

Role of TLR4 in Chikungunya virus (CHIKV) infection and associated altered cell mediated immune responses

By

CHANDAN MAHISH

LIFE11201604005

**National Institute of Science Education and Research,
Bhubaneswar**

*A thesis submitted to the
Board of Studies in Life Sciences
In partial fulfillment of the requirements
For the Degree of*

DOCTOR OF PHILOSOPHY

Of

HOMI BHABHA NATIONAL INSTITUTE



October, 2023

Homi Bhaba National Institute

Recommendations of the Viva Voce Committee

As members of the Viva Voce Committee, we certify that we have read the dissertation prepared by **Chandan Mahish** entitled "**Role of TLR4 in Chikungunya virus (CHIKV) infection and associated altered cell mediated immune responses**" and recommend that it may be accepted as fulfilling the thesis requirement for the award of Degree of Doctor of Philosophy.

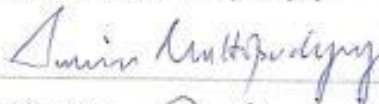
Chairman – Dr. Chandan Goswami

Date: 31/10/2023



Guide / Convener – Dr. Subhasis Chattopadhyay

Date: 31/10/2023



Examiner – Dr. Debashis Mitra

Date: 31/10/2023



Member 1 – Dr. Asima Bhattacharyya

Date: 31-10-2023

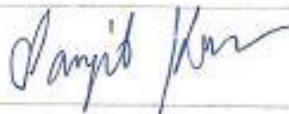


Member 2 – Dr. Harapriya Mohapatra

Date: 31-10-2023

Member 3 – Dr. Sanjib Kar

Date: 31-10-2023



Final approval and acceptance of this thesis is contingent upon the candidate's submission of the final copies of the thesis to HBNI.

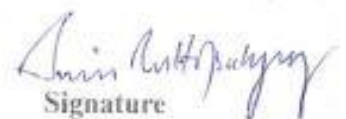
I/We hereby certify that I/we have read this thesis prepared under my/our direction and recommend that it may be accepted as fulfilling the thesis requirement.

Date:

Place:

Signature

Co-guide (if any)



Signature

Guide

STATEMENT BY AUTHOR

This dissertation has been submitted in partial fulfillment of requirements for an advanced degree at Homi Bhabha National Institute (HBNI) and is deposited in the library of NISER, Bhubaneswar to be made available to borrowers under the rules of the HBNI.

Brief quotations from this dissertation are allowable without special permission, provided that accurate acknowledgment of the source is made. Requests for permission for extended quotation from or reproduction of this manuscript in whole or in part may be granted by the Competent Authority of HBNI when in his or her judgment the proposed use of the material is in the interests of scholarship. In all other instances, however, permission must be obtained from the author.

Chandan Mahish

DECLARATION

I, hereby declare that the investigation presented in the thesis has been carried out by me. The work is original and has not been submitted earlier as a whole or in part for a degree/diploma at this or any other Institution / University.

Chandan Mahish

LIST OF PUBLICATIONS

Publications in refereed journal:

• Pertaining to thesis:

1. **Mahish C**, De S, Chatterjee S, Ghosh S, Keshry SS, Mukherjee T, Khamaru S, Tung KS, Subudhi BB, Chattopadhyay S & Chattopadhyay S. TLR4 is one of the receptors for Chikungunya virus envelope protein E2 and regulates virus induced pro-inflammatory responses in host macrophages. *Frontiers in Immunology* (2023) 14: doi: 10.3389/fimmu.2023.1139808.
2. Nayak TK, Mamidi P, Sahoo SS, Kumar PS, **Mahish C**, Chatterjee S, Subudhi BB, Chattopadhyay S & Chattopadhyay S. P38 and JNK Mitogen-Activated Protein Kinases Interact with Chikungunya Virus Non-structural Protein-2 and Regulate TNF Induction During Viral Infection in Macrophages. *Frontiers in Immunology* (2019) 10: doi: 10.3389/fimmu.2019.00786.

• Other publications:

1. Chatterjee S, Ghosh S, Datey A, **Mahish C**, Chattopadhyay S, Chattopadhyay S. Chikungunya virus perturbs the Wnt/ β -catenin signaling pathway for efficient viral infection. *Journal of Virology* (2023) doi: 10.1128/jvi.01430-23.
2. Shikha D, **Mahish C**, Sing R, Chattopadhyay S, Goswami C. Modulation of TRPM8 alters the phagocytic activity of microglia and induces changes in sub-cellular organelle functions. *Biochemical and Biophysical Research Communications* (2023) 682:56–63. doi: 10.1016/j.bbrc.2023.09.078.
3. Radhakrishnan A[†], Mukherjee T[†], **Mahish C**[†], Kumar PS, Goswami C, Chattopadhyay S. TRPA1 activation and Hsp90 inhibition synergistically downregulate macrophage activation and inflammatory responses in vitro. *BMC Immunology* (2023) 24:16. doi: 10.1186/s12865-023-00549-0. (†- **Equal contribution for joint**

first authorship).

4. Chatterjee S, Kumar S, Mamidi P, Datey A, Sengupta S, **Mahish C**, Laha E, De S, Keshry SS, Nayak TK, Ghosh S, Singh S, Subudhi BB, Chattopadhyay S & Chattopadhyay S. DNA Damage Response Signaling Is Crucial for Effective Chikungunya Virus Replication. *Journal of Virology* (2022) doi: 10.1128/jvi.01334-2.
5. De S, Ghosh S, Keshry SS, **Mahish C**, Mohapatra C, Guru A, Mamidi P, Datey A, Pani SS, Vasudevan D, Beuria TK, Chattopadhyay S, Subudhi BB & Chattopadhyay S. MBZM-N-IBT, a Novel Small Molecule, Restricts Chikungunya Virus Infection by Targeting nsP2 Protease Activity *In Vitro*, *In Vivo*, and *Ex Vivo*. *Antimicrobial Agents and Chemotherapy* (2022) 66: doi: 10.1128/aac.00463-22.
6. De S, Mamidi P, Ghosh S, Keshry SS, **Mahish C**, Pani SS, Laha E, Ray A, Datey A, Chatterjee S, Singh S, Mukherjee T, Khamaru S, Chattopadhyay S, Subudhi BB & Chattopadhyay S. Telmisartan restricts Chikungunya virus infection *in vitro* and *in vivo* through the AT1/PPAR- γ /MAPKs pathways. *Antimicrobial Agents and Chemotherapy* (2021) doi: 10.1128/AAC.01489-21.
7. Sanjai Kumar P, Nayak TK, **Mahish C**, Sahoo SS, Radhakrishnan A, De S, Datey A, Sahu RP, Goswami C, Chattopadhyay S, & Chattopadhyay S. Inhibition of transient receptor potential vanilloid 1 (TRPV1) channel regulates chikungunya virus infection in macrophages. *Archives of Virology* (2021) 166:139–155. doi: 10.1007/s00705-020-04852-8.

Conference Proceedings:

1. **Chandan Mahish**, Tapas Kumar Nayak, Soma Chattopadhyay, Subhasis Chattopadhyay. A poster entitled “*CHIKV Induced TNF Activates T Cells Using p38 And JNK-MAPK Mediated Pathway: A Brief Insight*” was presented in “Functional nucleic acids: Recent landscapes and therapeutic applications”- India | EMBO lecture course- RCB, Aug 16-19th, 2022, Faridabad, India.
2. **Chandan Mahish**, Tapas Kumar Nayak, Soma Chattopadhyay, Subhasis Chattopadhyay. A poster entitled “*The Bridging of Host Innate and Adaptive Immune Responses During Chikungunya Virus Infection: An Outline*” was presented in “Infections, Vaccines & Immuno-Innovations for Human Health”- Indian Immunology Society-BHU, July 8th and 9th, Varanasi, India.
3. **Chandan Mahish**, Tapas Kumar Nayak, Soma Chattopadhyay, Subhasis Chattopadhyay. A poster entitled “*Association of Pro-inflammatory Responses and Cell-Mediated Immune Responses During Chikungunya Virus Infection: An Outline*” was presented at International Conference on Recent Trends in Biotechnology (ICRTB)- Centurion University of Technology and Management, June 22nd & 23rd, 2022 Odisha, India.
4. **Chandan Mahish**, Tapas Kumar Nayak, Puspen Mondol, Priyanshu Singh, Soma Chattopadhyay, Subhasis Chattopadhyay. A poster entitled “*An Immunological Approach Towards DRDE-06 and S 27 Strains of Chikungunya Virus*” was presented in “Emerging and Reemerging viral diseases- Climate change impacts and Mitigations”- Indian Virological Society- AIIMS Bibinagar, March 26-28th, 2022, Hyderabad, Telangana, India. (Published as the conference proceedings in *Virus Disease* (July-September 2022) 33:338–361 - <https://doi.org/10.1007/s13337-022-00787-7>).
5. Tapas Kumar Nayak, Prabhudutta Mamidi, P Sanjai Kumar, Subhransu S. Sahoo, **Chandan Mahish**, Soma Chattopadhyay Subhasis Chattopadhyay. Participated as a member in the poster presentation entitled “*Modulation of Macrophages during Chikungunya Virus infection*” at “Global viral

- epidemics: a challenging threat’’- Indian Virological Society- PGIMER, Nov 12-14th, 2018, Chandigarh, India. (Published as the conference proceedings in *Virus disease* (January–March 2019) 30(1):112–169 - <https://doi.org/10.1007/s13337-019-00523-8>).
6. Tapas Kumar Nayak, P Sanjai Kumar, **Chandan Mahish**, Saumya Bandyopadhyay, Soma Chattopadhyay, Subhasis Chattopadhyay. Participated as a member in the presentation entitled “*Analysis of Altered Host Cell Immunity of Macrophages during Chikungunya Virus (CHIKV) Infection, in vitro*” at “International Congress of Cell Biology”- CCMB, Jan 27th -31st, 2018, Hyderabad, India (P217).
 7. Attended the hands-on workshop on different virological methods organized by the Indian Virological Society at Nitte University, Deralakatte, Mangalore-575018, India from Dec 10–13th, 2017.
 8. Subhransu Sekhar Sahoo, P Sanjai Kumar, Dalai Jupiter Nanda Kishore, Tathagata Mukherjee, **Chandan Mahish**, Soma Chattopadhyay, Chandan Goswami, Subhasis Chattopadhyay. Participated as a member in the presentation entitled “*Functional Expression of Sensory Receptor Channels in Cell-Mediated Immunity Implications in Infection and Tumor Immunity*” (BS-32) at Indian Science Congress, Bhubaneswar chapter- KIIT University, Dec 12th & 13th, 2016, Bhubaneswar, Odisha, India.

Chandan Mahish

*Dedicated to my family, teachers, and all those kind hearts
who had crossed path during my journey*

Acknowledgment

The 7 years long journey wasn't easy. Ultimately, the end of the journey came at the cost of lots of sacrifices, support, hard work, and dedication from my family, well-wishers, friends, and last but not least, me. I sincerely acknowledge their notable contributions from the bottom of my heart. You all made it possible.

Firstly, I would like to acknowledge my parents. Their continuous encouragement and support have driven me to follow the right track to success. Their values towards life have always guided me to differentiate between the right and the wrong things, time to time. Throughout this voyage, I have realized that they have sacrificed a lot to support my higher education in reputed institutions. No matter what I would try to repay, I won't be able to neutralize the balance sheet.

I wish to sincerely acknowledge the contribution of my biology teacher in high-school time, Mr. Tapan Kumar Ghati. His extraordinary way of teaching had directed my preference for biology for the very first time. Moreover, his mental support and guidance to choose the right path was one of the stepping stones of today.

I have completed my bachelor's in science at Ramakrishna Mission Vidyamandira, Belur, West Bengal. I am fortunate enough to learn the cultural heritage and moral values to be a better person during my residential life at RKM Vidyamandira. Those values have continuously kept my head high during the tough days. Moreover, the timely advises from Debanjan Maharaj, Sanjib Maharaj, and also from my departmental teachers always enriched my knowledge and guided me for the future.

During my postgraduation, I was fortunate enough to be guided by Dr. Arup Kumar Mitra at St. Xavier's College, Kolkata. He is the first person who taught me the basics of research and continuously motivated me to persue my career in the field of research. Moreover, the generous

support from Dr. Riddhi Majumder, St. Xavier's College, Kolkata, has further guided me for the next step of my journey.

During my PhD tenure, my supervisor, Dr. Subhasis Chattopadhyay has encouraged me to learn the different aspects of research. First of all, he never refrained from trying anything new for experimentation purposes. I believe this is the most important aspect of research. This freedom of experimentation as well as several responsibilities like lab management and teaching assistantship have shaped me a lot to take on new challenges nowadays. Moreover, he patiently supported me while I was facing technical issues and gave me useful suggestions as well as opened scopes of collaboration to facilitate the project as well as my scientific career. To my understanding, a Ph.D. supervisor is not for only scientific discussions. Rather, he/she shapes the future of a student in both scientific as well as philosophical aspects. I feel delightful to have my expectations fulfilled. He used to tell us that a Ph.D. degree cannot be given rather one must have to earn it. Now, I can say that I have tried my level best to earn the same. Thank you for showing the path, sir.

Dr. Soma Chattopadhyay from DBT-Institute of Life Sciences, Bhubaneswar, always was kind enough to support my research work. Whenever, I have requested her for scientific discussions, I have never felt differentiated from her Ph.D. students. I can clearly remember those days when despite having a tight schedule, she used to evaluate my research project on a regular basis and gave useful suggestions for possible upgradation of the work. Moreover, during my research period, sometimes I had felt depressed or to be precise, lack of motivation due to several reasons. During those days, a conversation with madam used to change my way of thinking. Once madam advised me not to go for what I could have got, rather think what I have already got. I have understood the philosophy behind this simple statement and have implemented the lesson which I will try to remember for lifetime. Thank you for your generosity, madam.

My long Ph.D. tenure would not have been such exiting without my friends. During the initial days of joining, Aranya, Bratati, and Tathagata used to have a long chit-chat, leg pulling, and lots of roaming around Bhubaneswar. The coursework examination of advanced molecular biology became easier because of our group study, where Aranya had explained the research papers. Also, how can I forget buying of my first expensive watch with them from the very first stipend? I can remember our PhD departmental trip to Simlipal and Keonjhar which was organized by our batch, i.e., August batch 2016. This was an achievement for me as a tour manager. Out of the many events, I can remember our cooking venture in collaboration with Raktim, Nishant, and Uday. I can bet that the taste of the food by our inexperienced hands was far better than the usual canteen meals. Also, lots of discussions and outings with Debashis, Raktim, Arjama, Nishant, Uday, Tapas, Bidyadhar, and Prafulla were rejuvenating after a tedious day in the lab. Most of them have risked their valuable lives several times to facilitate my learning of two-wheeler vehicles inside as well as outside of the campus.

It would be an injustice if I don't acknowledge another special friend, Deep Shikha from the January, 2018 PhD batch of Biology. Her positive mindset continuously supported me in my tough times and kept me mentally positive. Starting from the departmental journal club events to arranging a tour at Phulbani-Mandasuru-Daringbadi along with Rojalin, Rashmita di, Bimal Vaiya, and Tathagata, we had developed our bond which further became support for each other during the tough time. Thank you for being with me and tolerating all my high level stupidities, time to time.

I would like to thank DBT-ILS Bhubaneswar friends like Saikat, Soumyajit, Sanchari, Ankita, Supriya, Eshna, Sharad, Prabhu bhaiya, Kaustav da, Udvas and many more people. Together, we have enjoyed a lot on several group trips like Puri-Chilika, Satkosia, Koraput, etc., and parties at different places.

I would like to talk a few more words about our laboratory. When I joined the lab in July, 2016, initially I was taught lab protocols, experiments, lab managements and many more things by

Tapas Vaiya, Subhransu Vaiya, and Sanjai Vaiya. I would like to humbly acknowledge their guidance. Next, Upasana di had also contributed to initial experimental planning and designing of my project. For, different scientific, technical, or lab management purposes I have always received unconditional cooperation from Tathagata, my batchmate as well as my lab mate and also my partner of many crimes. Moreover, my juniors, Somlata and Kshyama also have supported the regular research work. They have contributed significantly in terms of different lab responsibilities. This change of baton had helped me to focus on my research during the final days. I wish to sincerely acknowledge their contributions. From time to time, M.Sc. students such as Manas, Avinash, Supriya, Anukrishna, Aniruddha, Hemendra, Puspen, Priyanshu, Ayush, Gayatri, Tanishka, Uditanshu, Mrithika, Prajwal, Harshit, Situl and Mrinalini have raised their helpful hands to continue the scientific contribution of SC lab, SBS, NISER.

Lastly, I would like to acknowledge all of my departmental professors, my doctoral committee members, all of the official staff of the School of Biological Sciences, the purchase & finance section, and the Animal House Facility for their immense support throughout my journey. I would love to express my regards and gratitude to all of my seniors and juniors for keeping their imprint during the last seven years.

Chandan Mahish

INDEX

	Page No.
SYNOPSIS	16-33
ABBREVIATIONS	34-39
LIST OF FIGURES	40-43
LIST OF TABLES	43
CHAPTER-1: Introduction and Review of literature	44-91
1. Introduction	45-67
1.1. Introduction to the Immune System.....	45-57
1.2. Introduction to the viruses.....	57-60
1.3. <i>Alphavirus</i> and its pathobiology.....	60-63
1.4. Role of PRRs in Different Microbial Infections: A Gateway Strategy.....	63
1.5. Macrophage-dependent Microbial Elimination: A Salient Innate Immune Response.....	64-67
2. Review of Literature	68-91
2.1. The Clinical, Pathobiological and Epidemiological Severity of Chikungunya Virus (CHIKV): A Brief Overview.....	68- 77
2.2. The importance of cellular pathways and host factors on CHIKV entry into the host.....	77-81
2.3. Immunological Aspects of Host-CHIKV Interaction.....	81-84
2.4. The significance of Toll like receptors (TLRs) during CHIKV infection.....	84-86
2.5. TLR4: An Unprecedented Regulator of Inflammation.....	86-91
CHAPTER-2: HYPOTHESIS AND OBJECTIVES	92-93
3.1. Hypothesis	93

3.2. Objectives.....	93
CHAPTER-3: MATERIALS AND METHODS.....	94-118
4. Materials.....	94-103
4.1. Cells and Viruses.....	95
4.2. Animals.....	95-96
4.3. Antibodies.....	96-98
4.4. Chemicals, reagents, and modulators.....	98-101
4.5. Kits.....	101-102
4.6. Primers for PCR amplifications.....	102
4.7. Buffers and other reagents preparation.....	102-103
5. Methods.....	104-118
5.1. Isolation of Mouse Peritoneal Macrophages.....	104
5.2. Isolation of hPBMC-derived Adherent Myeloid Lineage of Cells.....	104-105
5.3. PMA-induced Differentiation of THP-1 Cells.....	105
5.4. MTT-based Viability Assay.....	106
5.5. AnnexinV-7AAD-based Viability Assay.....	106
5.6. LPS Stimulation in RAW264.7 Cells.....	106
5.7. The Treatment of Modulators in Macrophages.....	106-107
5.8. CHIKV Infection in Absence/ Presence of TLR4 Inhibition.....	107-108
5.9. Plaque Assay.....	108
5.10. qRT-PCR Analysis.....	109-110
5.11. Flow Cytometry (FC)-based Analysis.....	110-111

5.12. Sandwich ELISA for Cytokine Analysis.....	111
5.13. Western Blot Analysis.....	111-112
5.14. Co-immunoprecipitation Study.....	113
5.15. <i>In silico</i> Analysis.....	113-114
5.16. Anti-TLR4-antibody-driven Neutralization Assay.....	114
5.17. Time of addition assay.....	115
5.18. Effect of TLR4 inhibition before, during, and after CHIKV infection.....	115
5.19. Temperature-shift assay.....	115
5.20. Viral Attachment Assay.....	115-116
5.21. <i>In vivo</i> effect of TLR4 inhibition in BALB/c mice.....	116-117
5.22. Splenocyte isolation and T cell purification.....	117
5.23. Indirect Co-culture of syngeneic T cell and Macrophage, <i>in vitro</i>	117-118
5.24. Statistical Analysis.....	118

CHAPTER-4: RESULTS AND DISCUSSION.....119-164

6.1. TLR4 inhibition abrogates LPS-induced macrophage activation and pro-inflammatory responses in the host macrophages, <i>in vitro</i>	122-125
6.2. TLR4 antagonism reduces CHIKV infection in the host macrophages of different origins, <i>in vitro</i>	125-140
6.3. CHIKV-induced TNF promotes naive T cell activation in p38 and JNK-MAPK pathway-dependent manner, <i>in vitro</i>	140-142
6.4. TLR4 antagonism lowers LPS or CHIKV-induced p38 and SAPK-JNK phosphorylation in host macrophages, <i>in vitro</i>	142-145

6.5. Functional TLR4 and CHIKV-E2 interact to promote efficient infection in host macrophages.....145-153

6.6. TLR4 is required to regulate the CHIKV entry in host macrophages, *in vitro*.....153-158

6.7. TLR4 inhibition efficiently reduces the CHIKV infection and inflammation in mice, *in vivo*.....158-160

DISCUSSION AND CONCLUSION.....160-164

BIBLIOGRAPHY.....165-180

PUBLICATIONS



Homi Bhabha National Institute

SYNOPSIS OF Ph. D. THESIS

- 1. Name of the Student:** Chandan Mahish
- 2. Name of the Constituent Institution:** NISER Bhubaneswar, an off-campus center (OCC) of HBNI
- 3. Enrolment No.:** LIFE11201604005
- 4. Title of the Thesis:** Role of TLR4 in Chikungunya virus (CHIKV) infection and associated altered cell mediated immune responses
- 5. Board of Studies:** Life Sciences

SYNOPSIS

(Limited to 10 pages in double spacing)

Abstract:

Toll like receptor 4 (TLR4), one of the major innate immune system components, is already reported to be directly associated with inflammation in various cases of microbial infection, cancer, and autoimmune responses. However, no such published report is available on TLR4 in regulating Chikungunya virus (CHIKV) infection, inflammation, and interaction with the viral proteins. Hence, the possible regulatory role of TLR4 on CHIKV infection and subsequent immuno-modulations in the host were investigated using mouse macrophage cell line namely, RAW264.7, primary macrophage cells of mouse and human origins, and *in vivo* mice model. The findings depict that TLR4 inhibition may reduce CHIKV infection and host immune activation in terms of reduced expression of macrophage activation markers and pro-inflammatory cytokines *in vitro* and *in vivo*. The regulatory

role of TLR4 on CHIKV infection was further validated by a comparative study between the RAW264.7 and TLR4 KO RAW cell lines, which shows the absence of functional TLR4 significantly reduces CHIKV infection and associated host immune responses. The specific interactions between TLR4 and CHIKV envelope protein E2 demonstrated TLR4 as a potential receptor of CHIKV-E2, *in vitro* and *in silico*. Moreover, an anti-TLR4 blocking study reconfirmed the role of TLR4 as a possible host entry factor of CHIKV-E2 in the macrophages. Altogether, the results infer that the TLR4 interacts with viral E2 protein and therefore, has a positive regulatory role in CHIKV infection and modulation of pro-inflammatory responses, which might bear a translational approach for designing potential medication against CHIKV infection.

Introduction:

Starting from its discovery in 1952, the Chikungunya virus (CHIKV), a member of genus: *Alphavirus* and family: *Togaviridae*, has shown its re-emergence across the globe several times. As it is a mosquito-borne disease (vector is *Aedes sp.*), the densely populated areas with a lack of effective mosquito-control facilities were specifically reported for the repeated CHIKV outbreaks. To date, the lack of available vaccines or specific medications also demonstrates the severity of the disease (1,2). The major initial symptoms of CHIKV-infected patients are high fever, headache, polyarthralgia, and myalgia which may further lead to failure of cardiovascular, neuronal, renal, or respiratory systems in later stages and therefore, permanent physical disability(2–4).

The crucial factor of CHIKV pathogenesis is massive pro-inflammatory cytokine burst due to the activation of host immune responses. The reports reveal that the marked upregulation of tumor necrosis factor (TNF), interleukin (IL)- 6, 4, 1 β and 12 in mouse as well as human macrophages via p38 and Jun N-terminal protein kinase (JNK)-mitogen-activated protein kinase (MAPK) mediated pathway is associated with polyarthralgia and CHIKV infection mediated fever (CHIKF)(5–8). However, the initial cellular pathways associated with CHIKV-driven activation of the host immune

system are yet to be explored. Interestingly, the literature reveals that toll like receptor 4 (TLR4), an innate immune system component, regulates pro-inflammatory responses in various cases of microbial infection, cancer, and autoimmunity (9–11). Several pro-inflammatory clinical irregularities such as necrotizing enterocolitis (NEC), and inflammatory bowel disease (IBD) are well-reported to be associated with TLR4-directed regulation (12,13). Moreover, *in vivo* inflammation models such as mouse sepsis or lung injury model specifically demonstrate the positive regulation of TLR4 towards inflammation and modulation of host immune responses. Furthermore, some of the structural proteins of respiratory syncytial virus (RSV), foot and mouth disease virus (FMDV), and SARS-CoV2 have recently been reported to interact with host TLR4 (14–16). Therefore, the above-mentioned studies reveal the possibility that TLR4 might play a pivotal role in viral entry as well as disease manifestation in the host.

The CHIKV-driven activation of host immune systems and rise in pro-inflammatory cytokines (**cytokine storm**) via the MAPK pathway are already reported by us and others(7,17,18). Since host TLR4 activation is already reported to be associated with MAPK activation and pro-inflammatory cytokine release (such as TNF), the possible connection between CHIKV infection and host TLR4 activation is yet to be explored (19,20). Hence, it was hypothesized that host TLR4 might be associated with the regulation of CHIKV infection and subsequent host immune responses. Therefore, the study is designed to explore the possible regulation of TLR4 on CHIKV infection and associated host immune responses using *in vitro* models of different origins, *in silico* as well as *in vivo* mice models.

Hypothesis and Objectives:

Hypothesis

The functional expression of the toll like receptor 4 (TLR4) during Chikungunya virus (CHIKV) infection may regulate host cell mediated immune responses.

Specific objectives

1. To investigate the requirement of TLR4 in CHIKV infection in macrophages and associated immune responses, *in vitro*.
2. To study the TLR4-directed modulation of altered cellular signaling of macrophages during CHIKV infection, *in vitro*.
3. To examine the possible interaction of TLR4 and CHIKV structural proteins, *in vitro*.
4. To find out the role of TLR4 towards CHIKV infection in mice, *in vivo*.

Materials and Methods

Cells and virus and reagents: The RAW264.7 (ATCC® TIB-71™), peritoneal macrophages obtained from BALB/c and C57BL/6 derived mice and human peripheral blood mononuclear cells (hPBMC) derived monocyte-macrophages were cultured in complete RPMI 1640 in a sterile humidified atmosphere at 37°C with 5% CO₂ as described earlier(7,8,21). The Vero and TLR4-knock-out (KO) cells were similarly cultured in complete DMEM media as described before(7,22). The CHIKV-Indian Strain (IS) (accession no- EF210157.2), Vero cells, and anti-CHIKV-E2 antibody were kind gifts from Dr. M.M. Parida, DRDE, Gwalior, India. The anti-CHIKV-E1 antibody was a generous gift from Dr. T.K. Chowdary, NISER, Bhubaneswar, India. TAK-242 (catalog no: 614316-5MG), a well-cited TLR4 inhibitor was purchased from Merck Millipore, USA (10,20,23).

Human peripheral blood mononuclear cells (hPBMC) isolation: Following the guidelines issued by Institutional Ethics Committee, NISER, Bhubaneswar (NISER/IEC/2022-04), hPBMC-derived adherent myeloid cells were isolated from healthy donors and further experimentation was done as described previously (24–26).

Cell viability assay: The working concentration/s of TAK2-242 was determined using an MTT-based assay or annexin V-7-AAD-based method as per the manufacturer's protocol (7).

LPS induction in RAW264.7 cells: The RAW264.7 cells were treated with LPS as per the protocol mentioned earlier (27).

CHIKV infection: The macrophage cells of different sources were infected with the CHIKV-Indian strain (CHIKV-IS) at MOI 5 for 2 h and processed further for downstream experiments as per the protocol described before (7,8,25,26).

Flow cytometry: The differentially treated macrophage cells of different origins were subjected to surface and/or intracellular staining as per the methods described earlier (7,8). The stained cells were acquired in BD LSR Fortessa and analyzed further using FlowJo™ software (BD Biosciences, USA). Around ten thousand cells were acquired per sample of each set (a minimum of three independent sets were performed).

ELISA: The cell culture supernatant/mouse serum of different conditions was analyzed using the BD OptEIA™ Sandwich ELISA kit (BD Biosciences, USA) as per the manufacturer's instructions. The standard curves of different cytokines were prepared and the quantification was performed as described earlier (7,8,25,26).

T cells isolation and co-culture assay: The splenic T cells were isolated from 6-8 weeks old BALB/c mice as described earlier (28). The anti-TCR-antibody-driven T cell activation in the presence and absence of the CHIKV-infected RAW264.7 culture supernatants in the presence/absence of either SB203580 (p-p38 inhibitor, SB), SP600125 (p-JNK inhibitor, SP) or anti-TNF neutralizing antibody following the protocol described before with little modifications (29).

qRT-PCR and Plaque assay: To quantify the viral copy number in cell culture supernatants/inside the cells, qRT-PCR-based analysis was performed for the CHIKV-E1 gene as described earlier (7,25).

The plaque assay was also performed for some cases to quantify the viral titer obeying the protocol described earlier(7,8,21,25,26,30).

Effect of TAK-242 before, during, and after CHIKV infection: To determine the effectiveness of the TLR4 inhibitor namely TAK-242 in different stages of viral infection, the cells were treated with the drug at different points of CHIKV infection, for example, before infection, during infection and after infection obeying the protocol as described earlier (25,26).

Viral attachment assay: To quantitate the unbound virus particles after infection, the infection volume was collected and q-RT and plaque assay-based analysis were performed as per the protocol mentioned earlier.

Time of addition experiment: To investigate the role of TLR4 in different stages of the CHIKV life cycle, the time of addition experiment was performed as per the protocol described earlier (21).

Western blot: The differential protein expressions were assessed using the Western blot-based analysis as per the protocol described earlier (7,8,30).

In silico analysis: The possible interactions between TLR4 and the viral proteins responsible for attachment and internalization in the host were analyzed using molecular docking-based studies as per the protocol described earlier (31).

Co-immunoprecipitation: To investigate the protein-protein interactions associated with CHIKV and host interaction, Co-immunoprecipitation-based studies were performed using a similar protocol as described earlier (8,30).

Anti-TLR4 blocking assay: An anti-TLR4 antibody-based blocking experiment was performed to validate the specific role of TLR4 in the regulation of CHIKV infection in the host macrophages following the similar protocol described earlier with little modifications (32).

Animal Studies: The peritoneal macrophages from BALB/c and C57BL/6 mice were collected following the method described before. The *in vivo* effect of TLR4 inhibition during CHIKV infection was studied in C57BL/6 mice following the protocols as performed earlier (25,26).

Statistical analysis: The GraphPad Prism 9 software was used to perform one-way ANOVA or unpaired t-tests. All data were represented as Mean \pm SEM. $p < 0.05$ was considered statistically significant among different groups.

Results:

1. TLR4 antagonism overcomes LPS-induced macrophage activation, *in vitro*

Although the positive regulation of TLR4 over LPS-induced pro-inflammatory responses was established earlier, it was re-explored as an experimental control to bridge the possible TLR4 dependent-CHIKV-induced inflammation in host macrophages. The results delineated that TAK-242-driven TLR4 inhibition significantly abrogated the LPS-driven expression of macrophage activation markers such as CD86, MHC-II, and CD14 and proinflammatory cytokines such as TNF. As reported earlier, surface expression of TLR4 was found to reduce and total expression of TLR4 and was found to increase during LPS/ LPS + TAK-242 stimulation concerning mock treatment. Moreover, the TAK-242 treatment restored the LPS-induced increased level of p-NF- κ B and p-p38, and p-JNK MAPK proteins. In conclusion, it was found that TLR4 antagonism regulates LPS-induced macrophage activation in the current experimental setup.

2. TLR4 inhibition decreases CHIKV infection and associated host immune responses in macrophages of different origins, *in vitro*

In correlation to the TLR4-dependent regulation of pro-inflammatory responses due to LPS induction, the possible involvement of TLR4 was studied in CHIKV infection in host macrophages. The results depicted that TAK-242 was used to pre-incubate the RAW264.7 cells as well as peritoneal macrophages obtained from BALB/c and C57BL/6 mice for 3 h followed by CHIKV infection at MOI

5 for 2 h. The cells were harvested at 8 hours post-infection (hpi). The flow cytometry-based study revealed that the CHIKV structural protein E2 was reduced in the presence of TAK-242. The surface and the total TLR4 expressions were reduced and increased respectively during CHIKV infection compared to the mock. The viral copy number, macrophage activation markers, such as CD86, MHC-II, and CD14, the final molecule of TLR4 signaling pathway i.e., p-NF-KB, and pro-inflammatory cytokines such as TNF, IL-6, and MCP-1 reduced significantly up on TAK-242 directed TLR4 inhibition.

Moreover, the TAK-242-directed TLR4 inhibition reduced the CHIKV infection in hPBMC-derived host macrophages in terms of reduced CHIKV-E2 levels determined by flow cytometry, plaque assay-based reduction in viral titer and ELISA-based reduction in secretory TNF expression. Together, TLR4 inhibition lowered CHIKV infection and associated host macrophage activation, *in vitro*.

3. TLR4 inhibition reduces CHIKV-induced activation of p38 and JNK MAPK pathways in host macrophages, *in vitro*

To investigate the specific pathways involved in CHIKV-induced cytokine burst, the RAW264.7 cells were subjected to CHIKV infection in MOI 5 for 2 h and the possible involvement of MAPK pathways was analyzed in the presence of specific p-p38 MAPK and p-JNK MAPK inhibitors namely SB203580 (SB) and SP600125 (SP), respectively. The data confer that the activation of MAPK pathways augments TNF secretion in RAW264.7 cells.

To correlate the role of TLR4 in the activation of MAPK pathways-induced pro-inflammatory cytokine production, p38, and JNK-MAPK levels were assessed in the presence and absence of TAK-242-driven TLR4 antagonism in CHIKV-infected RAW264.7 cells. The results depicted that the TAK-242 treatment lowered the p-p38 and p-JNK expression in a concentration-dependent manner. Therefore, the reduction in MAPK proteins reconfirms the positive regulation of TLR4 in CHIKV

infection and the associated rise in pro-inflammatory cytokines.

4. CHIKV infection-derived secretory TNF upregulates T cell activations, *in vitro*

To further investigate the effect of CHIKV infection-induced cell-mediated immune responses an indirect co-culture study was performed. The culture supernatants of CHIKV infected RAW264.7 cells in the presence or absence of anti-TNF neutralizing antibody, SB203580 (SB) and SP600125 (SP) were collected and splenic T cells isolated from BALB/c mice were co-cultured for 36 h in presence of TCR stimulation to explore the possible differential activation status. It was found that the early activation marker of T cells, CD69 showed reduced activation in the presence of anti-TNF antibody-treated culture supernatant and reduced further in the presence of SB and SP-treated CHIKV-infected culture supernatants. Therefore, the study concludes that CHIKV infection-induced upregulation of p38 and JNK MAPK pathways promote pro-inflammatory cytokine burst in macrophages which further aggravates T cell-mediated host immune responses.

5. Efficient interaction of CHIKV-E2 and host TLR4 is required for CHIKV infection and subsequent disease pathogenesis.

To determine whether functional TLR4 interacts with CHIKV envelope proteins and therefore facilitates viral entry into host macrophages, a comparative study between TLR4KO RAW cells and RAW264.7 cells was performed. The results denoted the significant reduction in CHIKV-E2, non-significant changes in the macrophage activation markers, and reduced proinflammatory cytokines generation in the case of CHIKV-infected TLR4KO RAW cells. Next, the protein-protein interaction study revealed positive interaction between CHIKV-E2 and host TLR4, *in vitro*. Moreover, molecular docking study revealed the existence of multiple high-affinity polar interactions which supports the TLR4-dependent CHIKV entry and further regulation of pathogenesis in host macrophages. Furthermore, the anti-TLR4-antibody dependent blocking assay was performed in RAW264.7 cells and it was found that pre-treatment of the macrophages with anti-TLR4-antibody effectively reduced

CHIKV infection which further supports the essentiality of TLR4-dependent CHIKV entry in host macrophages.

6. TLR4 is essential in the entry of CHIKV in host macrophages, *in vitro*

To investigate the specific stage(s) of the CHIKV life cycle where TLR4 effectively regulates CHIKV infection and further host immune responses, an experimental study was performed. TAK-242 was added before infection, during infection, both before and during infection, and post-infection. It was found that the TLR4 inhibitor is most effective when added before infection. However, post-infection treatment did not show any anti-viral role. Moreover, no effect of TLR4 inhibition was observed in viral transcription or translation. Therefore, the overall observation signifies the TLR4-dependent CHIKV entry in host macrophages.

7. TLR4 antagonism improves survival and reduces inflammation of CHIKV-infected mice, *in vivo*

To investigate the role of TLR4 antagonism against CHIKV infection in mice, *in vivo*, 10-12 days old C57BL/6 mice pups (n=6) were infected with CHIKV-IS in the presence/absence of oral TAK-242 treatment. The results delineated that the TAK-242 treated group showed significant improvement in terms of reduced E2 level and viral titer in muscle and spleen, reduced serum TNF level, and improved survival (75%) and disease score in comparison to only CHIKV infected group. Therefore, the study again supports the association of TLR4 with CHIKV infection and subsequent disease pathogenesis.

Discussion:

As one of the major early determinants of foreign immunogenic components, TLR4 contributes a regulatory role in studying host-pathogen interactions and associated pro-inflammatory host immune responses. Modern-age biomedical research in the field of inflammation, for example, rheumatoid arthritis, necrotizing enterocolitis, inflammatory bowel disease, severe sepsis, and acute

alcoholic hepatitis (<https://clinicaltrials.gov/ct2/show/NCT04620148>) has shown a profound TLR4-specific regulatory role in disease progression and therefore the anti-TLR4-based remedy is currently under consideration for different levels of phase trials (9,12,13,33). As CHIKV is already reported to cause massive pro-inflammatory cytokine burst (7,8) in the host and there is a lack of availability of specific anti-CHIKV treatment, the current study is intended to demonstrate the possible involvement of TLR4 in CHIKV pathogenesis and specific anti-TLR4-driven anti-viral remedy.

The current findings report that TLR4 antagonism with TAK-242 (a cyclohexene derivative small molecule that preferentially binds to only TLR4 as Cys747 residue and therefore, inhibits TLR4-specific downstream signalling) reduced CHIKV infection and associated macrophage activation in terms of activation markers and pro-inflammatory cytokine secretion in host macrophages of different origins in p38 and SAPK-JNK MAPK dependent way. The comparative study between RAW264.7 and TLR4 KO RAW cells validated the necessity of functional TLR4 for efficient CHIKV infection and subsequent pro-inflammatory responses, *in vitro*. Moreover, it was found that CHIKV envelope protein E2 interacts with host TLR4, *in vitro* as well as *in silico*, which indicated the possible alliance of CHIKV entry using host TLR4. Further, the anti-TLR4-driven blocking of host TLR4 reconfirmed the association of TLR4 in CHIKV entry in host macrophages, *in vitro*. Mechanistically, it was found that TLR4 inhibition before CHIKV infection is most effective in reducing the viral infection, and once entered into the host, TLR4 inhibition does not have any significant role to regulate the CHIKV life cycle. Nonetheless, the *in vivo* mice model study revealed that TLR4 inhibition significantly reduces disease symptoms and inflammation and improves survival. Collectively, for the first time, the study reveals the positive regulation of TLR4 towards CHIKV infection and pathogenesis and also detects the future possibility of TLR4-directed anti-CHIKV measure.

Although the study reveals the association of TLR4 with CHIKV entry, TLR4 inhibition doesn't completely hinder viral entry. Therefore, the possible association of other known CHIKV receptors(34) in the presence or absence of TLR4 antagonism could be further investigated. Moreover, the *in-silico* study shows that Thr546, Ser550, and Tyr454 residues of TLR4 and Gln307 and Glu303 residues of CHIKV-E2 protein exhibit multiple high-affinity polar interactions, which might be subjected to mutational analysis in future to explore the detailed mechanism(s). Furthermore, the effectiveness of TLR4 inhibition in hPBMC-derived macrophages might be indicative for further detailed investigation of higher-order systems. In conclusion, the positive regulation of TLR4 in CHIKV infection and further disease pathogenesis in the host might have translational implications to design future therapeutics.

References:

1. Suhrbier A. Rheumatic manifestations of chikungunya: emerging concepts and interventions. *Nat Rev Rheumatol* (2019) 15:597–611. doi: 10.1038/s41584-019-0276-9
2. Webb E, Michelen M, Rigby I, Dagens A, Dahmash D, Cheng V, Joseph R, Lipworth S, Harriss E, Cai E, et al. An evaluation of global Chikungunya clinical management guidelines: A systematic review. *EClinicalMedicine* (2022) 54:101672. doi: 10.1016/j.eclinm.2022.101672
3. Cunha RV da, Trinta KS. Chikungunya virus: clinical aspects and treatment - A Review. *Mem Inst Oswaldo Cruz* (2017) 112:523–531. doi: 10.1590/0074-02760170044
4. Simon F, Javelle E, Cabie A, Bouquillard E, Troisgros O, Gentile G, Leparç-Goffart I, Hoen B, Gandjbakhch F, Rene-Corail P, et al. French guidelines for the management of chikungunya (acute and persistent presentations). November 2014. *Med Mal Infect* (2015) 45:243–263. doi: 10.1016/j.medmal.2015.05.007
5. Guerrero-Arguero I, Høj TR, Tass ES, Berges BK, Robison RA. A comparison of Chikungunya virus infection, progression, and cytokine profiles in human PMA-differentiated U937 and murine RAW264.7 monocyte derived macrophages. *PLoS One* (2020) 15:e0230328. doi: 10.1371/journal.pone.0230328
6. Jacob-Nascimento LC, Carvalho CX, Silva MMO, Kikuti M, Anjos RO, Fradico JRB, Campi-Azevedo AC, Tauro LB, Campos GS, Moreira PS dos S, et al. Acute-Phase Levels of CXCL8 as Risk Factor for Chronic Arthralgia Following Chikungunya Virus Infection. *Front Immunol* (2021) 12: doi: 10.3389/fimmu.2021.744183

7. Nayak T, Mamidi P, Kumar A, Singh L, Sahoo S, Chattopadhyay S, Chattopadhyay S. Regulation of Viral Replication, Apoptosis and Pro-Inflammatory Responses by 17-AAG during Chikungunya Virus Infection in Macrophages. *Viruses* (2017) 9:3. doi: 10.3390/v9010003
8. Nayak TK, Mamidi P, Sahoo SS, Kumar PS, Mahish C, Chatterjee S, Subudhi BB, Chattopadhyay S, Chattopadhyay S. P38 and JNK Mitogen-Activated Protein Kinases Interact With Chikungunya Virus Non-structural Protein-2 and Regulate TNF Induction During Viral Infection in Macrophages. *Front Immunol* (2019) 10: doi: 10.3389/fimmu.2019.00786
9. Samarpita S, Kim JY, Rasool MK, Kim KS. Investigation of toll-like receptor (TLR) 4 inhibitor TAK-242 as a new potential anti-rheumatoid arthritis drug. *Arthritis Res Ther* (2020) 22:16. doi: 10.1186/s13075-020-2097-2
10. Takashima K, Matsunaga N, Yoshimatsu M, Hazeki K, Kaisho T, Uekata M, Hazeki O, Akira S, Iizawa Y, Ii M. Analysis of binding site for the novel small-molecule TLR4 signal transduction inhibitor TAK-242 and its therapeutic effect on mouse sepsis model. *Br J Pharmacol* (2009) 157:1250–1262. doi: 10.1111/j.1476-5381.2009.00297.x
11. Wu K, Zhang H, Fu Y, Zhu Y, Kong L, Chen L, Zhao F, Yu L, Chen X. TLR4/MyD88 signaling determines the metastatic potential of breast cancer cells. *Mol Med Rep* (2018) doi: 10.3892/mmr.2018.9326
12. Han C, Guo L, Sheng Y, Yang Y, Wang J, Gu Y, Li W, Zhou X, Jiao Q. FoxO1 regulates TLR4/MyD88/MD2-NF- κ B inflammatory signalling in mucosal barrier injury of inflammatory bowel disease. *J Cell Mol Med* (2020) 24:3712–3723. doi: 10.1111/jcmm.15075
13. Yu R, Jiang S, Tao Y, Li P, Yin J, Zhou Q. Inhibition of HMGB1 improves necrotizing enterocolitis by inhibiting NLRP3 via TLR4 and NF- κ B signaling pathways. *J Cell Physiol* (2019) 234:13431–13438. doi: 10.1002/jcp.28022
14. Marzec J, Cho H-Y, High M, McCaw ZR, Polack F, Kleeberger SR. Toll-like receptor 4-mediated respiratory syncytial virus disease and lung transcriptomics in differentially susceptible inbred mouse strains. *Physiol Genomics* (2019) 51:630–643. doi: 10.1152/physiolgenomics.00101.2019
15. Zhang J, Li D, Yang W, Wang Y, Li L, Zheng H. Foot-and-Mouth Disease Virus VP3 Protein Acts as a Critical Proinflammatory Factor by Promoting Toll-Like Receptor 4-Mediated Signaling. *J Virol* (2021) 95: doi: 10.1128/JVI.01120-21
16. Zhao Y, Kuang M, Li J, Zhu L, Jia Z, Guo X, Hu Y, Kong J, Yin H, Wang X, et al. SARS-CoV-2 spike protein interacts with and activates TLR4. *Cell Res* (2021) 31:818–820. doi: 10.1038/s41422-021-00495-9
17. Felipe VLJ, Paula A V, Silvio U-I. Chikungunya virus infection induces differential inflammatory and antiviral responses in human monocytes and monocyte-derived macrophages. *Acta Trop* (2020) 211:105619. doi: 10.1016/j.actatropica.2020.105619

18. Nayak TK, Mamidi P, Sahoo SS, Sanjai Kumar P, Mahish C, Chatterjee S, Subudhi BB, Chattopadhyay S, Chattopadhyay S. P38 and JNK Mitogen-Activated Protein Kinases Interact with Chikungunya Virus Non-structural Protein-2 and Regulate TNF Induction during Viral Infection in Macrophages. *Front Immunol* (2019) 10:1–15. doi: 10.3389/fimmu.2019.00786
19. Lin F-Y, Chen Y-H, Tasi J-S, Chen J-W, Yang T-L, Wang H-J, Li C-Y, Chen Y-L, Lin S-J. Endotoxin Induces Toll-Like Receptor 4 Expression in Vascular Smooth Muscle Cells via NADPH Oxidase Activation and Mitogen-Activated Protein Kinase Signaling Pathways. *Arterioscler Thromb Vasc Biol* (2006) 26:2630–2637. doi: 10.1161/01.ATV.0000247259.01257.b3
20. Matsunaga N, Tsuchimori N, Matsumoto T, Ii M. TAK-242 (Resatorvid), a Small-Molecule Inhibitor of Toll-Like Receptor (TLR) 4 Signaling, Binds Selectively to TLR4 and Interferes with Interactions between TLR4 and Its Adaptor Molecules. *Mol Pharmacol* (2011) 79:34–41. doi: 10.1124/mol.110.068064
21. Sanjai Kumar P, Nayak TK, Mahish C, Sahoo SS, Radhakrishnan A, De S, Datey A, Sahu RP, Goswami C, Chattopadhyay S, et al. Inhibition of transient receptor potential vanilloid 1 (TRPV1) channel regulates chikungunya virus infection in macrophages. *Arch Virol* (2021) 166:139–155. doi: 10.1007/s00705-020-04852-8
22. Anand G, Perry AM, Cummings CL, St. Raymond E, Clemens RA, Steed AL. Surface Proteins of SARS-CoV-2 Drive Airway Epithelial Cells to Induce IFN-Dependent Inflammation. *The Journal of Immunology* (2021) 206:3000–3009. doi: 10.4049/jimmunol.2001407
23. Sha T, Sunamoto M, Kitazaki T, Sato J, Ii M, Iizawa Y. Therapeutic effects of TAK-242, a novel selective Toll-like receptor 4 signal transduction inhibitor, in mouse endotoxin shock model. *Eur J Pharmacol* (2007) 571:231–239. doi: 10.1016/j.ejphar.2007.06.027
24. Chattopadhyay S, Chakraborty NG. Continuous Presence of Th1 Conditions Is Necessary for Longer Lasting Tumor-Specific CTL Activity in Stimulation Cultures With PBL. *Hum Immunol* (2005) 66:884–891. doi: 10.1016/j.humimm.2005.06.002
25. De S, Mamidi P, Ghosh S, Keshry SS, Mahish C, Pani SS, Laha E, Ray A, Datey A, Chatterjee S, et al. Telmisartan restricts Chikungunya virus infection *in vitro* and *in vivo* through the AT1/PPAR- γ /MAPKs pathways. *Antimicrob Agents Chemother* (2021) doi: 10.1128/AAC.01489-21
26. De S, Ghosh S, Keshry SS, Mahish C, Mohapatra C, Guru A, Mamidi P, Datey A, Pani SS, Vasudevan D, et al. MBZM-N-IBT, a Novel Small Molecule, Restricts Chikungunya Virus Infection by Targeting nsP2 Protease Activity *In Vitro*, *In Vivo*, and *Ex Vivo*. *Antimicrob Agents Chemother* (2022) 66: doi: 10.1128/aac.00463-22
27. Liu G, Xie J, Shi Y, Chen R, Li L, Wang M, Zheng M, Xu J. Sec-O-glucosylhamaudol suppressed inflammatory reaction induced by LPS in RAW264.7 cells through inhibition of NF- κ B and MAPKs signaling. *Biosci Rep* (2020) 40: doi: 10.1042/BSR20194230
28. Sahoo SS, Pratheek BM, Meena VS, Nayak TK, Kumar PS, Bandyopadhyay S, Maiti PK, Chattopadhyay S. VIPER regulates naive T cell activation and effector responses: Implication

- in TLR4 associated acute stage T cell responses. *Sci Rep* (2018) 8:7118. doi: 10.1038/s41598-018-25549-8
29. Feng H, Zhang D, Palliser D, Zhu P, Cai S, Schlesinger A, Maliszewski L, Lieberman J. *Listeria* - Infected Myeloid Dendritic Cells Produce IFN- β , Priming T Cell Activation. *The Journal of Immunology* (2005) 175:421–432. doi: 10.4049/jimmunol.175.1.421
 30. Chatterjee S, Kumar S, Mamidi P, Datey A, Sengupta S, Mahish C, Laha E, De S, Keshry SS, Nayak TK, et al. DNA Damage Response Signaling Is Crucial for Effective Chikungunya Virus Replication. *J Virol* (2022) doi: 10.1128/jvi.01334-22
 31. Pierce BG, Wiehe K, Hwang H, Kim B-H, Vreven T, Weng Z. ZDOCK server: interactive docking prediction of protein-protein complexes and symmetric multimers. *Bioinformatics* (2014) 30:1771–1773. doi: 10.1093/bioinformatics/btu097
 32. Yang K, Zhang XJ, Cao LJ, Liu XH, Liu ZH, Wang XQ, Chen QJ, Lu L, Shen WF, Liu Y. Toll-Like Receptor 4 Mediates Inflammatory Cytokine Secretion in Smooth Muscle Cells Induced by Oxidized Low-Density Lipoprotein. *PLoS One* (2014) 9:e95935. doi: 10.1371/journal.pone.0095935
 33. Rice TW, Wheeler AP, Bernard GR, Vincent J-L, Angus DC, Aikawa N, Demeyer I, Sainati S, Amlot N, Cao C, et al. A randomized, double-blind, placebo-controlled trial of TAK-242 for the treatment of severe sepsis*. *Crit Care Med* (2010) 38:1685–1694. doi: 10.1097/CCM.0b013e3181e7c5c9
 34. Zhang R, Kim AS, Fox JM, Nair S, Basore K, Klimstra WB, Rimkunas R, Fong RH, Lin H, Poddar S, et al. Mxra8 is a receptor for multiple arthritogenic alphaviruses. *Nature* (2018) 557:570–574. doi: 10.1038/s41586-018-0121-3
 35. Grubbs H, Kahwaji CI. *Physiology, Active Immunity*. (2023).183. Wang J, Feng X, Zeng Y, Fan J, Wu J, Li Z, Liu X, Huang R, Huang F, Yu X, et al. Lipopolysaccharide (LPS)-induced autophagy is involved in the restriction of *Escherichia coli* in peritoneal mesothelial cells. *BMC Microbiol* (2013) 13:255. doi: 10.1186/1471-2180-13-255

Publications in Refereed Journal:

a. Published

- # **1. Mahish C**, De S, Chatterjee S, Ghosh S, Keshry SS, Mukherjee T, Khamaru S, Tung KS, Subudhi BB, Chattopadhyay S & Chattopadhyay S. TLR4 is one of the receptors for Chikungunya virus envelope protein E2 and regulates virus induced pro-inflammatory responses in host macrophages. *Frontiers in Immunology* (2023) 14: doi: 10.3389/fimmu.2023.1139808.
- # **2. Nayak TK**, Mamidi P, Sahoo SS, Kumar PS, **Mahish C**, Chatterjee S, Subudhi BB,

Chattopadhyay S & Chattopadhyay S. P38 and JNK Mitogen-Activated Protein Kinases Interact with Chikungunya Virus Non-structural Protein-2 and Regulate TNF Induction During Viral Infection in Macrophages. *Frontiers in Immunology* (2019) 10: doi: 10.3389/fimmu.2019.00786.

3. Chatterjee S, Kumar S, Mamidi P, Datey A, Sengupta S, **Mahish C**, Laha E, De S, Keshry SS, Nayak TK, Ghosh S, Singh S, Subudhi BB, Chattopadhyay S & Chattopadhyay S. DNA Damage Response Signaling Is Crucial for Effective Chikungunya Virus Replication. *Journal of Virology* (2022) doi: 10.1128/jvi.01334-2.

4. De S, Ghosh S, Keshry SS, **Mahish C**, Mohapatra C, Guru A, Mamidi P, Datey A, Pani SS, Vasudevan D, Beuria TK, Chattopadhyay S, Subudhi BB & Chattopadhyay S. MBZM-N-IBT, a Novel Small Molecule, Restricts Chikungunya Virus Infection by Targeting nsP2 Protease Activity *In Vitro*, *In Vivo*, and *Ex Vivo*. *Antimicrobial Agents and Chemotherapy* (2022) 66: doi: 10.1128/aac.00463-22.

5. De S, Mamidi P, Ghosh S, Keshry SS, **Mahish C**, Pani SS, Laha E, Ray A, Datey A, Chatterjee S, Singh S, Mukherjee T, Khamaru S, Chattopadhyay S, Subudhi BB & Chattopadhyay S. Telmisartan restricts Chikungunya virus infection *in vitro* and *in vivo* through the AT1/PPAR- γ /MAPKs pathways. *Antimicrobial Agents and Chemotherapy* (2021) doi: 10.1128/AAC.01489-21.

6. Sanjai Kumar P, Nayak TK, **Mahish C**, Sahoo SS, Radhakrishnan A, De S, Datey A, Sahu RP, Goswami C, Chattopadhyay S, & Chattopadhyay S. Inhibition of transient receptor potential vanilloid 1 (TRPV1) channel regulates chikungunya virus infection in macrophages. *Archives of Virology* (2021) 166:139–155. doi: 10.1007/s00705-020-04852-8.

7. Radhakrishnan A[†], Mukherjee T[†], **Mahish C**[†], Kumar PS, Goswami C, Chattopadhyay S. TRPA1 activation and Hsp90 inhibition synergistically downregulate macrophage activation and inflammatory responses *in vitro*. *BMC Immunology* (2023) 24:16. doi: 10.1186/s12865-023-00549-0.

#- Pertaining to thesis

†- Equal contribution for joint first authorship

b. Accepted: NA

c. Communicated: NA

Other Publications:

a. Book/Book Chapter- NA

b. Conference/Symposium

1. **Chandan Mahish**, Tapas Kumar Nayak, Soma Chattopadhyay, Subhasis Chattopadhyay. A poster entitled “*CHIKV Induced TNF Activates T Cells Using p38 And JNK-MAPK Mediated Pathway: A Brief Insight*” was presented in “Functional nucleic acids: Recent landscapes and therapeutic applications”- India | EMBO lecture course- RCB, Aug 16-19th, 2022, Faridabad, India.
2. **Chandan Mahish**, Tapas Kumar Nayak, Soma Chattopadhyay, Subhasis Chattopadhyay. A poster entitled “*The Bridging of Host Innate and Adaptive Immune Responses During Chikungunya Virus Infection: An Outline*” was presented in “Infections, Vaccines & Immuno-Innovations for Human Health”- Indian Immunology Society-BHU, July 8th and 9th, Varanasi, India.
3. **Chandan Mahish**, Tapas Kumar Nayak, Soma Chattopadhyay, Subhasis Chattopadhyay. A poster entitled “*Association of Pro-inflammatory Responses and Cell-Mediated Immune Responses During Chikungunya Virus Infection: An Outline*” was presented at International Conference on Recent Trends in Biotechnology (ICRTB)- Centurion University of Technology and Management, June 22nd & 23rd, 2022 Odisha, India.
4. **Chandan Mahish**, Tapas Kumar Nayak, Puspun Mondol, Priyanshu Singh, Soma Chattopadhyay, Subhasis Chattopadhyay. A poster entitled “*An Immunological Approach Towards DRDE-06 and S 27 Strains of Chikungunya Virus*” was presented in “Emerging and Reemerging viral diseases-Climate change impacts and Mitigations”- Indian Virological Society- AIIMS Bibinagar, March 26-28th, 2022, Hyderabad, Telangana, India. (Published as the conference proceedings in Virus Disease (July-September 2022) 33:338–361 - <https://doi.org/10.1007/s13337-022-00787-7>).
5. Tapas Kumar Nayak, Prabhudutta Mamidi, P Sanjai Kumar, Subhransu S. Sahoo, **Chandan Mahish**, Soma Chattopadhyay Subhasis Chattopadhyay. Participated as a member in the poster presentation entitled “*Modulation of Macrophages during Chikungunya Virus infection*” at “Global viral epidemics: a challenging threat”- Indian Virological Society- PGIMER, Nov 12-14th, 2018, Chandigarh, India. (Published as the conference proceedings in Virus disease (January–March 2019) 30(1):112–169 - <https://doi.org/10.1007/s13337-019-00523-8>).
6. Tapas Kumar Nayak, P Sanjai Kumar, **Chandan Mahish**, Saumya Bandyopadhyay, Soma Chattopadhyay, Subhasis Chattopadhyay. Participated as a member in the presentation entitled “*Analysis of Altered Host Cell Immunity of Macrophages during Chikungunya Virus (CHIKV) Infection, in vitro*” at “International Congress of Cell Biology”- CCMB, Jan 27th -31st, 2018, Hyderabad, India (P217).
7. Attended the hands-on workshop on different virological methods organized by the Indian Virological Society at Nitte University, Deralakatte, Mangalore-575018, India from Dec 10–13th, 2017.
8. Subhransu Sekhar Sahoo, P Sanjai Kumar, Dalai Jupiter Nanda Kishore, Tathagata Mukherjee, **Chandan Mahish**, Soma Chattopadhyay, Chandan Goswami, Subhasis Chattopadhyay. Participated as a member in the presentation entitled “*Functional Expression of Sensory Receptor Channels in Cell-Mediated Immunity Implications in Infection and Tumor Immunity*” (BS-32) at Indian Science Congress, Bhubaneswar chapter- KIIT University, Dec 12th & 13th, 2016, Bhubaneswar, Odisha, India.

Signature of Student:

Chandan Mahish

Date:

*30/05/23***Doctoral Committee:**

S. No.	Name	Designation	Signature	Date
1.	Dr. Chandan Goswami, Associate Professor, SBS, NISER	Chairman	<i>Chandan Goswami</i>	<i>30/05/2023</i>
2.	Dr. Subhasis Chattopadhyay, Associate Professor, SBS, NISER	Guide/ Convener	<i>Subhasis Chattopadhyay</i>	<i>30/05/2023</i>
3.	NA	Co-guide (If any)		
4.	Dr. Asima Bhattacharyya, Associate Professor, SBS, NISER	Member	<i>Asima Bhattacharyya</i>	<i>30.5.2023</i>
5.	Dr. Harapriya Mohapatra, Associate Professor, SBS, NISER	Member	<i>Harapriya Mohapatra</i>	<i>30.05.2023</i>
6.	Dr. Sanjib Kar, Associate Professor, SCS, NISER	Member	<i>Sanjib Kar</i>	<i>30.05.2023</i>

ABBREVIATIONS

7-AAD: 7-Aminoactinomycin D

AF488: Alexa Fluor 488

AF647: Alexa Fluor 647

ANOVA: Analysis of Variance

APC: Allophycocyanin

APC: Antigen Presenting Cells

APS: Ammonium Persulfate

ATP: Adenosine Triphosphate

CD: Cluster of Differentiation

cDNA: complementary DNA

CHIKF: Chikungunya Fever

CHIKV: Chikungunya Virus

CLIP: Class II-associated Invariant Chain Peptide

CMI: Cell Mediated Immunity

CPE: Cytopathic Effect

CTL: Cytotoxic T Lymphocytes

DC: Dendritic Cell

DC-SIGN: Dendritic Cell-Specific Intercellular adhesion molecule-3-Grabbing Non-integrin

DDT: Dithiothreitol

DMEM: Dulbecco's modified Eagle's Medium

DMSO: Dimethyl Sulfoxide

DNA: Deoxyribonucleic Acid

EDTA: Ethylenediaminetetraacetic Acid

EGTA: Ethylene Glycol-bis (β -aminoethyl ether)-N, N, N', N'-tetraacetic Acid

ELISA: Enzyme-Linked Immunosorbent Assay

ER: Endoplasmic Reticulum

ERK: Extracellular-signal-Regulated Kinase

Fab: Fragment Antigen Binding

FACS: Fluorescence-Activated Cell Sorting

FBS: Fetal Bovine Serum

FC analysis: Flow Cytometry analysis

Fc: Fragment Crystallizable

FcR: Fragment Crystallizable Receptor

FSC-A: Forward Scatter-area

GAPDH: Glyceraldehyde 3-phosphate dehydrogenase

GM-CSF: Granulocyte-Macrophage Colony-Stimulating Factor

HLA-DM: Human Leukocyte Antigen DM

hpi: Hours Post Infection

HPLC: High-Performance Liquid Chromatography

HRP: Horseradish Peroxidase

HSCs: Hematopoietic Stem Cells

HSP: Heat Shock Protein

IAEC: Institutional Animal Ethics Committee

ICS: Intracellular Staining

IFN: Interferon

IFN- γ : Interferon- γ

Ig: Immunoglobulin

IgG: Immunoglobulin G

IL: Interleukin

ip: Intraperitoneal

IRF-3: Interferon Regulatory Factor 3

JNK: c-Jun N-terminal Kinase

LPS: Lipopolysaccharide

mAb: monoclonal Antibodies

MALT: Mucus Associated Lymphoid Tissues

MAPK: Mitogen-Activated Protein Kinase

MCP-1: Monocyte Chemoattractant Protein-1

mDC: *Myeloid Dendritic Cell*

MFI: Mean Fluorescence Intensity

MHC: Major Histocompatibility Complex

MIP: Macrophage Inflammatory Proteins

mM: millimolar

MOI: Multiplicity of Infection

MTT: 3-(4,5-dimethylthiazol-2-yl)-2,5-diphenyltetrazolium bromide

M Φ : Macrophage

NK Cell: Natural Killer Cell

NKT cells: Natural Killer T cells

nsP: Non-structural protein

OD: Optical Density

ORF: Open Reading Frame

PAMP: *Pathogen-Associated Molecular Patterns*

pAPCs: Professional Antigen Presenting Cells

PBS: *Phosphate-Buffered Saline*

PCR: Polymerase Chain Reaction

PE: Phycoerythrin

PEC: Peritoneal Exudate Cells

PFA: Paraformaldehyde

PFU: Plaque Forming Units

PHSC: Pluripotent Hematopoietic Stem Cell

PRR: Pattern Recognition Receptor

PVDF: Polyvinylidene Fluoride or Polyvinylidene Difluoride

RA: Rheumatoid Arthritis

RBCs: Red Blood Cells

RIPA: Radio Immunoprecipitation Assay

RLR: Rig-1 like Receptor

RNA: Ribonucleic acid

RNS: Reactive Nitrogen Species

ROS: Reactive Oxygen Species

RPMI-1640: Roswell Park Memorial Institute-1640

RT: Room Temperature

RT-PCR: Reverse Transcription Polymerase Chain Reaction

SAPK: Stress-Activated Protein Kinase

SDS: Sodium Dodecyl Sulphate

SDS-PAGE: Sodium Dodecyl Sulfate Polyacrylamide Gel Electrophoresis

SEM: Standard Error of the Mean

SFM: Serum Free Media

SP: Single Positive

SS: Surface Staining

SSC-A: Side Scatter-area

TAP: Transporters Associated with Antigen Processing

TBS: Tris-Buffered Saline

TBST: Tris-Buffered Saline Tween-20

Tc Cells: Cytotoxic T Cells

TCR: T Cell Receptor

TCR β : T Cell Receptors β

TEMED: Tetra-methyl ethylenediamine

TG: Thioglycolate

TGF- β : Transforming Growth Factor beta

TGS: Tris-Glycine-SDS

T_H Cells: T helper Cells

TLR: Toll-like Receptor

TMB: 3,3',5,5'-Tetramethylbenzidine

TNF: Tumor Necrosis Factor

Tregs: Regulatory T cells

v/v: Volume/Volume

w/v: Weight/Volume

WCL: Whole Cell Lysate

LIST OF FIGURES

Descriptions	Page No.
Figure 1. The cells of the immune system.....	50
Figure 2. Endogenous and exogenous antigen processing and further presentation to T cells...52	
Figure 3. The general structure of an antibody.....	53
Figure 4. T cell-APC interaction.....	56
Figure 5. Cytotoxic T cell responses.....	57
Figure 6. The central dogma scheme.....	58
Figure7. The phylogenetic classification scheme of <i>Alphaviruses</i>	60
Figure 8. The structure of <i>Alphaviral</i> genome.....	61
Figure 9. The different stages of the life cycle of an <i>Alphavirus</i>	62
Figure 10. An illustration depicting macrophage-dependent phagocytosis process to entrap and degrade evading pathogens.....	65
Figure 11. An illustration depicting macrophage-dependent METosis process to entrap and degrade evading pathogens	66
Figure 12. The illustration depicting the pandemic CHIKV transmission in past decades.....	68
Figure13. The modes of CHIKV transmission in human.....	70

Figure 14. Different stages of CHIKV replication in mosquitoes.	71
Figure 15. A schematic illustration of CHIKV non-structural and structural proteins expression.....	72
Figure 16. The domain structure of CHIKV-nsPs.....	73
Figure 17. A schematic representation of the CHIKV E2-E1 heterocomplex.....	75
Figure 18. A schematic illustration of CHIKV entry in the host cell.....	78
Figure 19. A schematic representation of CHIKV-E2-E1-Mxra8 interaction.....	80
Figure 20. Mouse TLR4-MD2-LPS complex in dimerized structure.....	87
Figure 21. TLR4 signaling pathway.....	88
Figure 22. The bi-directional role of TLR4 in cancer.....	90
Figure 23. The cell viability assay using different sources of macrophages to determine the working concentration of TAK-242.....	120
Figure 24. TLR4 expression in mock RAW264.7 cells in the presence or absence of TAK-242.....	121
Figure 25. LPS-driven pro-inflammatory responses in RAW264.7 macrophage cells are regulated in TLR4-dependent way.....	124
Figure 26. TLR4 antagonism reduces the CHIKV-induced proinflammatory responses in RAW264.7 macrophages, <i>in vitro</i>	128
Figure 27. TLR4 antagonism reduces the CHIKV infection and CHIKV-induced TNF level RAW264.7 macrophages, <i>in vitro</i>	130

Figure 28. TLR4 antagonism reduces the CHIKV-induced proinflammatory responses in peritoneal macrophages of BALB/c mice, *in vitro*.....133

Figure 29. TLR4 antagonism reduces the CHIKV-induced proinflammatory responses in peritoneal macrophages of C57BL/6 mice, *in vitro*.....136

Figure 30. TLR4 antagonism reduces the CHIKV-induced proinflammatory responses in hPBMC-derived monocyte-macrophages, *in vitro*.....138

Figure 31. TLR4 antagonism reduces the CHIKV-induced proinflammatory responses in PMA-induced THP-I cells, *in vitro*.....139

Figure 32. The CHIKV infection-induced TNF promotes naïve primary T cell activation, *in vitro*.
.....141

Figure 33. TLR4 antagonism reduces LPS-induced MAPK-activation in RAW264.7 cells...143

Figure 34. TLR4 antagonism reduces the CHIKV-induced MAPK-activation in RAW264.7 macrophages, *in vitro*.....144

Figure 35. The functional TLR4 is essential to promote CHIKV infection in host macrophages.
.....147

Figure 36. The functional TLR4-CHIKV-E2 interaction promotes CHIKV infection in host macrophages, *in vitro*.....149

Figure 37. The functional TLR4-CHIKV-E2 interaction promotes CHIKV infection in host macrophages, *in silico*.....150

Figure 38. Anti-TLR4 antibody-driven blocking of cellular TLR4 reduces CHIKV infection in RAW264.7 cells, *in vitro*.....152

Figure 39. TLR4 regulates CHIKV entry in early stages of viral infection in RAW264.7 cells, *in vitro*.....157

Figure 40. TLR4-antagonims protects and increases survival of CHIKV infected mice, *in vivo*.....159

LIST OF TABLES

Descriptions	Page No.
Table 1. The Baltimore classification of viruses.....	59
Table 2. Different DAMPs and corresponding PRRS-mediated responses in the host.....	64
Table 3. CHIKV replication and structural proteins: An overview.....	76
Table 4. Cells and cell lines of different origins which are susceptible to CHIKV infection..	83
Table 5. Different model systems to study CHIKV infection.....	84
Table 6. Details of the antibodies used	96-98
Table 7. Details of the chemicals used.....	98-101
Table 8. Details of the kits used.....	101-102
Table 9. Details of the primers used.....	102
Table 10. Details of the buffer and other reagents.....	102-103

Chapter# 1

Introduction

and

Review of Literature

1. Introduction

1.1. Introduction to the Immune System

Immunology (**immunis** meaning exempt and **logos** meaning science) is the branch of science that preferentially encompasses the host responses upon foreign or in some rare cases, self-stimuli. Alternatively, a particular host is immune against pathogen X means that the host possesses a counter-regulatory mechanism to neutralize the effect of pathogen X. The immune system comprises two major wings, namely the innate and adaptive immune systems.

1.1.1. The innate immune system

The innate immune system is a non-selective and immediate response of the host against invading foreign immunogens. This particular defense mechanism has been functional in the host since birth and doesn't depend on the previous exposure-based memory response of the host. That's why it is often referred to as the first line of defense of the host. The innate immune system consists of several components,

- **Physical barriers:** It consist of skin and mucus membranes. Most of the microbes cannot penetrate the intact skin. Moreover, the acidic pH, secretory fatty acids, sebum from sebaceous glands, and hydrolytic enzymes such as lysozyme inhibit microbial infection and colonization. Moreover, the presence of mucus membranes and cilia in the respiratory tract entrap the invading microorganisms and finally propel them out of the host.
- **Chemical barriers:** In order to maintain physiological homeostasis, several secretory components such as complement proteins, cationic peptides, acute phase proteins (c-reactive proteins, serum amyloid protein A, and mannose-binding protein), enzymes like lysozyme, defensins and most importantly pattern recognition molecules present over different cells and tissues to promote an immediate non-specific response against invading microbes. A phagocytic engulfment process, namely opsonization is one of the key mechanisms to establish a chemical barrier-mediated innate

immune response. In this process, foreign immunogens bind with several complement proteins or antibodies which make them more prone to macrophage-dependent phagocytosis either by oxygen-dependent killing mechanism (reactive oxygen, and nitrogen species-mediated process) or by oxygen-independent process (lysozyme, defensin, and various hydrolytic enzymes-mediated process).

- **Inflammatory barriers:** Classically, inflammation has been defined by its characteristic symptoms, namely, calor (heat generation), dolor (pain), rubor (redness), tumor (swelling), and in extreme cases, functio leasa (loss of function). Microbial invasion leads to the activation of tissue-resident or circulating macrophages which further promotes the recruitment of neutrophils at the site of infection in a secretory chemokine signaling-dependent manner. Later, other cells such as dendritic cells and monocytes are also recruited to enhance the phagocytic lysis of the pathogen and initiate cell-mediated immune responses. During the process, histamine (secreted by natural killer cells and mast cells upon tissue damage) and kinin (the inactive form is always present in the blood) cause vasodilation and increased capillary permeabilization, therefore the reason for heat generation, pain, redness, and swelling. Moreover, kinin, being a potent nerve stimulator, is the major cause of inflammation-induced pain sensation (35–38).

1.1.2. The adaptive immune system

The adaptive immune system employs a more specific and robust immune response against foreign immunogens although the process takes longer time than innate immune responses. The distinct features of adaptive immune responses are,

- **Specificity:** The adaptive immune response is generated in an epitope-specific manner.
- **Immunologic memory:** A re-exposure of the same epitope gets recognized and results in faster and more profound adaptive immune responses.
- **Diversified responses:** A huge number of epitopes get recognized and specific immune responses are generated.

- **Self/non-self-recognition:** The adaptive immune system can recognize self and non-self-immunogens and therefore, respond in a specific way.

The adaptive immune responses might be active or passive in nature. In the case of active immunity, the host generates specific immune responses against naturally invading foreign immunogens. Whereas, passive immunity deals with the introduction of naturally or artificially generated antibodies or vaccines into the host.

Adaptive immunity has two branches, humoral and cell-mediated immunity. Humoral (humor means fluid) immunity deals with the B cell-mediated antibody-driven responses, whereas, cell-mediated immunity deals with the antigen presentation to T cells by antigen-presenting cells and subsequently, T cell-derived cytokine-driven immune responses to different cells against the immunogen. However, these two interconnected arms together carry the adaptive immune response of the host against a specific immunogen (38,39).

1.1.3. The cells and organs associated with the immune system

The cells of the immune system originate from a common multipotent progenitor, i.e., hematopoietic progenitor cells, which are further classified into two groups, namely, myeloid and lymphoid progenitor cells (**Fig: 1**).

The different cells of myeloid progenitor cells are,

- **Monocyte and Macrophages:** Monocytes are mononuclear phagocytic leucocytes that circulate in the blood stream (around 8 h after origin) during which they proliferate and finally migrate into the tissues where they differentiate into either dendritic cells or macrophages. The macrophages are terminally differentiated forms of monocytes that perform several crucial functions such as phagocytosis, opsonization, and antigen presentation to T cells. Moreover, the macrophages contain several types of receptors associated with antigenic determination, such as complement receptors, pattern recognition receptors, cytokine receptors, Fc γ receptors, etc. Most of the tissue systems contain specialized macrophages such as alveolar macrophages (lung), microglial cells (brain),

Kupffer cells (liver), splenic macrophages (spleen), osteoclasts (bone), and peritoneal macrophages (peritoneal cavity), etc. One of the signature characteristics of macrophages is the secretion of pro-inflammatory cytokines such as interleukin-6,10,12, tumor necrosis factor (TNF)- α , fibroblast growth factor, etc.

- **Dendritic cells:** Dendritic cells can be either myeloid or lymphoid progenitor cells, by origin. These are one type of professional antigen-presenting cells (APC) with constitutive high levels of class-II MHC molecules. There are several types of dendritic cells, for example, Langerhans cells, myeloid dendritic cells, lymphoid dendritic cells, and interstitial dendritic cells. Moreover, another subset, namely, follicular dendritic cells don't express high levels of MHC-II molecules, therefore, don't act as APC. They recognize antigen-antibody complexes via non-specific receptors.

- **Mast cells:** Mast cells originate from bone marrow-derived myeloid progenitor cells. Before residing in tissues, mast cells generally circulate in the blood stream. Mast cell secretes histamine, a mediator of allergic response into the host.

- **Granulocytes:** Granulocytes are polymorphonuclear leukocytes which include neutrophils, eosinophils, and basophils. Neutrophils are the mostly abundant leukocyte (around 60-70% of total cells) in the bloodstream. The circulating neutrophils originate from bone marrow and stay in blood flow for 8-10 days post origin. Then the cells finally migrate into free spaces inside the tissue by a process, namely, extravasation. Eosinophils are primarily effective against protozoan and helminths and produce cationic peptides and reactive oxygen and nitrogen species to promote innate immune responses. Basophils are known to secrete histamine, prostaglandins, leukotrienes, etc. to promote innate immune responses and associated inflammation.

The different cells originate from lymphoid progenitor cells are,

- **Natural killer cells:** Natural killer (NK) cells are an essential component of host innate immune responses. They comprise around 5-10% of the total population of all white blood cells. Although they functionally exhibit similar effects to cytotoxic T cells, i.e., perforin or granzyme-mediated

elimination of foreign immunogens, NK cells are unique in terms of their non-specific killing mechanism. NK cells follow two separate mechanisms for pathogen clearance. Firstly, NK cell receptors recognize the possible target cell in terms of cellular markers such as MHC-I expression. If abnormalities are detected (in the case of cancerous or virus-infected cells), they release anti-microbial chemicals such as perforin and granzyme. The second mechanism is known as antibody-dependent cell-mediated cytotoxicity (ADCC). Here, the foreign immunogens first encounter specific antibody-dependent neutralization which further gets recognized by NK cell markers such as CD16, and subsequently, NK cells release perforin and granzyme for pathogen elimination.

- **B cells:** B cells originate from bone marrow-derived lymphoid progenitor cells and are distributed over lymphoid tissues, lymph nodes, spleen, and bone marrow. This is a single antibody-producing cell; therefore, it possesses a central role in humoral immunity. Moreover, B cells are a type of professional APC and, therefore, act as a bridge between the innate and adaptive immunity of the host.

- **T cells:** T cells originate from bone marrow-derived lymphoid progenitor cells and further get educated at the thymus i.e., maturation of T cells in terms of specific T cell receptor accumulation occurs at the thymus. There are mainly two subsets of T cells, CD4⁺ T helper (T_H) cells and CD8⁺ T effector cells or cytotoxic T (T_C) cells. T cells are responsible for sensing the processed and presented immunogenic components and thereafter, sending cytokine-driven signals to B cells for humoral immune response or may initiate T_C mediated elimination of foreign immunogen. There is also another class of T cells, namely, regulatory T cells are present which is essential to contribute physiological homeostasis in different immunological up/down regulation.

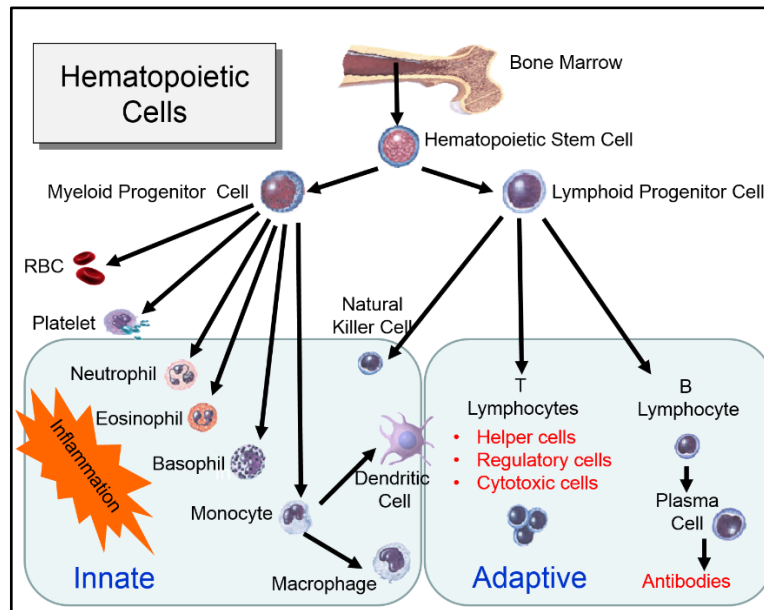


Figure 1: The cells of the immune system (The source of the image: www.sphweb.bumc.bu.edu (40)).

The different organs associated with the immune system are,

- **Thymus:** Thymus is one of the primary lymphoid organs where undifferentiated myeloid progenitor cells migrate and further differentiate and proliferate into mature T cells. Moreover, T cells undergo thymic selection to differentiate self and non-self-antigens. Next, the matured and selected T cells come into the peripheral bloodstream followed by storage at secondary lymphoid organs.
- **Bone marrow:** Bone marrow, a primary lymphoid organ, is the site of the generation of all immune cells from hematopoietic stem cells. Also, bone marrow serves as the site for B cell proliferation and further maturation.
- **Spleen:** Spleen is the largest secondary lymphoid organ where foreign immunogenic elements come via blood circulation and therefore, get entrapped. Moreover, this is the site where antibodies are synthesized and finally approach blood circulation. There are two compartments of the spleen. The red pulp region is often described as the graveyard of red blood cells (RBCs) due to the degeneration

of old and defective RBCs at this site. The white pulp region forms a T cells-enriched layer, namely, periarteriolar lymphoid sheath (PALS). Around 50% of the cells of the spleen are B cells and 34-40% of cells are T cells.

- **Lymph nodes:** Lymph nodes are encapsulated bean-like structures rich in lymphocytes, macrophages and dendritic cells. In response to foreign invasion, the processed immunogens are presented to the T cells at the lymph nodes, and subsequent immune responses are initiated.

- **Mucosa-associated lymphoid tissue (MALT):** This is a specialized secondary lymphoid tissue, present over the lining of respiratory, gastrointestinal, and genitourinary tracts. Tonsil, adenoid, a specialized region in the small intestine, namely, Payer's patch is classified under MALT to initiate immune responses in different local regions of a host (38,39).

1.1.4. Antigen-presenting cells (APCs)

Antigen-presenting cells are a type of specialized immune cells that process and present various antigenic determinants to T cells and therefore, initiate cell-mediated immune responses. There are two classes of APCs, namely, professional APCs and non-professional APCs. Professional APCs such as macrophages, B cells, and dendritic cells are rich in MHC-II molecules and recognize exogenous antigens in MHC-II and other co-stimulatory molecules such as pattern recognition receptor (PRR)-dependent way. Finally, the processed antigens are presented to either T_H or T_C cells. Non-professional APCs such as mast cells, neutrophils, lymphatic endothelial cells, and virus-infected cells present the endogenous antigens via MHC-I dependent way to T_H cells only (38).

1.1.5. Antigen processing and presentation

Based on the origin of the antigens, it can be two types, exogenous and endogenous (**Fig: 2**). The exogenous antigens are processed and presented by professional APCs in a class II MHC-dependent manner. The process starts with the engulfment of exogenous antigens by APCs. The engulfed antigens enter the cytosol entrapped in an early endosome. Next, the recruitment of lysosomes promotes phagolysosome formation and the acidic pH-dependent degradation of the antigen into

smaller parts. On the other hand, a newly formed class II MHC molecule gets vesicle entrapped as well and its binding groove gets covered with a small invariant chain peptide (CLIP: Class II-associated invariant chain peptide) to prevent any premature binding. Once the vesicle with Class II MHC fuses with phagolysosome, acidic pH promotes the removal of CLIP followed by interaction of class II MHC with cleaved antigenic determinants. The newly formed complexes with class II MHC-antigenic determinants are now presented in the cellular membrane to initiate further cell-mediated immune responses.

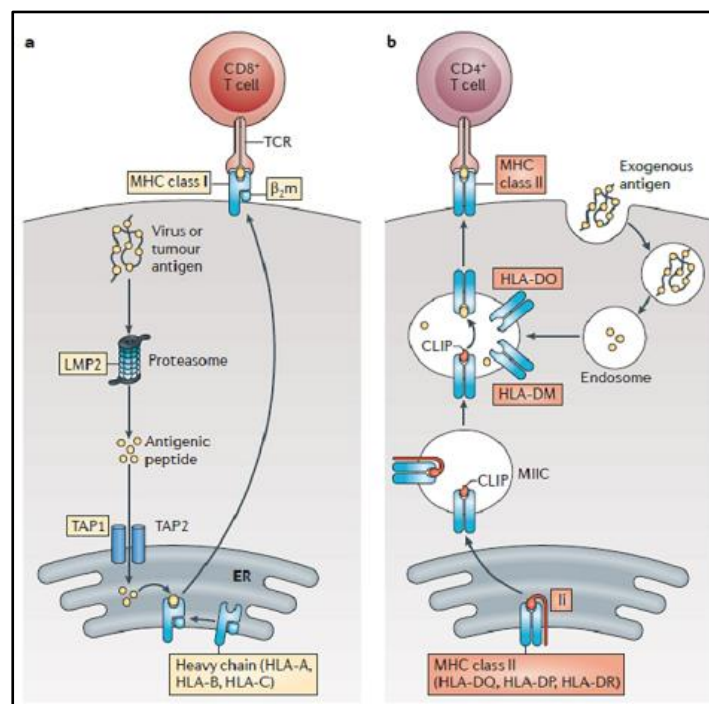


Figure 2: Endogenous and exogenous antigen processing and further presentation to T cells (The source of the image: www.medicalbiochemist.com (41)).

Endogenous antigen processing and presentation is class I MHC molecule dependent. MHC-I is found in all nucleated cells. The endogenous antigens are first ubiquitinated to promote proteasomal degradation. Now, the cleaved antigenic determinants are transported to the endoplasmic reticulum (ER) with the help of a transporter protein, namely, transporters associated with antigen processing (TAP). Now, class I MHC molecules come in the vicinity of TAP-bound antigenic fragments (agretope) with the help of molecular chaperone proteins, such as calnexin, calreticulin, tapasin, and

ERp57. Next, the Class I MHC-antigen complex gets presented over the cell membrane which is further recognized by T_C cells and promotes perforin and granzyme-based immune responses (38,41).

1.1.6. Antibodies

Immunoglobulins or antibodies are soluble glycoproteins secreted by plasma B cells to neutralize specific antigens. They comprise a total of around 20% of all proteins found in blood plasma. Therefore, one of the most abundant proteins with high variability in terms of antigenic determination.

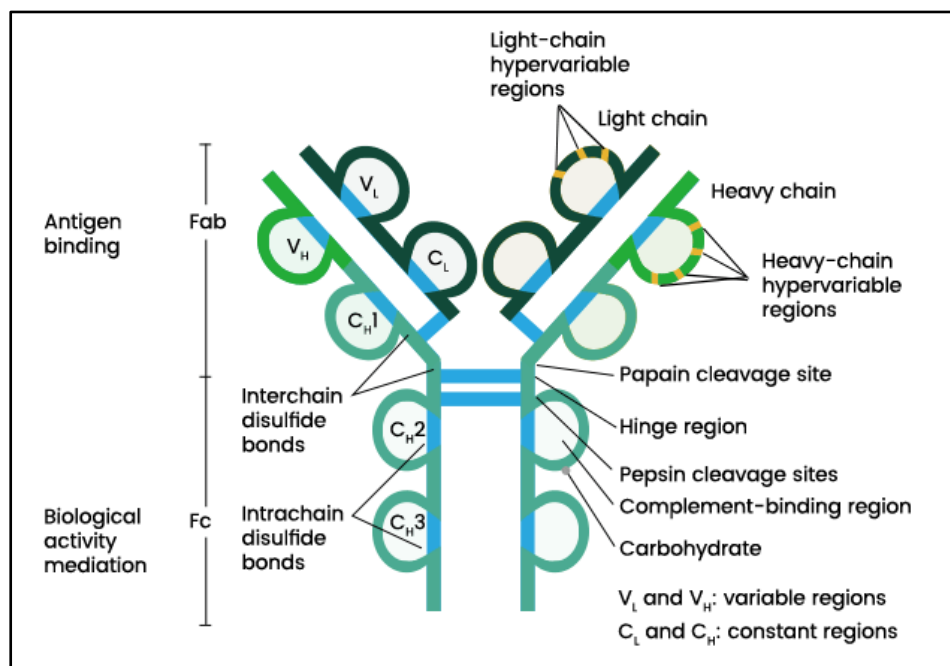


Figure 3: The general structure of an antibody (The source of the image:

www.sinobiological.com (42))

- **Structure of antibodies:** In a simpler way, an antibody is a Y-shaped glycoprotein consisting of two light (**L**) and two heavy (**H**) chains to form a bi-variant assembly (**Fig: 3**). Each light chain is linked to its heavy chain counterpart by di-sulfide and other non-covalent bonds. Therefore, an antibody is simply a dimer of H-L chains. The L chains have two classes, namely, κ and λ . Whereas, the H-chains have five classes, namely, α , γ , δ , ϵ , and μ . In a given antibody molecule, both H and L chains will have the same class variant only although different combinations of H and L chains classes

are found in any individual. Additionally, the α class of the H chain has two sub-classes, namely, $\alpha 1$ and $\alpha 2$, whereas, the γ class has four sub-classes such as $\gamma 1, \gamma 2, \gamma 3, \gamma 4$.

The N-terminal domain of both L and H chains possess a variable region that further is subdivided into hypervariable regions or complementary determining regions (CDR) and residual framework regions. The CDRs are associated with epitope-specific interactions. The constant regions form an F_c domain that has several immunological significances, for example, in ADCC or opsonization process.

Types of the antibodies: Based on the heavy chain diversity, there are five major types of antibodies; IgG (γ), IgD (δ), IgM (μ), IgA (α), and IgE (ϵ). Antibodies of a particular class show around 90% homology in amino acid sequences, whereas, different classes have around 50-60% homology.

- **Function of antibodies:** IgG is the most abundant antibody with the longest half-life of all other types of human antibodies. It can pass through the placenta and may provide immunity to the fetus. IgM is the main antibody that is produced as a primary response against immunogens. Moreover, IgM is the first antibody produced in neonates and it also has the most effective role in generating complement pathway activation and therefore, initiating innate immune responses against invading pathogens. IgA subclass of antibodies is mainly found in the body secretions, such as tears, mother's milk, saliva, and mucus fluid from several organs. IgE promotes hypersensitivity reactions and IgD mainly serves its role on B cell maturation.

In general, antibodies perform various functions against foreign antigens such as opsonization, neutralization of toxins, complement pathway activation, and immune complex, i.e., antigen-antibody complex formation and ADCC.

- **Other soluble factors:** There are various soluble proteins in blood plasma to mediate several immune responses associated with pathogen clearance. For example, liver-derived C reactive proteins

(CRP), complement proteins, NK and T_C-derived perforins and granzymes, basophil and mast cells derived histamines, etc. cover different aspects of innate as well as adaptive immune systems (38).

1.1.7. T cells and cell-mediated immunity (CMI)

T cells are lymphoid progenitor cells that interact with processed immunogens presented over APCs at secondary lymphoid organs to proliferate and differentiate into effector T cells. These effector T cells either move to the site of infection or interact with other immune cells to promote further antibody-mediated neutralization or cytotoxic responses.

- **T cell receptor:** The T cell receptor (TCR) consists of two membrane-embedded glycosylated chains (generally, α and β) connected by disulfide bonds. Each of the chains consists of variable and constant regions. Essentially, the variable chains are the reason for differential immunogenic determination. Moreover, there is another class of TCR available which has γ and δ glycoprotein chains. Functionally, $\alpha\beta$ T cells recognize peptide antigens presented by classical MHC molecules whereas, $\gamma\delta$ T cells recognize phospholipid antigens in MHC independent manner. The co-receptor of TCR is either CD4 (for MHC-II restricted antigens) or CD8 (for MHC-I restricted antigens). TCR molecules along with CD3 are often referred to as T cell receptor complex.

- **Activation of T cells:** The T cell activation followed by proliferation and differentiation of T cells is dependent on two types of immunogenic stimulations by APCs (**Fig: 4**). Signal 1 deals with the interaction of TCR and MHC-immunogenic determinants complex, whereas, signal 2 deals with the interaction of CD28 of T cells and B7 molecule of APCs. The absence of signal 2 results in apoptosis and/or altered immune responses by T cells. Therefore, functional interactions for both signals are necessary for subsequent immunogenic responses. Another two cellular interactions are essential to stabilize the T cell activation. One is intracellular adhesion molecule-1 (ICAM-1) of APC and leucocyte function-associated antigen 1 (LFA or CD11a/CD18) of T cells. Another one is CD2 of T cells and CD58 (LFA-3) of APCs. Activated T_H cells promote secretory cytokines-driven B cell

activation followed by the generation of antigen-specific antibodies. Also, T_H cells may activate T_C cells mediated cytotoxic cell death.

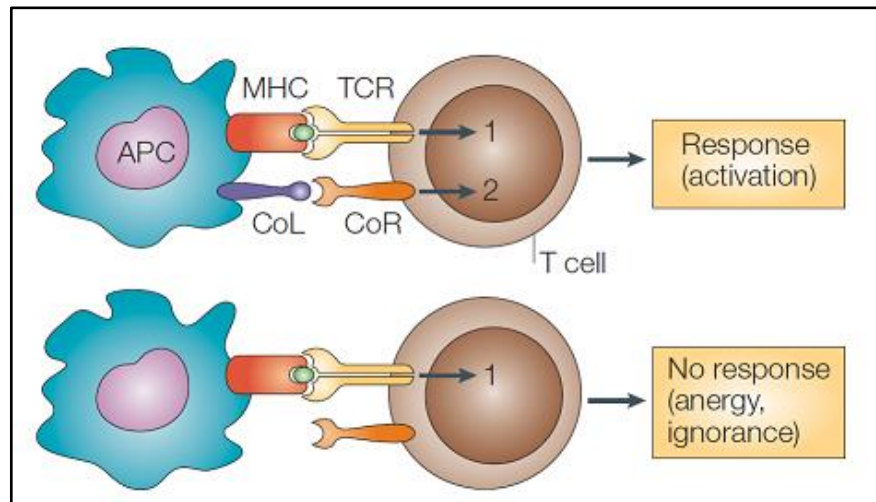


Figure 4: T cell-APC interaction (The source of the image: www.astro.org (43))

- **T_C -mediated cytotoxicity:** Class I MHC-restricted cytotoxic T lymphocyte (CTL) response requires Ca^{2+} ion dependent attachment of CTL and target host cells to promote apoptosis of target cell in mainly two pathways (**Fig: 5**). Firstly, attachment of abnormal host cells promotes the secretion of cytolytic compounds such as perforin, granzymes, etc. by CTLs. Ca^{2+} -dependent polymerization of perforin promotes the formation of transmembrane pores in the target cell. Granzymes, a type of serine protease utilize the pore to enter inside the target cell to imbalance several essential cellular pathways and therefore, the induction of apoptosis. Secondly, the Fas ligand of the CTL also interacts with the Fas receptor of host cells. This interaction promotes the activation Fas receptor-associated death domain and consequently, caspase-8-dependent apoptosis in the target host cells (38).

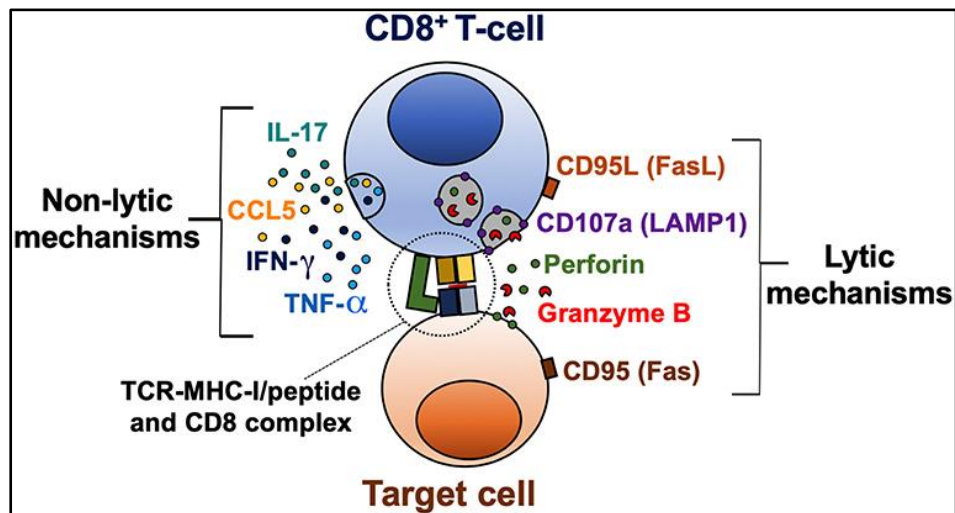


Figure 5: Cytotoxic T-cell responses (The source of the image: *Perdomo-Celis F et al, Frontiers in Immunology, 2019, doi:10.3389/fimmu.2019.01896*).

1.2. An Introduction to The Viruses

The viruses are obligatory intracellular and sub-microscopic infectious agents that infect different types of hosts, like, animals, plants, fungi, bacteria any many others to replicate inside the host modulating host replication machinery. The life cycle of all viruses has two cycles: the **dormant stage**: The virus particle remains outside of the host and is often considered an inanimate object and the **virulent stage**: where the virus enters inside its specific host, replicates inside the host using the host machinery and therefore, forms progenies. The virulent stage of the virus is similar to other living pathogens. Therefore, the virus is considered a living and non-living entity. The genetic material of viruses is covered within a viral protein-based structure namely, capsid. However, the capsid might be further covered with a host cell membrane-derived layer, namely, envelope, depending on a case-to-case basis (44).

organisms. The presence of viroid and infection-mechanism of Hepatitis delta viruses are supportive of this hypothesis (44).

Table 1: The Baltimore classification of viruses (*The image courtesy- Koonin EV et al, Microbiology and Molecular Biology Reviews, 2021, doi: 10.1128/MMBR.00053-21*)

BC	Virion nucleic acid	Genome structure	Genome size (kb)	Genome segmentation	Packaging of components of replication/transcription machineries	Host range
I	dsDNA	Mostly linear	5–2,500	None	No replication, transcription in some	Bacteria and archaea, protists, animals; none in plants, rare in fungi
II	ssDNA	Mostly circular	1.7–25	Mostly non segmented	None	Bacteria, rare in archaea; most eukaryotes
III	dsRNA	linear	4–30	Mostly segmented	All packaged	Protists, animals, plants; one family in bacteria, none in archaea
IV	(+) RNA	linear	3.5–40	Mostly non segmented but many segmented	None	All eukaryotes; one class with six families in bacteria, none in archaea
V	(-) RNA	Mostly linear	1.7–20	Roughly half segmented	Nearly all packaged	Animals, plants, rare in fungi, protists; none in bacteria or archaea
VI	(+) RNA, RT	Linear	5–13	Non segmented	All packaged	All eukaryotes; none in bacteria or archaea
VII	dsDNA, RT	Circular	3–10	Non segmented	Mostly packaged	Animals, plants; unknown in protists; none in bacteria or archaea

In 1971, David Baltimore first summarized all known viruses into different groups based on the replication of nucleic acids to form viral proteins and subsequently matured viruses (**Table: 1**). The Baltimore classification of viruses (B71) was groundbreaking research work at that time as it was a stepping stone for several modern virological researches. For example, the discovery of retroviral reverse transcriptase by Tamin and Baltimore (Nobel prize in Physiology,1975), which was an amendment of the conventional central dogma theory given by Francis Crick (1960), was based on the B71 classification scheme (45,46) (**Fig: 6**).

There is another Gold-standard classification scheme for viruses was proposed in 1962, based on a variety of attributes, most notably morphological characteristics, by the **International Committee**

on **Taxonomy of Viruses** or ICTV. The ICTV classifies viruses into seven orders: *Herpesvirales*, large eukaryotic double-stranded DNA viruses; *Caudovirales*, tailed double-stranded DNA viruses typically infecting bacteria; *Ligamenvirales*, linear double-stranded viruses infecting archaea; *Mononegavirales*, non-segmented negative (or antisense) strand single-stranded RNA viruses of plants and animals; *Nidovirales*, positive (or sense) strand single-stranded RNA viruses of vertebrates; *Picornavirales*, small positive-strand single-stranded RNA viruses infecting plants, insects, and animals; and finally, the *Tymovirales*, monopartite positive single-stranded RNA viruses of plants. In addition to these orders, there are ICTV families, some of which have not been assigned to an ICTV order (47).

1.3. *Alphavirus* and Its Pathobiology

1.3.1. What are the *Alphaviruses*?

Taxonomically, *Alphaviruses* (group IV of the B71 classification system of viruses) are the sole genus of the *Togaviridae* family (**Fig: 7**). The genetic material of *Alphaviruses* is an 11.8 kb long, single-stranded positive-sense RNA, which replicates inside several types of vertebrates as well as invertebrate hosts. Predominantly, *Alphaviruses* infect individuals of a species via mosquitoes. Therefore, this group of viruses is considered arthropod-borne viruses (Arbovirus).

Classification scheme of <i>Alphaviruses</i>	
Unranked	Virus
Realm	<i>Riboviria</i>
Kingdom	<i>Orthornavirae</i>
Phylum	<i>Kitrinovircota</i>
Class	<i>Alsuviricetes</i>
Order	<i>Martellivirales</i>
Family	<i>Togaviridae</i>
Genus	<i>Alphavirus</i>

Figure 7: The phylogenetic classification scheme of *Alphaviruses*. (The image was adapted from

the Taxonomy browser of NCBI (48))

The *Alphavirus* envelope is 70 nm wide with an icosahedral symmetry. The single-stranded positive-sense genomic RNA with a 5' cap and a 3'-poly A tail contains two open reading frames to code replication/non-structural proteins (nsP1-4) and structural proteins (E1-3, capsid, and 6k) (**Fig: 8**).

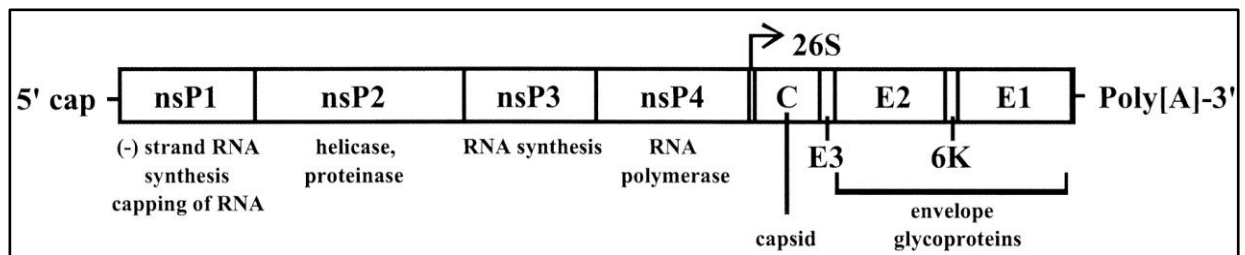


Figure 8: The structure of *Alphaviral* genome (The Image courtesy: *Powers AM et al, Journal of Virology, 2001, doi: 10.1128/jvi.75.21.10118-10131.2001*)

1.3.2. The life cycle of *Alphaviruses*

Alphaviruses contain a single copy of around 11.8 kb positive sense RNA which comes out from the envelope and capsid coat into the host cytosol upon viral entry (**Fig: 9**). Next, the replication-associated proteins nsP1-4 are directly translated into a polyprotein complex. nsP4 is the first protein that is cleaved from the polyprotein unit and acts as an RNA-dependent RNA polymerase to synthesize a sub-genomic RNA from the 3' end of the genomic RNA. This sub-genomic RNA is further translated into structural proteins i.e., E1-3, capsid, and 6k protein. For non-structural proteins, the cleavage between nsP3 and nsP4 of the polyprotein complex occurs in a *cis* position which favors the formation of an unstable replication complex. Next, the cleavage between nsP1 and nsP23 occurs at the *trans* position subject to the availability of a high concentration of the polyprotein complex. All of the products i.e., nsP1, nsP23, and nsP4 stay with virus-induced cytopathic vacuoles (CPV1) and

are designed to synthesize only the negative strand from viral genomic RNA. The cleavage of nsP23 to form functional nsP2 and nsP3 is the rate-limiting step of the viral replication. All processed replication proteins finally form the stable replication complex and therefore, can synthesize positive-strand genomic and sub-genomic RNA (49–51).

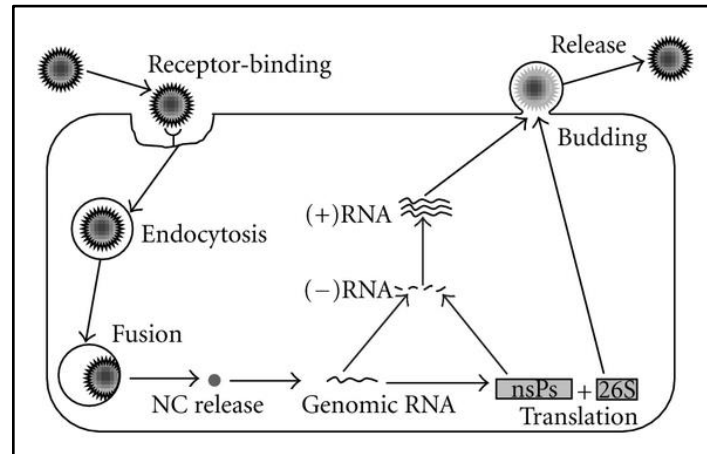


Figure 9: The different stages of the life cycle of an *Alphavirus* (The source of the image: *Leung JS et al, Advances in Virology, doi: 10.1155/2011/249640*)

1.3.3. Disease manifestation, and possible remedy to date.

Out of the total 32 members, there are many *Alphaviruses* such as Chikungunya virus, Barmah Forest virus, Mayaro virus, Ross River virus, O’nyong’nyong virus, Tonate virus, Una virus, and Western equine encephalitis virus predominantly infect human and other mammals and therefore, promote massive pro-inflammatory cytokine release in the host. The common disease symptoms are high fever, body aches, joint pain, rashes, myalgia, and viremia-induced encephalitis in some cases. There is no specific vaccine or direct therapy available for *Alphavirus* infections to date. However, several vaccine-based drugs are already in the trial phase for certain *Alphaviruses*, for example, CHIKV. Moreover, gene therapy-based medications are currently under research and development for the Sindbis virus, Ross River virus (RRV), Venezuelan equine encephalitis virus (VEEV), and

Semliki Forest virus (SFV).

1.4. Role of PRRs in Different Microbial Infections: A Gateway Strategy

In 1989, Dr. C.A. Janeway, one of the pioneering scientists in the field of modern innate immunological research, first predicted the presence of a specific type of receptors over the immune cells associated with early non-specific recognition of pathogens followed by prompt clearance and also the presentation of antigenic determinants to T cells. A Nobel prize-winning research work (2011) on Toll-like receptors and other contemporary research finally proved his unparalleled vision of these receptors, which are now collectively called pattern recognition receptors (PRRs) (52,53).

The immune cells associated with PRRs predominantly serve as an essential tool of host innate immune responses. PRRs mainly identify some conserved structures present over microbial outer surfaces, namely, pathogen-associated molecular patterns (PAMPs) or secreted or lysed cellular components from stressed cells, namely, damage-associated molecular patterns (DAMPs) and therefore, employ inflammation in the host immune system (**Table: 2**). Depending on their, localization and PAMP they recognize, PRRs are mainly divided into four exclusive groups, namely, toll-like receptors (TLRs), retinoic acid-inducible gene 1-like receptors (RLRs), the leucine-repeat-rich nucleotide-binding oligomerization domain (NOD)- containing receptors (NLRs) and C-type lectin-like receptors (CLRs). These PRRs induce several prompt microbicidal activities such as induction of apoptosis in the infected cells, promotion of pro-inflammatory cytokines secretion, and activation of nearby immune cells of the infected cells/ tissue via the paracrine signaling mechanism. Moreover, PRRs are present in invading microbial antigens to the T cells to promote adaptive immune responses (52–54).

Table 2: Different DAMPs and corresponding PRRS-mediated responses in the host. (The source of the image: *Amarante-Mendes et al, Frontiers in Immunology, 2018, doi-10.3389/fimmu.2018.02379*)

DAMPs	Immunogenic function	Receptors	Related cell death
Adenosine triphosphate (ATP)	DC and M ϕ activation Inflammasome activation	P2Y2,6,12, P2X1,3,7 NLRP3	Apoptosis Pyroptosis Necroptosis NCD
Annexin A1 (ANXA1)	"Eat me" signal Immunogenicity	FPR1	Apoptosis
ASC specks	Lysosomal damage IL-1 β activation	unknown	Pyroptosis
Calreticulin	"Eat me signal" Immunogenicity	CD91	Apoptosis
Cyclophilin A	Cytokine induction	CD147	Necroptosis NCD
Defensin α	Antimicrobial Anti-inflammatory	CCR2, CCR6, TLR4	Apoptosis NCD
Heat shock proteins (HSPs)	Monocytes and neutrophils attraction DC maturation	CD91, TLR2, TLR4, SREC1 and FEEL1	Necroptosis NCD
HMGB1	DCs and M ϕ activation Cytokine activation	CXCR4, RAGE, TLR2,4,9	Apoptosis Necroptosis Pyroptosis
HMGN1	Leukocyte recruitment DC maturation	TLR4	Necroptosis NCD
IL-1 α	DC and M ϕ activation Cytokine induction	IL-1R	Necroptosis Pyroptosis NCD
IL-33	Cytokine induction DC activation	ST2	Necroptosis NCD
IL-6	Immune responses T cell differentiation	IL6R and GP130	Necroptosis NCD
Lysophosphatidylcholine (LPC)	Monocyte and M ϕ recruitment DC maturation "Eat me" signal	G2A	Apoptosis
Mitochondrial DNA (mtDNA)	M ϕ activation PMNs activation NLRP3 activation	TLR9	Necroptosis Pyroptosis
N-formyl peptides (NFP)	PMNs activation Monocyte activation	FPR1	NCD
Nucleic acids (dsDNA/dsRNA)	DC activation Inflammasome activation Cytokine induction	TLR3, TLR7/8, TLR9, AIM2	Apoptosis Necroptosis Pyroptosis NCD
Peroxiredoxin 1 (Prx1)	Cytokine induction CD maturation	TLR4	NCD
S100	Leukocyte recruitment Cytokine induction	RAGE, TLR4	Necroptosis NCD
SAP130	M ϕ activation Neutrophil recruitment Cytokine induction	Mincle	Necroptosis NCD
Uric acid	DC activation Inflammasome activation	P2X7, NLRP3	NCD

1.5. Macrophage-dependent Microbial Elimination: A Salient Innate Immune Response

Macrophages play a crucial role in promoting initial nonspecific host immune responses against invading microorganisms. Generally, macrophages follow three different types of mechanisms to

establish a quick onset of innate immune responses. The first one is **phagocytosis** (Phagos means engulfment; Cytos means cells) (**Fig: 10**). To locate the invading microbes or phagocytic targets, macrophages extend their actin-rich dendrites (a protrusion of cells that may or may not have a branched structure) in the nearby extracellular surfaces. Next, macrophages interact with the pathogen/damage-associated molecular patterns (PAMPs or DAMPs: a conserved structural component of microbes) via several types of pattern recognition receptors (PRR) like TLRs, NLRs, CLRs, RLRs, and cytoplasmic-ds DNA receptors. Next, a successful receptor-ligand interaction facilitates membrane remodeling followed by engulfment of the target inside a vesicular structure (nascent endosome/phagosome). The nascent phagosome undergoes Rab-5 (a GTPase)-directed phagosome remodeling (early phagosome) followed by Rab-remodeling where Rab-7 (Another GTPase and a lysosomal marker) gets recruited in place of Rab-5 to promote lysosomal fusion to form phagolysosome/ late phagosome. The successive stages also gradually decrease the vesicular pH towards a more acidic end. The acidic nature of phagolysosome (pH~ 5.5) activates several proteases, lipases, nucleases, phosphatases, and glycosidases along with reactive nitrogen and oxygens catalyzed by NADPH oxidase (Nox2) and oxidase synthase 2, respectively, to degrade the engulfed microorganism/s (55,56).

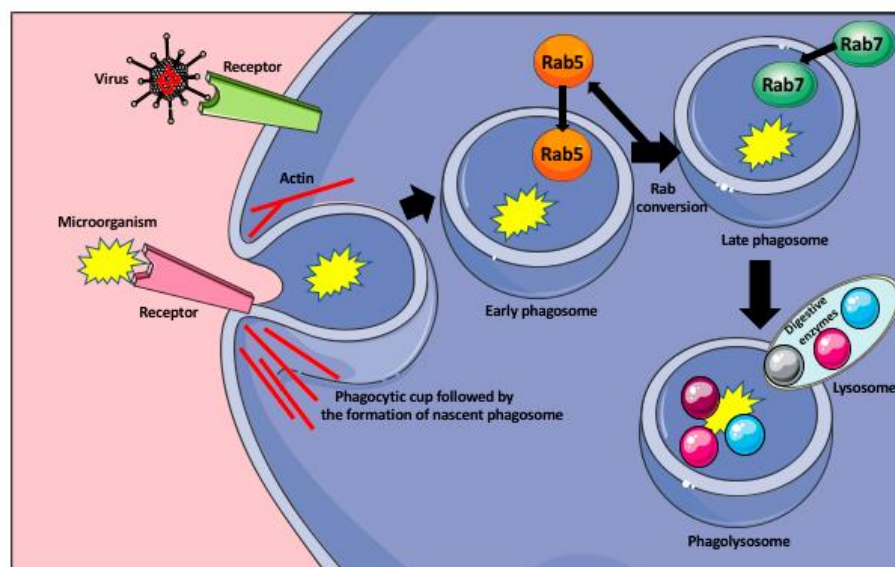


Figure 10: An illustration depicting macrophage-dependent phagocytosis process to entrap and degrade evading pathogens (The courtesy of the image: *Kloc M et al, Int. J. Mol. Sc, 2020, doi: 10.3390/ijms21249669*).

Secondly, the macrophages are known to sequester some minerals, for example, iron and manganese ions through a process called, **nutritional immunity**. Natural resistance-associated macrophage protein 1 (NRAMP-1) is found at the phagosome and it catalyzes the export of Fe and Mn ions from the phagosomal lumen to the cytosol. The exported ions are further delivered to the storage proteins at cytosol, such as ferritin and calprotectin in the chaperone-dependent way (55,56).

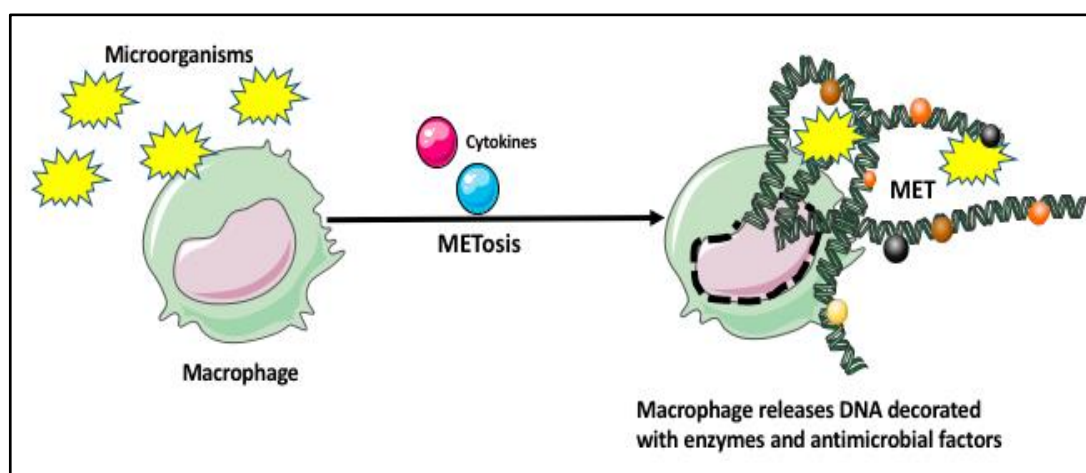


Figure 11: An illustration depicting macrophage-dependent METosis process to entrap and degrade evading pathogens (The courtesy of the image: *Kloc M et al, Int. J. Mol. Sc, 2020, doi: 10.3390/ijms21249669*).

Third and lastly, macrophages as well as granulocytes and mast cells have recently been found to form an extracellular trap as a sensory response against microorganisms and/or elevated cytokine

levels. This macrophage extracellular traps (MET) induce breakage of the nuclear envelope and therefore release of ds DNA decorated with different metalloproteinases, lysozymes, myeloperoxidases, lactoferrin, elastases, hypercitrullinated histones and different antimicrobial peptides to promote a unique cell death mechanism, **METosis (Fig: 11)**. This mechanism also stimulates neighboring macrophages and immune cells to recognize MET and release pro-inflammatory cytokines release (55–59).

Besides the non-specific innate Immune responses, macrophages also present the phagocytosed foreign antigens to the T cells via MHC-II mediated way to initiate an antigen-specific cell-mediated immune response. Therefore, the macrophages have a bi-directional role in balancing host innate and adaptive immune responses against invading microorganisms (55,57,60,61).

2. Review of Literature

2.1. The Clinical, Pathobiological and Epidemiological Severity of Chikungunya Virus (CHIKV) in human: A Brief Overview

2.1.1. A historical perspective of Chikungunya

Chikungunya virus (CHIKV), one of the major arthritogenic arbovirus (Genus: *Alphavirus* within the *Togaviridae* family), has been considered one of the potent epidemic threats across the globe, specifically in densely populated tropical and sub-tropical countries with inappropriate mosquito control strategies and hygiene. The CHIKV was isolated and characterized from Tanzania, east Africa in 1952 for the very first time. Later, CHIKV has shown repeated outbreaks throughout the world in past decades (62) (**Fig: 12**). A total of approximately 110 countries in Asia, Europe, Africa, and America have been affected by the disease severity (63). The most severe outbreaks were documented in 1967 in Thailand (the first reported urban outbreak), 1970 in India, and 2005-06 at La Reunion Island in the Indian ocean, Italy, and the USA (2007) (64–67). As per the latest report by European Center for Disease control and Prevention, a total of 214317 cases were listed in 2023, mostly from Brazil, Paraguay, Argentina, Bolivia and Thailand (68).

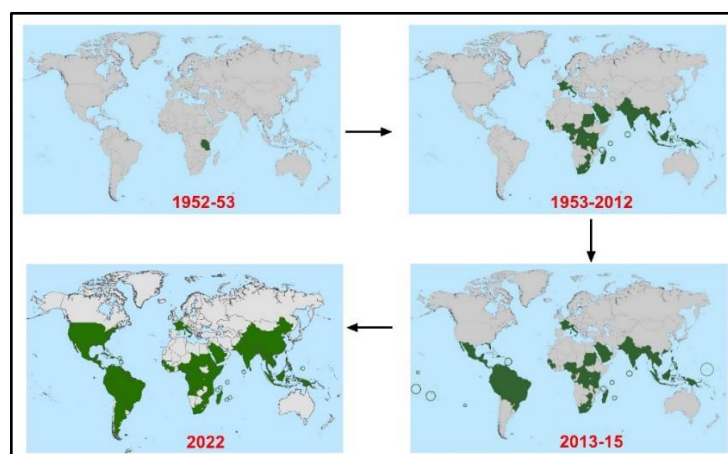


Figure 12: The illustration depicts the pandemic CHIKV transmission in past decades

(Courtesy:Centers for Disease Control and Prevention report;www.cdc.gov/chikungunya/geo/index.html).

2.1.2. Symptoms

The clinical symptoms of CHIKV infection are quite similar to Zika and dengue fever, although CHIKV-induced host immune responses have several characteristic aspects. A latency period of 3-7 days for viral replication and propagation into different host tissues before disease onset has been reported after CHIKV infection. The overall symptoms of CHIKV infection can be classified into three stages namely, acute, sub-acute, and chronic stages. The acute stage of infection has symptoms like high fever, body ache, severe joint pain, nausea, vomiting, loss of appetite and head ache. For the sub-acute stage of infection, these symptoms may last for approximately 3-5 months. The chronic stage of CHIKV infection is quite lethal in neonates and people with ages over 65 years, patients suffering from co-morbidity and during pregnancy. The major symptoms are chronic polyarthralgia, myalgia, severe joint swelling due to cytokine burst (a massive production of pro-inflammatory cytokines), long term fatigue which ultimately may lead to cardio-vascular, renal, ocular, neuronal, or respiratory system failure (1,2,69).

2.1.3. Mode of infection

The CHIKV is a mosquito-borne disease. Mainly, *Aedes aegypti* and *Aedes albopictus* are the prime vectors for CHIKV transmission in humans. Also, there are some lesser common modes of transmission such as intra-uterine, intrapartum, needlestick injury, and laboratory exposure of the virus due to mishandling or accidental cases (**Fig: 13**).

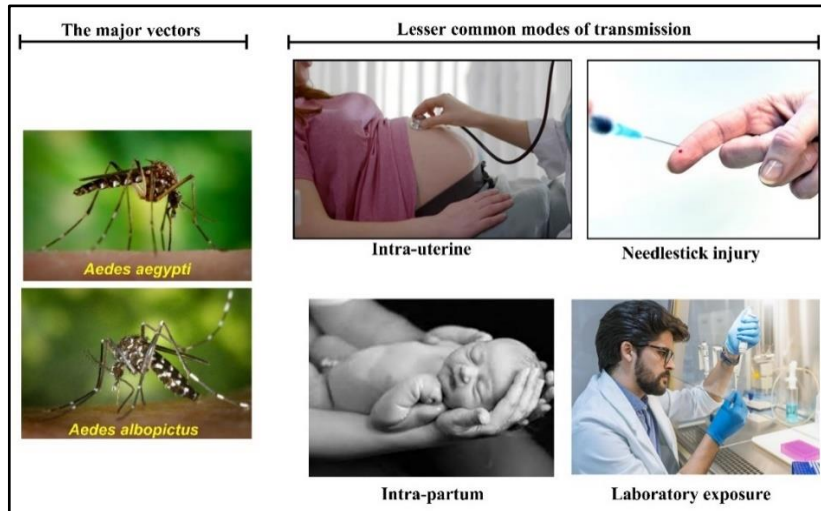


Figure 13: The modes of CHIKV transmission in humans (Courtesy: Study report of National Center for Emerging and Zoonotic Infectious Diseases).

2.1.4. Vector-CHIKV interaction

CHIKV transmission can be classified into two distinct but interconnected cyclic stages: the sylvatic and urban cycle. The forest-dwelling *Aedes* mosquitoes and non-human primates participate in a classical sylvatic cycle which may result in discrete small outbreaks of Chikungunya. Whereas, for the urban cycle, CHIKV gets transmitted from an infected to an uninfected human individual with the aid of *Aedes aegypti* or *Aedes albopictus*. Existing literature suggests that a point mutation in the CHIKV-E1 gene (A226V) of the ESCA strain plays a dominant role in more severe infection and subsequent transmission by the above-mentioned species of mosquitos (70,71).

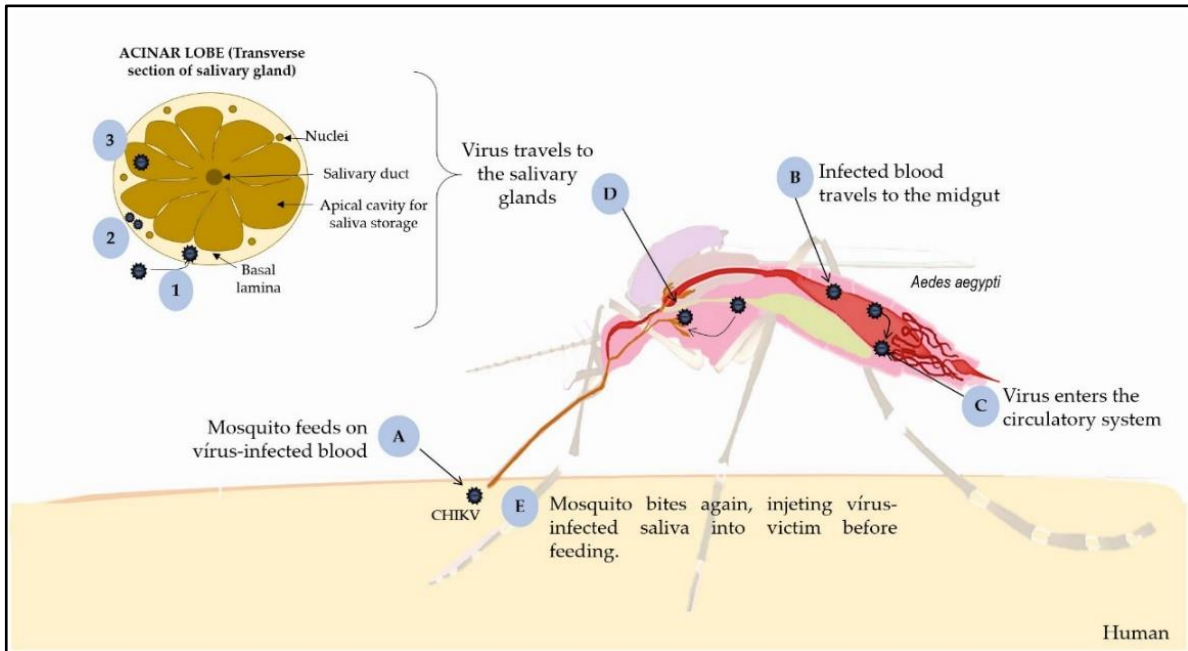


Figure 14: Different stages of CHIKV replication in mosquitoes. (A) The mosquito bite results in the entrance of CHIKV from the infected human. CHIKV stays in a latent period in this stage for 3-7 days. (B) The mid-gut cells of the mosquito get infected with CHIKV. (C) CHIKV transmission to hemocoel and other organs like (D) salivary gland: 1. Penetration of the virus to the basal lamina of the salivary gland surrounding the acinar cells, 2. Viral replication in, 3. Deposition of CHIKV particles in the apical portion. (E) the storage of mosquito saliva before feeding (The source of the image: *Monteiro VVS et al, Frontiers in Microbiology, 2019, doi: 10.3389/fmicb.2019.00492*).

The transmission of CHIKV into a mosquito is through two different ways: horizontal transmission, where a female *Aedes* mosquito gets blood-derived CHIKV from an infected human, and vertical transmission, where the mosquito eggs of an infected mother get infected with CHIKV and therefore, progenies become an auto-choice carrier of the virus. Following entry into a mosquito, CHIKV initially infects the mid-gut cells followed by dissemination into the hemocoel and salivary gland (extrinsic incubation). CHIKV replicates inside the basal lamina of acinar cells and finally

matured viruses are stored at the apical surface of the salivary gland, where mosquitoes store their saliva before biting (72–74).

2.1.5. Genomic structure

The genomic structure of CHIKV consists of a single 11.8 kb long positive sense RNA. The internalization of CHIKV particles into the host cells manipulates host cell replication machinery to synthesize two viral protein precursor complexes namely, viral non-structural proteins and structural proteins (essential to form the virus structure and facilitate host cell attachment and entry) (**Fig: 15**). Next, the proteolytic cleavage mechanism of the host finally generates the functional non-structural proteins (nsPs) namely, nsP1,2, 3 and 4, which are essential for viral replication inside the host cell and structural proteins namely, capsid, envelope (E)1,2,3 and 6K proteins, which are essential to construct the viral structure, promote attachment and entry processes into the host (75,76) (**Table:3**).

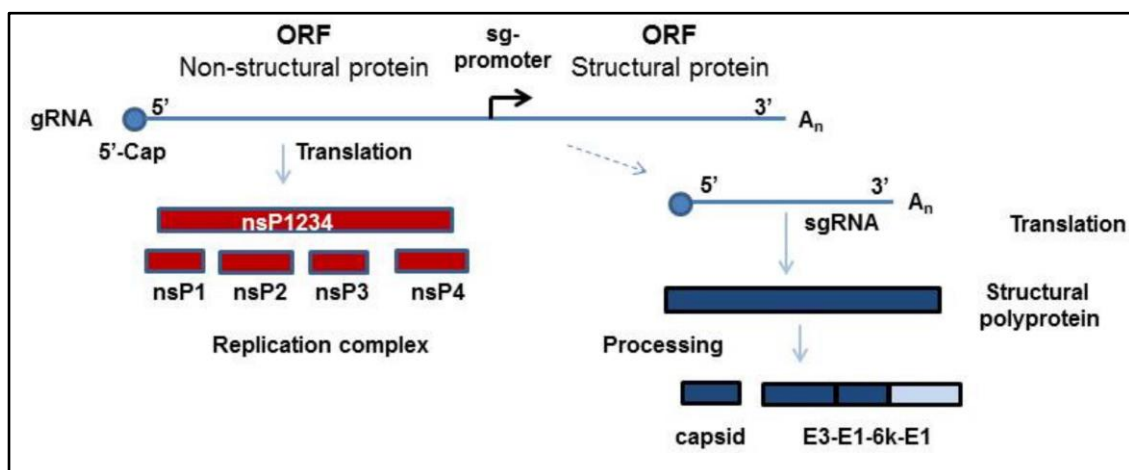


Figure 15: A schematic illustration depicting the expression of CHIKV non-structural and structural proteins. The non-structural proteins (nsPs) are processed from genomic RNA (gRNA), whereas, the structural proteins are processed from sub-genomic RNA (sgRNA) synthesized from the minus strand of genomic RNA. (The source of the image: *Schnierle BS et al, viruses, 2019, doi: 10.3390/v11111078*).

The non-structural or viral replication-associated proteins are major key regulators of viral replication, immune evasion mechanism/s and interaction with host factors. These proteins, encoded at the 5' end of the viral genome, are immediately translated after the entry of viral genomic RNA at the host cytoplasm to facilitate the viral replication process (77) (**Fig: 16**).

The CHIKV-nsP1 protein has been reported to catalyze the 5' capping of genomic and sub-genomic viral RNA (78). The sequence analysis and prediction studies reveal that CHIKV-nsP1 is around 400 amino acid residues long, where amino acids, namely, histidine 37 (H37), aspartate 89 (D89) arginine 92 (R92), and tyrosine 248 (Y248) are conserved throughout the *Alphavirus* superfamily. H37 is thought to act as the covalent binding site of m⁷GMP, whereas D89 binds with the methyl group donor S-Adenosyl-methionine (SAM/ AdoMet). R92 and Y248 contribute to the methyltransferase activity. nsP1 of the CHIKV replication complex interacts with the membrane in a monotopic fashion due to having a palmitoyl moiety (77–80).

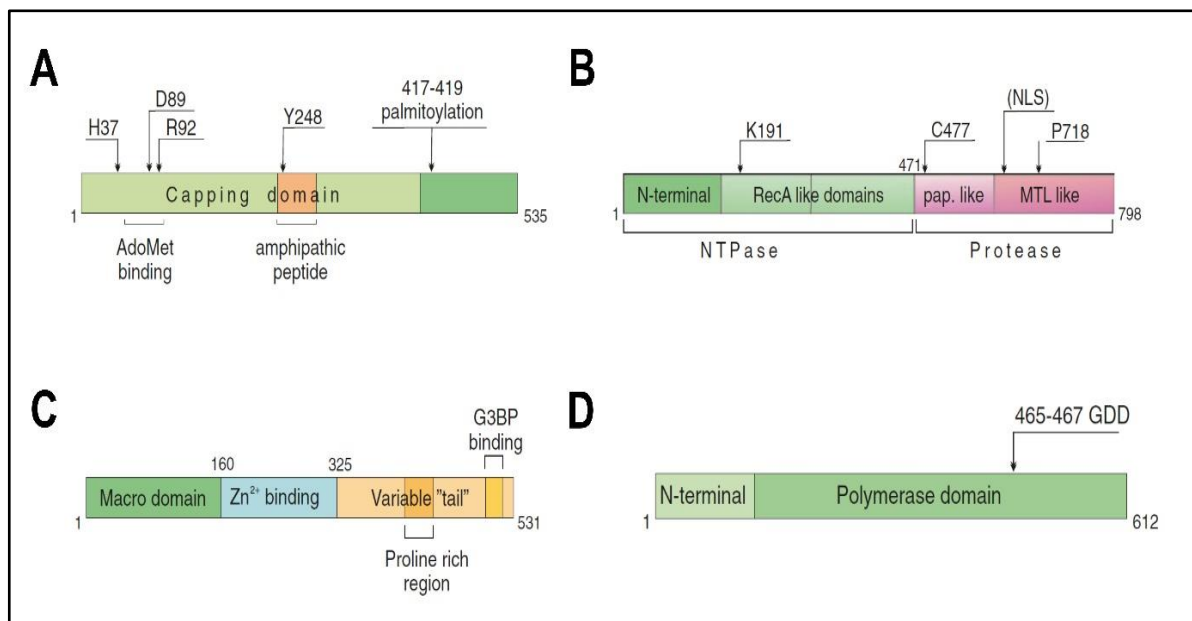


Figure 16: The domain structure of CHIKV-nsPs. The domain structure of (A) nsP1 (B) nsP2 (C) nsP3 and (D) nsP4 were depicted. The conserved residues of different domains were pointed. (The source of the image: *Ahola T et al, Springer Nature, 2016, doi: 10.1007/978-3-319-42958-8_6*)

The CHIKV-nsP2 is a multidomain protein with around 800 amino acids long. It has mainly

two functions, NTPase activity where the N-terminal domain and Rec A domains form the functional unit. The second is, protease activity (nsP2 is a papain-like-Cys protease) where a papain-like domain and an Ftsj methyltransferase-like (MTL) domain forms the core structure. Despite having a methyltransferase domain at the C-terminal, CHIKV-nsP2 does not possess any methyltransferase activity due to having conformational deformity(77,81).

The CHIKV-nsP3 is around 531 amino acid long protein which consists of an N-terminal macro domain, a Zn^{2+} binding domain, and a C terminal proline rich variable tail domain. The macro domain acts as mono-ADP-ribosyl hydrolase which removes the mono or poly-ADP ribose from post-translationally modified proteins of host cells as well as may bind to RNA containing its substrate analog, ADP-ribose-1" phosphate to cleave it. The next macrodomain is a small globular region, where the binding of a Zn^{2+} ion coordinated by four cysteines promotes viral replication. The detailed role of the Zn^{2+} binding domain is yet to come to light to date. The C terminus variable tail region domain consists of heavily phosphorylated serine and threonine residues which promote variable interaction with different host factors. The proline-rich region interacts with host amphiphysin 1 and 2 to induce the formation of membrane replication spherule (77,82–84)

The CHIKV-nsP4 is around 612 amino acids long RNA-dependent RNA polymerase and the C terminal end also has a terminal adenylyl transferase activity to promote poly(A) tailing of positive-stranded RNAs in template independent manner (85,86). The presence of an in-frame terminator codon upstream of the nsP4 coding region and rapid proteasomal degradation make CHIKV-nsP4 the least abundant viral protein inside the host cells (87). The α subunit of heat shock protein 90 and CHIKV-nsP4 is crucial to construct the CHIKV replication complex (88).

The CHIKV-E1 protein, a type II membrane protein, consists of 3 β -barrel domains. The domain II is anchored with the fusion peptide at the distal end and domain I is present in between domain II and III. Together, CHIKV-E1 and E2 form the heterodimer where E1 along with the fusion peptide promotes fusion with the host cell membrane and E2 acts as the regulator of the fusion process.

This heterodimer further forms a trimeric structure on the virus surface which is known as the spike (75,76) (**Fig: 17**).

The CHIKV-E2 protein, a member of the immunoglobulin (Ig) superfamily, has been predicted as one of the major attachment and entry factors into the host cells due to its interaction with the neutralizing antibodies. The CHIKV-E2 consists of three Ig domains. Domain A is present at the center, Domain B is present just below the spike and Domain C is oriented towards the membrane. A long β -ribbon connects all three domains keeping Domain B at the top most surface. The structure prediction studies revealed that E2-Domain A resides at the top of the spike with a three-layered contact and E2-Domain B occupies the side space, therefore, contributing to the propeller-like shape of the spike. The epitope mapping of CHIKV-neutralizing monoclonal antibodies reveals that Domain B along with the acid-sensitive regions (ASRs) present over neighbouring β -ribbon connector serve as one of the major epitopes of CHIKV (75,76,89). As per the structural prediction studies on the CHIKV entry mechanism, Domain B and the associated ASRs of the E2-E1 heterodimer rearrange to expose the fusion peptide of E1 protein at low pH to facilitate viral entry into host cells (75,76).

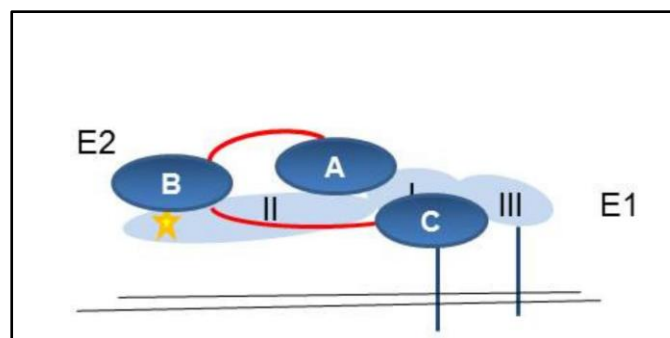


Figure 17: A schematic representation of the CHIKV E2-E1 heterocomplex. E2 (dark blue) interacts with E1 (light blue) via a fusion peptide (yellow). The β ribbon connectors assemble the three domains of the E2 protein (The source of the image: *Schnierle BS et al, viruses, 2019, doi: 10.3390/v11111078*).

CHIKV-E2 and E3 proteins are processed from a common precursor polypeptide, p62 at

trans-Golgi apparatus by Furin-mediated proteolytic cleavage. The functional CHIKV-E3 may be associated with E2 by electrostatic interactions until the release of the matured virion from the host cell (76).

Table 3: CHIKV replication and structural proteins: An overview (The source of the table: *Constant LC et al, Frontiers in Microbiology, 2021, doi:10.3389/fmicb.2021.744164*)

Protein	Length (aa)	Functions and characteristics	Function by domain	Pest-translational modification	References
nsP1	535	<ul style="list-style-type: none"> Membrane anchor for replication complex Capping viral RNA Association with lipid-rafts Affinity with cholesterol 	<ul style="list-style-type: none"> N-terminal: methyltransferase (MTase) and guanylyl transferase (GTase) Intermediary: membrane binding domain (MB) C-terminal: D3 domain 	Palmitoylated	Lampio et al.,2000; Rana et al.,2014; Feibelman et al.,2018; Zhang N. et al.,2019; Bakhache et al.,2020; Gotipati et al.,2020
nsP2	798	<ul style="list-style-type: none"> Essential for capping process Nonstructural polyprotein cleavage Shut-off host transcription and translation Localized in both cytoplasm and cell nucleus Repression of host antiviral response 	<ul style="list-style-type: none"> N-terminal: helicase, nucleoside-triphosphatase (NTPase) and RNA-triphosphatase (RTPase) C-terminal: cysteine protease and methyltransferase-like 	Gluthathionylated	Peränen et al.,1990; Pastorino et al., 2008; Karpe et al.,2011; Das et al.,2014; Rana et al.,2014; Stapleford et al.,2015; Rausalu et al.,2016; Saisawang et al.,2017; Göertz et al.,2018; Meshram et al.,2019
nsP3	530	<ul style="list-style-type: none"> Contribution to viral genome replication Contribution to virus assembly Binding to ADP-ribose ADP-ribosyl hydrolase activity Interaction with host factors 	<ul style="list-style-type: none"> N-terminal: macrodomain Intermediary: alphavirus unique domain (AUD) C-terminal: hypervariable domain 	Phosphorylated	Li et al.,1990; Vihinen et al.,2001; Dé et al.,2003; Fros et al.,2012; McPherson et al.,2017; Remenyi et al.,2017; Agback et al.,2019; Gao et al., 2019; Shimizu et al.,2020
nsP4	611	<ul style="list-style-type: none"> Responsible for viral RNA synthesis Terminal adenylyl transferase (TdT) activity 	<ul style="list-style-type: none"> N-terminal: disordered region C-terminal: RNA-dependent RNA polymerase (RdRp) 		Tomar et al.,2006; Rubach et al.,2009; Rupp et al.,2011; Rathore et al.,2013, 2014; Chen et al.,2017
C	261	<ul style="list-style-type: none"> Nucleocapsid assembly Initiation of virus budding process Self-cleavage Cytoplasm localization Contains nuclear localization signals (NLS) 	<ul style="list-style-type: none"> N-terminal: RNA binding domain C-terminal: serine protease domain 		Hong et al.,2006; Thomas et al.,2010,2013; Sharma et al.,2018
pE2 (or p62)	487	<ul style="list-style-type: none"> E2-E3 precursor Cleaved by host furin Contains signal peptide sequence for transportation of nsP1234 to ER 		Glycosylated	Strauss and Strauss,1994; Singh A. et al.,2018
E1	439	<ul style="list-style-type: none"> Major envelope protein Interaction with E2 to form spike-like structure Contains the fusion loop Target of neutralizing antibodies 	<ul style="list-style-type: none"> Domain I Domain II: type II fusion class Domain III: Ig-like domain Transmembrane domain: type I integral membrane 	Glycosylated	Metz et al.,2011; Sanchez-San Martin et al.,2013; Masrinoul et al.,2014
E2	423	<ul style="list-style-type: none"> Major envelope protein Interaction with E1 to form spike-like structure Main target of neutralizing antibodies E3 	<ul style="list-style-type: none"> Domain A: receptor binding Domain B: receptor binding Domain C Subdomain D: stem region 	Glycosylated	Glasgow et al.,1991; Metz et al.,2011; Silva et al.,2014; Weber et al.,2017; Holmes et al.,2020; Kumar et al.,2020
	64	<ul style="list-style-type: none"> E1-p62 heterodimer synthesis control Prevention of premature fusion of E1-E2 with host membrane Protection of fusion loop at E1 domain 		Glycosylated	Singh A. et al.,2018
6K	61	<ul style="list-style-type: none"> Signal peptide for E1 Present in virus envelope Assistance of E1 translocation to ER Ion channel activity Important to virus budding 		Glycosylated	Snyder et al. 2013; Silva and Dermody, 2017; Singh A. et al.,2018; Dey et al.,2019
TF	76	<ul style="list-style-type: none"> Ion channel activity Associated to virus production, pathogenesis and budding 		Palmitoylated	Snyder et al.,2013; Silva and Dermody, 2017; Singh A. et al.,2018; Dey et al.,2019

CHIKV-6K proteins are around 60 amino acid residues long and act as signal peptides for CHIKV-E1 at the viral envelope. It also promotes the translocation of CHIKV-E1 at the endoplasmic reticulum (ER) and the budding of the matured virion (62).

2.1.6. Available or clinical phase trial medicines

Currently, no specific anti-CHIKV medication is available in the market, till date. However, several anti-CHIKV vaccines are on different clinical phase trial levels. For example, a live attenuated virus-based vaccine by Valneva is under phase III clinical trial. Also, a virus-like particle-based vaccine by Emergent BioSolutions is under phase III trial. Recently, Merck has developed a measles virus vectored live attenuated vaccine which has completed phase II clinical trial. The International Vaccine Institute in collaboration with Bharat Biotech has developed another anti-CHIKV specific vaccine which is based on inactivated whole virus. The research and development of most of these vaccines are co-funded by the Coalition for Epidemic Preparedness Innovations (CEPI) (90,91).

2.2. The importance of cellular pathways and host factors on CHIKV entry into the host

A potent virus-host cell interaction consists of two separate events namely, attachment and entry. An efficient attachment step concentrates the virus particles over the cell surface in the presence of the attachment factors. However, these attachment factors are not necessarily involved with the cellular entry-dependent conformational switching of the virus membrane. This characteristic makes the attachment factors quite non-specific for different classes of viruses. On the other hand, viral entry becomes facilitated by canonical entry receptors which promote conformational switching of the envelope, a pre-requisite for membrane fusion followed by insertion of the capsid and genetic material into the host cell. Also, the entry factors determine the host range of viruses due to their specificity.

For example, as the mammalian vector of CHIKV transmission is arthropod origin, it is predicted that the virus follows similar entry mechanisms for host cell entry using evolutionarily conserved entry factors (75,92).

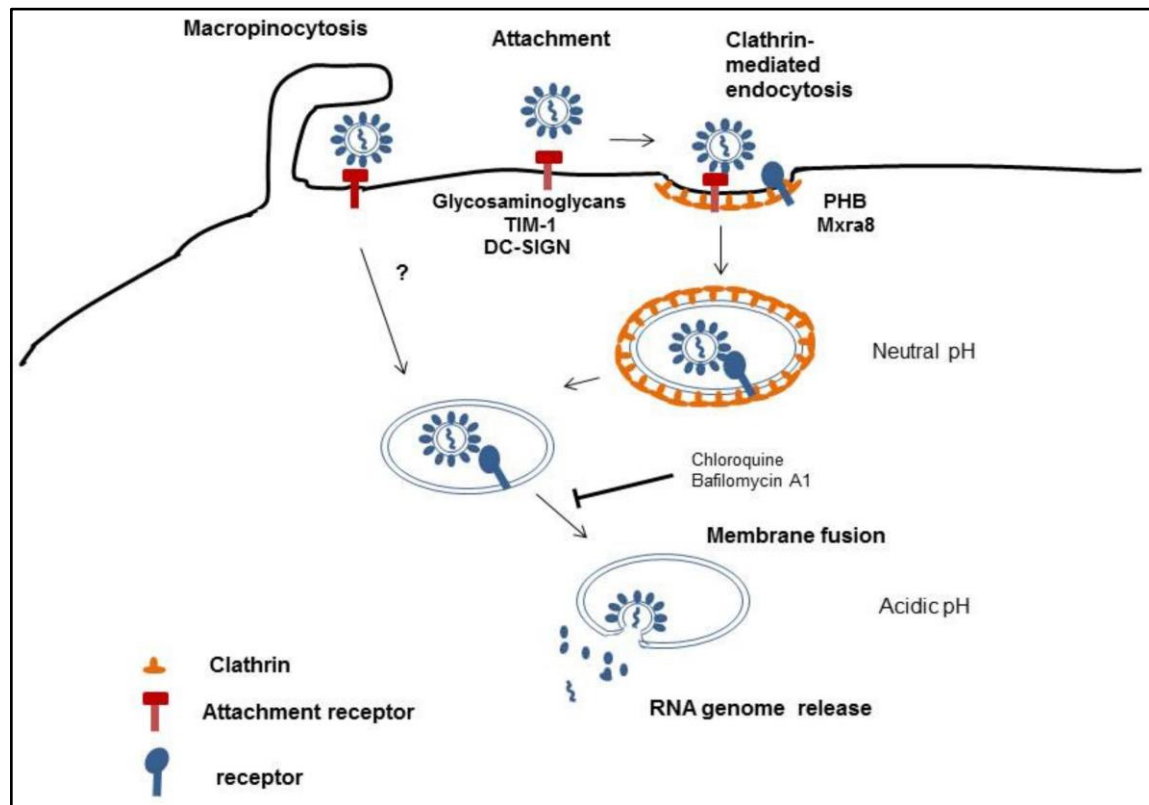


Figure 18: A schematic illustration of CHIKV entry in the host cell (The source of the image: *Schnierle BS et al, viruses, 2019, doi: 10.3390/v11111078*).

Detailed insight into CHIKV entry pathways into the host cells is yet to come to light. However, several mechanisms such as clathrin-mediated endocytosis, epidermal growth factor receptor substrate 15 (Eps-15)-dependent pathway, and most recently macropinocytosis are described to facilitate CHIKV entry and subsequent viral replication and propagation into the host cell (**Fig: 18**). The clathrin-coated endocytic vesicles are already reported to efficiently deliver the cargo into the cytoplasm. The acidic pH inside the endosome stimulates the CHIKV and other *Alphaviruses* for penetration and subsequent uncoating. Knockdown studies have reported that Eps-15 dependent

pathway has a role in CHIKV entry into the host cells, although, this is not an exclusive pathway. Moreover, macropinocytosis has been reported to non-specifically uptake CHIKV and other *Alphaviruses* into human muscle cells in large uncoated vesicles. The virus-dependent stimulation of growth factor receptors on the cell surface promotes the polarization of actin filaments followed by the formation of ruffles to the extracellular side of the membrane. Some but not all of these ruffles move back and therefore, fuse with the membrane to form a vesicle-like structure containing the virus, which further moves into the cytoplasm (75,92–98).

One of the major host-derived entry factors of CHIKV is glycosaminoglycans (GAGs) which include heparan, keratan, chondroitin and dermatan sulfates (99). A report on point mutation study of CHIKV-E2 reveals that E79K, G82R and E166K mutations result in the generation of live attenuated vaccine like CHIKV strain which shows reduced *in vivo* replication and enhanced attachment to cell surface GAGs. Except for cellular entry, no other direct pro or anti-CHIKV role of GAGs is reported (100–102). Another cell surface marker, namely, T-cell immunoglobulin and mucin 1 (TIM-1) is expressed in a wide variety of cells and the extracellular domain of TIM-1 interacts with phosphatidylserine (PtdSer) of viral membrane and therefore, facilitates the viral attachment into the host cells (103,104). Likewise, a few other PtdSer-interacting proteins such as Axl and TIM-4 are also reported to promote the CHIKV attachment process in a similar fashion (105,106). As the transmembrane and intracellular domain of these PtdSer interacting proteins have no functional role in terms of enhanced viral entry, therefore, it has been hypothesized that these markers act as attachment factors rather than having a role of specific receptor facilitating viral entry (75). Another attachment factor, the C-type calcium-dependent lectin DC-SIGN (Dendritic Cell-specific intracellular adhesion molecule-3-grabbing-non-integrin) also serves the role of attachment factor of CHIKV (107,108). Moreover, some cellular proteins such as actin gamma 1, collagen type1-alpha-2, and tyrosine phosphatase non-receptor-type 2 are also reported to interact with CHIKV-E2 (109). Loss-of-function-based screening study has reported Tetraspanin membrane 9 and FUZZ proteins to

positively modulate early endosome formation and therefore, regulate membrane fusion of CHIKV (110).

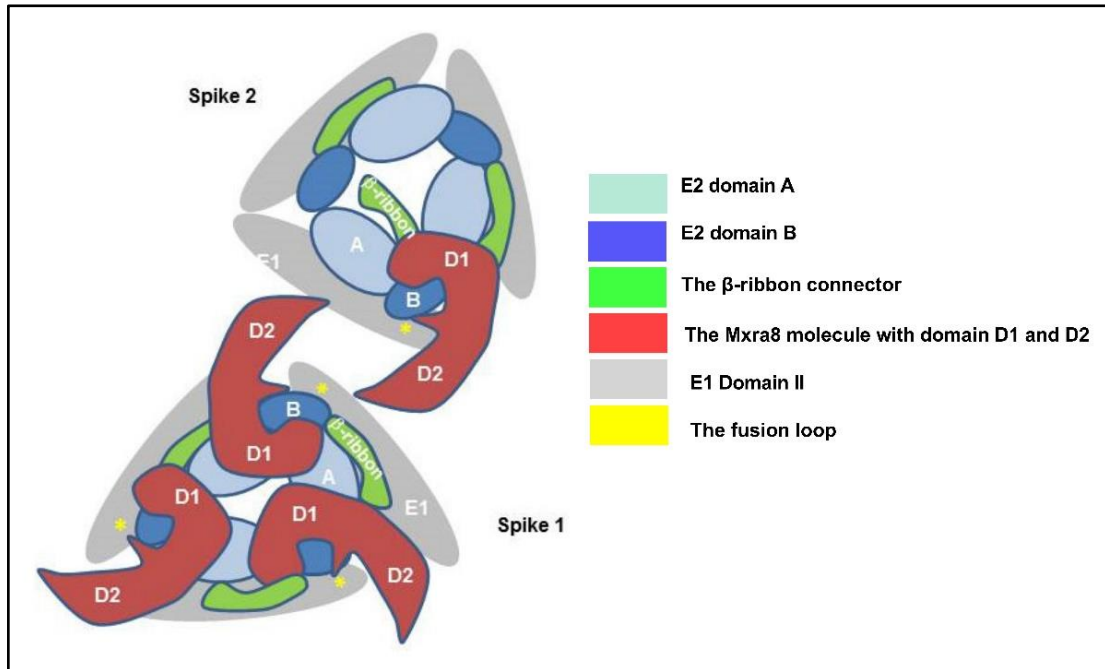


Figure 19: A schematic representation of CHIKV-E2-E1-Mxra8 interaction (The source of the image: *Schnierle BS et al, viruses, 2019, doi: 10.3390/v11111078*).

Loss-of-function-based screening has also reported interferon-induced transmembrane protein 3 (IFITM3) and tetherin/BST-2 to negatively regulate the release of CHIKV (111–113) The positive interactions of CHIKV-E2 with prohibitin 1 and 2 have been demonstrated to regulate the CHIKV attachment over host cell membrane (114,115). Likewise, the ATP synthase- β subunit (ATPS β), a mitochondrial and plasma membrane-bound protein, has been reported to interact with CHIKV-E2 and take a positive role in viral entry in mosquito cells (116).

In recent times, Mxra8 (also known as limiting, DICAM, or ASP3), another mediator of CHIKV infection, has been screened out based on a CRISPR-Cas9-based study. The direct interaction of CHIKV-Mxra8 has been found to promote enhanced attachment and internalization of virus particles into the host cells (**Fig: 19**). Moreover, anti-Mxra8 monoclonal antibody-mediated blocking

has been found to almost block CHIKV infection completely. The residual CHIKV infection and absence of Mxra8 in mosquitoes are supportive of the presence of other possible functional receptors (34,117).

2.3. Immunological Aspects of Host-CHIKV Interaction

2.3.1. Cytokine burst: an inevitable response of host-CHIKV interaction

CHIKV is an arthritogenic *Alphavirus*, responsible for infection-induced massive pro-inflammatory cytokine responses. Previous studies on CHIKV-infected interferon (IFN) knock-out mice revealed that CHIKV infection promotes a quick and massive onset of type I IFN response. However, *in vivo* followed by *in vitro* studies reveal that the CHIKV-infected fibroblast cells are the key player to generate type I IFNs. CARDF (CARD adaptor inducing IFN β), a downstream adaptor protein of two patterns recognizing receptor (PRR) namely RIG-1 and MDA-5, possibly degrades ss RNA and therefore, acts as a regulator of fibroblast-induced type I IFN responses. On the other side, CHIKV-nsP2 promotes viral multiplication and rapid disease onset by inhibiting IFN- α/β pathways. Moreover, pro-inflammatory cytokines such as interleukin 1- β , 6, 12, tumor necrosis factor (TNF) and IFN- γ ; growth factors such as granulocyte-macrophage colony-stimulating factor (GM-CSF) and chemokines such as monocyte chemoattractant protein 1 (MCP-1) are characteristically upregulated during CHIKV infection which might lead towards CHIKV induced fever (CHIKF) (7,118–129). This rapid production of host-induced pro-inflammatory cytokines is known as cytokine burst, a characteristic feature of CHIKV and other *Alphavirus* infections.

Furthermore, heat shock proteins such as HSP 90 interact with CHIKV-nsP3 and 4 and therefore, promote viral replication inside the host (130). Additionally, HSPs are also reported to activate neighboring cells against infection in a paracrine signaling-dependent manner. The role of mitogen-associated protein kinases (MAPKs) such as p38 and stress-associated protein kinase- c-Jun N terminal Kinase (SAPK-JNK) are well cited to promote CHIKV-induced inflammation (8,25).

2.3.2. Importance of host macrophages in CHIKV infection

CHIKV predominantly infects a variety of host cells for example skin fibroblasts, and epithelial cells, and also penetrates lymphoid tissues. Several human and non-human laboratory cell lines were reported to be infected by CHIKV, for example, HeLa (a cervical carcinoma cell line), HEK-293T (a human kidney epithelial cell line), HUH-7 (a hepatocarcinoma cell line), SH-SY5Y (a neuroblastoma cell line), Vero (African green monkey kidney epithelial cell line) and many more (131–133) (**Table:4**). Moreover, the RAW264.7 cells (a murine macrophage cell line) has been well reported as a suitable target for CHIKV, which might imply different immune evasion strategies of the virus (7,8,21,25).

Antigen-presenting cells (APCs) specifically monocyte-macrophages bear a significant role in initiating the innate immune responses in the early stages of CHIKV infection and also, promoting antigen-specific adaptive immune responses in the host immune system. Along with macaque and mouse models, multiple *in vitro* and *in vivo studies* on humans report that monocyte-derived macrophages are susceptible to CHIKV infections and promote subsequent immune alteration in the host. Along with macaque and mouse models, human-derived multiple *in vitro* and *in vivo studies* report that monocyte-derived macrophages are susceptible to CHIKV infections and promote subsequent immune alteration in the host (134–137) (**Table:5**). Macrophage scavenger receptor 1 (MSR1) induce autophagy to restrict *in vivo* CHIKV infection in mice model (138). Moreover, CHIKV infection-induced activation of different tissue macrophages contributes to a significantly higher amount of secretory pro-inflammatory cytokines such as IL-1 β , TNF, IL-6, and chemokines such as MCP-1, which in turn promote CHIKF and joint pain and subsequently chronic polyarthralgia and myalgia (5,6).

Table 4: Cells and cell lines of different origins that are susceptible to CHIKV infection (The source of the table: *Constant LC et al, Frontiers in Microbiology, 2021, doi:10.3389/fmicb.2021.744164*).

Name of Cells	Origin
Hs. 789.Sk	Human primary skin fibroblast
MRC5	Human primary lung fibroblast
hSMM	Human primary skeletal muscle myoblast
PBMC	Human primary blood monocytes
FLS	Human primary fibroblast-like synoviocyte
Osteoblasts	Human primary osteoblast
Vero E6	Monkey kidney epithelial-derived cell line
BHK-21	Baby hamster kidney fibroblast-derived cell line
HeLa	Human cervical carcinoma epithelia-derived cell line
HEK-293T	Human embryonic kidney epithelia-derived cell line
293T	Human kidney epithelia-derived cell line
BEAS-2B	Human bronchial epithelia-derived cell line
BGM	Buffalo green monkey kidney-derived cell line
THP-1	Human peripheral blood monocyte-derived cell line
Huh7	Human hepatocellular carcinoma-derived cell line
C6/36	<i>Aedes albopictus</i> intestine-derived cell line
A20	Mouse B lymphocyte-derived cell line
AAg2	<i>Aedes aegypti</i> -derived cell line
RD	Human rhabdomyosarcoma-derived cell line
U4.4	<i>Aedes albopictus</i> -derived cell line
A549	Human lung adenocarcinoma-derived cell line
U251MG	Human malignant glioblastoma-derived cell line
Vero CCL-81	<i>Cercopithecus aethiops</i> kidney-derived cell line
HFF	Human foreskin fibroblast-derived cell line
C2C12	Mouse myoblast-derived cell line
SVG-A	Human astrocyte-derived cell line

Intriguingly, CHIKV is known to exhibit immune evasion followed by reappearance even after several years in a macrophage-dependent manner (139). Earlier studies depict that CHIKV infection promotes IFN- β and ISG mRNA synthesis in an IRF3-dependent manner and also blocks host cell translation machinery. Therefore, the effector response of ISG activation remains inhibited. Also, after viral replication into the host cell, the cellular transcription process gets shut off, where CHIKV-nsP2 might have a possible implication (140–142).

Therefore, the path-immunological significance of CHIKV infection in macrophages has gained immense importance in clinical and experimental studies.

Table 5: Different model systems to study CHIKV infection (The source of the table: *Constant LC et al, Frontiers in Microbiology, 2021, doi:10.3389/fmicb.2021.744164*).

Category/model	Animal	Main outcome	References
Aged model	WT C57BL/6	Severe disease progression.	Uhrlaub et al., 2016; Arévalo et al., 2019; Jain et al., 2019
Anti-CHIKV treatment	WT C57BL/6, C1q ^{-/-} , FcRγ ^{-/-}	Limitation on CHIKV infection.	Abdelnabi et al., 2018; Fox et al., 2019; Patil et al., 2021
Arthritis	WT C57BL/6, ISG15 ^{-/-} , Ube1L ^{-/-} , MHCII ^{A/A} , IFNγ ^{-/-} , Sting ^{9/9t} , CCR2 ^{-/-}	CHIKV arthritis signature.	Gardner et al., 2010; Werneke et al., 2011; Nakaya et al., 2012; Poo et al., 2014a; Geng et al., 2021
CHIK vaccine development	WT C57BL/6; AG129; BALB/c (H2 ^d)	Rapid and long-lasting against CHIKV responses. Protection against lethal challenge.	Wang et al., 2011; Arévalo et al., 2019; Campos et al., 2019; López-Camacho et al., 2019; Chen et al., 2020; Adam et al., 2021
Chronic/Persistent model	WT C57BL/6, CD8 _α ^{-/-} , Baff3 ^{-/-} , Wdfy4 ^{-/-} , Rag1 ^{-/-} , μMT C57BL/6; Golden hamster	Viral persistence in joint tissues. Severe inflammation of the musculoskeletal and joints tissues.	Morrison et al., 2011; Bosco-Lauth et al., 2015; Hawman et al., 2016, 2017; Davenport et al., 2020
IFN receptor-deficient	IFNAR ^{-/-} , ISG15 ^{-/-} , IFN-α/βR ^{-/-}	High mortality, paralysis, severe disease.	Couderc et al., 2008; Werneke et al., 2011; Hiroki et al., 2020; McCarthy et al., 2020
Lethal challenge	BALB/c, AG129, DBA1/J, Swiss Webster	Death after 2–13 days post infection*.	ROSS, 1956; Campos et al., 2019; Zhang H.-L. et al., 2019; Chen et al., 2020; Julander et al., 2020
Leukocyte deficient	TLR ₃ ^{-/-} , TLR _{3/7/9} ^{-/-} , TLR ₉ ^{-/-} , CCR2 ^{-/-}	Increased viral load and enhanced disease susceptibility.	Poo et al., 2014a; Hiroki et al., 2020; McCarthy et al., 2020
Acute disease and Innate immune model	Rhesus macaques, Bonnet macaques, Cynomologus macaques	Clinical symptoms, viremia, immune cells, cytokines, persistence	Chen et al., 2010; Messaoudi et al., 2013; Roy et al., 2014
Aged model	Rhesus macaques	viremia, clinical symptoms and immune response age dependent	Messaoudi et al., 2013
Pregnant model	Rhesus macaques	Viral detection in tissues during pregnancy	Chen et al., 2010
Vaccine and therapies	Rhesus macaques, Cynomologus macaques	Viremia and immune response during therapy	Akahata et al., 2010; Chang et al., 2014; Kam et al., 2014; Pal et al., 2014

2.4. The significance of Toll like receptors (TLRs) in CHIKV infection

Being one of the prime sub-family of pattern recognition receptors, TLRs contribute significantly to initiate host innate immune responses against different foreign antigenic molecules. Therefore, the role of TLRs during different inflammation-induced physiological abnormalities is of immense significance in experimental immunological research as well as pharmacological remedies. The earlier reports suggest a possible involvement of several TLRs such as TLR, 3, 7, and 8 in the pathogenesis and modulation of host immune responses during CHIKV-induced altered cellular

responses. The possible association of TLR3 is well investigated from different perspectives. Priya et al, have shown that the activation of TLR3 using a pharmacological agonist (**Poly I:C**) provides 100% survival of CHIKV-infected mice by reducing the viral titer in different tissues including brain, decreasing interferon responses and inflammation in the host immune system, *in vivo* (123). Another interesting observation was reported by Her et al, which summarizes that CHIKV-specific antibodies from TLR3^{-/-} mice exhibited significantly lower *in vitro* neutralization capacity, due to altered virus-neutralizing epitope specificity. They also have shown that TLR3-specific SNP genotyping analysis of CHIKF patients and have identified SNP **rs6552950** to be associated with disease severity and CHIKV-specific neutralizing antibody response (143). Genetic polymorphisms of TLR7 and 8 have also been reported to be associated with CHIKV susceptibility in human patients. Three polymorphisms of TLR-7 (viz. rs179010, rs5741880, rs3853839) and one of TLR-8 (rs3764879) are found to be positively associated with chikungunya infection. Both CC and CT genotypes of rs179010, GC and CC genotype and G allele of rs3853839, and GC genotype of rs3764879 were significantly more prevalent among CHIKV-infected patients (144). Another pioneering study has shown that human monocytes and monocyte-derived macrophages (MDMs) are susceptible to Chikungunya virus (CHIKV) infection *in vitro*. The signature pro-inflammatory responses during CHIKV infection in host macrophages such as upregulation of macrophage activation markers and raise in pro-inflammatory cytokines levels such as IL-1 β , IL-6, TNF, etc., and interferon- α responses are observed in their experimental model. The recognition of structural components of CHIKV promotes the generation of pro-inflammatory cytokines but not ISGs. Next, an m-RNA-based qRT-PCR study reveals that the CHIKV infection induces the fold expression of toll like receptor (TLR) 2, 7, and 8 in monocytes, whereas, TLR3 and 7 are involved in CHIKV-induced MDMs. Therefore, there might be a possible differential regulation of CHIKV infection in human monocytes and MDMs. Interestingly, the expression of TLR4 at the mRNA level was found to increase during CHIKV infection in a time point-dependent manner in both monocytes as well as MDMs, although the fold

increase of expression is higher in MDMs. Altogether, the study reports for the first time that there might be modulation of expressions of different TLRs such as TLR2, 3, 4, 7, and 8 at m-RNA level along with raised pro-inflammatory responses and macrophage activation during CHIKV infection hPBMC-derived monocytes and MDMs (17).

2.5. TLR4: An Unprecedented Regulator of Inflammation

2.5.1. An introduction to TLR4 and associated immune regulation

Toll-like receptor 4 (TLR4) or CD284, a frontline member of toll-like receptors is of interest to immunologists because of its pivotal immune-regulatory role against invading pathogens as the initial innate immune response of the host. TLR4, a transmembrane helical protein, consists of an evolutionarily conserved toll-interleukin-1 receptor (TIR) domain like all other TLRs at the cytosolic face (**Fig:20**). In terms of cell-specific localization, TLR4 is well abundant in granulocytes, T cells and professional antigen-presenting cells such as macrophages and dendritic cells. Although the signaling mechanism and activation-induced inflammatory response of TLR4 were first described with lipopolysaccharide (LPS) (a Gram-negative cell wall component that acts as specific TLR4 ligand), there are several endogenous as well as exogenous ligands from different bacterial and viral components have been discovered till date (**Table X**). Due to having a direct regulatory role over different pro-inflammatory as well as anti-inflammatory conditions, TLR4 is currently being considered as an alternative drug-designing target.

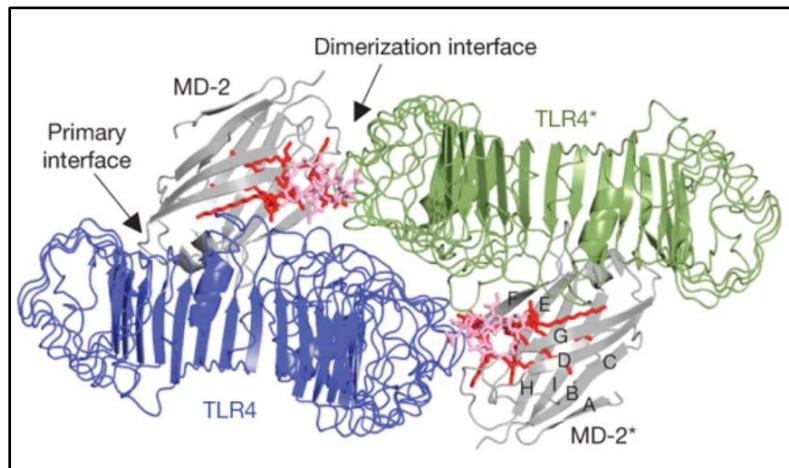


Figure 20: Mouse TLR4-MD2-LPS complex in dimerized structure (The image courtesy: *Park B et al, Nature, 2009, doi.org/10.1038/nature07830*).

2.5.2. TLR4 signaling pathway

The molecular mechanism of the TLR4 signaling pathway in the presence of lipopolysaccharide (LPS), a Gram-negative bacterial cell wall component and a specific agonist of TLR4, has been well characterized (**Fig:21**). Initially, LPS binding protein (LBP), an extracellular protein, first interacts with LPS present over bacterial outer membrane or in micelle form. Single LPS-LBP complex then interacts with either soluble or membrane-bound CD14, a co-stimulator of the TLR4 signaling pathway. CD14 acts as a carrier to transfer a single molecule of LPS to MD2 which in turn facilitates TLR4-MD2 heterodimer formation representing functional LPS receptor (145). Next, the TLR4 dimer recruits two adapter proteins, namely, TIRAP (Toll-interleukin 1 receptor (TIR) domain-containing adapter protein) and TRAM (TRIF-related adaptor molecule) to initiate MyD88 (Myeloid differentiation primary response 88) and TRIF (TIR Domain-containing Adaptor-inducing Interferon- β)-dependent pathway, respectively. The MyD88-dependent pathway ultimately induces early NF- κ B activation followed by pro-inflammatory cytokines production, whereas the TRIF-dependent pathway leads to late NF- κ B activation followed by IRF-3 (Interferon regulatory

factor-3) and type I IFN activation. TRIF-dependent activation of TLR4 leads to activation of co-stimulatory markers such as CD86 and chemokines such as CCL-5 (10,20,146). Intriguingly, TLR4 along with endocytosed LPS is co-localized on the early endosomes followed by ubiquitination. It has been observed that blockade of endosomal pathways results in marked elevation of LPS-induced NF- κ B activation. Moreover, antigen-bound LPS receptor complex is presented via MHC-II to CD4⁺ helper T cells (147).

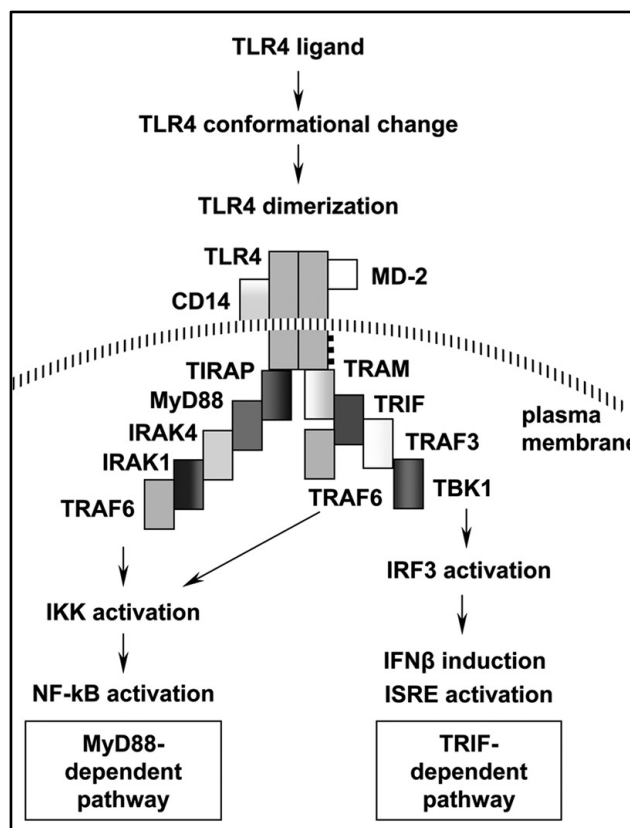


Figure 21: TLR4 signaling pathway (The source of the image: **Matsunaga et al, Molecular Pharmacology, 2010, doi: 10.1124/mol.110.068064**)

2.5.3. Role of TLR4 in infection-induced inflammation

The mechanistic role of TLR4 in the presence of its specific ligand, LPS, is well understood and well described. Therefore, Gram-negative bacterial infection-mediated severe sepsis and acute

lung injury are currently being studied for TLR4-directed remedy (148,149). Moreover, the association of TLR4 with chronic obstructive pulmonary disease (COPD) is also a current bio-medical research topic (150). Also, bacterial LPS-mediated necrotizing enterocolitis and inflammatory bowel disease (IBS) such as Crohn's disease and ulcerative colitis are well reported to be regulated by TLR4 (151,152).

TLR4 is also known to exert pro-inflammatory responses in the host due to several viral infections. A comparative study of TLR4 mutant C3H-HeJ mice shows reduced inflammation due to respiratory syncytial virus (RSV) infection concerning the wild-type C3H-OUJ mice. Moreover, infection-induced infiltration of lymphocytes, epithelial proliferation, and lung neutrophilia were significantly reduced in TLR4-mutant C3H-HeJ mice (14).

To promote viral replication, the VP3 protein of the foot-and-mouth-disease virus interacts with TLR4. To elevate TLR4 expression, therefore, infection-induced inflammation, VP3 also inhibits a lysosomal protein, Rab7b. Henceforth, VP3-mediated upregulation of TLR4 promotes FMDV infection and subsequent inflammation in the host (15).

Gene knockout study has revealed that the hexameric nsP1 protein of the Dengue virus promotes pro-inflammatory responses in mouse and human macrophages in a TLR4-dependent manner. Therefore, the possibility of TLR4-targeted therapy might be a promising aid in future drug development (153).

Most recently, SARS-CoV2 spike protein has been found to interact with TLR4 and promote TLR4-dependent pro-inflammatory responses in different cell lines and primary cells.

Together, all of these reports suggest the notion that the association of TLR4 with inflammation is an integral part of promoting pro-inflammatory viral and Gram-negative bacterial disease in the host.

2.5.4. Role of TLR4 in physiological inflammatory condition

For acute alcoholic hepatitis, TLR4 has a potent role in mediating pro-inflammatory responses in a TRIF-dependent pathway (154–156). This experimental fact is further applied in current biomedical research. TAK-242, a cyclohexane derivative small molecule, a specific antagonist of TLR4 now recently been promoted to clinical phase trial under the U.S. Food and Drug administration (FDA) as a possible remedy against acute alcoholic hepatitis ([ClinicalTrials.gov Identifier: NCT04620148](https://clinicaltrials.gov/ct2/show/study/NCT04620148)).

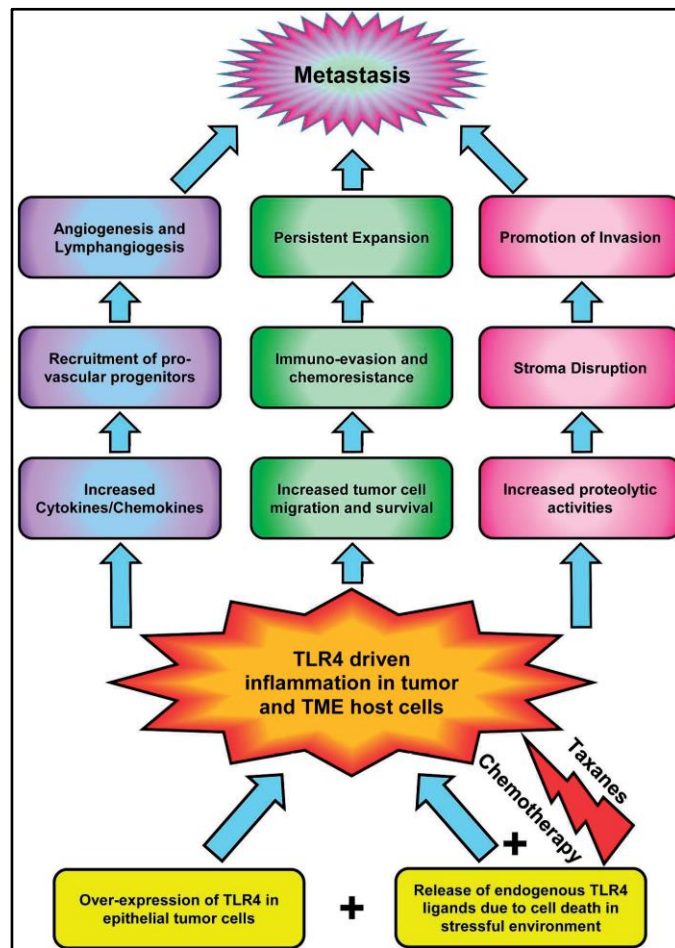


Figure 22: The bi-directional role of TLR4 in cancer (The source of the image: *Ran et al, Translational studies on inflammation, IntechOpen.com, doi: 10.5772/intechopen.78112*).

Moreover, TLR4 is reported to exert a sharp rise in pro-inflammatory responses followed by apoptosis in mice astrocytes and glial cells due to alcohol-driven stimulation (157).

Although immune suppression is a key feature for most types of cancer, TLR4 exhibits a “double-edged sword” effect in terms of tumor development (158) (**Fig:22**). TLR4 pathway promotes several key cellular and subcellular functions such as cell proliferation, differentiation, migration, tissue invasion, and heat shock proteins-driven survival. A few systemic responses of tumorigenesis are enhanced migration, maturation, and antigen presentation by dendritic cells in a TLR4-dependent manner to further activate cytotoxic T cells and therefore, increased apoptosis of tumor cells. Therefore, TLR4 agonist-driven antitumor medication is nowadays a suitable target for bio-medical research (159–161). However, TLR4 activation promotes bone marrow-derived myeloid progenitor cells to promote metastasis and blood vessel formation to facilitate tumorigenesis (162–165).

Together, all of the reports suggest that TLR4 has an integral role in altered host immune system-induced inflammation and therefore, might be a suitable target to regulate infection-induced inflammation, host cell activation and ultimately maintain physiological homeostasis.

Chapter#2
Hypothesis
and
Objectives

3.1. Hypothesis:

The functional expression of the toll like receptor 4 (TLR4) during Chikungunya virus (CHIKV) infection may regulate host cell mediated immune responses.

3.2. Objectives:

1. To investigate the requirement of TLR4 in CHIKV infection in macrophages and associated immune responses, *in vitro*.
2. To study the TLR4-directed modulation of altered cellular signaling of macrophages during CHIKV infection, *in vitro*.
3. To examine the possible interaction of TLR4 and CHIKV structural proteins, *in vitro*.
4. To find out the role of TLR4 towards CHIKV infection in mice, *in vivo*.

Chapter #3

Materials and Methods

4. Materials

4.1. Cells and Virus

The RAW264.7 cell line (ATCC® TIB-71™), THP-1 cell line (ATCC® TIB-202™), primary peritoneal macrophages obtained from BALB/c and C57BL/6 mice, and primary macrophages obtained from human peripheral blood mononuclear cells (hPBMC) were cultured in complete Roswell Park Memorial Institute (RPMI) media i.e., RPMI 1640 GlutaMAX™ (Gibco, USA), 1X antibiotic-antimycotic solution (HiMedia Laboratories Pvt. Ltd, MH, India) and 10% heat-inactivated Fetal Bovine Serum (FBS) (Gibco, USA) in a humidified sterile chamber at 37°C with 5% CO₂. The Vero (ATCC® CCL-81™) and TLR4-knockout (KO) RAW cells (Invivogen, USA) were cultured in complete Dulbecco's Modified Eagle's Medium (DMEM) i.e., DMEM Glutamax (Gibco, USA), 1X antibiotic-antimycotic solution and 10% heat-inactivated FBS. For TLR4KO RAW cells, a selection antibiotic, namely, zeocin (Invivogen, USA) was used in alternative passages to maintain the selection pressure. The Chikungunya virus-Indian Strain (CHIKV-IS; Accession number: EF210157.2) and the Vero cells were kind gifts from Dr. M.M. Parida (DRDE, Gwalior, India). Zymefree (HiMedia Laboratories Pvt. Ltd, MH, India), an enzyme-free cell detachment solution, or Trypsin (HiMedia Laboratories Pvt. Ltd, MH, India) was used for regular cell maintenance and culture.

4.2. Animals

All of the animal experiments in the current project were performed as per the guidelines issued by the Committee for the Purpose of Control and Supervision of Experiments on Animals (CPCSEA) of India. The Institutional Animal Ethics Committee of NISER, Bhubaneswar (1634/GO/ReBi/S/12/CPCSEA) and ILS, Bhubaneswar (76/Go/ReBi/S/1999/CPCSEA) approved the experimental protocols. 6-8 weeks old BALB/c or C57BL/6 male mice were used to harvest peritoneal macrophages. 6-8 weeks old male BALB/c mice were used for splenic T cell isolation. 8-9 days old C57BL/6 pups of both sexes were subjected to *in vivo* CHIKV infection to investigate

the role of TLR4. All animals were kept in a sterile environment with an alternative 12 h of light and dark cycle with food and water provided ad libitum.

4.3. Antibodies

The antibodies used in flow cytometry and/or Western blot-based analysis to investigate the different aspects of the current project are listed below in the Table format (**Table number 6**),

Si No.	Antibodies	Company	Catalog no/Clone no
1	AF488 anti-mouse TLR4	eBiosciences, USA	53-9041-82/(UT41)
2	AF647 Anti-m-TLR4	Novus Biologicals, USA	NBP2-24865AF647/(MTS 510)
3	APC Annexin V	BD Biosciences, USA	550474/(G155-178)
4	APC anti-human CD14	eBiosciences, USA	17-0149-42/(61D3)
5	APC anti-mouse CD80 (B7-1)	eBiosciences, USA	17-0801-82/(16-10A1)
6	APC Anti-mouse CD80 (B7-2)	eBiosciences, USA	17-086282/(GL1)
7	APC anti-mouse CD90.2	Tonbo Biosciences	20-0903-U100/(30-H12)
8	APC Rat IgG2a k isotype control	BD Biosciences, USA	553932/(R35-95)
9	Chicken anti-mouse AF488	Invitrogen, CA, USA	A21200/NA
10	FITC anti-human CD19	BD Biosciences, CA, USA	555412/(H1B19)
11	FITC anti-mouse CD69	eBiosciences, USA	11-0691-85/(H1.2F3)
12	Goat anti-rabbit AF647	Invitrogen, CA, USA	A21244/NA
13	Hamster anti-mouse CD28 (NA/LE)	BD Biosciences, CA, USA	553294/37.51
14	HRP-goat anti-mouse IgG	BD Biosciences, CA, USA	554002/NA
15	HRP-goat anti-rabbit IgG	BD Biosciences, CA, USA	554021/NA

16	Monoclonal Antibody to GAPDH	Abgenex India Pvt. Ltd., India	10-10011/(ABM22C5)
17	Mouse anti-mouse CHIKV-E2	A gift from Dr. M.M Parida, DRDE, Gwalior, India	
18	Mouse IgG1 Isotype Control	Abgenex India Pvt. Ltd., India	10-101/(MOPC31C)
19	PE anti-human CD11b	eBiosciences, USA	12-0112-82/(M1/70)
20	PE anti-mouse CD25	BD Biosciences, USA	553866/(PC61)
21	PE anti-mouse H-2k ^b	BD Biosciences, USA	561072/(AF6-88.5)
22	PE anti-mouse H-2k ^d	BD Biosciences, USA	553566/(SF1-1.1)
23	PE Rat anti-mouse I-Ad/I-Ed,	BD Biosciences, USA	558593/(2G9)
24	PE Rat IgG2c, k isotype control	BD Biosciences, USA	559841/(A23-1)
25	PE-anti-mouse TNF	BD Biosciences, USA	51-18135Z
26	PerCP-Cy5.5 anti-human CD90	BD Biosciences, CA, USA	561557/(5E10)
27	PerCP-Cy5.5 anti-mouse CD14	BD Biosciences, USA	560638/(rmc5-3)
28	Polyclonal Beta-actin antibody	Abgenex India Pvt. Ltd., India	IMG-5142A/NA
29	Rabbit anti-mouse CHIKV-E1	A gift from Dr. T.K. Chowdary, SBS, NISER Bhubaneswar, India	
30	Rabbit anti-mouse p38 MAPK	Cell Signaling Technology, USA	9212/NA
31	Rabbit anti-mouse p44/42 MAPK	Cell Signaling Technology, USA	4695/(137F5)
32	Rabbit anti-mouse p-NF- κ B	Cell Signaling Technology, USA	3033S/(93H1)
33	Rabbit anti-mouse p-p38 MAPK	Cell Signaling Technology, USA	4511/(D3F9)
34	Rabbit anti-mouse p-p44/42 MAPK	Cell Signaling Technology, USA	4370/(D13.14.4E)
35	Rabbit anti-mouse p-SAPK/JNK	Cell Signaling Technology, USA	4668/(81E11)
36	Rabbit anti-mouse SAPK/JNK	Cell Signaling Technology, USA	9258/(56G8)

37	Rabbit Anti-mouse TLR4	Invitrogen, USA	48-2300/NA
38	Rabbit anti-mouse-TLR4	Cell Signaling Technology, USA	14358/(D8L5W)
39	Rat anti-mouse CD3 (NA/LE)	BD Biosciences, CA, USA	555273/17A2

4.4. Chemicals, reagents and modulators

The chemicals used to investigate the different aspects of the current project are listed below in Table (Table number 7),

Si no	Chemicals	Company	Catalog no
1	10x Annexin V binding buffer	BD Biosciences, USA	556454
2	10X Phosphate buffer saline	Himedia Laboratories Pvt. Ltd., India	TL1032
3	10x RBC lysis buffer	Himedia Laboratories Pvt. Ltd., India	R075-100ML
4	20x TMB/H2O2	Bangalore Genei, Bangalore, India	62160118010A
5	2-mercaptoethanol	Sigma Aldrich, USA	63689
6	7-AAD	BD Biosciences, USA	559925
7	Acrylamide	Himedia Laboratories Pvt. Ltd., India	MB068
8	Ammonium persulfate (APS)	Bio-Rad, CA, USA	161-0700
9	Antibiotic-antimycotic solution	Himedia Laboratories Pvt. Ltd., India	A002
10	Bis-Acrylamide	Himedia Laboratories Pvt. Ltd., India	MB005-250G
11	Bovine serum albumin fraction-V	Himedia Laboratories Pvt. Ltd., India	GRM105-100G
12	Bradford reagent	Sigma Aldrich, USA	B6916
13	Bromophenol blue	Sigma Aldrich, USA	114391

14	Complete EDTA-free protease inhibitor	Sigma Aldrich, USA	05892970001
15	Concanavalin A (ConA)	Sigma Aldrich, USA	C0412-5MG
16	Crystal violet	Sigma Aldrich, USA	C6158
17	Di-Sodium mono-hydrogen phosphate	Himedia Laboratories Pvt. Ltd., India	GRM1417
18	DMEM	Gibco, USA	10566016
19	DMSO	Himedia Laboratories Pvt. Ltd., India	TC185-250ML
20	EDTA	Himedia Laboratories Pvt. Ltd., India	R066-500ML
21	EGTA	Sigma Aldrich, USA	E3889
22	FcR blocking reagent, mouse	Macs Miltenyi Biotech, Germany	130-092-575
23	Fetal Bovine Serum (FBS),	Gibco, USA	10270106
24	Glycerol	Himedia Laboratories Pvt. Ltd., India	MB060-500ML
25	Glycine	Himedia Laboratories Pvt. Ltd., India	MB013-1KG
26	HiSEP LSM	Himedia Laboratories Pvt. Ltd., India	LSM LS001
27	HPLC grade Methanol	Himedia Laboratories Pvt. Ltd., India	AS061-2.5L
28	immobilon ECL ultra–Western HRP substrate	Merck Millipore, USA	WBULS0100
29	Methylcellulose	Sigma Aldrich, USA	M0387-250g
30	Molecular Biology grade ethanol	Merck Millipore, Germany	108543
31	Molecular biology grade water	Himedia Laboratories Pvt. Ltd., India	ML-024
32	Mono-Sodium di-hydrogen phosphate	Himedia Laboratories Pvt. Ltd., India	GRM256
33	Paraformaldehyde	Himedia Laboratories Pvt. Ltd., India	GRM-3660
34	Phorbol-12-myristate-13 acetate (PMA)	Sigma Aldrich, USA	P8139

35	PhosStop™ (phosphatase inhibitors cocktail)	Sigma Aldrich, USA	04906837001
36	RPMI 1640 Glutamax	Gibco, USA	61870036
37	RPMI 1640 without phenol red	PAN Biotech, Germany	P04-16515
38	Saponin	Sigma Aldrich, USA	47036-50GM
39	SB203580	Merck Millipore, USA	559389
40	SDS (sodium dodecyl sulfate)	Sigma Aldrich, USA	L6026
41	Sodium azide	Himedia Laboratories Pvt. Ltd., India	GRM123-100G
42	Sodium bicarbonate	Himedia Laboratories Pvt. Ltd., India	GRM849
43	Sodium Carbonate	Himedia Laboratories Pvt. Ltd., India	GRM1189
44	Sodium chloride	Himedia Laboratories Pvt. Ltd., India	GRM031-1 kg
45	Sodium deoxycholate	Sigma Aldrich, USA	D6750-25G
46	SP600125	Merck Millipore, USA	420119
47	Sulfuric acid (H ₂ SO ₄)	Himedia Laboratories Pvt. Ltd., India	AS016-500ML
48	SuperSignal™ West Femto Maximum Sensitivity Substrate	Thermo Fisher Scientific, USA	34094
49	SyBR Green	Applied Biosystems, USA	A25741
50	TAK-242	Calbiochem, USA	614316-5MG
51	TEMED	Himedia Laboratories Pvt. Ltd., India	MB026
52	Thioglycolate (TG) medium brewer modified	BD Biosciences, USA	211716
53	Tris-base	Himedia Laboratories Pvt. Ltd., India	TC072-1KG
54	Triton X-100	Sigma Aldrich, USA	MB031-500ML

55	Trypan blue	Himedia Laboratories Pvt. Ltd., India	TC193
56	Trypsin-EDTA	Himedia Laboratories Pvt. Ltd., India	TCL-014
57	Tween-20	Himedia Laboratories Pvt. Ltd., India	GRM156-500G
58	Zeocin	Invivogen, USA	ant-zn-05
59	Zymefree	Himedia Laboratories Pvt. Ltd., India	TCL-028

4.5. Kits

The following table (**Table number 8**) consists of the kits used to conduct different experiments for the current project.

Si no	Name of the kit	Make	Catalog no
1	Annexin V apoptosis detection kit I	BD Biosciences, USA	556547
2	BD OptEIA™ ELISA kit for human TNF	BD Biosciences, USA	550610
3	BD OptEIA™ ELISA kit for mouse IL-6	BD Biosciences, USA	555240
4	BD OptEIA™ ELISA kit for mouse MCP-1	BD Biosciences, USA	555260
5	BD OptEIA™ ELISA kit for mouse TNF	BD Biosciences, USA	560478
6	Dynabeads Protein G Immunoprecipitation kit	Thermo Scientific, USA	10007D
7	Dynabeads untouched mouse T cell kit	Thermo Scientific, USA	11413D
8	EZcount™ MTT Cell Assay Kit	Himedia Laboratories Pvt. Ltd, India	CCK-003
9	First Strand cDNA synthesis kit	Takara Biosciences, Japan	6110A
10	First Strand cDNA synthesis kit	Thermo Scientific, USA	K1621
11	Genomic RNA isolation kit	Himedia Laboratories Pvt. Ltd, India	MB602-50 PR

12	Intracellular cytokine staining kit	BD Biosciences, USA	559302
13	Viral RNA Isolation kit	Qiagen, Germany	52904

4.6. Primers for PCR amplifications

The following primers were used in gene expression analysis for the current project (**Table number 9**).

Si no	Gene	Make	Sequence
1	E1	IDT, USA	(F)-5'TGCCGTCACAGTTAAGGACG3' (R)-5'CCTCGCATGACATGTCCG3'
2	GAPDH	IDT, USA	(F)- 5'CAAGGTCATCCATGACAACCTTTG3' (R)- 5'GTCCACCACCCTGTTGCTGTAG3'

4.7. Buffers and other reagents preparation

The different buffers used in the current project are given below with the details of composition (**Table number 10**).

Si no	Buffers and other reagents	Composition
1	1x TGS or SDS-PAGE running buffer	25 mM Tris base, 190 mM glycine, 0.1% SDS (w/v)
2	1x Transfer buffer for Western blot	25 mM Tris base, 190 mM glycine, 20% HPLC grade methanol (v/v)

3	2x Laemmli buffer 1	4% SDS (w/v), 10% 2-mercaptoethanol (v/v), 20% glycerol (v/v), 0.004% bromophenol blue (w/v), 0.125 M Tris HCl (pH 6.8)
4	4% paraformaldehyde (PFA)	1x PBS (pH 7.4-7.6), 4% paraformaldehyde (w/v)
5	Blocking buffer for flow cytometry-based intracellular staining	1x PBS (pH 7.4-7.6), 0.01% NaN ₃ (w/v), 1% BSA fraction-V (w/v), 0.1% saponin (w/v)
6	Blocking reagent for Western blotting	3% BSA fraction-V in TBST
7	Methylcellulose media for plaque assay	Complete DMEM media, 2% Methylcellulose (w/v)
8	Permeabilization buffer for flow cytometry-based intracellular staining	1x PBS (pH 7.4-7.6), 0.01% NaN ₃ (w/v), 0.5% BSA fraction-V (w/v), 0.1% saponin (w/v)
9	RIPA (Radio Immunoprecipitation Assay buffer) lysis buffer for Western blot and Co-IP method	150 mM sodium chloride, 1.0% NP-40 or Triton X-100 (v/v), 0.5% sodium deoxycholate (w/v), 0.1% SDS (sodium dodecyl sulfate) (w/v), 50 mM Tris, pH 8.0
10	Tris-buffered saline (TBS)	0.0153 M Trizma-HCl, 0.147 M NaCl in ultrapure water (Milli Q), pH adjusted to 7.6 by HCl
11	Tris-buffered saline Tween-20 (TBST)	0.05% (v/v) Tween-20 in 1x TBS

5. Methods

5.1. Isolation of Mouse Peritoneal Macrophages

6-8 weeks old BALB/c and C57BL/6 mice were used to isolate peritoneal macrophages as per the protocol described earlier. In brief, each of 5-6 male mice per set was injected with 1ml of 3.8% Brewer's thioglycolate solution. The mice were euthanized after 72 h and the peritoneum lavage was collected in a sterile manner using chilled 1X PBS+3% FBS in a laminar air flow hood. The cells were washed two times with room temperature (RT) 1X PBS at 350g for 5 minutes at 4°C. Then the cells were resuspended in complete RPMI media and plated in 90 mm dishes at a density of 6×10^6 cells/dish. After 12-15 h of seeding, the cells were washed once with 1X PBS (RT) and subjected to further experimentation with the adherent monocyte-macrophage population.

5.2. Isolation of hPBMC-derived Adherent Myeloid Lineage of Cells

To isolate human peripheral blood mononuclear cells (hPBMC)-derived adherent myeloid cells, blood was drawn from healthy human participants obeying the guidelines issued by Institutional Ethics Committee, NISER, Bhubaneswar (NISER/IEC/2022-04). The protocol to generate adherent myeloid lineage of cells was followed as described elsewhere with little modifications. Briefly, the collected blood was initially diluted with an equal volume of chilled 1X PBS and mixed thoroughly with a serological pipette. Then 2-3 ml of cold Hi-Sep LSM solution was added in a sterile 15 ml tube. While the tube was held in a tilted fashion, slowly the diluted blood was added over the Hi-Sep LSM up to the total volume of 12-13 ml in a dropwise manner. Next, all of the 15 ml tubes were centrifuged at 350 RCF, 25°C for 32 minutes with slow acceleration and slow decrease of the rotation. After centrifugation, the middle layer containing hPBMC i.e., the buffy coat was collected in another 15 ml tube and washed twice with 1X PBS (RT) at 350g, 25°C for 5 minutes. Then, the cells were counted and plated in 6 well plates at a

density of 10×10^6 cells/ well with 1 ml RPMI complete media. Following the enrichment of adherent circulating monocytes for 2 h, the nonadherent cells were separated by washing with 1X PBS (RT). After 96-120 h, the adherent cells were found to be of monocyte-macrophage lineage (>97% of the cells showed $CD11b^+CD14^+$) (166,167). The culture media was changed in each 24 h after 1X PBS (RT) wash.

5.3. PMA-induced Differentiation of THP-1 Cells

Phorbol-12-myristate-13 acetate (PMA) induced differentiation of THP-1 cells was performed as mentioned elsewhere with a little modification (168). In brief, 2×10^6 THP-1 cells were plated in each well of a 6-well plate with 2 ml of complete RPMI media and stimulated with PMA at 100 ng/ml concentration for 48 h followed by culture in PMA-free complete RPMI media for another 48 h before experiments.

5.4. MTT-based Viability Assay

The working concentration of TAK-242, a well-cited TLR4 inhibitor, was determined using the 3-(4,5-Dimethylthiazol-2-yl)-2,5-diphenyltetrazolium bromide (MTT)-based viability assay in THP-1 and hPBMC-derived monocyte-macrophage cells obeying the manufacturer's protocol (169). Briefly, 5×10^3 cells were seeded per well of a 96-well cell culture plate for 16-18 h. Next, the cells were washed with 1X PBS (RT) two times and the drug with different concentrations was added in a triplicate manner. DMSO was used as solvent control. After 24 h of incubation, the cells were washed and 100 μ l of RPMI without phenol red mixed with 10% MTT solution was added per well and the cells were further incubated at 37°C to form the formazan crystals. After visible crystal formation, the solution was carefully discarded and 100 μ l of solubilization buffer was added per well. The cells were incubated for 15 minutes at 37°C and the absorbance reading was taken at 550 nm in the microplate reader (BioTek, USA). The percent of

viable cells upon drug treatment was calculated concerning solvent control (DMSO).

5.5. AnnexinV-7AAD-based Viability Assay

The working concentration of TAK-242 in RAW264.7 and peritoneal macrophages was determined by AnnexinV-7-AAD-based viability assay as per the manufacturer's protocol (170). Briefly, the cells with differential treatments were harvested into microcentrifuge tubes by gentle scraping and washed with cold 1X PBS 2 times at 350g, 4°C for 5 minutes. Next, 100 µl of 1X AnnexinV binding buffer along with 2.5 µl of Annexin V and 7-AAD was added in each tube for 1×10^6 cells. The cells were incubated at dark for 15 minutes in RT. Further, 400 µl of AnnexinV binding buffer was added per tube and the samples were transferred in RIA vials for immediate acquisition in BD LSRFortessa (BD Biosciences, USA). The data were analyzed in FlowJo (BD Biosciences, USA). A total of ten thousand cells per sample was acquired.

1.6. LPS Stimulation in RAW264.7 Cells

To study the TLR4-dependent pro-inflammatory responses, lipopolysaccharide (LPS) was used to induce RAW264.7 cells as per the protocol mentioned earlier with little modifications (27). In brief, 4.5×10^6 cells were seeded in 90 mm dishes in 10 ml RPMI complete media. After 16-18 h incubation, the cells were washed twice with 1X PBS (RT) and pre-incubated with either DMSO or TAK-242 for 3 h. Next, the cells were washed with 1X PBS once and LPS was added in 500 ng/ml concentration in the respective dishes. After 6 h of incubation, the cells were washed, harvested with a cell scraper, and subjected to further experimentation.

1.7. The Treatment of Modulators in Macrophages

TAK-242 is a specific pharmacological antagonist of TLR4, which has been currently in wide use to explore the role of TLR4 in different clinical abnormalities at final phase trial levels (10,20). This cyclohexene derivative was used to investigate the possible association of TLR4 during CHIKV infection in the current project. The drug was used to pre-incubate the macrophages 3 h prior to CHIKV infection, during infection and post-infection incubation.

SB203580 (p-P38 inhibitor) and SP600125 (p-SAPK/p-JNK inhibitor) were used to pre-incubate the RAW264.7 cells 2 h prior to CHIKV infection, during infection and post-infection incubation. The culture supernatant was collected at 8 hours post-infection (hpi) and subjected to indirect co-culture with syngeneic naive T cells to investigate the possible association of p38 and JNK-MAPK pathways on T cell activation upon CHIKV infection.

1.8. CHIKV Infection in Absence/ Presence of TLR4 Inhibition

The macrophage cells of different origins were infected with CHIKV as per the method described below,

5.8.1. CHIKV infection in RAW274.7 and Murine Peritoneal Macrophages

The dose and time kinetics of CHIKV-IS infection in RAW264.7 cells were earlier standardized and reported by us (7). In brief, RAW264.7 cells with low passage number (passage no.-16-22) were cultured at 60-80% confluency in cell culture flasks. 6×10^6 cells were seeded in 90 mm cell culture dishes in 10 ml volume. After 16-18 h incubation, the cells were washed with 1X PBS (RT) twice and pre-incubated with either DMSO or the drug in serum-free media (SFM) for 3 h. Next, the cells were washed once with 1X PBS (RT). The CHIKV infection was given at MOI 5 for 2 h in the absence/ presence of the drug with an infection volume of 900 μ l SFM. During the CHIKV infection, the dishes were shaken at 10-minute intervals to avoid non-homogeneity of virus infection. After CHIKV infection, the cells were washed with 1X PBS twice and supplemented with RPMI complete media comprising 5% FBS with/without the drug. The cells were harvested at 8 hpi using a sterile cell scraper and subjected to further downstream experiments.

5.8.2. CHIKV infection in hPBMC-derived Primary Macrophages

hPBMC-derived adherent monocyte-macrophage cells were seeded in 12 well plates at a density of $0.8-1 \times 10^6$ cells/well in 1.5 ml complete RPMI media and incubated for 24 h. Next, the

cells were washed two times with 1X PBS (RT) and preincubation with the drug was given in SFM. The cells were further washed once with 1X PBS (RT) and CHIKV infection was given at MOI 5 for 2 h in 200 µl volume. After CHIKV infection, the cells were washed two times with 1X PBS (RT) and supplemented with complete RPMI media with 5% FBS. Finally, the cells were harvested at 8 hpi and subjected to flow cytometry staining.

5.8.3. CHIKV infection in THP-1-derived Macrophage-like Cells

To infect the PMA-induced macrophage-like cells, 2×10^6 monocyte cells were initially seeded in each well of a 6-well cell culture plate. Following the PMA-driven differentiation process as described above, the cells were washed once with 1X PBS (RT), and the drug treatment was given in SFM for 3 h. The cells were washed and CHIKV infection was given at MOI 5 for 2 h in SFM with a volume of 250 µl/well. After CHIKV infection, the cells were washed twice with 1X PBS (RT) and were supplemented with complete RPMI media consisting of 5% FBS. Finally, the cells were harvested at 8 hpi and processed for further experimental steps.

1.9. Plaque Assay

The plaque assay was performed in Vero cells to determine the viral titer present in cell-free culture supernatant as per the protocol described earlier (7,8). In brief, CHIKV-infected cell-free culture supernatants were serially diluted and used to infect the Vero cells. The Vero cells were seeded at a density of 2×10^6 cells/well in 1 ml of complete DMEM media. After 16-18 h of post-seeding, the cells were washed twice with 1X PBS (RT), and the serially diluted cell culture supernatants were added in respective wells at a volume of 200 µl. The cells were infected for 90 minutes and washed twice with 1X PBS (RT) followed by the application of 5% FBS-supplemented DMEM media mixed with 2% methyl-cellulose over the infected cells. After 4-5 days, the cells were fixed using 8% formaldehyde and further stained with crystal violet. The plaque-forming units (PFU) were manually counted under the white light of a trans-illuminator (Vilber Lourmat, France).

5.10. qRT-PCR Analysis

The viral RNA from cell-free culture supernatants was isolated using the QIAamp Viral RNA mini kit (Qiagen, Hilden, Germany) as per the manufacturer's protocol (25). In brief, 140 μ l of undiluted cell culture supernatant was added with 560 μ l of AVL buffer and 5.6 μ l of carrier RNA in a microcentrifuge tube. The components were mixed by pulse vortexing for 15 seconds and kept at RT for 10 minutes. The tubes were centrifuged at 1000g for 30 seconds to remove the droplets in the lid. Next, 560 μ l of 70% ethanol (MB grade) was added to each tube followed by centrifugation at 1000g for 30 seconds. Then, 630 μ l out of a total 1260 μ l volume was added in a spin column and centrifuged at 6000g for 1 minute. The columns with absorbed viral RNA were washed sequentially with 500 μ l of AW1 and AW2 buffer at 6000 and 15000 g for 1 minute respectively followed by a blank centrifugation at 15000 g for 1 minute. Finally, the washed RNA samples were eluted in a new tube in 20 μ l of AVE buffer.

HiPurA[®] Total RNA Miniprep Purification Kit (HiMedia Laboratories Pvt. Ltd., MH, India) was used to isolate cellular RNA including intracellular viral RNA copies as per the manufacturer's instructions (171). Briefly, the harvested cells were washed twice with 1X PBS (RT). The RNA lysis buffer (350 μ l/sample) along with beta-mercaptoethanol (3.5 μ l/sample) was added into the cells (up to 5×10^6 cells/sample) followed by vigorous vortexing for two minutes. Next, 350 μ l of 70% MB grade ethanol was added to each sample. To isolate the RNA copies, the total 700 μ l volume was added into the HiSpin column and centrifuged at 8000g for 15 seconds. Next, the column-bound RNA copies were washed with pre-wash and wash solutions respectively followed by elution into 25 μ l of elution buffer.

For viral RNA copies quantification from the cell-free culture supernatant, equal volumes of RNA from all experimental conditions were taken for cDNA synthesis using Primescript[™] 1st strand cDNA synthesis kit (Takara Bio Inc, Kusatsu, Shiga, Japan). The E1 gene was amplified using E1 primer (the primer sequence is given in Table X) and PowerUp[™] SYBR[™] Green Master Mix (Thermo Fisher Scientific, USA). The C_t values were plotted against the aforementioned standard curve to determine the corresponding viral copy number.

To quantitate the intracellular viral RNA copies, 1 µg of RNA was converted to cDNA using either First Strand cDNA synthesis kit (Thermo Fisher Scientific, USA) or Primescript™ 1st strand cDNA synthesis kit (Takara Bio Inc, Kusatsu, Shiga, Japan). This cDNA was used to amplify the E1 gene and GAPDH as corresponding housekeeping gene control (the primer sequences were given in Table number X) in Applied Biosystem QS7 flex real-time PCR system (Applied Biosystem, USA).

5.11. Flow Cytometry (FC)-based Analysis

The percent cellular expression of different cellular markers and viral proteins such as CHIKV-E2 were investigated in flow-cytometry-based analysis using either surface staining (SS) or intracellular staining (ICS) as per their localization obeying the protocol as described before (7). The cells were stained for either SS or ICS as per the protocol described elsewhere with little modifications. For ICS, the harvested cells were washed with 1X PBS and fixed with 4% PFA for 10 minutes at RT. After washing, the fixed cells were permeabilized using the permeabilization buffer (0.5% BSA, 0.1% Saponin, 0.01% Sodium azide in 1X PBS) for 10 minutes at RT followed by blocking using the blocking buffer (1% BSA, 0.1% Saponin, 0.01% Sodium azide in 1X PBS) for 30 mins at RT. The primary antibodies diluted in permeabilization buffer were added for 30 minutes at RT followed by AF647 or AF488 tagged secondary antibodies were added for 30 mins at room temperature at dark. Next, the cells were washed in permeabilization buffer, resuspended in FACS buffer (1% BSA, 0.05% Sodium azide in 1X PBS), and kept at 4°C until the acquisition in the flow cytometer.

For, SS, the harvested cells were washed twice with 1X PBS (RT), and FcR blocking reagent (Miltenyi Biotec, Germany) was added during the staining of macrophages at 1:20 dilution to reduce nonspecific interactions. Next, the cells were washed with FACS buffer, and fluorophore-conjugated or unconjugated primary antibodies were added followed by an incubation of 30 minutes at 4°C. For unconjugated antibodies, the primary antibody-tagged cells were washed twice

with FACS buffer, and corresponding secondary antibodies were added. After 30 minutes of incubation, the cells were washed and resuspended in FACS buffer followed by immediate acquisition in BD LSRFortessa and analysis by FlowJo software (BD Biosciences, USA). The anti-mouse and rabbit IgG antibodies were used as isotype control during staining. The gating was performed based on isotype scattering. Around ten thousand cells were acquired for each sample.

5.12. Sandwich ELISA for Cytokine Analysis

The cell-free culture supernatants were collected from different experimental conditions and kept at -80°C prior to the quantification using BD OptEIA™ Sandwich ELISA kit (BD biosciences, USA) as per the manufacturer's protocol (172–175). In brief, the 96-well strip immunoplates were coated with the capture antibody diluted in coating buffer overnight at 4°C to facilitate optimum coating. On the next day, the plates were washed with the wash buffer 3 times and blocked with the assay diluent for 1 h at RT. Next, the diluted samples and standards were added after washing the wells and the plate was incubated for 2 h at RT. After the antigen binding, a working detector (detection antibody+ HRP) was added followed by an incubation of 1 h at RT. Then, the wells were washed with wash buffer 7 times and the 1X substrate solution (TMB/ H_2O_2) was added to the wells followed by an incubation for 15-30 minutes in dark at RT. After the development of a bluish color, the enzyme-substrate reaction was stopped by the addition of the stop solution i.e., $2\text{N H}_2\text{SO}_4$. Immediately, the optical density reading was taken in an Epoch2 Microplate reader (BioTek, USA) at 450 nm. The concentration of the cytokines at different conditions was calculated based on the corresponding standard curve.

5.13. Western Blot Analysis

The differential expression of MAPK-pathway proteins and TLR4 was assessed by a Western-blot-based method following the same protocol as described earlier (7). The cells of different conditions were harvested by gentle scraping with a cell scraper followed by washing

with 1X PBS (RT). Next, the cells were lysed by Radio Immuno Precipitation Assay (RIPA) lysis buffer. In brief, after lysis buffer addition, the cells were kept at 4°C and were vortexed in every 15-minute interval for up to 1 h followed by centrifugation at 15000 rpm, 4°C for 30 minutes. The clear supernatants were collected and quantified using the Bradford method. Next, equal amounts and volumes of proteins (20-30 µg of protein in 10-25 µl volume) mixed with Laemmli buffer were loaded in 10% SDS-PAGE gel along with molecular weight markers. After the gel run step, the gel was washed with excess distilled water to remove any trace of excess salts and soaked in 1X transfer buffer for 5-10 minutes. In the meantime, PVDF membranes were charged with ice-cold methanol for 5 minutes followed by washing in 1X transfer buffer to remove the excess charge. Then, the transfer cassette was prepared and the proteins on the SDS-PAGE gel were transferred into the PVDF membrane for either 2 h or overnight (12-15 h) depending on the experimental requirements. Next, the PVDF membrane was blocked with blocking buffer (3% BSA in TBST) for 1 h, and the primary antibodies were added for overnight incubation at 4°C. The next day, the blots were washed with 1X TBST 3 times to remove nonspecific background and probed with HRP-tagged secondary anti-mouse or rabbit antibodies for 2 h at RT. Lastly, the blots were washed with 1X TBST 5 times and kept in 1X TBS until detection. The blots were detected using Immobilon Western chemiluminescent HRP substrate (Millipore Merck, USA) or SuperSignal West Femto (Thermo Fisher Scientific, USA) in ChemiDoc XRS⁺ imaging system and analyzed in Image Lab software (Bio-Rad, USA).

Fold change calculation: GAPDH or Beta-actin was used as the housekeeping gene. To calculate the differential fold change, the density of a particular marker and corresponding housekeeping gene was determined in different conditions (Density-adjusted volume of the band / Area of the band). Then, the differential fold change of the marker was calculated (Density of protein X at condition Y/ Density of housekeeping gene at Condition Y). Next, the differential fold change was normalized concerning untreated/ mock conditions (Fold change of marker X in all conditions/Fold change of marker X in mock or untreated conditions).

5.14. Co-immunoprecipitation Study

To study the probable protein-protein interaction, the RAW264.7, and TLR4KO RAW cells were infected with CHIKV at MOI 5 as described above. To harvest the cells, The culture dishes were washed twice with 1X PBS (RT) to remove traces of FBS, and RIPA lysis buffer (the same composition as used in Western blot analysis) was directly added to the culture dishes. The cell lysate was collected and processed as per the protocol described in the Western blot section. Next, the cell lysates were used for co-immunoprecipitation studies using Dynabeads[®] Protein G kit (Thermo Fisher Scientific, USA) as per manufacturer's instructions. Briefly, the cell lysates were incubated with the anti-CHIKV-E2 antibody (the antibody used to pull down its interacting partner) overnight at 4°C. On the next day, the protein G beads were washed with wash buffer 3 times and finally resuspended in wash and binding buffer. The beads were added to the cell lysates and incubated at 4°C for 3 h. Next, the beads were separated from the lysate with the help of a magnet and washed 3 times with the wash buffer. Then elution buffer and 4X Laemmli buffer were added to the beads and incubated at RT for 10 minutes. Finally, the beads were heated at 100°C for 10 minutes in a dry bath (Labnet, USA) and the solution devoid of beads was collected to a new microcentrifuge tube with the help of a magnetic separation process. The final solution was loaded in a 10% SDS-PAGE gel along with the input samples (the crude lysate) in a Western blot-based method.

5.15. *In silico* Analysis

The ClusPro2.0 web server (176,177) was used to study the protein-protein interaction. Three computational steps are used by this program to generate the output. The first step involves rigid-body docking based on the Fast Fourier Transform (FFT) correlation approach with a scoring function, $E = w_1E_{rep} + w_2E_{attr} + w_3E_{elec} + w_4EDARS$. The E_{rep} , E_{attr} , and E_{elec} represent the repulsive, attractive, and electrostatic energy terms respectively. The contribution of the pairwise structure-based potential is represented as EDARS (177,178). Following this scoring, the 1,000

lowest energy-docked structures are clustered in the second step. Based on the pairwise interface RMSD (IRMSD)(177,179), the center of the first cluster is defined as the structure with the highest neighbors within a 9 Å radius. This is followed by the clustering of the remaining structures to generate 30 clusters. The energy is minimized in the third step(177). Following this, the 10 clusters with the highest members are given as the output in the third step. The myeloid differentiation factor 2 (MD-2) was used as the receptor in the study. This structure was extracted from the crystal structure of mouse TLR4 and mouse MD-2 complex (PDB ID: 2Z64) available in the protein data bank (PDB) database(180) using the Discovery Studio Visualizer program and minimized. The CHIKV E1 and E2 structures were similarly extracted from the crystal structure of the mature envelope glycoprotein complex of CHIKV (PDB ID: 3N41) (181). The co-crystallized ligands and water molecules were removed from each of these structures and energy was minimized. The structures of CHIKV E1 and E2 were used as ligands for the protein-protein interaction study. The protein-protein interaction study in the ClusPro2.0 web server generated four different types of results. Based on the scoring algorithms these are categorized as “balanced”, “electrostatic-favored”, “hydrophobic-favored”, and “Van der Waals+ electrostatic”. In the absence of any experimental data, balanced outputs are generally preferred for further analysis (8). The first docking solution clusters usually have the largest members. Therefore, this was taken for further visualization in the PyMol software.

5.16. Anti-TLR4-antibody-driven Neutralization Assay

To investigate the possible role of TLR4 as a receptor of the CHIKV-E2 protein, an anti-TLR4 antibody-driven neutralization assay was performed in RAW264.7 cells obeying the similar protocol as described earlier (32). Briefly, the cells were seeded in cell culture plates and incubated for 16-18 h. Next, the cells were washed once with 1X PBS (RT) and pre-incubated with an anti-TLR4 antibody with or without TAK-242 (a TLR4 inhibitor) for 3 h before CHIKV infection. The cells were finally harvested at 8 hpi and further processed for downstream experiments.

5.17. Time of addition assay

To study the possible association of TLR4 in the post-entry CHIKV life cycle, a time of addition experiment was performed in RAW264.7 cells as per the protocol described earlier with little modifications (21,25,26,30). In brief, no drug treatment was given to inhibit TLR4 before or during CHIKV infection. The drug was only given at different time points of post-infection incubation starting from 0 to 14 hpi at 2 hpi intervals and the cell culture supernatants were collected at 15 hpi. The supernatants were subjected to analysis by plaque assay-based method.

5.18. Effect of TLR4 inhibition before, during and after CHIKV infection

To investigate the specific stages of viral infection where TLR4 inhibition is most effective, TAK-242 was added in RAW264.7 cells at different stages of CHIKV infection, likely, pre-incubation, during infection, pre+ during infection, post-infection incubation at 0 and 8 hpi. The culture supernatants were collected at 9 hpi and qRT-PCR-based analysis was performed to quantitate the CHIKV-E1 gene copy number.

5.19. Temperature-shift assay

To further understand the role of TLR4 in CHIKV attachment and/or entry procedure in detail, the temperature shift assay was performed as mentioned earlier with certain modifications (182). The RAW264.7 cells were either treated with DMSO or TAK-242 for 3 h prior to CHIKV infection (Pre-incubation). Following the pre-incubation, the cells were infected with CHIKV with MOI 5 for 2 h at 4°C for allowing only attachment of viral particles to the cells and the next 2 h at 37°C for viral entry. The inoculum volume was collected to estimate the unbound virus particles by qRT-PCR. Next, the cells were gently washed with 1X PBS once and supplemented with an equal volume of fresh serum-free media (SFM). Following that, the cells were placed at 45°C for 30 minutes to detach the un-internalized viral particles. Next, the supernatants were collected and qRT-PCR analysis of the E1 gene was performed.

5.20. Viral Attachment Assay

To understand the possible role of TLR4 inhibition on viral adsorption during CHIKV infection, a viral attachment assay was performed to quantify the unbound virus particles during CHIKV infection in the absence or presence of CHIKV infection in RAW264.7 cells. In brief, the RAW264.7 cells were treated with DMSO or TAK-242, a TLR4 antagonist for 3 h and then CHIKV infection was given at MOI 5 for 2 h. After CHIKV infection, the infection volume/ wash containing unbound viruses was collected and further analyzed by plaque assay and qRT-PCR-based method.

5.21. *In vivo* effect of TLR4 inhibition in BALB/c mice

The *in vivo* animal experiments were conducted strictly under the guidelines of The Committee for the Purpose of Control and Supervision of Experiments on Animals (CPCSEA) of India. All experimental procedures were reviewed and approved by the Institutional Animal Ethics Committee (76/Go/Rebi/S/1999/CPCSEA, 28.02.17).

The mice were housed and kept for breeding under specific pathogen-free conditions at the animal house facility. For CHIKV infection, 8-9 days-old mice were infected with 1×10^6 pfu of CHIKV-IS subcutaneously at the flank region of the right hind limb. For uninfected control (mock), SFM was injected in the same region of mice. The drug, TAK-242 (specific antagonist of TLR4), was given orally to the CHIKV-treated group of mice (n=5) from one day before CHIKV infection to 4 days post-infection at every 24 h interval. The CHIKV-untreated group received the solvent only. All of the animals were monitored every day for the disease symptoms. The mice were sacrificed at 5 dpi and the serum was isolated from blood. Different tissues were kept in SFM and were snap-frozen in liquid nitrogen for Western blot analysis. An equal quantity of tissues was homogenized in an equal volume of SFM. After that homogenous mixture was passed through the 0.22 μ m syringe filter and subjected to the plaque assay. For the survival curve and clinical score studies, the above-mentioned infection and treatment protocols were followed (n=5 mice in three groups). However, the compound was administrated from one day before infection to 6 dpi at

every 24 h interval. The clinical score was given to each mouse daily according to the phenotypic symptom-based disease outcomes [no symptoms-0, fur rise-1, hunchback-2, one hind limb paralysis-3, both hind limb paralysis-4, death-5]. The mice mortality was noted for the survival curve analysis.

5.22. Splenocyte isolation and purification of T cells

The splenocytes were isolated from the spleen of 6-8 weeks old male BALB/c mice as demonstrated earlier. In brief, the dissected spleens were crushed in a Petri plate using a sterile plunger of a 2 ml injection syringe and a 70 μ M cell strainer to remove the debris. Next, the RBCs were lysed by 1X RBC lysis buffer followed by washing in 1X PBS (RT) for once. After removal of lysed debris, the splenocytes were pelleted down and T cell purification was done using Untouched Mouse T Cell Isolation Kit (Invitrogen, USA) as per manufacturer's protocol. In brief, the splenocytes were resuspended in FBS and biotinylated antibody cocktail (antibodies against all types of splenocytes except T cells) for 20 minutes at 4°C. Next, the cells were washed with an isolation buffer and resuspended in streptavidin-coated magnetic beads for 15 minutes at RT. Lastly, the T cells were enriched (purity > 95%; determined by flow cytometry) through a magnetic separation mechanism.

5.23. Indirect Co-culture of syngeneic T cell and Macrophage, *in vitro*

The RAW264.7 cells were infected with CHIKV in the presence or absence of p-p38 and p-JNK inhibitors namely, SB203580 and SP600125, respectively. Next, the culture supernatants were collected at 8 hpi and stored at -80°C until the co-culture experiment. Prior to the experimentation, the anti-TNF antibody was added to the CHIKV-infected supernatant and incubated for 4 h at RT to prepare TNF-neutralized CHIKV-infected supernatant condition.

The purified syngeneic T cells were seeded in 24-well cell culture plates (SPL Biosciences, South Korea) with macrophage supernatants and fresh RPMI media at a 1:1 ratio for 36 h with/without T cell receptor (TCR) stimulation. For TCR-treated conditions, 2-3 μ g of anti-

CD3 antibody was coated in the corresponding wells and 2-4 µg of anti-CD28 antibody was added in the final culture media. For, ConA driven activation, 5 µg/ml concentration was used to stimulate the T cells. After, 36 h of incubation, the cells were harvested and processed for flow cytometry-based staining.

5.24. Statistical Analysis

GraphPad Prism 9 software (GraphPad Software Inc., San Diego, CA, USA) was used for statistical analysis. All comparisons between different groups were performed by One/Two-way ANOVA with Tuckey post-hoc test and all data were represented as Mean ± SEM. All analyzed data are representative of at least 3 independent experiments with $p < 0.05$ taken as statistically significant.

Chapter #4

Results and Discussion

6. Results:

To investigate the role of TLR4 inhibition in different primary cells and cell lines, TAK-242, a cyclohexene derivative small molecule acting as a specific antagonist of TLR4, was used. Earlier, it was reported that TAK-242 effectively reduces LPS-driven pro-inflammatory responses at 1 μ M concentration in RAW264.7 and peritoneal macrophages obtained from BALB/c mice. However, the working concentration of TAK-242 was further validated and determined in RAW264.7 cells, peritoneal macrophages obtained from BALB/c, and C57/BL/6 mice using the Annexin V-7-AAD-based method. Also, the viability assay for TAK-242 was performed in hPBMC-derived macrophages and PMA-induced THP-1 cells using MTT assay. It was noticed that after 24 h incubation with the drug, more than 95% of cells from all sources remained viable at 1 μ M concentration (**Fig: 23-A-E**). Hence, 0.5 and 1 μ M concentrations were selected for all in vitro experiments of the current project.

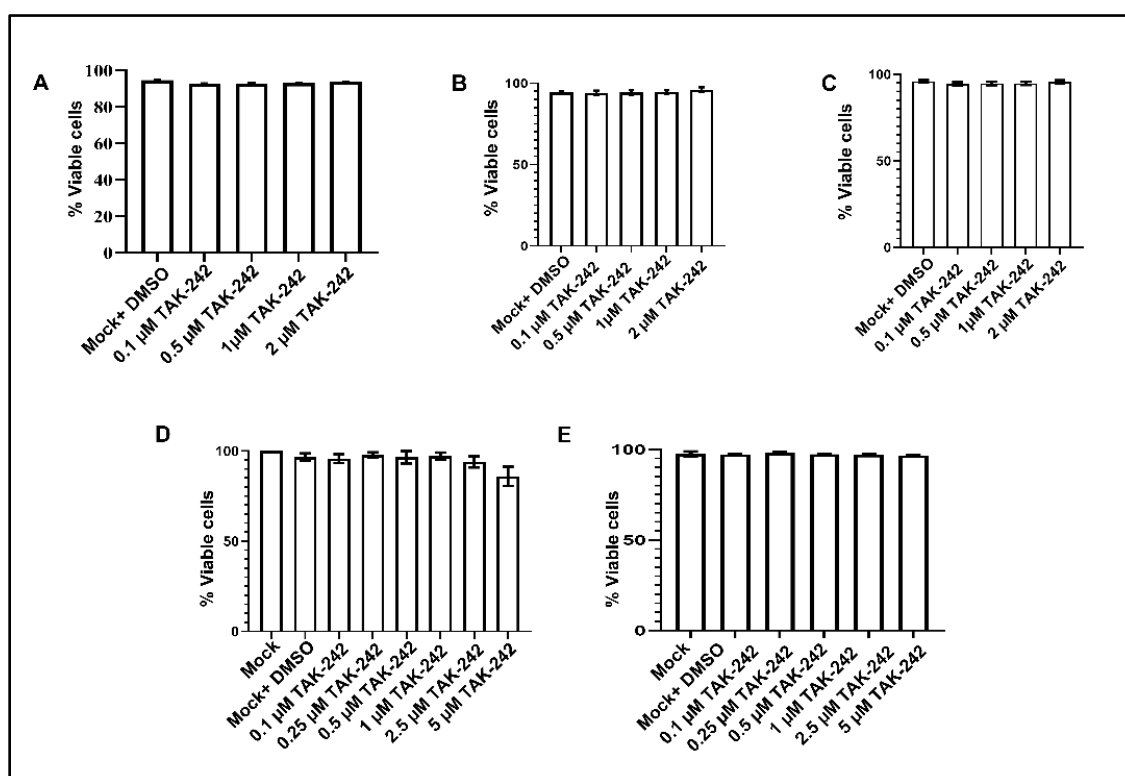


Figure 23: The cell viability assay using different sources of macrophages to determine the working concentration of TAK-242. Annexin V-7-AAD-based cell viability assay has been

performed in (A) RAW264.7 cells, peritoneal macrophages obtained from (B) BALB/c and (C) C57BL/6 mice. MTT-assay-based viability assay has been performed to determine the effective concentration of TAK-242 in (D) hPBMC-derived macrophages and (E) PMA-induced THP-1 cells.

TAK-242 was incubated with mock RAW264.7 cells for 3 h to investigate whether the drug alone may modulate surface and/or total TLR4 expression. It was observed that there was no significant change in cellular TLR4 level in terms of surface or total expression in the presence of 1 μ M TAK-242 (Fig: 24-A-C). Hence, TAK-242-driven TLR4 inhibition is only effective in the presence of LPS or CHIKV-induced proinflammatory conditions.

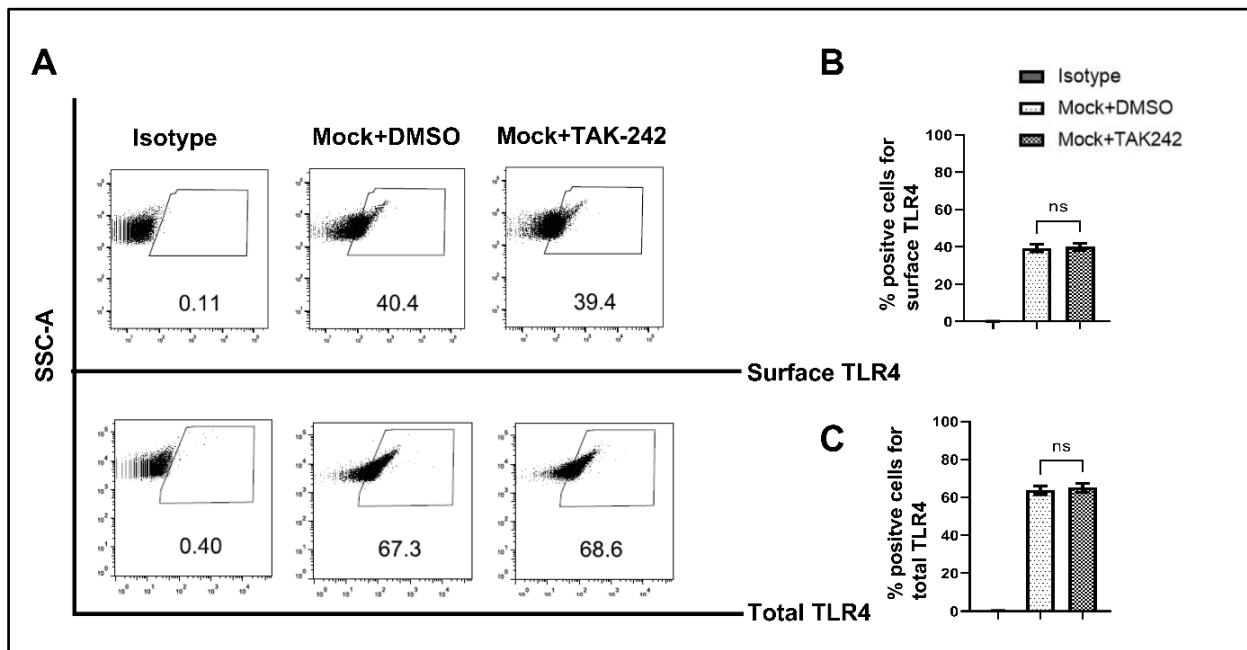


Figure 24: TLR4 expression in mock RAW264.7 cells in the presence or absence of TAK-242. The RAW264.7 cells were either treated with DMSO or TAK-242 for 12 h and harvested for further experiments. (A) The flow cytometry-based dot plot analysis revealed percent positive cells for surface and total TLR4 and the corresponding bar diagrams, (B) and (C) respectively, denoting the results obtained from 3 independent experiments. Data represent the Mean \pm SEM of three independent replicates. (ns=non-significant)

6.1. TLR4 inhibition abrogates LPS-induced macrophage activation and pro-inflammatory responses in the host macrophages, *in vitro*.

Earlier published reports had already shown that TAK-242-mediated TLR4-inhibition efficiently reduces LPS-driven pro-inflammatory responses in macrophages the RAW264.7 and peritoneal macrophages obtained from BALB/c mice (20). Therefore, the immune-modulatory role of TAK-242 in LPS-treated RAW264.7 cells was studied as the experimental control of the current investigation.

As per the previous reports, the reduction in surface expression and increase in total expression of cellular TLR4 had been observed due to LPS or virus-induced immune activation (15,183,184). Similarly, the flow cytometry dot plot-based analysis showed a significant increase in total TLR4 during LPS treatment in the presence or absence of pre-incubated TAK-242 [66.5 ±2.22 % (Mock) to 89.5±1.59 % (LPS) and 85.5±1.68 % (TAK-242+LPS)] (**Fig: 25-A, B**). Also, the surface expression of TLR4 was significantly reduced during LPS treatment in the presence or absence of TAK-242 [43.4±1.42% (Mock) to 27.6±1.1% (LPS) and 36.1±0.757% (LPS+TAK-242)] (**Fig: 25-A, C**).

The expression of CD14, a macrophage activation marker as well as an upstream molecule of the LPS-driven TLR4 signaling pathway, was investigated in the current study (167,185,186). The flow cytometry-based dot plot analysis showed a significant increase in percent positive cells for CD14 during LPS treatment, which had reduced in TAK-242-treated condition [16.233±2.44% (Mock) to 25.2 ±2.97% (LPS) and 21±3.03% (LPS+TAK-242)] (**Fig: 25-A, D**).

The inducible macrophage activation markers such as CD86 and MHC-II were already reported to be associated with immune-activation (7). Therefore, the modulation of these two markers was again studied using flow cytometry-based dot plot analysis in the current experimental setup. The percent positive cells expressing CD86 were found to increase during LPS

treatment and reduced further in the presence of pre-incubated TAK-242 [65.17±1.337% (Mock) to 71.30±1.553 % (LPS) and 66.13±1.325% (LPS+TAK-242)] (**Fig: 25-A, E**). Also, MHC-II showed a similar pattern of expression [40.07±1.707% (Mock) to 51.07±1.598% (LPS) and 47.33±1.338% (LPS+TAK-242)] (**Fig: 25-A, F**).

As per the earlier report, activation of TLR4 promotes phosphorylation and therefore, nuclear translocation of NF-κB, which further induces pro-inflammatory cytokines such as TNF responses (20,187). Therefore, p- NF-κB expression was studied in current experiments to investigate the regulatory role of TLR4 activation on pro-inflammatory cytokine responses. The flow cytometry-based study revealed the increase in percent positive cells for p-NF-κB during LPS treatment and a decrease upon TLR4 inhibition [14.73±2.153 % (Mock) to 37.15.6±3.762 % (LPS) and 25.23±2.533% (LPS+TAK-242)] (**Fig: 25-A, G**).

TAK-242-driven TLR4 inhibition in LPS-induced RAW cells was reported to reduce secretory TNF levels (20). ELISA-based quantification of secretory TNF levels was studied in the current experiment. In correlation to the earlier reports, it was noticed that TLR4 inhibition had significantly reduced secretory TNF level in LPS-induced macrophages [394.4±17.4 pg/mL (Mock) to 2585 ±57.69 pg/mL (LPS) and 552.5±13.06 pg/mL (LPS+TAK-242)] (**Fig: 25-H**).

Together, the results delineate the positive regulation of TLR4 in LPS-induced pro-inflammatory responses in RAW264.7 macrophages.

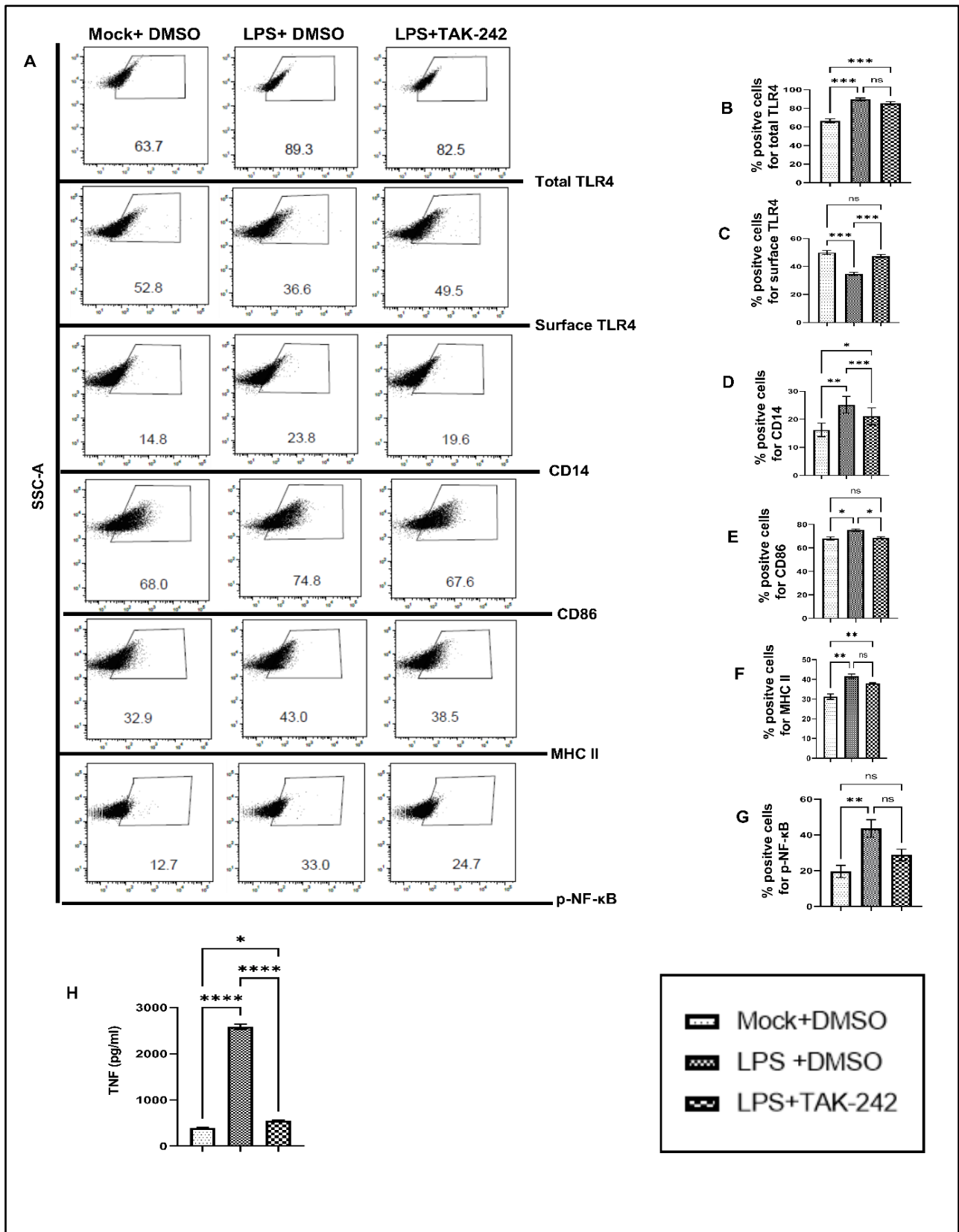


Figure 25: LPS-driven pro-inflammatory responses in RAW264.7 macrophage cells are regulated in a TLR4-dependent way. The RAW264.7 macrophages were pre-treated with either

DMSO or TAK-242 for 3h followed by LPS stimulation at 1µg/ml for 6 h. Next, the cells were harvested and stained further for flow cytometry-based analysis. The cell culture supernatants were also collected for ELISA-based cytokine analysis. (A) The flow cytometry-based dot plot analysis of percent positive cells shows the expression of (B) Total TLR4 (C) Surface TLR4 (D) CD14 (E) CD86 (F) MHC-II & (G) p-NF-κB. (H) The ELISA-based study depicts the secretory level of TNF in different conditions. Data represent the Mean ± SEM of three independent replicates. (ns=non-significant, * $p<0.05$, ** $p\leq0.01$, *** $p\leq0.001$, **** $p\leq0.0001$).

6.2. TLR4 antagonism reduces CHIKV infection in the host macrophages of different origins, *in vitro*.

6.2.1. Inhibition of TLR4 abrogates CHIKV infection in the RAW264.7 cells, significantly.

The protocol for CHIKV infection in the RAW264.7 cells was already standardized and published earlier by us. The previous kinetics study had reported that CHIKV-IS infection at MOI 5 for 2 h directs maximum infection in RAW264.7 macrophages at 8 hours post-infection (hpi) time point. Therefore, the 8 hpi time point was used in all *in vitro* experiments (7,8). The CHIKV envelope protein E2 was selected as a marker to assess CHIKV infection in different host macrophages (7,21,25,26,30).

To investigate the possible role of TLR4 in CHIKV infection, the RAW264.7 cells were pre-incubated with TAK-242, a selective antagonist of TLR4, for 3 h before virus treatment. Next, the cells were infected with CHIKV-IS at MOI 5 for 2 h. The infected cells were harvested at 8 hpi and further stained for flow cytometry-based analysis of viral E2 protein and macrophage activation markers. Moreover, the culture supernatants were assessed for qRT-PCR-based CHIKV-E1 gene copy number analysis and ELISA-based pro-inflammatory cytokine analysis. The TAK-242-treated condition showed a significant decrease in percent positive cells for CHIKV-E2 [15.43 ±0.5175 % (CHIKV) to 9.813±0.8411% (TAK-242)] (**Fig: 26-A, B**) and a

significant reduction in CHIKV-E1 copy number [58%] (**Fig: 26-C**), which might be indicative towards anti-viral role of TLR4 antagonism.

Next, the surface expression of TLR4 was found to significantly decrease during CHIKV infection and a further decrease was observed due to TAK-242-pretreatment in CHIKV-infected cells [from 45.33 ± 1.805 % (Mock) to 23.03 ± 2.266 % (CHIKV) and 18.2 ± 0.76 % ($1 \mu\text{M}$ TAK-242)] (**Fig: 26-A, D**). However, the total expression of TLR4 significantly increased during CHIKV infection in the presence or absence of TAK-242-mediated TLR4 inhibition [from 56.3 ± 2.066 (mock) to 75.5 ± 3.057 (CHIKV) and 73.2 ± 1.172 ($1 \mu\text{M}$ TAK-242)] (**Fig: 26-A, E**). The data was found linear with earlier LPS-mediated activation of TLR4. Therefore, the data might indicate CHIKV-induced activation and the internalization of surface TLR4 in host macrophages.

To determine the status of macrophage activation, the percent positive cells of CD14, CD86, and MHC-II were investigated during CHIKV infection with or without TLR4 inhibition. The results showed an increase in the percent positive cells of CD14 during CHIKV infection and further reduction in TLR4 inhibited condition) [from 5.57 ± 0.13 % (mock) to 27.9 ± 2.088 % (CHIKV) and 10.24 ± 1.157 % ($1 \mu\text{M}$ TAK-242)] (**Fig:26-A, F**). Another activation marker, CD86 showed a similar pattern of expression in terms of percent positive cells [from 71.67 ± 0.29 % (mock) to 89.03 ± 1.467 % (CHIKV) and 77.6 ± 0.7234 % ($1 \mu\text{M}$ TAK-242)] (**Fig:26-A, G**). Next, the percent positive cells for MHC-II also re-confirmed TLR4-inhibition-dependent reduction in macrophage activation [from 42.87 ± 4.889 % (mock) to 63.53 ± 1.12 % (CHIKV) and 50.07 ± 2.896 % ($1 \mu\text{M}$ TAK-242)] (**Fig: 26-A, H**). Together, the data reveals reduced macrophage activation status during TAK-242-driven TLR4 inhibition.

As per existing reports, phosphorylation of NF- κ B was shown to be linked with inflammation and an inducer of pro-inflammatory cytokines such as TNF, and IL-6 upregulation

(188,189). The massive cytokine burst in the form of a marked increase in TNF, IL-6, and MCP-1 was already reported by us and others (7,17). Therefore, flow cytometry-based dot plot analysis of p- NF- κ B was studied, which showed a significant upregulation of percent positive cells during CHIKV infection was regulated in the presence of TAK-242-driven TLR4 inhibition [from 19.37 ± 2.87 % (mock) to 33.43 ± 3.083 % (CHIKV) and 17.03 ± 2.854 % ($1 \mu\text{M}$ TAK-242)] (**Fig: 26-A, D**).

To explore the status of pro-inflammatory cytokines and chemokines, secretory levels of TNF, IL-6, and MCP-1 were assessed. ELISA-based quantification of TNF showed a significant increase during CHIKV infection and a reduction due to TLR4 inhibition [from 161.2 ± 28.34 (Mock) to 1340 ± 79.26 pg/mL (CHIKV) to 681.5 ± 97.3 pg/mL ($1 \mu\text{M}$ TAK-242)] (**Fig: 26-J**). Similarly, secretory IL-6 showed similar trend [from 411.1 ± 25.34 pg/mL (CHIKV) to 73.61 ± 8.047 pg/mL ($1 \mu\text{M}$ TAK-242)] (**Fig: 26-K**). MCP-1, a chemokine also showed a similar trend of expression [from 951.6 ± 17.19 pg/mL (Mock) to 1342 ± 12.85 pg/mL (CHIKV) and 286.2 ± 4.242 pg/mL (TAK-242)] (**Fig: 26-L**).

Together, the results indicate that TAK-242-directed TLR4 inhibition might reduce the CHIKV infection (around 58%) and pro-inflammatory responses, significantly, in the RAW264.7 cells.

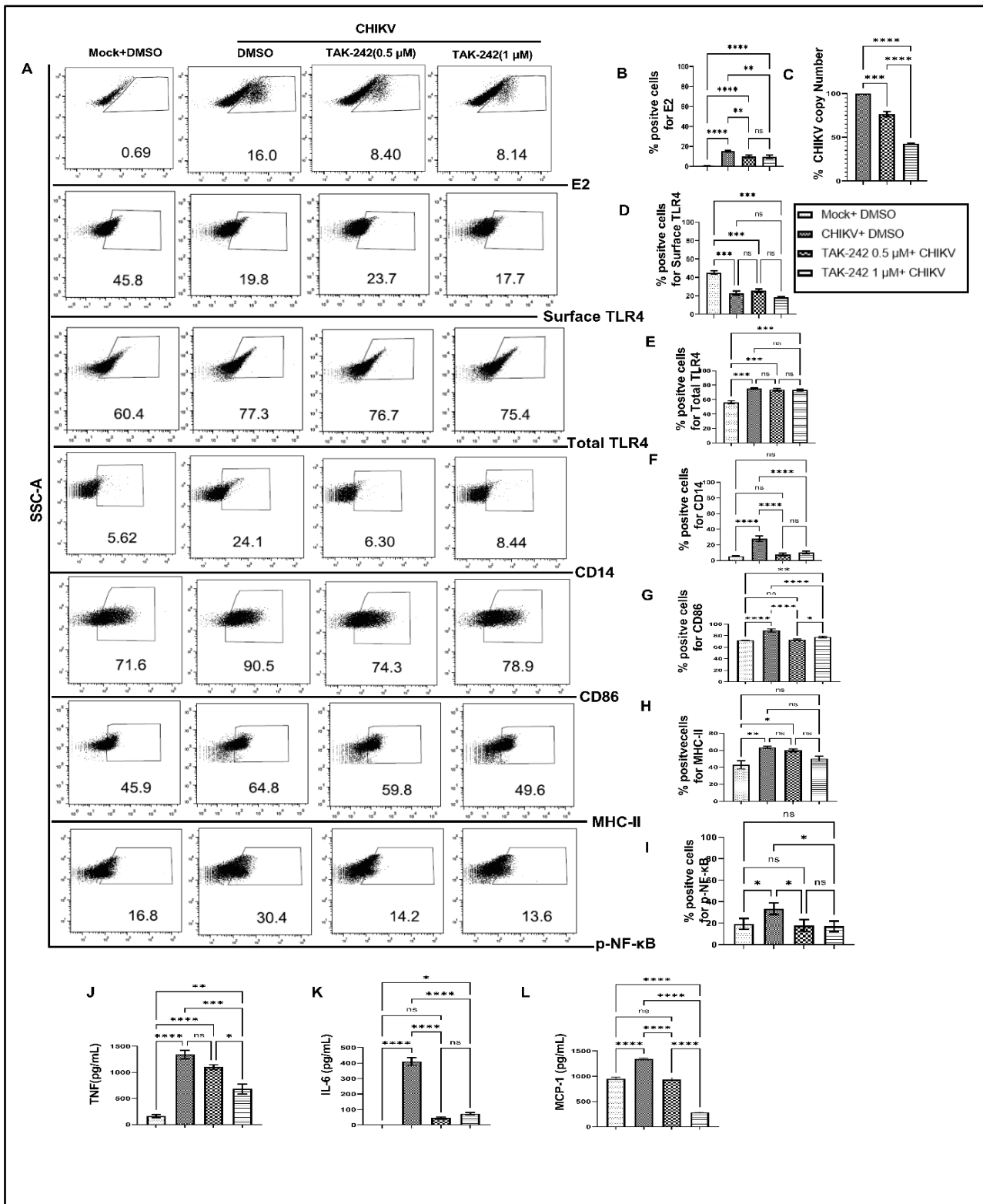


Figure 26: TLR4 antagonism reduces the CHIKV-induced proinflammatory responses in RAW264.7 macrophages, *in vitro*. The RAW264.7 cells were pre-incubated with TAK-242 for 3 h prior to CHIKV infection at MOI 5 for 2 h. Next, the cells were harvested at 8 hpi and further downstream experiments were performed. (A) The flow cytometry-based dot plot analysis of all

markers was shown. **(B)** The bar diagram denotes the percent positive cells for CHIKV-E2. **(C)** The bar diagram denotes q-RT PCR based CHIKV-E1 copy numbers of different conditions. The bar diagrams denote flow-cytometry-derived percent positive cells for **(D)** surface TLR4, **(E)** total TLR4, **(F)** CD14, **(G)** CD86, **(H)** MHC-II and **(I)** p-NF- κ B. The ELISA-based cytokine analysis of **(J)** TNF **(K)** IL-6 and **(L)** MCP-1 were represented in respective bar diagrams. Data represent the Mean \pm SEM of three independent replicates. (ns=non-significant, * p <0.05, ** p ≤0.01, *** p ≤0.001, **** p ≤0.0001).

Next, the current study further aimed to investigate whether TAK-242-directed TLR4 antagonism promotes reduced activation of macrophages or whether overall macrophage activation is solely dependent on the number/percentage of CHIKV-infected cells. To get a detailed clarity, the flow cytometry-based intracellular cytokine staining analysis of TNF-producing population was performed in CHIKV-E2 positive cells (**Fig: 27**). TLR4 inhibition with 1 μ M of TAK-242 significantly reduced the E2-positive RAW264.7 cells [15.67 \pm 1.477% (DMSO+CHIKV) and 9.49 \pm 0.9% (TAK-242+CHIKV)]. Corresponding E2 populations from TAK-242 untreated and treated groups were assessed further to investigate the frequency and expression of TNF in the aforementioned populations. The % positive cells of TNF-positive cells in both TAK-242 treated and untreated cells was found to be comparable under the E2-selected (gated) population. Interestingly, the mean fluorescence intensity (MFI) of TNF in the E2-gated cells was reduced significantly, which complies with the ELISA data mentioned earlier. The expression of TNF is possibly decreased due to the lowered frequency of the E2-positive cells upon TAK-242 treatment. Therefore, the result may delineate that TLR4 inhibition might not affect the total percentage of TNF-producing cells, but rather might suppress the production of TNF molecules quantitatively in individual macrophage cells.

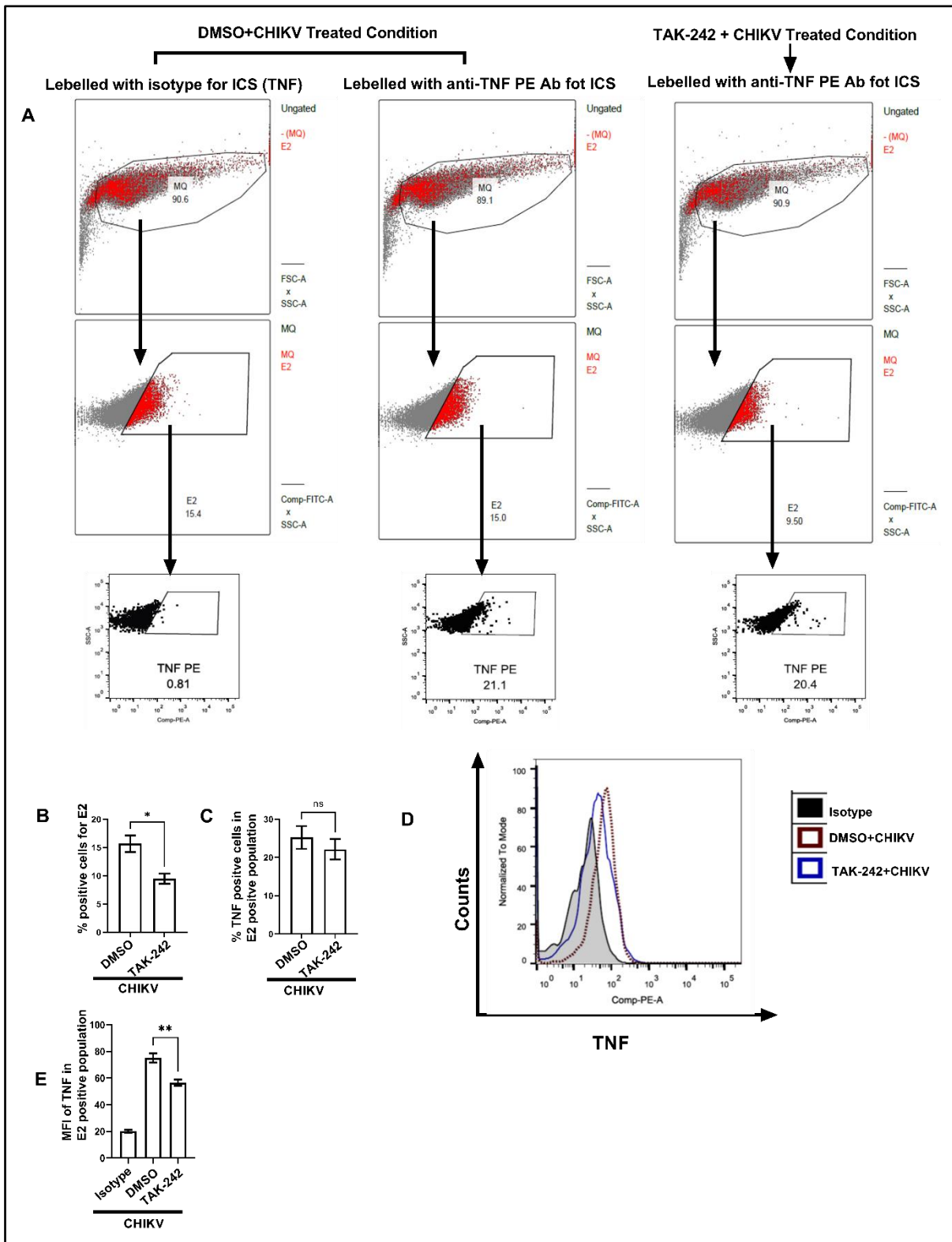


Figure 27: TLR4 antagonism reduces the CHIKV infection and CHIKV-induced TNF level RAW264.7 macrophages, *in vitro*. The RAW264.7 cells were incubated with TAK-242 for 3 h prior to CHIKV infection. The CHIKV infection was given at MOI 5 for 2 h. Next, the cells were treated with Golgistop at 4 hpi followed by incubation for next 4 hpi. The cells were harvested and

subjected to dual intracellular staining for CHIKV-E2 and TNF. **(A)** The scattered plots defining the main viable population (MQ) from where only E2 positive cells were further separated. **(B)** The bar representing percent E2-positive cells **(C)** The bar representation describing percent TNF positive cells in CHIKV-E2 positive population of different conditions, **(D, E)** The histogram and corresponding bar diagram representing the mean fluorescence intensity of TNF positive cells in CHIKV-E2 positive population of different conditions. Data represent Mean \pm SEM of three independent replicates. (ns=non-significant, * $p<0.05$, ** $p\leq0.01$, *** $p\leq0.001$, **** $p\leq0.0001$).

6.2.2. Inhibition of TLR4 abrogates CHIKV infection in the primary mouse peritoneal macrophages, significantly.

The positive regulatory role of TLR4 in RAW264.7 cells was validated in peritoneal macrophages obtained from BALB/c mice. Flow cytometry-based dot plot analysis revealed the reduction of percent CHIKV-E2 positive cells in the presence of TAK-242 treatment before CHIKV infection [from 26.73 ± 0.98 CHIKV) to 13.27 ± 0.5840 ($1\mu\text{M}$ TAK-242)] (**Fig:28-A, B**). The significant reduction of CHIKV-E1 copy numbers [60%] in the presence of drug treatment reconfirmed the role of TLR4 inhibition (**Fig: 28-C**). Next, the percent positive cells expressing surface TLR4 was found to decrease significantly upon CHIKV infection in the presence or absence of TLR4 inhibition [from 75.87 ± 1.247 to 51.07 ± 0.6360 % (CHIKV) and 53.5 ± 0.611 % ($1\mu\text{M}$ TAK-242)] (**Fig:28-A, D**). Although, the total expression of TLR4 increased significantly in CHIKV-infected macrophages treated with or without TAK-242 [from 81.5 ± 1.592 (Mock) to 90.73 ± 1.874 % (CHIKV) and 89.15 ± 1.084 % ($1\mu\text{M}$ TAK-242)] (**Fig:28-A, E**). CD14, an upstream regulator of the TLR4 signaling pathway as well as a macrophage activation marker, showed a significant increase in percent positive cells upon CHIKV infection, which further reduced upon TLR4 inhibition [from 22.53 ± 0.97 (Mock) to 30.73 ± 0.58 (CHIKV) and 26.37 ± 0.44 ($1\mu\text{M}$ TAK-242)] (**Fig:28-A, F**). Another macrophage activation marker, CD86 showed a significant increase

due to CHIKV infection, although a non-significant decrease in percent positive cells was observed upon TAK-242 pre-treated condition [from 37.47 ± 0.8 (Mock) to 65.23 ± 1.389 (CHIKV), 55.77 ± 0.67 ($0.5 \mu\text{M}$ TAK-242) and 60.93 ± 2.009 ($1 \mu\text{M}$ TAK-242)] (**Fig: 28-A, G**). Next, the percent positive cells expressing MHC-II reduced significantly due to TAK-242 pre-treatment [from 58.2 ± 1.25 (Mock) to 77.67 ± 0.09 (CHIKV) and 69.6 ± 1.513 ($1 \mu\text{M}$ TAK-242)] (**Fig: 28-A, H**). Furthermore, the percent positive cells expressing p-NF- κB was observed to significantly increase during CHIKV infection and decrease further upon TAK-242 treatment [from 29.2 ± 3.351 (Mock) to 52.63 ± 3.973 (CHIKV) and 40.87 ± 2.826 ($1 \mu\text{M}$ TAK-242)] (**Fig: 28-A, I**). The total TLR4 expression was validated by Western blot analysis. The result was found linear with flow cytometry data i.e., 2.123 ± 0.3 and 2.06 ± 0.16 -fold increased level in the absence and presence of $1 \mu\text{M}$ of TAK-242 pre-treatment in the CHIKV infected cells (**Fig: 28-J, K**). The pro-inflammatory responses associated with CHIKV infection were assessed in terms of ELISA-based quantification of TNF, IL-6, and MCP-1 levels. The level of secretory TNF reduced significantly upon TAK-242 pretreatment in CHIKV-infected cells [from 773.2 ± 62.88 pg/mL (CHIKV) to 398.6 ± 27.58 pg/mL ($1 \mu\text{M}$ TAK-242)] (**Fig: 28-L**). Next, IL-6 was found to maintain a similar trend as TNF [from 5.33 ± 1.294 pg/mL (Mock) to 1078 ± 147.9 pg/mL (CHIKV) and 186.4 ± 22.98 pg/mL ($1 \mu\text{M}$ TAK-242)] (**Fig: 28-M**). MCP-1, a chemokine, was also found to follow a similar pattern to denote the pro-inflammatory responses in host macrophages [from 145.4 ± 6.667 pg/mL (Mock) to 2117 ± 152.8 pg/mL (CHIKV) and 377.5 ± 76.98 pg/mL ($1 \mu\text{M}$ TAK-242)] (**Fig: 28-N**).

Together, the data might indicate that the TLR4 inhibition positively regulates the CHIKV infection and associated pro-inflammatory responses, significantly in the peritoneal monocyte-macrophages obtained from BALB/c mice.

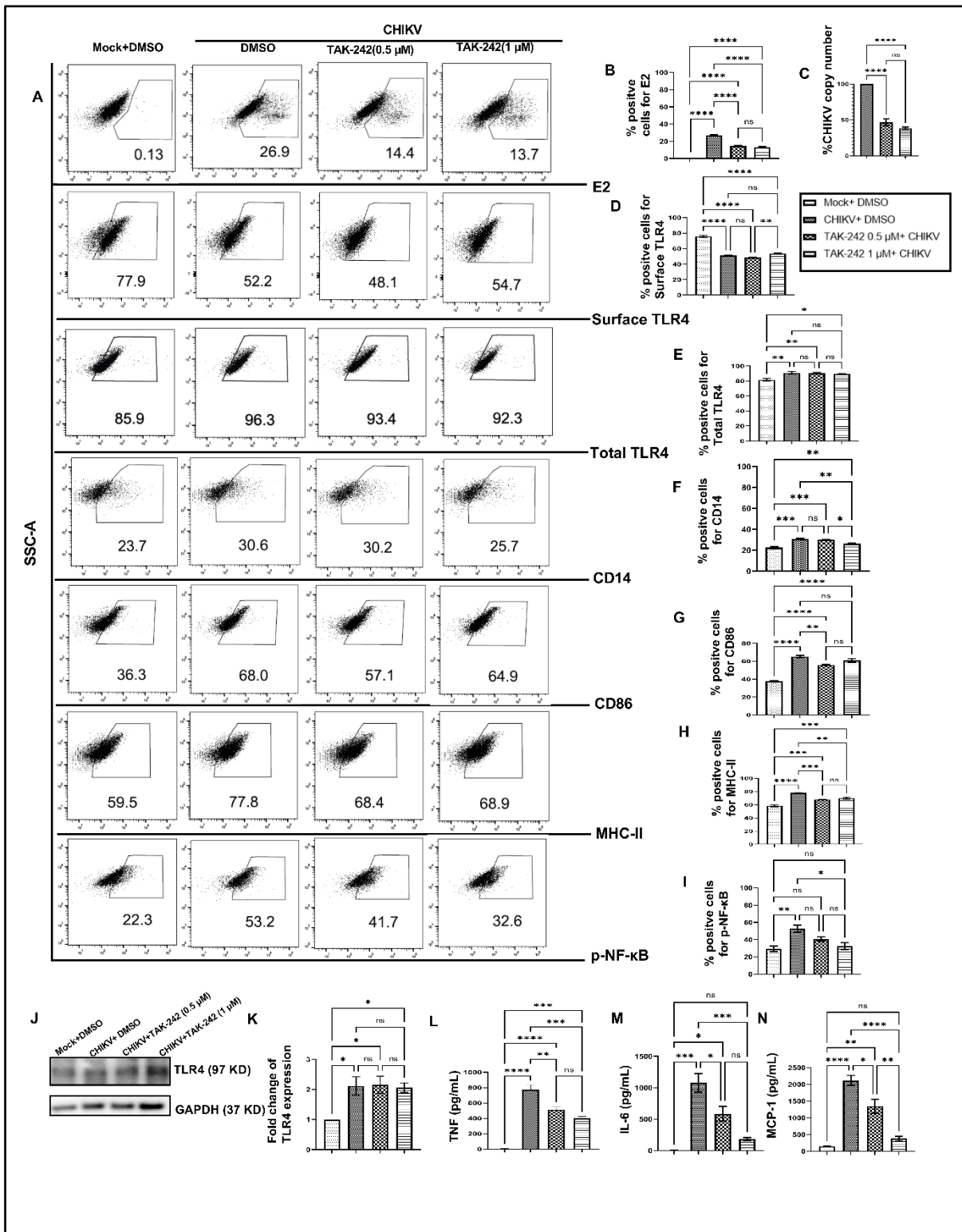


Figure 28: TLR4 antagonism reduces the CHIKV-induced proinflammatory responses in peritoneal macrophages of BALB/c mice, *in vitro*. Thioglycolate-induced peritoneal macrophages from BALB/c origin were pre-incubated with TAK-242 for 3 h prior to CHIKV infection at MOI 5 for 2 h. Next, the cells were harvested at 8 hpi, and further downstream

experiments were performed. **(A)** The flow cytometry-based dot plot analysis of all markers was shown. **(B)** The bar diagram denotes the percent positive cells for CHIKV-E2. **(C)** The bar diagram denotes q-RT PCR-based CHIKV-E1 copy numbers of different conditions. The bar diagrams denote flow-cytometry-derived percent positive cells for **(D)** surface TLR4, **(E)** total TLR4, **(F)** CD14, **(G)** CD86, **(H)** MHC-II and **(I)** p-NF- κ B. **(J, K)** Western blot analysis depicting the TLR4 level and its corresponding densitometry in different conditions. The ELISA-based cytokine analysis of **(L)** TNF **(M)** IL-6 and **(N)** MCP-1 were represented in respective bar diagrams. Data represent the Mean \pm SEM of three independent replicates. (ns=non-significant, * p <0.05, ** p \leq 0.01, *** p \leq 0.001, **** p \leq 0.0001).

Further, peritoneal macrophages obtained from C57BL/6 mice were used to conduct a similar study on the associative role of TLR4 during CHIKV infection. The flow cytometry-based dot plot analysis revealed a significant reduction of percent positive cells for CHIKV-E2 [from 18.6 ± 0.95 (CHIKV) to 6.558 ± 0.89 (1 μ M TAK-242)] (**Fig: 29-A, B**) as well as a significant 50% decrease of corresponding viral copy number in presence of TAK-242-driven TLR4 antagonism in CHIKV infected cells (**Fig: 29-C**). Next, the similar trend of change in the surface and total TLR4 expressions were determined by flow cytometry-based percent positive cells analysis (**Fig: 29-A, D, E**). It was further noticed that although the CD14 and MHC-II expressions were significantly modulated in a similar way, the CD86 expression showed a nonsignificant decrease in the presence of TAK-242 treatment (1 μ M) (**Fig: 29-A, F-H**). Moreover, the phosphorylation of NF- κ B was found to significantly increase during CHIKV infection and a marked decrease due to TLR4 inhibition was noticed [from 29.6 ± 1.793 (Mock) to 50.7 ± 0.66 (CHIKV) and 35.03 ± 0.5175 (1 μ M TAK-242)] (**Fig: 29-A, I**). The total TLR4 expression was further validated by Western blot analysis, which showed a significant increase during CHIKV infection in the presence or absence of TLR4 inhibition [1.553 ± 0.08 fold (CHIKV) and 1.489 ± 0.14 fold (1 μ M TAK-242)] (**Fig: 29-J, K**). Additionally, the ELISA-based cytokine analysis revealed a significant reduction of secretory

TNF, IL-6, and MCP-1 levels due to TLR4 antagonism before CHIKV infection in macrophage cells (**Fig: 29-L-N**).

Together the results indicate the regulatory role of TLR4 antagonism in decreasing the CHIKV infection and associated immune activation in peritoneal macrophages obtained from C57BL/6 mice as well.

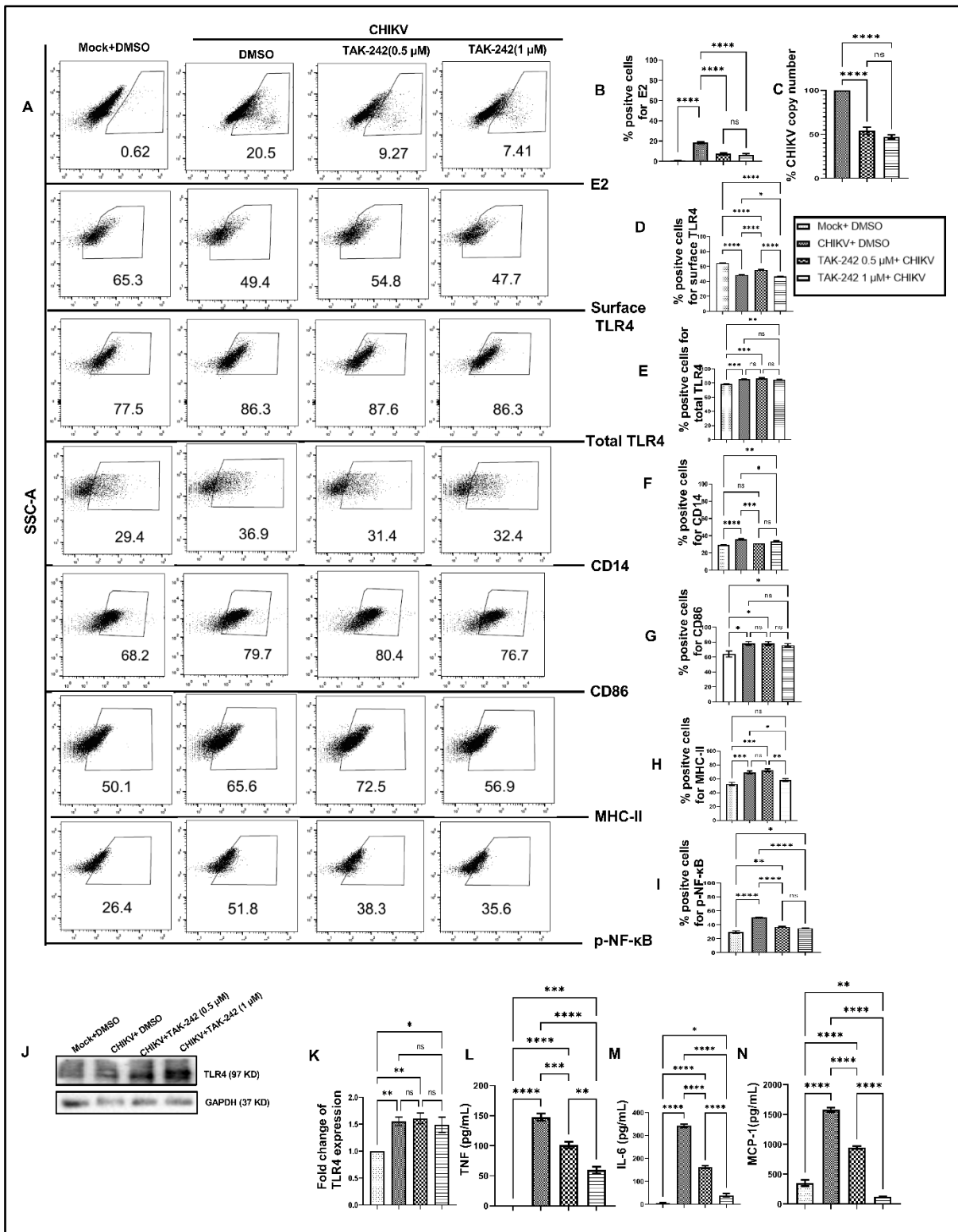


Figure 29: TLR4 antagonism reduces the CHIKV-induced proinflammatory responses in peritoneal macrophages of C57BL/6 mice, *in vitro*. Thioglycolate-induced peritoneal macrophages from C57BL/6 origin were pre-incubated with TAK-242 for 3 h prior to CHIKV infection at MOI 5 for 2 h. Next, the cells were harvested at 8 hpi, and further downstream

experiments were performed. **(A)** The flow cytometry-based dot plot analysis of all markers was shown. **(B)** The bar diagram denotes the percent positive cells for CHIKV-E2. **(C)** The bar diagram denotes q-RT PCR-based CHIKV-E1 copy numbers of different conditions. The bar diagrams denote flow-cytometry-derived percent positive cells for **(D)** surface TLR4, **(E)** total TLR4, **(F)** CD14, **(G)** CD86, **(H)** MHC-II and **(I)** p-NF- κ B. **(J, K)** Western blot analysis depicting the TLR4 level and its corresponding densitometry in different conditions. The ELISA-based cytokine analysis of **(L)** TNF **(M)** IL-6 and **(N)** MCP-1 were represented in respective bar diagrams. Data represent the Mean \pm SEM of three independent replicates. (ns=non-significant, * p <0.05, ** p ≤0.01, *** p ≤0.001, **** p ≤0.0001).

6.2.3. Inhibition of TLR4 abrogates CHIKV infection in the hPBMC-derived macrophages, significantly.

The effect of TAK-242-driven TLR4 inhibition was investigated in higher-order mammalian macrophage cells during CHIKV infection. hPBMC-derived adherent macrophage cells (~ 97% CD14⁺CD11b⁺) were separated from blood of healthy human donors (**Fig:30-A, B**). Next, the CHIKV infection was given to the cells at MOI 5 for 2 h in the presence and absence of TAK-242 pre-treatment. The cells were harvested at 8 hpi and flow-cytometry dot plot analysis showed around a 52% decrease of CHIKV-E2 positive cells due to TLR4 antagonism before CHIKV infection (**Fig:30-C, D**). The plaque assay-based viral titer analysis showed around 33% reduction in CHIKV particles from the collected cell culture supernatant, (**Fig:30-E**). Furthermore, ELISA-based cytokine analysis of soluble hTNF was performed to assess the CHIKV-induced pro-inflammatory responses. The data revealed around 44% reduction of hTNF level in TAK-242 treated condition (**Fig:30-F**).

Together, these data reveal the regulatory role of TLR4 in regulating CHIKV infection and subsequent pro-inflammatory responses in hPBMC-derived macrophages.

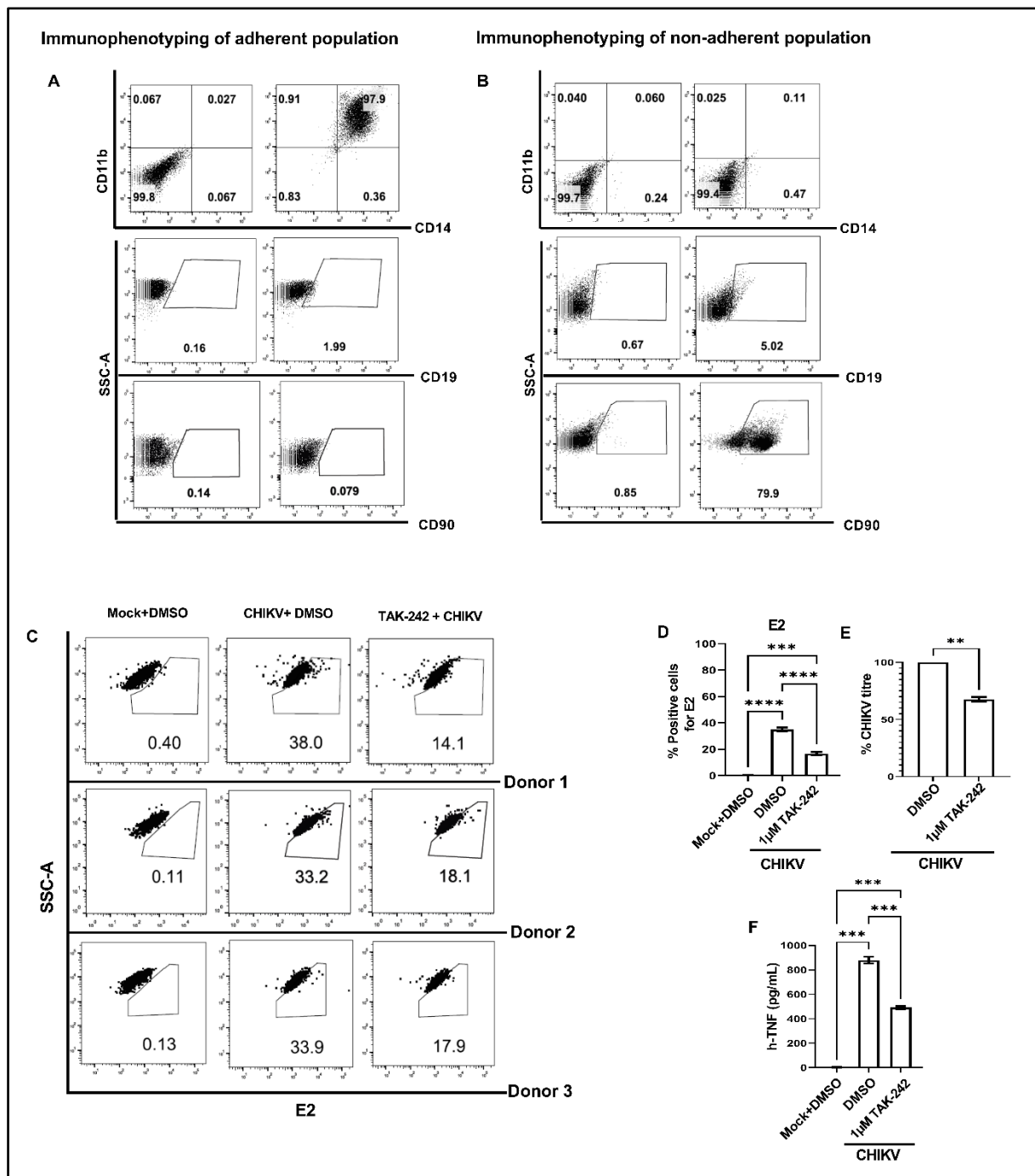


Figure 30: TLR4 antagonism reduces the CHIKV-induced proinflammatory responses in hPBMC-derived monocyte-macrophages, *in vitro*. hPBMC-derived adherent macrophages were pre-incubated with TAK-242 for 3 h prior to CHIKV infection at MOI 5 for 2 h. Next, the cells were harvested at 8 hpi, and further downstream experiments were performed. **(A, B)** The flow cytometry-based immunophenotyping of hPBMC-derived myeloid cells. **(C, D)** The percent positive cells for CHIKV-E2 in hPBMC-derived macrophages collected from three healthy donors were shown in the flow cytometry-based dot plot analysis and the corresponding bar diagram. **(E)**

The bar diagram depicts the percent CHIKV titer in different in different conditions. **(F)** The bar diagram depicting ELISA-based cytokine analysis of hTNF in different conditions. Data represent the Mean \pm SEM of three independent replicates. (ns=non-significant, * p <0.05, ** p ≤0.01, *** p ≤0.001, **** p ≤0.0001).

6.2.4. Inhibition of TLR4 abrogates CHIKV infection in PMA-induced THP-1 cells, significantly.

THP-1, a human monocyte cell line, was also studied to investigate the effect of TLR4 antagonism in CHIKV infection. The PMA-induced THP-1 cells are adherent by nature and are designated as macrophage-like cells. The PMA-induced macrophages were infected with CHIKV at MOI 5 for 2 h and harvested at 8 hpi. The flow cytometry-based study revealed around 40% reduction in CHIKV-E2 positive cells in the presence of 1 μ M of TAK-242 (**Fig:31-A, B**). Additionally, the plaque assay-based viral titer analysis revealed around 60% reduction of CHIKV particles in the presence of TAK-242 pre-treatment in CHIKV-infected cells (**Fig:31-C**).

Altogether, the results may delineate the anti-CHIKV effect of TAK-242-mediated TLR4 inhibition in PMA-induced THP-1 cells.

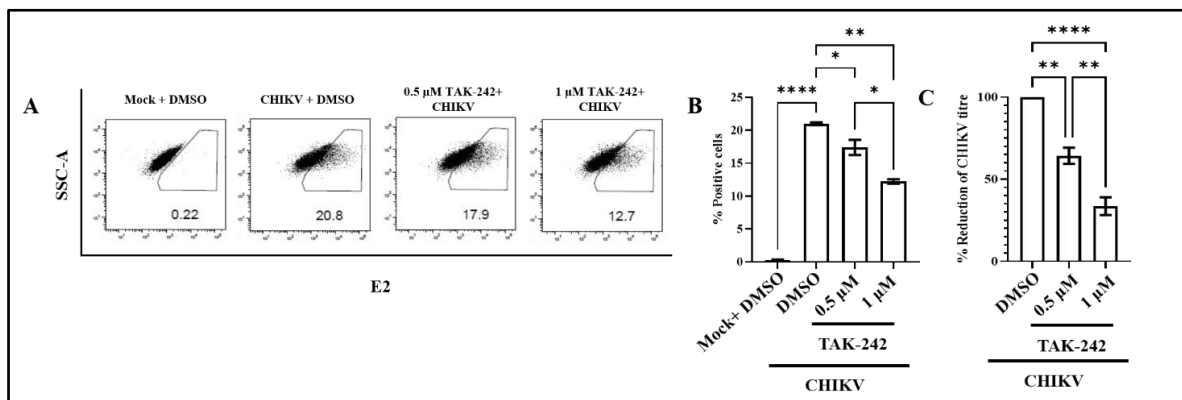


Figure 31: TLR4 antagonism reduces the CHIKV-induced proinflammatory responses in PMA-induced THP-1 cells, *in vitro*. PMA-induced THP-1 cells were differentiated and treated with TAK-242 3 h prior to CHIKV infection., Next cells were infected with CHIKV-IS at 5 MOI for 2 h. Finally, the cells were harvested and processed for further experiments. **(A, B)** The flow

cytometry-based dot plot analysis and corresponding bar diagram depicting the CHIKV-E2 expression in different conditions. (C) The bar diagram reveals the percent viral titer without/with TLR4 inhibition. Data represent the Mean \pm SEM of three independent replicates. (ns=non-significant, * $p < 0.05$, ** $p \leq 0.01$, *** $p \leq 0.001$, **** $p \leq 0.0001$).

6.3. CHIKV-induced TNF promotes naive T cell activation in p38 and JNK-MAPK pathway-dependent manner, *in vitro*.

TNF is one of the major factors behind the CHIKV-induced pro-inflammatory cytokine burst. However, TNF was also reported to accelerate T cell receptor (TCR)-dependent activation of T cells. Here, it was investigated the possibility of p38 and SAPK-JNK MAPK pathways of CHIKV-infected RAW264.7 cell in TCR dependent T cell activation. To achieve the possible connection, the culture supernatants of CHIKV-infected RAW264.7 cells treated with SB and SP (p-p38 and p-JNK antagonists, respectively) were collected at 8 hpi and further co-cultured with naive syngeneic primary mouse T cells for 36 h in presence or absence of TCR-driven stimulation. Moreover, the culture supernatant of only CHIKV infection was treated with an anti-TNF antibody to neutralize the soluble TNF molecules in the media and further used as a condition of the co-culture experiment.

Flow cytometry-based dot plot analysis of CD69, an early activation marker of T cells, showed an increase in the percent positive cells in TCR stimulated CHIKV infected culture supernatant in comparison to activated mock or resting conditions, which reduced in presence of anti-TNF antibody treated culture supernatant with TCR stimulation and also further reduced in SB and SP treated culture media in presence of TCR-driven stimulation [65.8 \pm 2.046 (Resting+TCR), 71.05 \pm 1.187 (Mock \pm TCR), 80.94 \pm 2.217 (CHIKV \pm TCR), 63.12 \pm 1.976 (CHIKV+anti-TNF Ab+TCR), 55.29 \pm 2.077 (CHIKV+SB+TCR), 49.31 \pm 0.2 (CHIKV+SP+TCR)] (**Fig: 32-A**).

Flow-cytometry-based dot plot analysis of CD25, a late activation marker of T cells, also showed similar pattern of percent positive cells in TCR stimulated condition [65.1 ± 0.6 (Resting+ TCR), 69.79 ± 1.897 (Mock+TCR), 77.37 ± 3.191 (CHIKV+TCR), 52.42 ± 1.632 (CHIKV+anti-TNF Ab+TCR), 59.61 ± 4.137 (CHIKV+SB+TCR), 52.80 ± 2.654 (CHIKV+SP+TCR)] (Fig: 32-B).

Together, the results decipher that the TNF within CHIKV-induced culture supernatant may activate naïve T cells in association with p38 and SAPK-JNK MAPK pathways.

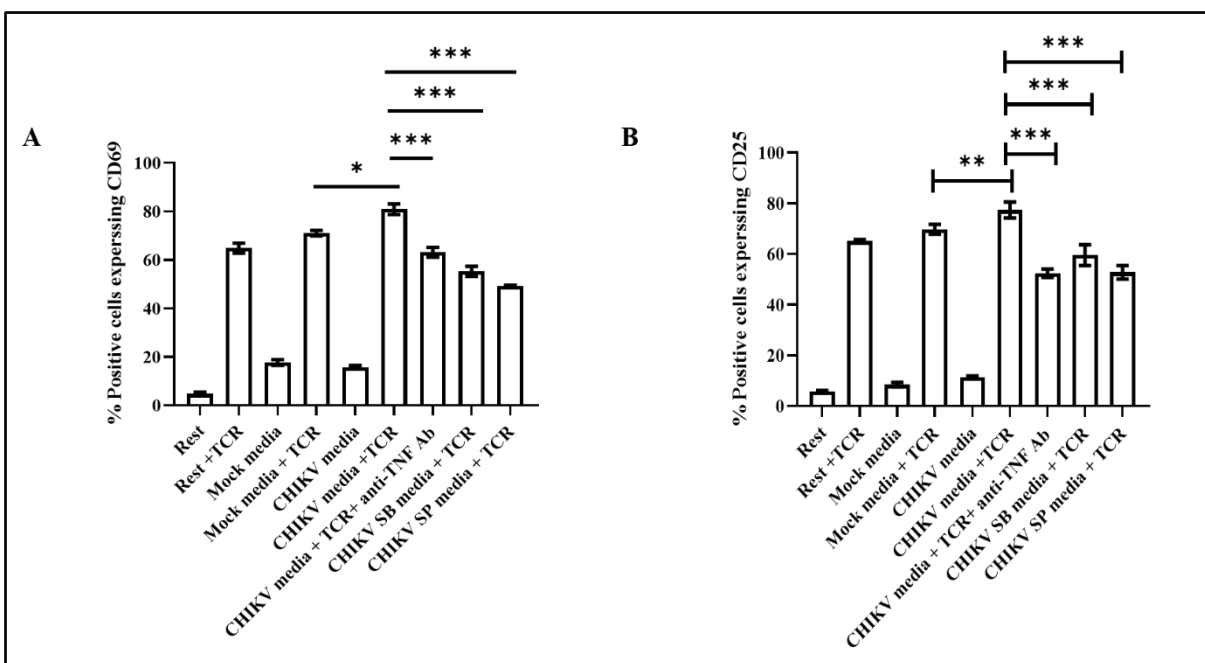


Figure 32: The CHIKV infection-induced TNF promotes naïve primary T cell activation, *in vitro*. The RAW264.7 cells were infected with CHIKV at MOI 5 for 2 h in the presence or absence of SB and SP (p-p38 and p-JNK antagonists, respectively) and the culture supernatants were collected at 8 hpi. An anti-TNF antibody was used to neutralize the soluble TNF in the CHIKV-infected culture supernatants. Next, naïve primary T cells from BALB/c origin were incubated with the syngeneic macrophage culture supernatants with TCR and appropriate controls. The cells were harvested at 36 h post-treatment and the flowcytometry-based staining was performed. (A) The flow-cytometry dot plot-based bar diagram depicting the percent positive cells for CD69 in different conditions. (B) The flow-cytometry dot plot-based bar diagram depicting the percent

positive cells for CD25 in different conditions. Data represent the Mean \pm SEM of three independent replicates. (ns=non-significant, * p <0.05, ** p \leq 0.01, *** p \leq 0.001, **** p \leq 0.0001).

6.4. TLR4 antagonism lowers LPS or CHIKV-induced p38 and SAPK-JNK phosphorylation in host macrophages, *in vitro*.

The previously published reports decipher the association of LPS with the upregulated phosphorylation of p38 and JNK-MAPK proteins in a TLR4-directed manner (190,191). Therefore, the current study is intended to serve as an experimental control of p38 and SAPK-JNK MAPK phosphorylation in pro-inflammatory conditions such as CHIKV infection. Western blot-based analysis showed a significant upregulation of TLR4 both in the presence and absence of TLR4 inhibition in LPS-induced RAW264.7 cells concerning mock condition [2.328 \pm 0.067 fold (LPS) and 2.205 \pm 0.25 fold (LPS+TAK-242)] (**Fig: 33-A, B**). Next, phosphorylation of SAPK-JNK exhibited a significant upregulation in LPS treatment by 9.826 \pm 0.62 fold which further reduced upon TAK-242 -directed TLR4 inhibition to 2.573 \pm 0.09 fold (**Fig: 33-A, C**). Further, a similar pattern of phosphorylation of p38 MAPK was observed [2.373 \pm 0.39 fold (LPS) and 1.044 \pm 0.2465 fold (LPS+TAK-242)] (**Fig: 33-A, D**). Together, the results delineate the positive association of p38 and SAPK-JNK MAPK phosphorylation during LPS-mediated pro-inflammatory conditions, *in vitro*.

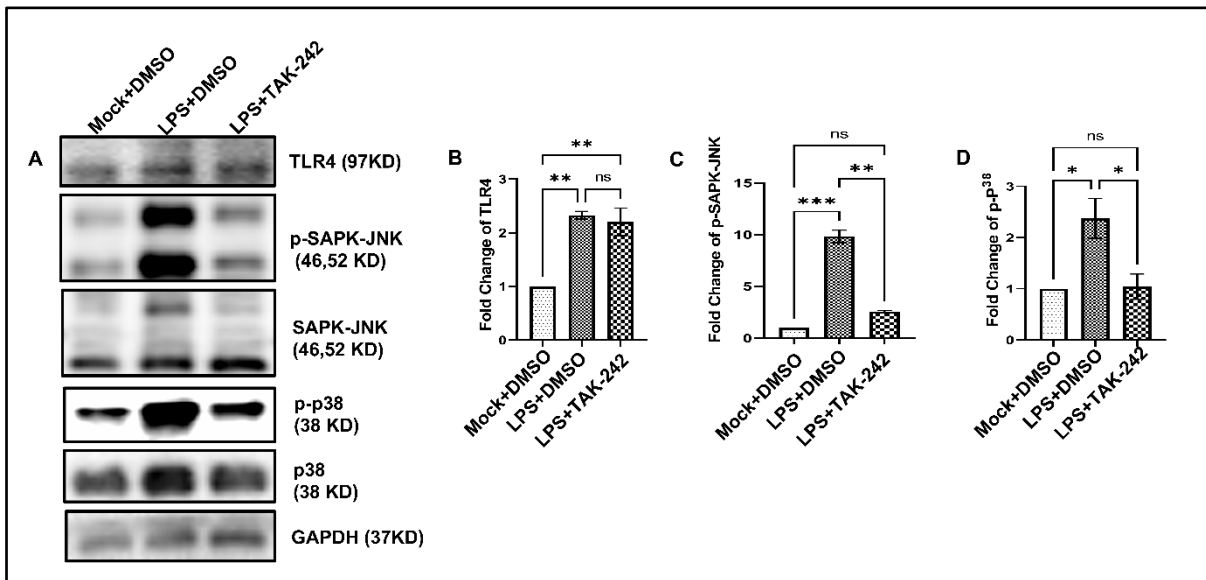


Figure 33: TLR4 antagonism reduces LPS-induced MAPK-activation in RAW264.7 cells.

The RAW264.7 macrophages were pre-treated with either DMSO or TAK-242 for 3h followed by LPS stimulation at $1\mu\text{g/ml}$ for 6 h. Next, the cells were harvested and processed for Western blot analysis. (A) The blot images show levels of TLR4, p-SAPK-JNK, t-SAPK-JNK, p-p38 MAPK, and t-p38 MAPK along with housekeeping control GAPDH in different conditions. (B-D) The bar diagrams depict the levels of TLR4, p-p38, and p-SAPK-JNK in different conditions of three individual sets of experiments. Data represent the Mean \pm SEM of three independent replicates. (ns=non-significant, * $p<0.05$, ** $p\leq 0.01$, *** $p\leq 0.001$, **** $p\leq 0.0001$).

The positive association of p38 and SAPK-JNK MAPK pathways with CHIKV infection was recently reported by this group and others. To investigate the possible role of TLR4 inhibition in the modulation of MAPK pathways, phosphorylation of p38 and SAPK-JNK were studied in CHIKV-infected RAW264.7 cells by Western blot experiment. A significant increase in p-p38 (2.9-fold) and p-SAPK-JNK (4.03-fold) during CHIKV infection was found to be reduced both in p-p38 (by 4.69-fold) and p-SAPK-JNK (by 1.61-fold) due to TAK-242 treatment (Fig: 34-A, B-C). To investigate the viral infection, CHIKV-E2 level was also measured which showed a 3.27-fold reduction in the presence of TLR4 inhibition (Fig: 34-A, D). The correlation of total

TLR4 expression with the current study showed an increase of 2.09-fold and 2.9-fold during only CHIKV infection and TAK-242 treatment, respectively (**Fig: 34-E-F**). Together, these data suggest that TAK-242-mediated TLR4 inhibition might reduce viral infection and p38 and SAPK-JNK MAPK induction.

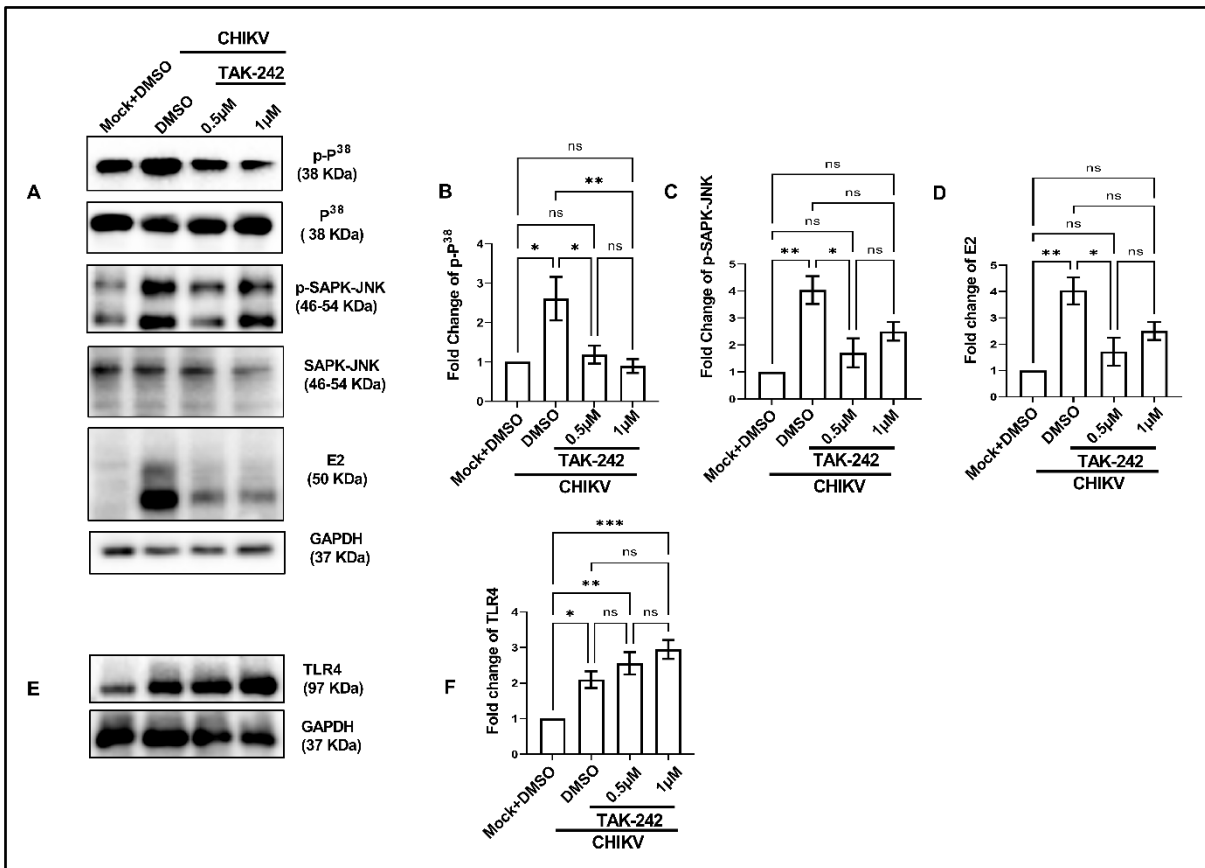


Figure 34: TLR4 antagonism reduces the CHIKV-induced MAPK-activation in RAW264.7 macrophages, *in vitro*. The RAW264.7 cells were pre-incubated with TAK-242 for 3 h prior to CHIKV infection at MOI 5 for 2 h. Next, the cells were harvested and processed for Western blot analysis. (A) The blot images show levels of p and t-p38, p and t-SAPK-JNK, CHIKV-E2, and housekeeping control GAPDH. (B-D) The graphical representations show the levels of p-p38, p-SAPK-JNK, and E2 of 3 independent experiments, respectively. (E) The blot images denote the levels of TLR4 and corresponding GAPDH levels in different conditions. (F) The bar diagram denotes the levels of TLR4 in different conditions of three individual experiments. Data represent

the Mean \pm SEM of three independent replicates. (ns=non-significant, * p <0.05, ** p ≤0.01, *** p ≤0.001, **** p ≤0.0001).

6.5. Functional TLR4 and CHIKV-E2 interact to promote efficient infection in host macrophages.

To get an insight on the possible regulatory role of TLR4, the status of CHIKV infection was studied in TLR4 knockout (KO) RAW cells. Earlier literature demonstrated the association of TLR4 in SARS-CoV2-induced immune-modulation. Interestingly, the TLR4KO RAW cells were found to generate reduced interferon response against SARS-CoV2-specific protein E antigens (22). Therefore, the requirement of functional TLR4 was found to be necessary to induce anti-viral response. The TLR4KO RAW cells and RAW264.7 cells were infected with CHIKV-IS at MOI 5 for 2 h. Both of the cells were harvested at 8 hpi and further processed for different experiments. The flow cytometry-based dot plot analysis study revealed a significant reduction of percent positive cells for CHIKV-E2 protein in TLR4 KO RAW cells [16.60±0.75 % (RAW264.7) to 3.877±0.43 % (TLR4KO RAW)] (**Fig: 35-A, B**). Western blot-based analysis of CHIKV-E2 level was found linear with the trend of flow cytometry data. It showed around 8.651±0.72-fold reduction of the E2 protein in CHIKV-infected TLR4KO RAW cells in comparison to wild-type RAW264.7 cells (**Fig: 35-C, D**). Next, a 48.11±3.23% reduction in viral titer in CHIKV-infected TLR4KO RAW cells was found supportive to the findings of both flow cytometry and Western blot data, i.e., TLR4 KO RAW cells were found to be less susceptible to CHIKV infection in comparison to the wild type (**Fig: 35-E**). Although it's a knockout cell line, the total and surface TLR4 expression were investigated for validation purposes. The flow cytometry dot plot analysis of total and surface TLR4 indicated no significant presence or change in the percent positive population in CHIKV-infected TLR4KO RAW cells (**Fig: 35-F, G-H**). Next, the other macrophage activation markers of TLR4KO RAW cells such as CD14, CD86, and

MHC-II were found to increase due to CHIKV infection in a nonsignificant manner (**Fig: 35-F, I-K**). However, p-NF- κ B expression showed a modest but significant change due to CHIKV infection in TLR4KO RAW cells (**Fig: 35-F, L**). The ELISA-based pro-inflammatory cytokine study revealed the rise of TNF, IL-6, and MCP-1 in RAW264.7 cells by 2.3, 1.7, and 1.5-fold respectively (**Fig:35-M-O**).

Therefore, the results obtained from TLR4KO-RAWcells indicate the functional requirement of TLR4 to promote effective viral infection and subsequent pro-inflammatory responses in host macrophages.

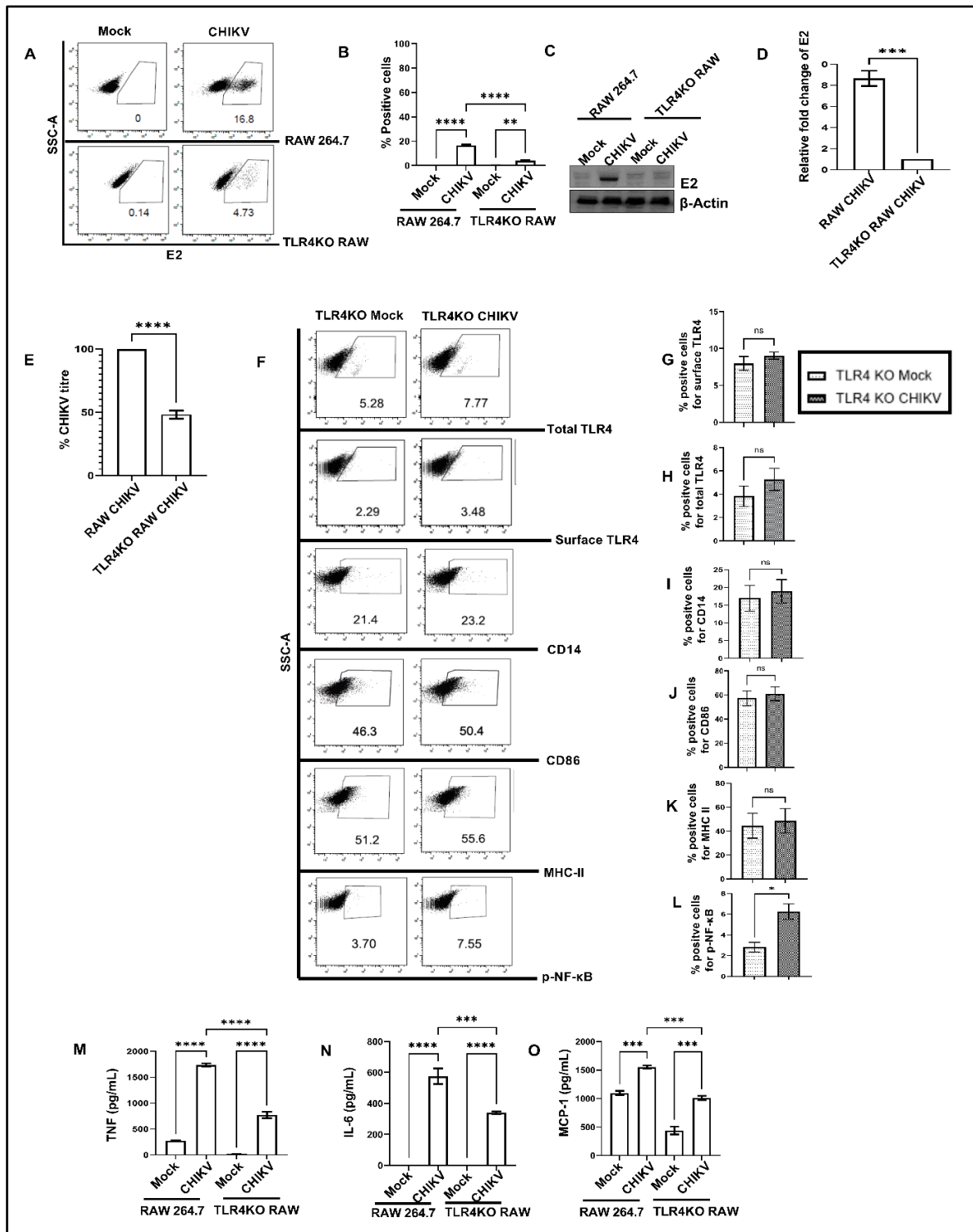


Figure 35: The functional TLR4 is essential to promote CHIKV infection in host macrophages. The RAW264.7 and TLR4KO RAW cells were infected with CHIKV at MOI 5 for 2 h and the cells were harvested at 8 hpi. Next, the cells were processed for further experiments. (A, B) The flow cytometry-based dot plot analysis and corresponding bar diagram depicting the percent CHIKV-E2-positive cells of RAW264.7 and TLR4KO RAW cells. (C, D) Western blot

images and corresponding bar diagram depicting the comparative CHIKV-E2 levels. **(E)** The bar diagram depicts the percent viral titer in CHIKV-infected RAW264.7 and TLR4KO RAW cells. **(F)** Flow cytometry-based dot plot images of all markers and corresponding bar diagrams for **(G)** total TLR4, **(H)** surface TLR4 **(I)** CD14, **(J)** CD86, **(K)** MHC-II, and **(L)** p-NF- κ B showing percent positive expression in mock and CHIKV infected TLR4KO RAW cells. **(M-O)** The bar diagrams denoting ELISA-based comparative TNF, IL-6, and MCP-1 levels, respectively in RAW264.7 and TLR4KO cells in the absence or presence of CHIKV infection. Data represent the Mean \pm SEM of three independent replicates. (ns=non-significant, * $p < 0.05$, ** $p \leq 0.01$, *** $p \leq 0.001$, **** $p \leq 0.0001$).

The study on TLR4KO RAW cells depicted the requirement of functional TLR4 to promote CHIKV infection in host macrophages. To investigate the probable direct interaction of TLR4 and CHIKV structural proteins such as E1 and E2, a co-immunoprecipitation study was performed. The RAW 264.7 and TLR4KO RAW cells were infected with CHIKV-IS at MOI 5 for 2 h and the cells were harvested at 8 hpi. Co-immunoprecipitation study followed by Western blot analysis revealed that functional TLR4 of RAW264.7 cells could be pulled out with CHIKV-E2 protein (**Fig: 36-A**). However, due to the absence of functional TLR4, there was no detectable interaction found in TLR4 KO RAW cells (**Fig: 36-B**). Next, to validate the specificity, the interaction between TLR4 and CHIKV-E1 protein was investigated in RAW264.7 cells, which showed no promising interaction (**Fig: 36-C**). Additionally, the interaction between CHIKV-E2 and TLR4 was further tested in the presence or absence of TAK-242-driven TLR4 inhibition in RAW264.7 cells. The lesser interaction between TLR4 and CHIKV-E2 in the presence of TLR4 inhibition re-confirmed the positive interaction of host TLR4 and CHIKV-E2 proteins (**Fig: 36-D**). Together, the immunoprecipitation studies indicate that the positive interaction of TLR4 and viral E2 protein promotes CHIKV infection and associated pro-inflammatory responses in host macrophages.

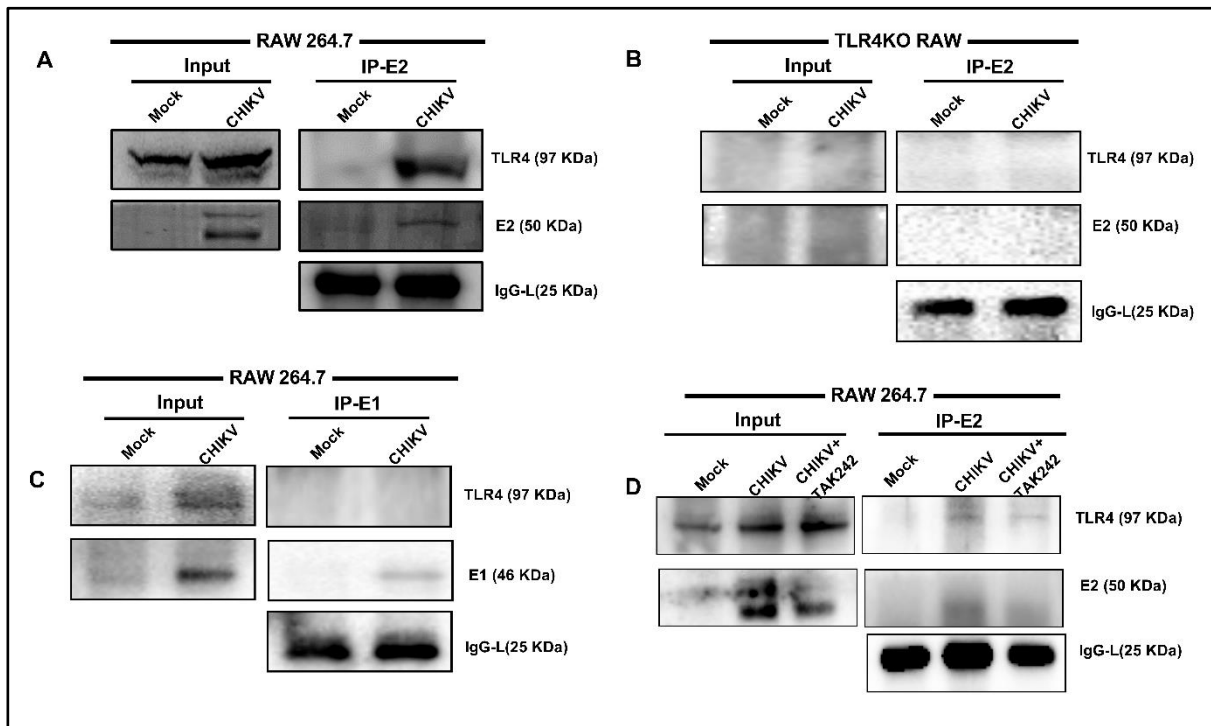


Figure 36: The functional TLR4-CHIKV-E2 interaction promotes CHIKV infection in host macrophages, *in vitro*. The RAW264.7 and TLR4KO RAW cells were infected with CHIKV at MOI 5 for 2 h and harvested at 8 hpi. The cells were further processed for immunoprecipitation followed by Western blot analysis to detect visible interaction between TLR4 and CHIKV-E2. **(A)** For RAW264.7 cells, the Western blot images denoting the E2 and TLR4 expression from the whole cell lysates (Left) and co-immunoprecipitation analysis denoting the positive interaction of E2 and TLR4 (Right) **(B)** For TLR4KO RAW cells, the Western blot images denoting the E2 and TLR4 expression from the whole cell lysates (Left) and co-immunoprecipitation analysis denoting the no interaction of E2 and TLR4 (Right) **(C)** For RAW264.7 cells, the Western blot images denoting the E1 and TLR4 expression from the whole cell lysates (Left) and co-immunoprecipitation analysis denoting the no interaction of E1 and TLR4 (Right) **(D)** For RAW264.7 cells, the Western blot images denoting the E2 and TLR4 expression from the whole cell lysates (Left) and co-immunoprecipitation analysis denoting the positive interaction of E2 and TLR4 (Right) in presence or absence of TAK-242 directed TLR4 antagonism.

In parallel to the *in vitro* studies, the probable *in silico* interaction of CHIKV-E2 and host TLR4 was also investigated by molecular docking study. The extracellular domain of TLR4 i.e., TLR4-MD2 complex (PDB ID: 2Z64) was fitted as the receptor and CHIKV structural protein E2 (PDB ID: 3N41) was fitted as the ligand (**Fig: 37-A**). The protein-protein interaction study demonstrated a total of 12 interactions between the ligand and the receptor. The Thr546, Ser550, and Tyr454 of TLR4-MD2 complex along with Gln307 and Glu303 of CHIKV-E2 showed multiple polar interactions (**Fig: 37-B**). Together, the protein-protein docking study revealed the possible interaction of CHIKV-E2 with the host TLR4-MD2 complex prior to the onset of CHIKV infection in host macrophages.

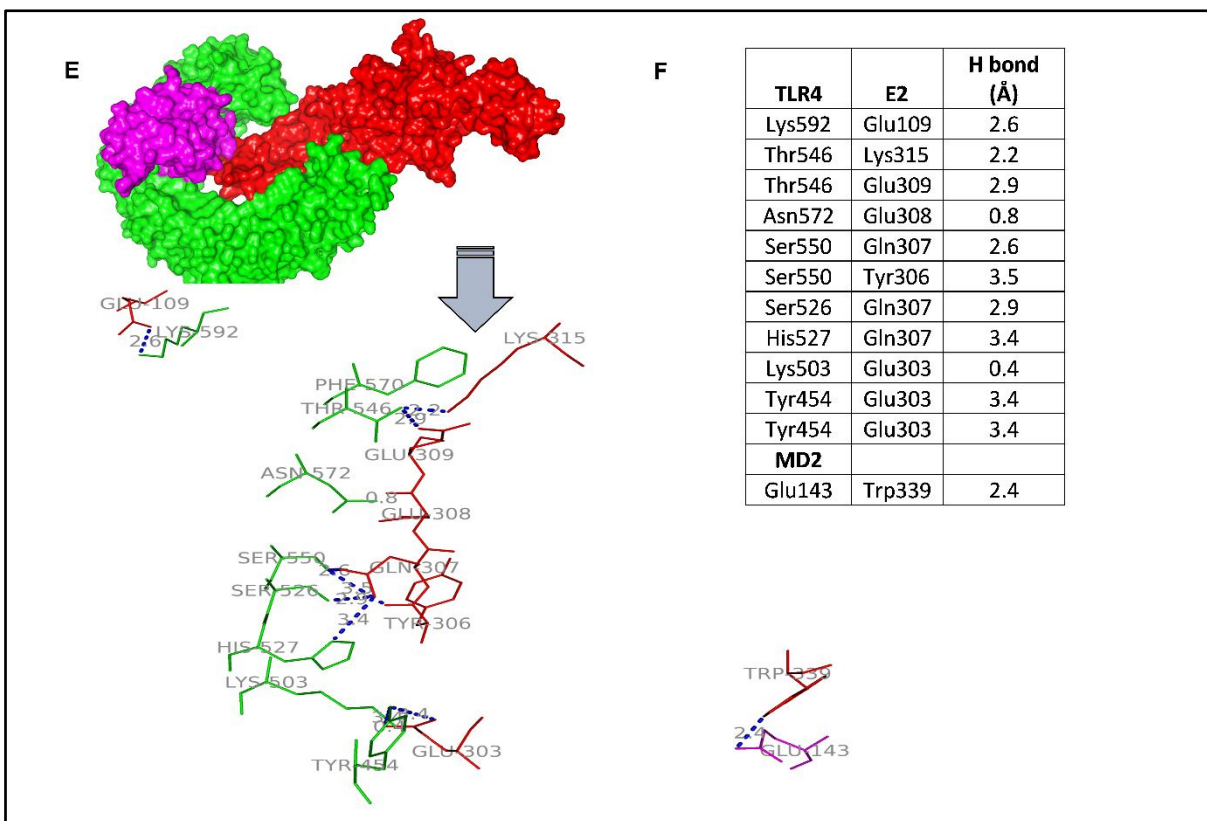


Figure 37: The functional TLR4-CHIKV-E2 interaction promotes CHIKV infection in host macrophages, *in silico*. The *in-silico* protein-protein interaction study between TLR4-MD2 (PDB ID: 2Z64) as the receptor and CHIKV-E2 (PDB ID: 3N41) as the ligand was performed using

ZDOCK web server **(A)** The representative image denoting the polar interactions (blue) of TLR4 (green) and MD2 (magenta) with CHIKV-E2 (red) **(B)** The residues contributing the polar interactions between TLR4-MD2 complex and CHIKV-E2.

The requirement of functional TLR4 during CHIKV infection and the positive interaction of TLR4 and CHIKV-E2 were further validated by an anti-TLR4-antibody-dependent blocking assay. The RAW264.7 cells were either pre-incubated with an anti-TLR4 antibody or its isotype in the presence or absence of TAK-242. Next, the cells were infected with CHIKV-IS at MOI 5 for 2 h and the cells were finally harvested at 8 hpi. The flow cytometry-based dot plot analysis revealed a similar extent of reduction in CHIKV infection in the presence of anti-TLR4-antibody-mediated blocking as well as only TLR4 inhibition. Interestingly, the dual presence of TAK-242 and anti-TLR4 antibody didn't markedly reduce the infection more than only anti-TLR4 antibody blocking or TAK-242 mediated inhibition. This incident might indicate the saturated inhibition of CHIKV infection [from $19.58 \pm 0.375\%$ (CHIKV) to $10.57 \pm 0.8168\%$ (TAK-242), $10.87 \pm 1.546\%$ (CHIKV+Antibody) to $11.88 \pm 1.316\%$ (TAK-242+CHIKV+Antibody)] (**Fig:38-A, B**). Next, Western blot analysis revealed a similar trend of CHIKV-E2 protein expression [from 8.212 ± 0.29 -fold (CHIKV) to 4.577 ± 1.062 -fold (TAK-242), 4.469 ± 0.42 -fold (CHIKV+Antibody) to 3.53 ± 0.45 -fold (TAK-242+CHIKV+Antibody)] (**Fig:38-C, D**). Moreover, the Western blot analysis of CHIKV-E1 protein also demonstrated a similar pattern of expression as CHIKV-E2 [from 11.56 ± 1.6775 -fold (CHIKV) to 3.868 ± 0.59 -fold (TAK-242), 6.725 ± 0.42 -fold (CHIKV+Antibody) to 4.315 ± 0.44 -fold (TAK-242+CHIKV+Antibody)] (**Fig:38-E, F**). Additionally, ELISA-based analysis of TNF showed a significant reduction in the presence of anti-TLR4-antibody-driven blocking study [from 98.84 ± 0.49 pg/ml (Mock) to 1673 ± 75.33 pg/ml (CHIKV), 1127 ± 6.685 pg/ml (TAK-242), 90.68 ± 17.12 pg/ml (Mock+Antibody) 1088 ± 136.6 pg/ml (CHIKV+Antibody) to 889.4 ± 48.26 pg/ml (TAK-242+CHIKV+Antibody)] (**Fig:38-G**).

Together the anti-TLR4-mediated blocking study reconfirms the engagement of CHIKV-E2 with host TLR4 and this interaction promotes CHIKV infection and subsequent pro-inflammatory responses in host.

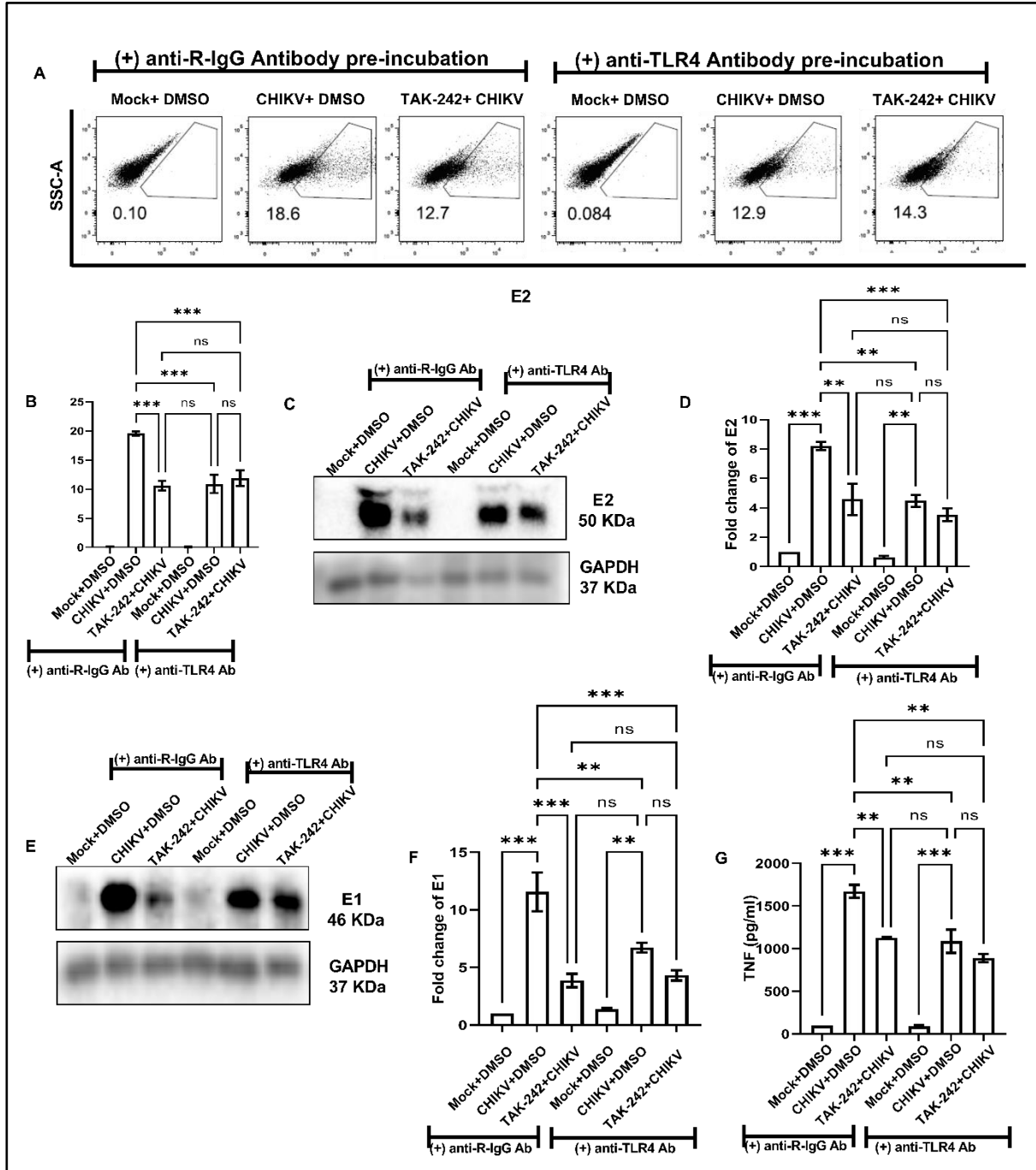


Figure 38: Anti-TLR4 antibody-driven blocking of cellular TLR4 reduces CHIKV infection in RAW264.7 cells, *in vitro*. The RAW264.7 cells were incubated with an anti-TLR4 antibody or the corresponding isotype in the presence or absence of TAK-242 before CHIKV infection. Next,

the cells were given CHIKV infection at MOI 5 for 2 h. The cells were harvested at 8 hpi and further processed for experiments. **(A, B)** The flow-cytometry dot plot analysis and corresponding bar graph represent the percent CHIKV-E2 positive cells in different conditions. **(C, D)** Western blot image and corresponding bar diagram representing CHIKV-E2 levels in different conditions. **(E, F)** Western blot image and corresponding bar diagram representing CHIKV-E1 levels in different conditions. **(G)** The bar diagram represents ELISA-based cytokine analysis of TNF in different conditions. Data represent the Mean \pm SEM of three independent replicates. (ns=non-significant, * $p < 0.05$, ** $p \leq 0.01$, *** $p \leq 0.001$, **** $p \leq 0.0001$).

6.6. TLR4 is required to regulate the CHIKV entry in host macrophages, *in vitro*.

So far, TAK-242-mediated TLR4 antagonism has been found to reduce CHIKV infection in different host macrophages. Next, TAK-242-mediated TLR4 antagonism was studied individually in different stages of viral infection to explore the most specific stage/s associated with TLR4 in RAW264.7 macrophages. The drug (1 μ M) was added before CHIKV infection (only pre-incubation), during CHIKV infection, both before and during CHIKV infection (pre+ during incubation), post-infection incubation at 0 hpi (the drug was added at 0 hpi) and post-infection incubation at 8 hpi (the drug was added at 8 hpi). The cell culture supernatants of all conditions were collected at 9 hpi and further processed for viral RNA isolation followed by qRT-PCR-based analysis of the CHIKV E1 gene. It was observed that pre-incubation as well as pre+ during incubation of TAK-242 most effectively regulated CHIKV infection (a reduction of 62% and 59% of CHIKV-E1 copy number, respectively). Interestingly, CHIKV infection in the presence of the drug (during infection) also promoted a 45% decrease in viral RNA copy number. However, post-infection treatment with the drug showed no anti-viral modulation. Therefore, the data suggest the

probable anti-CHIKV role of TLR4 antagonism might be associated with the initial entry and/or attachment stage (**Fig: 39-A**).

Viral entry assay: To validate the role of TLR4 in viral entry and /or attachment step, the RAW264.7 cells were pre-incubated with 1 μ M of TAK-242 for 3 h before infection followed by CHIKV infection at MOI 5 for 2 h at 37°C. Next, the unadsorbed virus particles of the wash solution (i.e., CHIKV in SFM) were collected after completion of CHIKV infection, and viral titer, as well as viral E1-copy number, were determined using plaque assay and qRT-PCR-based analysis, respectively. It was noticed that 24.38 ± 2.302 % more CHIKV particles and 10.86% more CHIKV-E1 RNA copy numbers were found in the TAK-242 pre-treated wash solution (**Fig: 39-B, C**). Therefore, the data reconfirm the requirement of TLR4 to facilitate CHIKV entry and/or attachment in host macrophages.

Time of addition assay: To re-confirm the role of TLR4 in post-CHIKV infection stages, a time of addition assay was performed. To experiment, the TLR4-antagonist was added at different time points post-infection, starting from 0 to 14 hpi with a gap of 2 hpi. All supernatants were collected at 15 hpi. The plaque assay-based viral titer analysis revealed no significant anti-viral role of post-infection TLR4 inhibition in RAW264.7 macrophages. Therefore, the data suggest no association of TLR4 with CHIKV infection once the virus is internalized into host macrophages (**Fig: 39-D**).

Temperature shift assay: To explore the importance of TLR4 in the CHIKV attachment and/or entry procedure, the “Temperature shift assay” was performed as mentioned in the materials and method section. The wash solutions containing unbound (37°C)/uninternalized (45°C) virus particles were collected after the incubation and were subjected to qRT-PCR analysis of the E1 gene. The results showed that around 25% more CHIKV particles were found in the wash solution of the TAK-242 treated condition (37°C), which indicated that around 25% less viruses were internalized/ attached in the TAK-242 treated condition. Moreover, around 46% more CHIKV

particles were found in TAK-242 treated supernatant at 45°C which depicts that around 46 % more viruses were attached to TAK-242 treated cells but unable to internalize inside the cells (**Fig: 39-E**). Taken together, the data suggest that TLR4 might play an impactful role in both the CHIKV attachment and entry process.

TAK-242-driven TLR4 inhibition was found to inhibit CHIKV entry and/or attachment. Next, the internal CHIKV-E1 RNA copy numbers were calculated in different time points post-infection in the same experimental setup to further validate the role of TLR4 as an entry and/or attachment factor of CHIKV. The RAW264.7 cells were pretreated with TAK-242 for 3 h followed by CHIKV infection at MOI 5 for 2 h. Next, the cells were harvested at 0, 2, and 4 hpi and subjected to internal RNA isolation followed by a qRT-PCR-based analysis of CHIKV-E1 copy numbers inside the cells. Interestingly, CHIKV-E1 copy numbers were found lower in TLR4-inhibited conditions of all three time points. Therefore, the data might conclude that pre-treatment of TLR4 inhibits viral entry and therefore, reduces viral replication inside the infected cells. The data supports the role of TLR4 as an entry and/or attachment factor of CHIKV infection in host macrophages (**Fig: 39-F**).

To explore the possible role of TLR4 in the viral transcription process in host macrophages, the RAW264.7 cells were infected with CHIKV at MOI 5 for 2 h and the infected cells were treated with TAK-242 at 0 hpi. Next, the cells, harvested at 2, 4, and 8 hpi, were subjected to cellular RNA isolation followed by qPCR-based viral RNA copy number analysis of the CHIKV-E1 gene. It was observed that no significant changes in CHIKV-E1 copy numbers in between TAK-242 post-treated or untreated groups at different hpi (**Fig: 39-G**). Therefore, the data emphasizes the non-associative role of TAK-242-driven TLR4 inhibition on viral RNA transcription.

The possible association of TLR4 inhibition with the viral translation process in host macrophages was also investigated similarly. The CHIKV-infected RAW264.7 cells were subjected to TAK-242 treatment at 0 hpi and the cells were harvested at 2, 4, and 8 hpi. Next, the

Western blot-based analysis revealed no significant changes in CHIKV-E2 protein expression in the presence or absence of TAK-242 treatment in all of the post-infection time points (**Fig: 39-H, I**). Therefore, the data indicate no possible association of TLR4 inhibition with the translation of viral proteins inside the host cells.

Together, all of these investigations were intended to determine the possible mechanism behind TLR4-dependent CHIKV infection in host macrophages. All of the studies may conclude the contribution of TLR4 as an entry and/or attachment factor of CHIKV in host macrophages.

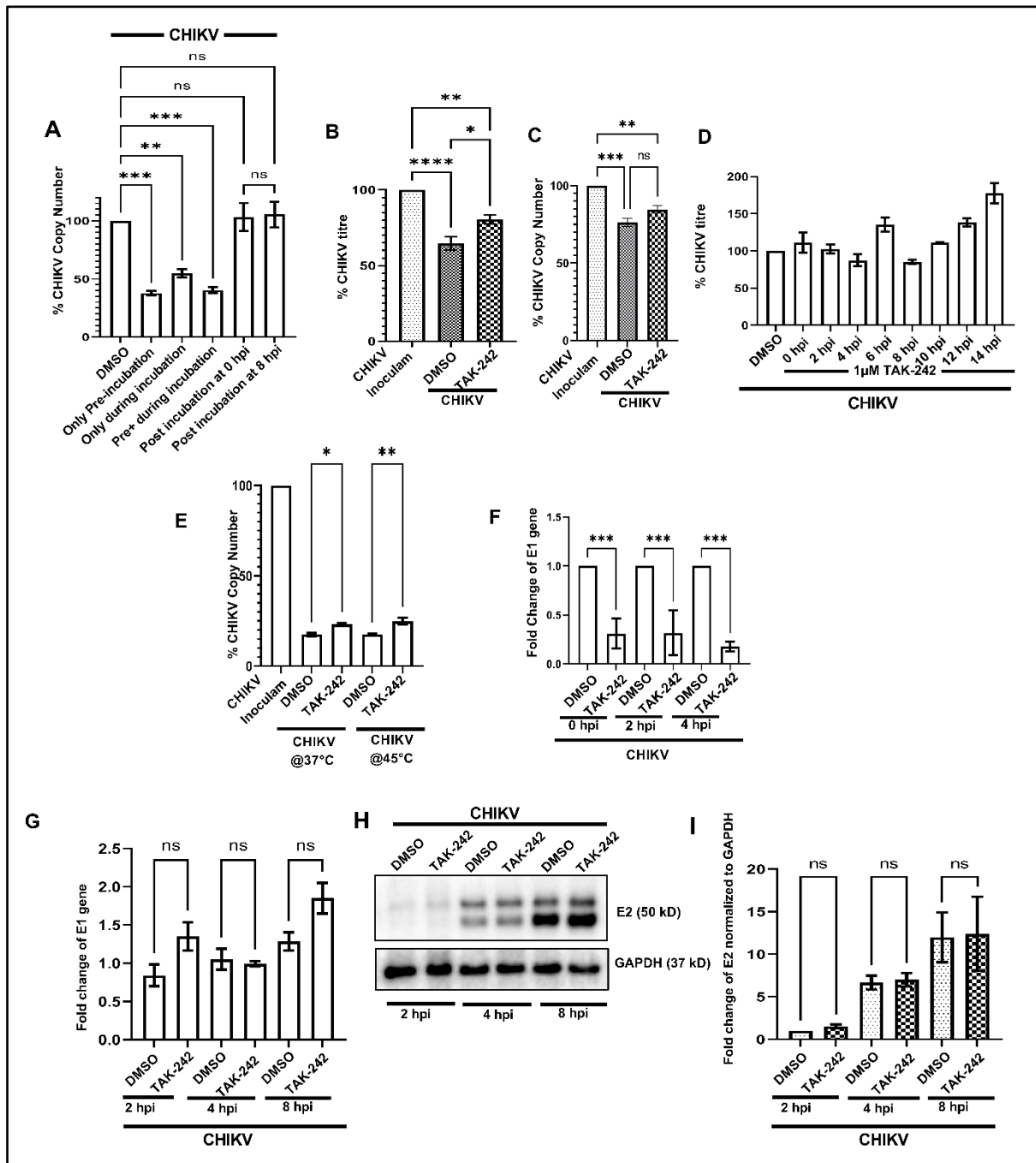


Figure 39: TLR4 regulates CHIKV entry in early stages of viral infection in RAW264.7 cells, *in vitro*. (A) TLR4 inhibition before or before and during CHIKV infection are most effective to reduce CHIKV infection. (B, C) **Viral entry assay:** Plaque assay-based viral titer and qRT-PCR-based viral RNA copy number analysis revealed 24 and 11% less viral entry and/or attachment, respectively, in TLR4-inhibited conditions. (D) **Time of addition assay:** TLR4 inhibition in post-infection incubated condition showing no significant role in reducing viral titer. (E) **Temperature shift assay:** The bar diagram depicting the presence of more unbound virus particles, therefore,

reduced viral entry in TLR4 inhibited conditions in different temperatures (F) TLR4 inhibition before CHIKV infection reducing CHIKV-E1 copy numbers in different time points (G) The bar diagram representing no role of post-infection inhibition of TLR4 at 0 hpi on CHIKV-E1 copy numbers in different timepoints (H, I) The Western blot image and corresponding bar diagram representing no role of post-infection inhibition of TLR4 at 0 hpi on CHIKV-E2 expression in different time points. Data represent the Mean \pm SEM of three independent replicates. (ns=non-significant, * p <0.05, ** p \leq 0.01, *** p \leq 0.001, **** p \leq 0.0001).

6.7. TLR4 inhibition efficiently reduces the CHIKV infection and inflammation in mice, *in vivo*

The possible inhibitory role of TAK-242-mediated TLR4 antagonism was investigated in 10-12 days old C57BL/6 mice (n=5). For the TAK-242 treated group of mice, the drug was orally administered at the dosage of 1mg/kg of body weight for one day before CHIKV infection to 4 days post-infection (dpi). All of the mice groups were sacrificed on 5 dpi. The phenotypic observations revealed a reduction of CHIKV-mediated impaired limb movements (indicated by red arrows) in the TAK-242-treated group (40-A). The plaque assay-based viral titer in quadriceps muscle and spleen showed a reduction of 41.26 \pm 2.664% and 47.01 \pm 0.4225% respectively, in TAK-242-driven TLR4 inhibited condition (40-B, C). Next, Western blot-based was performed to estimate viral protein levels in different tissues. A significant decrease of 56.08 \pm 2.020% and 50.04 \pm 0.6860% in CHIKV-E2 levels was found in tissue lysate obtained from quadriceps muscle and spleen of TLR4-inhibited mice group (40-D, F). To understand the CHIKV-induced inflammation, ELISA-based quantification of serum TNF was performed. The study revealed a significant decrease (38.47 \pm 2.128%) in serum TNF level in the TLR4-inhibited mice group (40-G). Additionally, the comparative arthritogenic symptoms of viral infection in terms of mean clinical scores were noted in CHIKV-infected mice groups treated with or without TAK-242.

TLR4 inhibition showed a visible decrease in the mean clinical score of CHIKV-infected mice (40-H). To determine the survival efficacy of CHIKV-infected mice in the presence of TAK-242-mediated TLR4 inhibition, a survival curve study was performed (n=6). The results showed that all of the CHIKV-infected mice died on 8th dpi whereas oral administration of TAK-242 showed a marked 75% survival of CHIKV-infected mice (40-I). Collectively, the data indicate the anti-viral role of TAK-242-directed TLR4 inhibition in CHIKV-infected mice model, *in vivo*.

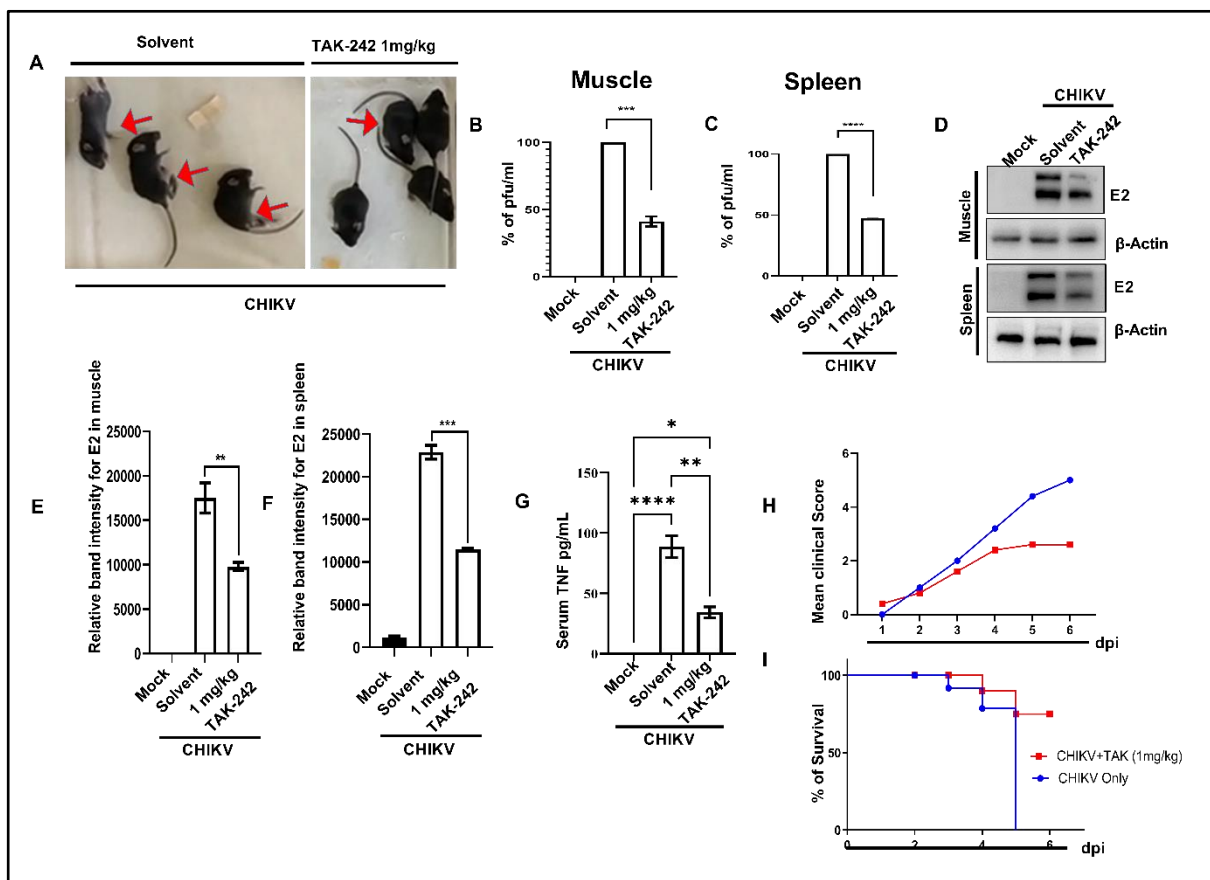


Figure 40: TLR4-antagonism protects and increases survival of CHIKV-infected mice, *in vivo*. C57BL/6 mice with an age of 10-12 days old (n=5) were orally administered TAK-242 (dosage:1mg/kg) from 24 h before to 96 h post-CHIKV infection at every 24 h interval. Both of the TAK-242 treated or untreated mice groups were subcutaneously injected with 10^6 PFU of CHIKV-IS. The mice groups were sacrificed at 5 days post-infection (dpi) and further experimentations were performed. (A) The image representing the healing role of TLR4 inhibition against CHIKV infection. The red arrows indicate the mice with impaired limb movement. (B, C)

The bar diagrams represent the percent CHIKV titer (PFU/ml) from the muscle and spleen of different groups of mice, respectively. **(D-F)** The Western blot image and corresponding graphical presentations denoting the CHIKV-E2 expression in muscles and spleens of different mice groups. **(G)** The graph representation of ELISA-based cytokine analysis of serum TNF collected from different groups of mice. **(H)** The diagram representing disease symptoms from 1 to 6 dpi in terms of mean clinical score of different groups of mice. **(I)** The survival curve denoting the effectiveness of TAK-242-mediated TLR4 inhibition in CHIKV-infected mice (n=6). Data represent the Mean \pm SEM of three independent replicates. (ns=non-significant, * $p<0.05$, ** $p\leq 0.01$, *** $p\leq 0.001$, **** $p\leq 0.0001$).

7. Discussion

TLR4, an important member of the innate immune system, acts as one of the earliest determinants of foreign immunogenic components associated with different sets of pathogens. From the very beginning of the discovery, the role of TLR4 has been studied critically to evaluate the functional aspects of host-pathogen interactions and subsequent pro-inflammatory immune responses. In this way, TLR4 has evolved as a suitable target for modern-age bio-medical research in the field of necrotizing enterocolitis, rheumatoid arthritis, and inflammatory bowel disease (9,12,13). Additionally, the exclusive regulatory role of TLR4 has also been investigated in the LPS-mediated endotoxin shock and sepsis model in mice using TAK-242 as a probable TLR4 antagonist (10,192). In the case of LPS-dependent TLR4 activation, LPS binding protein (LBP), an extracellular protein, first interacts with soluble or bacterial membrane-bound LPS molecules. A single LPS-LBP complex then interacts with either soluble or the membrane-bound CD14 protein, a co-stimulator of the TLR4 signaling pathway. CD14 has been designated as a carrier to transfer a single molecule of LPS to MD2, which further promotes the TLR4-MD2 heterodimer formation i.e., the functional LPS receptor. The TLR4-MD2 dimerization initiates a downstream

signaling cascade (145). The LPS induction promotes the internalization of cell surface TLR4 and also enhances the expression of macrophage activation markers like CD14, MHC-II, and CD86 (183,184,193–196). Notably, activation of TLR4 leads to phosphorylation of NF- κ B (187) and therefore, has a direct association with inflammation (188,189). TAK-242, a cyclohexene derivative small molecule, has been found to interact selectively to the Cys747 residue of the Toll/interleukin 1 receptor (TIR) domain of TLR4 and prohibits the downstream signaling cascade (10,20). As per the previous report, it has been shown that the pre-incubation with 1 μ M of TAK-242 for 5 minutes can reduce LPS-induced TNF production by 80% in the mouse peritoneal macrophages and the efficacy of the specific anti-inflammatory role of TAK-242 is concentration and time-dependent (20). This group has also shown TAK-242-mediated reduced activation of the NF- κ B pathway upon TLR4 inhibition (20). Therefore, the effect of TAK-242-driven TLR4 inhibition has been simultaneously studied in the LPS-induced pro-inflammatory model as an experimental control of the current study. The re-emergence of CHIKV is considered as one of the global public health threats especially due to the unavailability of possible anti-CHIKV drugs or vaccines to date. The available reports on CHIKV infection and pathogenesis demonstrate the cytokine burst in the host (7). Hence, the current study is intended to explore the involvement of TLR4 during CHIKV infection and associated pro-inflammatory responses.

Previous pieces of literature have already depicted the macrophages as a possible source of CHIKV-induced cytokine burst both *in vivo* as well as *in vitro*(7,8,197,198). The published literature on both mice and macaque models revealed the macrophages as one of the major immune cells to be recruited at the site of inoculation and therefore, are associated with strong immune responses by pro-inflammatory cytokine release, which might be associated with the tenosynovitis, CHIKV-induced arthritis and myositis (199,200). The CHIKV is already known for its immune evasion mechanisms, residing inside the macrophages followed by reappearance after several months or even years (197). Therefore, a detailed study of the modulation of the host

immune system due to CHIKV infection in macrophages might give a counterregulatory mechanism against CHIKV persistence and subsequent future therapeutic strategies.

TAK-242 (Resatorvid), a well-established TLR4-antagonist, is currently under clinical trials for several inflammatory diseases, such as severe sepsis (33) and acute alcoholic hepatitis (ClinicalTrials.gov.Identifier: NCT04620148,<https://clinicaltrials.gov/ct2/show/NCT04620148>). Therefore, this drug has been used to study the TLR4-driven immune regulation, if any, of CHIKV-induced pro-inflammatory responses. The current proceedings may decipher that TAK-242-mediated TLR4 inhibition may abrogate CHIKV infection, macrophage activation, and pro-inflammatory responses in mouse and human macrophages, *in vitro*. It also illuminates the positive association of TLR4 inhibition with the reduction in CHIKV-driven MAPK activation. Notably, it is found that CHIKV-E2 interacts with TLR4 during infection which is essential for efficient viral infection in host macrophages. The interaction of the extracellular domain of TLR4 and CHIKV-E2 has been further validated by *in-silico* analysis using the mouse TLR4-MD2 complex as the ligand and CHIKV structural protein, E2 as the receptor. The analysis highlights 12 possible interactions where Thr546, Ser550, and Tyr454 residues of TLR4 are found to be critically essential to interact with CHIKV-E2, *in silico*. Therefore, the study depicts TLR4 as one of the possible receptors of the CHIKV-E2 protein to facilitate viral infection. Moreover, the anti-TLR4 antibody-dependent blocking assay further strengthens the role of TLR4 as a possible receptor for CHIKV-E2 and therefore, TLR4-mediated CHIKV entry in the RAW264.7 macrophages. It has also been observed that TLR4 promotes the CHIKV attachment step. Therefore, TAK-242-driven TLR4 inhibition or absence of functional TLR4 might lead to an overall decrease in viral titer. The study also suggests that TLR4 inhibition has no role in post-entry stages of viral infection i.e., viral transcription, replication, and translation inside the host macrophages. Additionally, the TLR4 antagonism effectively reduces CHIKV infection and inflammation, *in vivo* by reducing the disease score, significantly with improved

survival of CHIKV-infected mice. Therefore, the positive regulation of TLR4 on CHIKV infection in different host systems could be associated with inflammation and viral pathogenesis.

An earlier report on the respiratory syncytial virus (RSV) describes that the functional TLR4 is an essential component to promote viral infection and the infection-induced inflammasome activation, vascular damage, T cell activation, B cell maturation and NK cell activation in mice model (14). Recent studies on SARS-CoV2 imply that TAK-242 mediated TLR4 inhibition significantly abolishes viral spike protein-induced pro-inflammatory cytokine responses in association with the p-NF- κ B protein in the murine and human macrophages (16,201). VP3, a structural protein of the foot and mouth disease virus (FMDV) is already reported to interact and induce TLR4 to promote viral infection and associated inflammation (15). Furthermore, previous reports on the reduction in the surface expression of TLR4 and increase in the total TLR4 upon LPS or virus-mediated stimulation are found to be similar to this current investigation (15,183,184). Hence, the current study suggests a positive regulation of TLR4 on CHIKV entry, infection, and associated inflammation in the host.

Although this study proposes probable TLR4-mediated CHIKV entry, TLR4 inhibition doesn't completely hinder viral entry in the host. Therefore, it seems that the possible involvement of other cellular receptor/s (34) to execute viral entry and pathogenesis might be crucial under the current experimental scenario, which is yet to be explored. Moreover, siRNA-mediated gene silencing could be explored as a suitable tool to investigate the detailed role of TLR4 during viral infection.

The *in-silico* study reveals the association of specific amino acids of TLR4-MD2 complex and CHIKV-E2 proteins in the current investigation. Two amino acid residues, Asn572 and Lys503 of TLR4 (PDB ID: 2Z64) have been found to show high-affinity polar interactions (< 2 Å) with Glu308 and Glu 303 of CHIKV-E2 (PDB ID: 3N41), respectively. Furthermore, Thr546, Ser550, and Tyr454 residues of TLR4 and Gln307 and Glu303 residues of CHIKV-E2 protein

have been shown to exhibit multiple polar interactions to emphasize their prominent role in terms of CHIKV-TLR4 association. Further, it will be interesting to investigate the role of these amino acid residues in this interaction through mutational studies in the future.

In addition to the mice model, earlier reports are also available on the CHIKV-driven pro-inflammatory cytokine burst and associated symptoms in human patient studies, *in vivo* (5,6). Accordingly, the effect of TLR4 inhibition could be further explored in experimental *in vitro* or *in vivo* setups with CHIKV-infected patient samples. Therefore, the probable efficacy of TLR4 inhibition against CHIKV infection might be explored in higher-order mammalian systems in future.

8. Conclusion

In conclusion, the current study reveals the probable regulatory role of TLR4 at the attachment as well as entry stages of viral infection via interaction with the CHIKV structural protein E2. Therefore, TLR4 could be considered as a possible receptor of CHIKV and a positive regulator of CHIKV-driven pro-inflammatory immune responses in the host. Considering this regulatory role of TLR4, this current study might have translational implications for designing future therapeutic strategies against CHIKV infection to modulate the disease pathogenesis.

References:

1. Suhrbier A. Rheumatic manifestations of chikungunya: emerging concepts and interventions. *Nat Rev Rheumatol* (2019) 15:597–611. doi: 10.1038/s41584-019-0276-9
2. Webb E, Michelen M, Rigby I, Dagens A, Dahmash D, Cheng V, Joseph R, Lipworth S, Harriss E, Cai E, et al. An evaluation of global Chikungunya clinical management guidelines: A systematic review. *EClinicalMedicine* (2022) 54:101672. doi: 10.1016/j.eclinm.2022.101672
3. Cunha RV da, Trinta KS. Chikungunya virus: clinical aspects and treatment - A Review. *Mem Inst Oswaldo Cruz* (2017) 112:523–531. doi: 10.1590/0074-02760170044
4. Simon F, Javelle E, Cabie A, Bouquillard E, Troisgros O, Gentile G, Leparç-Goffart I, Hoen B, Gandjbakhch F, Rene-Corail P, et al. French guidelines for the management of chikungunya (acute and persistent presentations). November 2014. *Med Mal Infect* (2015) 45:243–263. doi: 10.1016/j.medmal.2015.05.007
5. Guerrero-Arguero I, Høj TR, Tass ES, Berges BK, Robison RA. A comparison of Chikungunya virus infection, progression, and cytokine profiles in human PMA-differentiated U937 and murine RAW264.7 monocyte derived macrophages. *PLoS One* (2020) 15:e0230328. doi: 10.1371/journal.pone.0230328
6. Jacob-Nascimento LC, Carvalho CX, Silva MMO, Kikuti M, Anjos RO, Fradico JRB, Campi-Azevedo AC, Tauro LB, Campos GS, Moreira PS dos S, et al. Acute-Phase Levels of CXCL8 as Risk Factor for Chronic Arthralgia Following Chikungunya Virus Infection. *Front Immunol* (2021) 12: doi: 10.3389/fimmu.2021.744183
7. Nayak T, Mamidi P, Kumar A, Singh L, Sahoo S, Chattopadhyay S, Chattopadhyay S. Regulation of Viral Replication, Apoptosis and Pro-Inflammatory Responses by 17-AAG during Chikungunya Virus Infection in Macrophages. *Viruses* (2017) 9:3. doi: 10.3390/v9010003
8. Nayak TK, Mamidi P, Sahoo SS, Kumar PS, Mahish C, Chatterjee S, Subudhi BB, Chattopadhyay S, Chattopadhyay S. P38 and JNK Mitogen-Activated Protein Kinases Interact With Chikungunya Virus Non-structural Protein-2 and Regulate TNF Induction During Viral Infection in Macrophages. *Front Immunol* (2019) 10: doi: 10.3389/fimmu.2019.00786
9. Samarpita S, Kim JY, Rasool MK, Kim KS. Investigation of toll-like receptor (TLR) 4 inhibitor TAK-242 as a new potential anti-rheumatoid arthritis drug. *Arthritis Res Ther* (2020) 22:16. doi: 10.1186/s13075-020-2097-2
10. Takashima K, Matsunaga N, Yoshimatsu M, Hazeki K, Kaisho T, Uekata M, Hazeki O, Akira S, Iizawa Y, Ii M. Analysis of binding site for the novel small-molecule TLR4 signal transduction inhibitor TAK-242 and its therapeutic effect on mouse sepsis model. *Br J Pharmacol* (2009) 157:1250–1262. doi: 10.1111/j.1476-5381.2009.00297.x
11. Wu K, Zhang H, Fu Y, Zhu Y, Kong L, Chen L, Zhao F, Yu L, Chen X. TLR4/MyD88 signaling determines the metastatic potential of breast cancer cells. *Mol Med Rep* (2018) doi: 10.3892/mmr.2018.9326

12. Han C, Guo L, Sheng Y, Yang Y, Wang J, Gu Y, Li W, Zhou X, Jiao Q. FoxO1 regulates TLR4/MyD88/MD2-NF- κ B inflammatory signalling in mucosal barrier injury of inflammatory bowel disease. *J Cell Mol Med* (2020) 24:3712–3723. doi: 10.1111/jcmm.15075
13. Yu R, Jiang S, Tao Y, Li P, Yin J, Zhou Q. Inhibition of HMGB1 improves necrotizing enterocolitis by inhibiting NLRP3 via TLR4 and NF- κ B signaling pathways. *J Cell Physiol* (2019) 234:13431–13438. doi: 10.1002/jcp.28022
14. Marzec J, Cho H-Y, High M, McCaw ZR, Polack F, Kleeberger SR. Toll-like receptor 4-mediated respiratory syncytial virus disease and lung transcriptomics in differentially susceptible inbred mouse strains. *Physiol Genomics* (2019) 51:630–643. doi: 10.1152/physiolgenomics.00101.2019
15. Zhang J, Li D, Yang W, Wang Y, Li L, Zheng H. Foot-and-Mouth Disease Virus VP3 Protein Acts as a Critical Proinflammatory Factor by Promoting Toll-Like Receptor 4-Mediated Signaling. *J Virol* (2021) 95: doi: 10.1128/JVI.01120-21
16. Zhao Y, Kuang M, Li J, Zhu L, Jia Z, Guo X, Hu Y, Kong J, Yin H, Wang X, et al. SARS-CoV-2 spike protein interacts with and activates TLR41. *Cell Res* (2021) 31:818–820. doi: 10.1038/s41422-021-00495-9
17. Felipe VLJ, Paula A V, Silvio U-I. Chikungunya virus infection induces differential inflammatory and antiviral responses in human monocytes and monocyte-derived macrophages. *Acta Trop* (2020) 211:105619. doi: 10.1016/j.actatropica.2020.105619
18. Nayak TK, Mamidi P, Sahoo SS, Sanjai Kumar P, Mahish C, Chatterjee S, Subudhi BB, Chattopadhyay S, Chattopadhyay S. P38 and JNK Mitogen-Activated Protein Kinases Interact with Chikungunya Virus Non-structural Protein-2 and Regulate TNF Induction during Viral Infection in Macrophages. *Front Immunol* (2019) 10:1–15. doi: 10.3389/fimmu.2019.00786
19. Lin F-Y, Chen Y-H, Tasi J-S, Chen J-W, Yang T-L, Wang H-J, Li C-Y, Chen Y-L, Lin S-J. Endotoxin Induces Toll-Like Receptor 4 Expression in Vascular Smooth Muscle Cells via NADPH Oxidase Activation and Mitogen-Activated Protein Kinase Signaling Pathways. *Arterioscler Thromb Vasc Biol* (2006) 26:2630–2637. doi: 10.1161/01.ATV.0000247259.01257.b3
20. Matsunaga N, Tsuchimori N, Matsumoto T, li M. TAK-242 (Resatorvid), a Small-Molecule Inhibitor of Toll-Like Receptor (TLR) 4 Signaling, Binds Selectively to TLR4 and Interferes with Interactions between TLR4 and Its Adaptor Molecules. *Mol Pharmacol* (2011) 79:34–41. doi: 10.1124/mol.110.068064
21. Sanjai Kumar P, Nayak TK, Mahish C, Sahoo SS, Radhakrishnan A, De S, Datey A, Sahu RP, Goswami C, Chattopadhyay S, et al. Inhibition of transient receptor potential vanilloid 1 (TRPV1) channel regulates chikungunya virus infection in macrophages. *Arch Virol* (2021) 166:139–155. doi: 10.1007/s00705-020-04852-8
22. Anand G, Perry AM, Cummings CL, St. Raymond E, Clemens RA, Steed AL. Surface Proteins of SARS-CoV-2 Drive Airway Epithelial Cells to Induce IFN-Dependent Inflammation. *The Journal of Immunology* (2021) 206:3000–3009. doi: 10.4049/jimmunol.2001407

23. Sha T, Sunamoto M, Kitazaki T, Sato J, li M, Iizawa Y. Therapeutic effects of TAK-242, a novel selective Toll-like receptor 4 signal transduction inhibitor, in mouse endotoxin shock model. *Eur J Pharmacol* (2007) 571:231–239. doi: 10.1016/j.ejphar.2007.06.027
24. Chattopadhyay S, Chakraborty NG. Continuous Presence of Th1 Conditions Is Necessary for Longer Lasting Tumor-Specific CTL Activity in Stimulation Cultures With PBL. *Hum Immunol* (2005) 66:884–891. doi: 10.1016/j.humimm.2005.06.002
25. De S, Mamidi P, Ghosh S, Keshry SS, Mahish C, Pani SS, Laha E, Ray A, Datey A, Chatterjee S, et al. Telmisartan restricts Chikungunya virus infection *in vitro* and *in vivo* through the AT1/PPAR- γ /MAPKs pathways. *Antimicrob Agents Chemother* (2021) doi: 10.1128/AAC.01489-21
26. De S, Ghosh S, Keshry SS, Mahish C, Mohapatra C, Guru A, Mamidi P, Datey A, Pani SS, Vasudevan D, et al. MBZM-N-IBT, a Novel Small Molecule, Restricts Chikungunya Virus Infection by Targeting nsP2 Protease Activity *In Vitro*, *In Vivo*, and *Ex Vivo*. *Antimicrob Agents Chemother* (2022) 66: doi: 10.1128/aac.00463-22
27. Liu G, Xie J, Shi Y, Chen R, Li L, Wang M, Zheng M, Xu J. Sec-O-glucosylhamaudol suppressed inflammatory reaction induced by LPS in RAW264.7 cells through inhibition of NF- κ B and MAPKs signaling. *Biosci Rep* (2020) 40: doi: 10.1042/BSR20194230
28. Sahoo SS, Pratheek BM, Meena VS, Nayak TK, Kumar PS, Bandyopadhyay S, Maiti PK, Chattopadhyay S. VIPER regulates naive T cell activation and effector responses: Implication in TLR4 associated acute stage T cell responses. *Sci Rep* (2018) 8:7118. doi: 10.1038/s41598-018-25549-8
29. Feng H, Zhang D, Palliser D, Zhu P, Cai S, Schlesinger A, Maliszewski L, Lieberman J. *Listeria* - Infected Myeloid Dendritic Cells Produce IFN- β , Priming T Cell Activation. *The Journal of Immunology* (2005) 175:421–432. doi: 10.4049/jimmunol.175.1.421
30. Chatterjee S, Kumar S, Mamidi P, Datey A, Sengupta S, Mahish C, Laha E, De S, Keshry SS, Nayak TK, et al. DNA Damage Response Signaling Is Crucial for Effective Chikungunya Virus Replication. *J Virol* (2022) doi: 10.1128/jvi.01334-22
31. Pierce BG, Wiehe K, Hwang H, Kim B-H, Vreven T, Weng Z. ZDOCK server: interactive docking prediction of protein-protein complexes and symmetric multimers. *Bioinformatics* (2014) 30:1771–1773. doi: 10.1093/bioinformatics/btu097
32. Yang K, Zhang XJ, Cao LJ, Liu XH, Liu ZH, Wang XQ, Chen QJ, Lu L, Shen WF, Liu Y. Toll-Like Receptor 4 Mediates Inflammatory Cytokine Secretion in Smooth Muscle Cells Induced by Oxidized Low-Density Lipoprotein. *PLoS One* (2014) 9:e95935. doi: 10.1371/journal.pone.0095935
33. Rice TW, Wheeler AP, Bernard GR, Vincent J-L, Angus DC, Aikawa N, Demeyer I, Sainati S, Amlot N, Cao C, et al. A randomized, double-blind, placebo-controlled trial of TAK-242 for the treatment of severe sepsis*. *Crit Care Med* (2010) 38:1685–1694. doi: 10.1097/CCM.0b013e3181e7c5c9
34. Zhang R, Kim AS, Fox JM, Nair S, Basore K, Klimstra WB, Rimkunas R, Fong RH, Lin H, Poddar S, et al. Mxra8 is a receptor for multiple arthritogenic alphaviruses. *Nature* (2018) 557:570–574. doi: 10.1038/s41586-018-0121-3

35. Grubbs H, Kahwaji CI. *Physiology, Active Immunity*. (2023).
36. Justiz Vaillant AA, Sabir S, Jan A. *Physiology, Immune Response*. (2023).
37. Rahman M, Bordoni B. *Histology, Natural Killer Cells*. (2023).
38. Judith A. Owen JPSAS with contributions by PPJones. *Kuby immunology*.
39. Alberts B JALJ et al. *Molecular Biology of the Cell. 4th edition. New York: Garland Science; 2002. Chapter 24, The Adaptive Immune System*.
40. Different cells of immune system.
41. Exogenous and Endogenous antigen processing and presentation.
42. The general structure of an Antibody.
43. T cell activation.
44. Nasir A, Kim KM, Caetano-Anollés G. Viral evolution. *Mob Genet Elements* (2012) 2:247–252. doi: 10.4161/mge.22797
45. CRICK F. Central Dogma of Molecular Biology. *Nature* (1970) 227:561–563. doi: 10.1038/227561a0
46. Koonin E V., Krupovic M, Agol VI. The Baltimore Classification of Viruses 50 Years Later: How Does It Stand in the Light of Virus Evolution? *Microbiology and Molecular Biology Reviews* (2021) 85: doi: 10.1128/MMBR.00053-21
47. Mahmoudabadi G, Phillips R. A comprehensive and quantitative exploration of thousands of viral genomes. *Elife* (2018) 7: doi: 10.7554/eLife.31955
48. Taxonomy browser powered by NCBI.
49. Leung JY-S, Ng MM-L, Chu JH. Replication of Alphaviruses: A Review on the Entry Process of Alphaviruses into Cells. *Adv Virol* (2011) 2011:1–9. doi: 10.1155/2011/249640
50. Lemm JA, Rumenapf T, Strauss EG, Strauss JH, Rice CM. Polypeptide requirements for assembly of functional Sindbis virus replication complexes: a model for the temporal regulation of minus- and plus-strand RNA synthesis. *EMBO J* (1994) 13:2925–2934. doi: 10.1002/j.1460-2075.1994.tb06587.x
51. Shirako Y, Strauss JH. Regulation of Sindbis virus RNA replication: uncleaved P123 and nsP4 function in minus-strand RNA synthesis, whereas cleaved products from P123 are required for efficient plus-strand RNA synthesis. *J Virol* (1994) 68:1874–1885. doi: 10.1128/jvi.68.3.1874-1885.1994
52. Janeway CA. Approaching the Asymptote? Evolution and Revolution in Immunology. *Cold Spring Harb Symp Quant Biol* (1989) 54:1–13. doi: 10.1101/SQB.1989.054.01.003

53. Amarante-Mendes GP, Adjemian S, Branco LM, Zanetti LC, Weinlich R, Bortoluci KR. Pattern Recognition Receptors and the Host Cell Death Molecular Machinery. *Front Immunol* (2018) 9: doi: 10.3389/fimmu.2018.02379
54. Walsh D, McCarthy J, O'Driscoll C, Melgar S. Pattern recognition receptors—Molecular orchestrators of inflammation in inflammatory bowel disease. *Cytokine Growth Factor Rev* (2013) 24:91–104. doi: 10.1016/j.cytogfr.2012.09.003
55. Kloc M, Uosef A, Kubiak JZ, Ghobrial RM. Macrophage Proinflammatory Responses to Microorganisms and Transplanted Organs. *Int J Mol Sci* (2020) 21:9669. doi: 10.3390/ijms21249669
56. Flannagan R, Heit B, Heinrichs D. Antimicrobial Mechanisms of Macrophages and the Immune Evasion Strategies of *Staphylococcus aureus*. *Pathogens* (2015) 4:826–868. doi: 10.3390/pathogens4040826
57. Reddick LE, Alto NM. Bacteria Fighting Back: How Pathogens Target and Subvert the Host Innate Immune System. *Mol Cell* (2014) 54:321–328. doi: 10.1016/j.molcel.2014.03.010
58. Freeman SA, Grinstein S. Phagocytosis: receptors, signal integration, and the cytoskeleton. *Immunol Rev* (2014) 262:193–215. doi: 10.1111/imr.12212
59. Brophy MB, Nolan EM. Manganese and Microbial Pathogenesis: Sequestration by the Mammalian Immune System and Utilization by Microorganisms. *ACS Chem Biol* (2015) 10:641–651. doi: 10.1021/cb500792b
60. Boe DM, Curtis BJ, Chen MM, Ippolito JA, Kovacs EJ. Extracellular traps and macrophages: new roles for the versatile phagocyte. *J Leukoc Biol* (2015) 97:1023–1035. doi: 10.1189/jlb.4RI1014-521R
61. Doster RS, Rogers LM, Gaddy JA, Aronoff DM. Macrophage Extracellular Traps: A Scoping Review. *J Innate Immun* (2018) 10:3–13. doi: 10.1159/000480373
62. Constant LEC, Rajsfus BF, Carneiro PH, Sisnande T, Mohana-Borges R, Allonso D. Overview on Chikungunya Virus Infection: From Epidemiology to State-of-the-Art Experimental Models. *Front Microbiol* (2021) 12: doi: 10.3389/fmicb.2021.744164
63. WHO report.
64. Josseran L, Paquet C, Zehgnoun A, Caillere N, Le Tertre A, Solet J-L, Ledrans M. Chikungunya Disease Outbreak, Reunion Island. *Emerg Infect Dis* (2006) 12:1994–1995. doi: 10.3201/eid1212.060710
65. Halstead SB. Reappearance of Chikungunya, Formerly Called Dengue, in the Americas. *Emerg Infect Dis* (2015) 21: doi: 10.3201/eid2104.141723
66. Morens DM, Fauci AS. Chikungunya at the Door — Déjà Vu All Over Again? *New England Journal of Medicine* (2014) 371:885–887. doi: 10.1056/NEJMp1408509
67. Schwartz O, Albert ML. Biology and pathogenesis of chikungunya virus. *Nat Rev Microbiol* (2010) 8:491–500. doi: 10.1038/nrmicro2368

68. European Centre for Disease Prevention and Control Report.
69. Ganesan V, Duan B, Reid S. Chikungunya Virus: Pathophysiology, Mechanism, and Modeling. *Viruses* (2017) 9:368. doi: 10.3390/v9120368
70. Coffey L, Failloux A-B, Weaver S. Chikungunya Virus–Vector Interactions. *Viruses* (2014) 6:4628–4663. doi: 10.3390/v6114628
71. Monteiro VVS, Navegantes-Lima KC, de Lemos AB, da Silva GL, de Souza Gomes R, Reis JF, Rodrigues Junior LC, da Silva OS, Romão PRT, Monteiro MC. Aedes–Chikungunya Virus Interaction: Key Role of Vector Midguts Microbiota and Its Saliva in the Host Infection. *Front Microbiol* (2019) 10: doi: 10.3389/fmicb.2019.00492
72. Juhn J, Naeem-Ullah U, Maciel Guedes BA, Majid A, Coleman J, Paolucci Pimenta PF, Akram W, James AA, Marinotti O. Spatial mapping of gene expression in the salivary glands of the dengue vector mosquito, *Aedes aegypti*. *Parasit Vectors* (2011) 4:1. doi: 10.1186/1756-3305-4-1
73. Melo B, Silva N, Gomes R, Navegantes K, Oliveira A, Almeida L, Azevedo C, Monteiro M. Bioactive Compounds of the Salivary Glands from *Aedes aegypti* with Anti-Hemostatic Action. *Annu Res Rev Biol* (2015) 8:1–17. doi: 10.9734/ARRB/2015/20322
74. Vega-Rúa A, Lourenço-de-Oliveira R, Mousson L, Vazeille M, Fuchs S, Yébakima A, Gustave J, Girod R, Dusfour I, Leparç-Goffart I, et al. Chikungunya Virus Transmission Potential by Local *Aedes* Mosquitoes in the Americas and Europe. *PLoS Negl Trop Dis* (2015) 9:e0003780. doi: 10.1371/journal.pntd.0003780
75. Schnierle BS. Cellular Attachment and Entry Factors for Chikungunya Virus. *Viruses* (2019) 11:1078. doi: 10.3390/v11111078
76. Voss JE, Vaney M-C, Duquerroy S, Vonnrhein C, Girard-Blanc C, Crublet E, Thompson A, Bricogne G, Rey FA. Glycoprotein organization of Chikungunya virus particles revealed by X-ray crystallography. *Nature* (2010) 468:709–712. doi: 10.1038/nature09555
77. Ahola T, Merits A. “Functions of Chikungunya Virus Nonstructural Proteins.,” *Chikungunya Virus*. Cham: Springer International Publishing (2016). p. 75–98 doi: 10.1007/978-3-319-42958-8_6
78. Ahola T, Kääriäinen L. Reaction in alphavirus mRNA capping: formation of a covalent complex of nonstructural protein nsP1 with 7-methyl-GMP. *Proceedings of the National Academy of Sciences* (1995) 92:507–511. doi: 10.1073/pnas.92.2.507
79. Ahola T, Karlin DG. Sequence analysis reveals a conserved extension in the capping enzyme of the alphavirus supergroup, and a homologous domain in nodaviruses. *Biol Direct* (2015) 10:16. doi: 10.1186/s13062-015-0050-0
80. Ahola T, Laakkonen P, Vihinen H, Kääriäinen L. Critical residues of Semliki Forest virus RNA capping enzyme involved in methyltransferase and guanylyltransferase-like activities. *J Virol* (1997) 71:392–397. doi: 10.1128/jvi.71.1.392-397.1997
81. Pastorino BAM, Peyrefitte CN, Almeras L, Grandadam M, Rolland D, Tolou HJ, Bessaud M. Expression and biochemical characterization of nsP2 cysteine protease of Chikungunya virus. *Virus Res* (2008) 131:293–298. doi: 10.1016/j.virusres.2007.09.009

82. Malet H, Coutard B, Jamal S, Dutartre H, Papageorgiou N, Neuvonen M, Ahola T, Forrester N, Gould EA, Lafitte D, et al. The Crystal Structures of Chikungunya and Venezuelan Equine Encephalitis Virus nsP3 Macro Domains Define a Conserved Adenosine Binding Pocket. *J Virol* (2009) 83:6534–6545. doi: 10.1128/JVI.00189-09
83. Feijs KLH, Forst AH, Verheugd P, Lüscher B. Macrodomein-containing proteins: regulating new intracellular functions of mono(ADP-ribosyl)ation. *Nat Rev Mol Cell Biol* (2013) 14:443–451. doi: 10.1038/nrm3601
84. Li C, Debing Y, Jankevicius G, Neyts J, Ahel I, Coutard B, Canard B. Viral Macro Domains Reverse Protein ADP-Ribosylation. *J Virol* (2016) 90:8478–8486. doi: 10.1128/JVI.00705-16
85. Rubach JK, Wasik BR, Rupp JC, Kuhn RJ, Hardy RW, Smith JL. Characterization of purified Sindbis virus nsP4 RNA-dependent RNA polymerase activity in vitro. *Virology* (2009) 384:201–208. doi: 10.1016/j.virol.2008.10.030
86. Tomar S, Hardy RW, Smith JL, Kuhn RJ. Catalytic Core of Alphavirus Nonstructural Protein nsP4 Possesses Terminal Adenylyltransferase Activity. *J Virol* (2006) 80:9962–9969. doi: 10.1128/JVI.01067-06
87. de Groot RJ, Rümenapf T, Kuhn RJ, Strauss EG, Strauss JH. Sindbis virus RNA polymerase is degraded by the N-end rule pathway. *Proceedings of the National Academy of Sciences* (1991) 88:8967–8971. doi: 10.1073/pnas.88.20.8967
88. Rathore APS, Haystead T, Das PK, Merits A, Ng M-L, Vasudevan SG. Chikungunya virus nsP3 & nsP4 interacts with HSP-90 to promote virus replication: HSP-90 inhibitors reduce CHIKV infection and inflammation in vivo. *Antiviral Res* (2014) 103:7–16. doi: 10.1016/j.antiviral.2013.12.010
89. Kam Y, Lum F, Teo T, Lee WWL, Simarmata D, Harjanto S, Chua C, Chan Y, Wee J, Chow A, et al. Early neutralizing IgG response to Chikungunya virus in infected patients targets a dominant linear epitope on the E2 glycoprotein. *EMBO Mol Med* (2012) 4:330–343. doi: 10.1002/emmm.201200213
90. CHIKV vaccine development in collaboration with Coalition for Epidemic Preparedness Innovations (CEPI).
91. National Center for Emerging and Zoonotic Infectious Diseases.
92. Kielian M, Chanel-Vos C, Liao M. Alphavirus Entry and Membrane Fusion. *Viruses* (2010) 2:796–825. doi: 10.3390/v2040796
93. Lee RCH, Hapuarachchi HC, Chen KC, Hussain KM, Chen H, Low SL, Ng LC, Lin R, Ng MM-L, Chu JH. Mosquito Cellular Factors and Functions in Mediating the Infectious entry of Chikungunya Virus. *PLoS Negl Trop Dis* (2013) 7:e2050. doi: 10.1371/journal.pntd.0002050
94. Smith AE, Helenius A. How Viruses Enter Animal Cells. *Science* (1979) (2004) 304:237–242. doi: 10.1126/science.1094823
95. Mercer J, Helenius A. Virus entry by macropinocytosis. *Nat Cell Biol* (2009) 11:510–520. doi: 10.1038/ncb0509-510

96. Lee CHR, Mohamed Hussain K, Chu JJH. Macropinocytosis dependent entry of Chikungunya virus into human muscle cells. *PLoS Negl Trop Dis* (2019) 13:e0007610. doi: 10.1371/journal.pntd.0007610
97. Weber C, König R, Niedrig M, Emmerich P, Schnierle BS. A neutralization assay for chikungunya virus infections in a multiplex format. *J Virol Methods* (2014) 201:7–12. doi: 10.1016/j.jviromet.2014.02.001
98. Bernard E, Solignat M, Gay B, Chazal N, Higgs S, Devaux C, Briant L. Endocytosis of Chikungunya Virus into Mammalian Cells: Role of Clathrin and Early Endosomal Compartments. *PLoS One* (2010) 5:e11479. doi: 10.1371/journal.pone.0011479
99. Gandhi NS, Mancera RL. The Structure of Glycosaminoglycans and their Interactions with Proteins. *Chem Biol Drug Des* (2008) 72:455–482. doi: 10.1111/j.1747-0285.2008.00741.x
100. Silva LA, Khomandiak S, Ashbrook AW, Weller R, Heise MT, Morrison TE, Dermody TS. A Single-Amino-Acid Polymorphism in Chikungunya Virus E2 Glycoprotein Influences Glycosaminoglycan Utilization. *J Virol* (2014) 88:2385–2397. doi: 10.1128/JVI.03116-13
101. Ashbrook AW, Burrack KS, Silva LA, Montgomery SA, Heise MT, Morrison TE, Dermody TS. Residue 82 of the Chikungunya Virus E2 Attachment Protein Modulates Viral Dissemination and Arthritis in Mice. *J Virol* (2014) 88:12180–12192. doi: 10.1128/JVI.01672-14
102. Henrik Gad H, Paulous S, Belarbi E, Diancourt L, Drosten C, Kümmerer BM, Plate AE, Caro V, Desprès P. The E2-E166K substitution restores Chikungunya virus growth in OAS3 expressing cells by acting on viral entry. *Virology* (2012) 434:27–37. doi: 10.1016/j.virol.2012.07.019
103. Kondratowicz AS, Lennemann NJ, Sinn PL, Davey RA, Hunt CL, Moller-Tank S, Meyerholz DK, Rennert P, Mullins RF, Brindley M, et al. T-cell immunoglobulin and mucin domain 1 (TIM-1) is a receptor for Zaire Ebolavirus and Lake Victoria Marburgvirus. *Proceedings of the National Academy of Sciences* (2011) 108:8426–8431. doi: 10.1073/pnas.1019030108
104. Moller-Tank S, Kondratowicz AS, Davey RA, Rennert PD, Maury W. Role of the Phosphatidylserine Receptor TIM-1 in Enveloped-Virus Entry. *J Virol* (2013) 87:8327–8341. doi: 10.1128/JVI.01025-13
105. Jemielity S, Wang JJ, Chan YK, Ahmed AA, Li W, Monahan S, Bu X, Farzan M, Freeman GJ, Umetsu DT, et al. TIM-family Proteins Promote Infection of Multiple Enveloped Viruses through Virion-associated Phosphatidylserine. *PLoS Pathog* (2013) 9:e1003232. doi: 10.1371/journal.ppat.1003232
106. Moller-Tank S, Albritton LM, Rennert PD, Maury W. Characterizing Functional Domains for TIM-Mediated Enveloped Virus Entry. *J Virol* (2014) 88:6702–6713. doi: 10.1128/JVI.00300-14
107. Prado Acosta M, Geoghegan EM, Lepenies B, Ruzal S, Kielian M, Martinez MG. Surface (S) Layer Proteins of Lactobacillus acidophilus Block Virus Infection via DC-SIGN Interaction. *Front Microbiol* (2019) 10: doi: 10.3389/fmicb.2019.00810
108. Chaaithanya IK, Muruganandam N, Surya P, Anwesh M, Alagarasu K, Vijayachari P. Association of Oligoadenylate Synthetase Gene Cluster and DC-SIGN (CD209) Gene Polymorphisms with

- Clinical Symptoms in Chikungunya Virus Infection. *DNA Cell Biol* (2016) 35:44–50. doi: 10.1089/dna.2015.2819
109. Dudha N, Rana J, Rajasekharan S, Gabrani R, Gupta A, Chaudhary VK, Gupta S. Host–pathogen interactome analysis of Chikungunya virus envelope proteins E1 and E2. *Virus Genes* (2015) 50:200–209. doi: 10.1007/s11262-014-1161-x
 110. Ooi YS, Stiles KM, Liu CY, Taylor GM, Kielian M. Genome-Wide RNAi Screen Identifies Novel Host Proteins Required for Alphavirus Entry. *PLoS Pathog* (2013) 9:e1003835. doi: 10.1371/journal.ppat.1003835
 111. Zani A, Yount JS. Antiviral Protection by IFITM3 In Vivo. *Curr Clin Microbiol Rep* (2018) 5:229–237. doi: 10.1007/s40588-018-0103-0
 112. Poddar S, Hyde JL, Gorman MJ, Farzan M, Diamond MS. The Interferon-Stimulated Gene IFITM3 Restricts Infection and Pathogenesis of Arthritogenic and Encephalitic Alphaviruses. *J Virol* (2016) 90:8780–8794. doi: 10.1128/JVI.00655-16
 113. Ooi Y, Dubé M, Kielian M. BST2/Tetherin Inhibition of Alphavirus Exit. *Viruses* (2015) 7:2147–2167. doi: 10.3390/v7042147
 114. Wintachai P, Wikan N, Kuadkitkan A, Jaimipuk T, Ubol S, Pulmanusahakul R, Auewarakul P, Kasinrerak W, Weng W-Y, Panyasrivanit M, et al. Identification of prohibitin as a Chikungunya virus receptor protein. *J Med Virol* (2012) 84:1757–1770. doi: 10.1002/jmv.23403
 115. Sripathi SR, He W, Atkinson CL, Smith JJ, Liu Z, Elledge BM, Jahng WJ. Mitochondrial–Nuclear Communication by Prohibitin Shuttling under Oxidative Stress. *Biochemistry* (2011) 50:8342–8351. doi: 10.1021/bi2008933
 116. Fongsaran C, Jirakanwisal K, Kuadkitkan A, Wikan N, Wintachai P, Thepparit C, Ubol S, Phaonakrop N, Roytrakul S, Smith DR. Involvement of ATP synthase β subunit in chikungunya virus entry into insect cells. *Arch Virol* (2014) 159:3353–3364. doi: 10.1007/s00705-014-2210-4
 117. Zhang R, Earnest JT, Kim AS, Winkler ES, Desai P, Adams LJ, Hu G, Bullock C, Gold B, Cherry S, et al. Expression of the Mxra8 Receptor Promotes Alphavirus Infection and Pathogenesis in Mice and *Drosophila*. *Cell Rep* (2019) 28:2647–2658.e5. doi: 10.1016/j.celrep.2019.07.105
 118. Couderc T, Chrétien F, Schilte C, Disson O, Brigitte M, Guivel-Benhassine F, Touret Y, Barau G, Cayet N, Schuffenecker I, et al. A Mouse Model for Chikungunya: Young Age and Inefficient Type-I Interferon Signaling Are Risk Factors for Severe Disease. *PLoS Pathog* (2008) 4:e29. doi: 10.1371/journal.ppat.0040029
 119. Fros JJ, Liu WJ, Prow NA, Geertsema C, Ligtenberg M, Vanlandingham DL, Schnettler E, Vlak JM, Suhrbier A, Khromykh AA, et al. Chikungunya Virus Nonstructural Protein 2 Inhibits Type I/II Interferon-Stimulated JAK-STAT Signaling. *J Virol* (2010) 84:10877–10887. doi: 10.1128/JVI.00949-10
 120. Kelvin AA, Banner D, Silvi G, Moro ML, Spataro N, Gaibani P, Cavrini F, Pierro A, Rossini G, Cameron MJ, et al. Inflammatory Cytokine Expression Is Associated with Chikungunya Virus

- Resolution and Symptom Severity. *PLoS Negl Trop Dis* (2011) 5:e1279. doi: 10.1371/journal.pntd.0001279
121. Kumar S, Jaffar-Bandjee M-C, Giry C, Connen de Kerillis L, Merits A, Gasque P, Hoarau J-J. Mouse macrophage innate immune response to chikungunya virus infection. *Virology* (2012) 9:313. doi: 10.1186/1743-422X-9-313
 122. Priya R, Dhanwani R, Patro IK, Rao PVL, Parida MM. Differential regulation of TLR mediated innate immune response of mouse neuronal cells following infection with novel ECSA genotype of Chikungunya virus with and without E1:A226V mutation. *Infection, Genetics and Evolution* (2013) 20:396–406. doi: 10.1016/j.meegid.2013.09.030
 123. Priya R, Patro IK, Parida MM. TLR3 mediated innate immune response in mice brain following infection with Chikungunya virus. *Virus Res* (2014) 189:194–205. doi: 10.1016/j.virusres.2014.05.010
 124. Chirathaworn C, Poovorawan Y, Lertmaharit S, Wuttirattanakowit N. Cytokine levels in patients with chikungunya virus infection. *Asian Pac J Trop Med* (2013) 6:631–634. doi: 10.1016/S1995-7645(13)60108-X
 125. Chow A, Her Z, Ong EKS, Chen J, Dimatatac F, Kwek DJC, Barkham T, Yang H, Rénia L, Leo Y-S, et al. Persistent Arthralgia Induced by Chikungunya Virus Infection is Associated with Interleukin-6 and Granulocyte Macrophage Colony-Stimulating Factor. *J Infect Dis* (2011) 203:149–157. doi: 10.1093/infdis/jiq042
 126. Lohachanakul J, Phuklia W, Thannagith M, Thongsakulprasert T, Smith DR, Ubol S. Differences in response of primary human myoblasts to infection with recent epidemic strains of Chikungunya virus isolated from patients with and without myalgia. *J Med Virol* (2015) 87:733–739. doi: 10.1002/jmv.24081
 127. Phuklia W, Kasisith J, Modhiran N, Rodpai E, Thannagith M, Thongsakulprasert T, Smith DR, Ubol S. Osteoclastogenesis induced by CHIKV-infected fibroblast-like synoviocytes: A possible interplay between synoviocytes and monocytes/macrophages in CHIKV-induced arthralgia/arthritis. *Virus Res* (2013) 177:179–188. doi: 10.1016/j.virusres.2013.08.011
 128. Reddy V, Mani RS, Desai A, Ravi V. Correlation of plasma viral loads and presence of Chikungunya IgM antibodies with cytokine/chemokine levels during acute Chikungunya virus infection. *J Med Virol* (2014) 86:1393–1401. doi: 10.1002/jmv.23875
 129. Schilte C, Couderc T, Chretien F, Sourisseau M, Gangneux N, Guivel-Benhassine F, Kraxner A, Tschopp J, Higgs S, Michault A, et al. Type I IFN controls chikungunya virus via its action on nonhematopoietic cells. *Journal of Experimental Medicine* (2010) 207:429–442. doi: 10.1084/jem.20090851
 130. Rathore APS, Haystead T, Das PK, Merits A, Ng M-L, Vasudevan SG. Chikungunya virus nsP3 & nsP4 interacts with HSP-90 to promote virus replication: HSP-90 inhibitors reduce CHIKV infection and inflammation in vivo. *Antiviral Res* (2014) 103:7–16. doi: 10.1016/j.antiviral.2013.12.010

131. Tsetsarkin K, Higgs S, McGee CE, Lamballerie X De, Charrel RN, Vanlandingham DL. Infectious Clones of Chikungunya Virus (La Réunion Isolate) for Vector Competence Studies. *Vector-Borne and Zoonotic Diseases* (2006) 6:325–337. doi: 10.1089/vbz.2006.6.325
132. Solignat M, Gay B, Higgs S, Briant L, Devaux C. Replication cycle of chikungunya: A re-emerging arbovirus. *Virology* (2009) 393:183–197. doi: 10.1016/j.virol.2009.07.024
133. Tang BL. The cell biology of Chikungunya virus infection. *Cell Microbiol* (2012) 14:1354–1363. doi: 10.1111/j.1462-5822.2012.01825.x
134. Her Z, Malleret B, Chan M, Ong EKS, Wong S-C, Kwek DJC, Tolou H, Lin RTP, Tambyah PA, Rénia L, et al. Active Infection of Human Blood Monocytes by Chikungunya Virus Triggers an Innate Immune Response. *The Journal of Immunology* (2010) 184:5903–5913. doi: 10.4049/jimmunol.0904181
135. Kumar S, Jaffar-Bandjee M-C, Giry C, Connen de Kerillis L, Merits A, Gasque P, Hoarau J-J. Mouse macrophage innate immune response to chikungunya virus infection. *Virology* (2012) 9:313. doi: 10.1186/1743-422X-9-313
136. Labadie K, Larcher T, Joubert C, Mannioui A, Delache B, Brochard P, Guigand L, Dubreil L, Lebon P, Verrier B, et al. Chikungunya disease in nonhuman primates involves long-term viral persistence in macrophages. *Journal of Clinical Investigation* (2010) 120:894–906. doi: 10.1172/JCI40104
137. Gardner J, Anraku I, Le TT, Larcher T, Major L, Roques P, Schroder WA, Higgs S, Suhrbier A. Chikungunya Virus Arthritis in Adult Wild-Type Mice. *J Virol* (2010) 84:8021–8032. doi: 10.1128/JVI.02603-09
138. Yang L, Geng T, Yang G, Ma J, Wang L, Ketkar H, Yang D, Lin T, Hwang J, Zhu S, et al. Macrophage scavenger receptor 1 controls Chikungunya virus infection through autophagy in mice. *Commun Biol* (2020) 3:556. doi: 10.1038/s42003-020-01285-6
139. Srivastava P, Chaudhary S, Malhotra S, Varma B, Sunil S. Transcriptome analysis of human macrophages upon chikungunya virus (CHIKV) infection reveals regulation of distinct signaling and metabolic pathways during the early and late stages of infection. *Heliyon* (2023) 9:e17158. doi: 10.1016/j.heliyon.2023.e17158
140. Nelemans T, Kikkert M. Viral Innate Immune Evasion and the Pathogenesis of Emerging RNA Virus Infections. *Viruses* (2019) 11:961. doi: 10.3390/v11100961
141. Frolova EI, Fayzulin RZ, Cook SH, Griffin DE, Rice CM, Frolov I. Roles of Nonstructural Protein nsP2 and Alpha/Beta Interferons in Determining the Outcome of Sindbis Virus Infection. *J Virol* (2002) 76:11254–11264. doi: 10.1128/JVI.76.22.11254-11264.2002
142. White LK, Sali T, Alvarado D, Gatti E, Pierre P, Streblow D, DeFilippis VR. Chikungunya Virus Induces IPS-1-Dependent Innate Immune Activation and Protein Kinase R-Independent Translational Shutoff. *J Virol* (2011) 85:606–620. doi: 10.1128/JVI.00767-10
143. Her Z, Teng T, Tan JJ, Teo T, Kam Y, Lum F, Lee WW, Gabriel C, Melchioni R, Andiappan AK, et al. Loss of TLR3 aggravates CHIKV replication and pathology due to an altered virus-specific

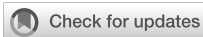
- neutralizing antibody response. *EMBO Mol Med* (2015) 7:24–41. doi: 10.15252/emmm.201404459
144. Dutta SK, Tripathi A. Association of toll-like receptor polymorphisms with susceptibility to chikungunya virus infection. *Virology* (2017) 511:207–213. doi: 10.1016/j.virol.2017.08.009
 145. Fitzgerald KA, Kagan JC. Toll-like Receptors and the Control of Immunity. *Cell* (2020) 180:1044–1066. doi: 10.1016/j.cell.2020.02.041
 146. Fitzgerald KA, Rowe DC, Barnes BJ, Caffrey DR, Visintin A, Latz E, Monks B, Pitha PM, Golenbock DT. LPS-TLR4 Signaling to IRF-3/7 and NF- κ B Involves the Toll Adapters TRAM and TRIF. *Journal of Experimental Medicine* (2003) 198:1043–1055. doi: 10.1084/jem.20031023
 147. Husebye H, Halaas Ø, Stenmark H, Tunheim G, Sandanger Ø, Bogen B, Brech A, Latz E, Espevik T. Endocytic pathways regulate Toll-like receptor 4 signaling and link innate and adaptive immunity. *EMBO J* (2006) 25:683–692. doi: 10.1038/sj.emboj.7600991
 148. Lv T, Shen X, Shi Y, Song Y. TLR4 is Essential in Acute Lung Injury Induced by Unresuscitated Hemorrhagic Shock. *Journal of Trauma: Injury, Infection & Critical Care* (2009) 66:124–131. doi: 10.1097/TA.0b013e318181e555
 149. Kuzmich N, Sivak K, Chubarev V, Porozov Y, Savateeva-Lyubimova T, Peri F. TLR4 Signaling Pathway Modulators as Potential Therapeutics in Inflammation and Sepsis. *Vaccines (Basel)* (2017) 5:34. doi: 10.3390/vaccines5040034
 150. Budulac SE, Boezen HM, Hiemstra PS, Lapperre TS, Vonk JM, Timens W, Postma DS. Toll-Like Receptor (TLR2 and TLR4) Polymorphisms and Chronic Obstructive Pulmonary Disease. *PLoS One* (2012) 7:e43124. doi: 10.1371/journal.pone.0043124
 151. Gomart A, Vallée A, Lecarpentier Y. Necrotizing Enterocolitis: LPS/TLR4-Induced Crosstalk Between Canonical TGF- β /Wnt/ β -Catenin Pathways and PPAR γ . *Front Pediatr* (2021) 9: doi: 10.3389/fped.2021.713344
 152. Lu Y, Li X, Liu S, Zhang Y, Zhang D. Toll-like Receptors and Inflammatory Bowel Disease. *Front Immunol* (2018) 9: doi: 10.3389/fimmu.2018.00072
 153. Modhiran N, Watterson D, Blumenthal A, Baxter AG, Young PR, Stacey KJ. Dengue virus NS1 protein activates immune cells via TLR4 but not TLR2 or TLR6. *Immunol Cell Biol* (2017) 95:491–495. doi: 10.1038/icb.2017.5
 154. Hritz I, Mandrekar P, Velayudham A, Catalano D, Dolganiuc A, Kodys K, Kurt-Jones E, Szabo G. The critical role of toll-like receptor (TLR) 4 in alcoholic liver disease is independent of the common TLR adapter MyD88. *Hepatology* (2008) 48:1224–1231. doi: 10.1002/hep.22470
 155. Engelmann C, Habtesion A, Hassan M, Kerbert AJC, Hammerich L, Novelli S, Fidaleo M, Philips A, Davies N, Ferreira-Gonzalez S, et al. Combination of G-CSF and a TLR4 inhibitor reduce inflammation and promote regeneration in a mouse model of ACLF. *J Hepatol* (2022) 77:1325–1338. doi: 10.1016/j.jhep.2022.07.006
 156. Yang L, Seki E. Toll-Like Receptors in Liver Fibrosis: Cellular Crosstalk and Mechanisms. *Front Physiol* (2012) 3: doi: 10.3389/fphys.2012.00138

157. Alfonso-Loeches S, Pascual-Lucas M, Blanco AM, Sanchez-Vera I, Guerri C. Pivotal Role of TLR4 Receptors in Alcohol-Induced Neuroinflammation and Brain Damage. *Journal of Neuroscience* (2010) 30:8285–8295. doi: 10.1523/JNEUROSCI.0976-10.2010
158. Basith S, Manavalan B, Yoo TH, Kim SG, Choi S. Roles of toll-like receptors in Cancer: A double-edged sword for defense and offense. *Arch Pharm Res* (2012) 35:1297–1316. doi: 10.1007/s12272-012-0802-7
159. Kim JY, Kim YJ, Kim JS, Ryu HS, Lee HK, Kang JS, Kim HM, Hong JT, Kim Y, Han S-B. Adjuvant effect of a natural TLR4 ligand on dendritic cell-based cancer immunotherapy. *Cancer Lett* (2011) 313:226–234. doi: 10.1016/j.canlet.2011.09.009
160. Gröbner S, Lukowski R, Autenrieth IB, Ruth P. Lipopolysaccharide induces cell volume increase and migration of dendritic cells. *Microbiol Immunol* (2014) 58:61–67. doi: 10.1111/1348-0421.12116
161. Apetoh L, Ghiringhelli F, Tesniere A, Obeid M, Ortiz C, Criollo A, Mignot G, Maiuri MC, Ullrich E, Saulnier P, et al. Toll-like receptor 4–dependent contribution of the immune system to anticancer chemotherapy and radiotherapy. *Nat Med* (2007) 13:1050–1059. doi: 10.1038/nm1622
162. He J, Xiao Z, Chen X, Chen M, Fang L, Yang M, Lv Q, Li Y, Li G, Hu J, et al. The expression of functional toll-like receptor 4 is associated with proliferation and maintenance of stem cell phenotype in endothelial progenitor cells (EPCs). *J Cell Biochem* (2010) 111:179–186. doi: 10.1002/jcb.22686
163. Volk-Draper LD, Hall KL, Wilber AC, Ran S. Lymphatic endothelial progenitors originate from plastic myeloid cells activated by toll-like receptor-4. *PLoS One* (2017) 12:e0179257. doi: 10.1371/journal.pone.0179257
164. Roodhart JML, He H, Daenen LGM, Monvoisin A, Barber CL, van Amersfoort M, Hofmann JJ, Radtke F, Lane TF, Voest EE, et al. Notch1 regulates angio-supportive bone marrow–derived cells in mice: relevance to chemoresistance. *Blood* (2013) 122:143–153. doi: 10.1182/blood-2012-11-459347
165. Ran S, Bhattarai N, Patel R, Volk-Draper L. “TLR4-Induced Inflammation Is a Key Promoter of Tumor Growth, Vascularization, and Metastasis.,” *Translational Studies on Inflammation*. IntechOpen (2020) doi: 10.5772/intechopen.85195
166. Hogg N, Palmer DG, Revell PA. Mononuclear phagocytes of normal and rheumatoid synovial membrane identified by monoclonal antibodies. *Immunology* (1985) 56:673–81.
167. Ziegler-Heitbrock HWL, Ulevitch RJ. CD14: Cell surface receptor and differentiation marker. *Immunol Today* (1993) 14:121–125. doi: 10.1016/0167-5699(93)90212-4
168. Chanput W, Mes JJ, Savelkoul HFJ, Wichers HJ. Characterization of polarized THP-1 macrophages and polarizing ability of LPS and food compounds. *Food Funct* (2013) 4:266–276. doi: 10.1039/C2FO30156C
169. HiMedia laboratories MI. MTT assay protocol.
170. BD Biosciences U. Annexin V-7-AAD assay details .

171. HiMedia Laboratories MI. HiPurA® Total RNA Miniprep Purification Kit protocol.
172. BD Biosciences U. BD mouse TNF ELISA kit details.
173. BD Biosciences U. BD human TNF ELISA details .
174. BD Biosciences USA. BD mouse MCP-1 ELISA details .
175. BD Biosciences U. BD mouse IL-6 ELISA kit details.
176. Kozakov D, Beglov D, Bohnuud T, Mottarella SE, Xia B, Hall DR, Vajda S. How good is automated protein docking? *Proteins: Structure, Function, and Bioinformatics* (2013) 81:2159–2166. doi: 10.1002/prot.24403
177. Kozakov D, Hall DR, Xia B, Porter KA, Padhorny D, Yueh C, Beglov D, Vajda S. The ClusPro web server for protein–protein docking. *Nat Protoc* (2017) 12:255–278. doi: 10.1038/nprot.2016.169
178. Chuang G-Y, Kozakov D, Brenke R, Comeau SR, Vajda S. DARS (Decoys As the Reference State) Potentials for Protein-Protein Docking. *Biophys J* (2008) 95:4217–4227. doi: 10.1529/biophysj.108.135814
179. Kozakov D, Clodfelter KH, Vajda S, Camacho CJ. Optimal Clustering for Detecting Near-Native Conformations in Protein Docking. *Biophys J* (2005) 89:867–875. doi: 10.1529/biophysj.104.058768
180. Kim HM, Park BS, Kim J-I, Kim SE, Lee J, Oh SC, Enkhbayar P, Matsushima N, Lee H, Yoo OJ, et al. Crystal structure of the TLR4-MD-2 complex with bound endotoxin antagonist Eritoran. *Cell* (2007) 130:906–17. doi: 10.1016/j.cell.2007.08.002
181. Voss JE, Vaney M-C, Duquerroy S, Vonnrhein C, Girard-Blanc C, Crublet E, Thompson A, Bricogne G, Rey FA. Glycoprotein organization of Chikungunya virus particles revealed by X-ray crystallography. *Nature* (2010) 468:709–12. doi: 10.1038/nature09555
182. Tong L, Wang L, Liao S, Xiao X, Qu J, Wu C, Zhu Y, Tai W, Huang Y, Wang P, et al. A Retinol Derivative Inhibits SARS-CoV-2 Infection by Interrupting Spike-Mediated Cellular Entry. *mBio* (2022) 13: doi: 10.1128/mbio.01485-22
183. Wang J, Feng X, Zeng Y, Fan J, Wu J, Li Z, Liu X, Huang R, Huang F, Yu X, et al. Lipopolysaccharide (LPS)-induced autophagy is involved in the restriction of Escherichia coli in peritoneal mesothelial cells. *BMC Microbiol* (2013) 13:255. doi: 10.1186/1471-2180-13-255
184. Akashi S, Shimazu R, Ogata H, Nagai Y, Takeda K, Kimoto M, Miyake K. Cutting Edge: Cell Surface Expression and Lipopolysaccharide Signaling Via the Toll-Like Receptor 4-MD-2 Complex on Mouse Peritoneal Macrophages. *The Journal of Immunology* (2000) 164:3471–3475. doi: 10.4049/jimmunol.164.7.3471
185. Giannini TL, Teghanemt A, Zhang D, Coussens NP, Dockstader W, Ramaswamy S, Weiss JP. Isolation of an endotoxin–MD-2 complex that produces Toll-like receptor 4-dependent cell activation at picomolar concentrations. *Proceedings of the National Academy of Sciences* (2004) 101:4186–4191. doi: 10.1073/pnas.0306906101

186. Schromm AB, Lien E, Henneke P, Chow JC, Yoshimura A, Heine H, Latz E, Monks BG, Schwartz DA, Miyake K, et al. Molecular Genetic Analysis of an Endotoxin Nonresponder Mutant Cell Line. *Journal of Experimental Medicine* (2001) 194:79–88. doi: 10.1084/jem.194.1.79
187. Küper C, Beck F-X, Neuhofer W. Toll-like receptor 4 activates NF- κ B and MAP kinase pathways to regulate expression of proinflammatory COX-2 in renal medullary collecting duct cells. *American Journal of Physiology-Renal Physiology* (2012) 302:F38–F46. doi: 10.1152/ajprenal.00590.2010
188. Li C, Zhao B, Lin C, Gong Z, An X. TREM2 inhibits inflammatory responses in mouse microglia by suppressing the PI3K/NF- κ B signaling. *Cell Biol Int* (2019) 43:360–372. doi: 10.1002/cbin.10975
189. Hop HT, Reyes AWB, Huy TXN, Arayan LT, Min W, Lee HJ, Rhee MH, Chang HH, Kim S. Activation of NF- κ B-Mediated TNF-Induced Antimicrobial Immunity Is Required for the Efficient *Brucella abortus* Clearance in RAW 264.7 Cells. *Front Cell Infect Microbiol* (2017) 7: doi: 10.3389/fcimb.2017.00437
190. Wang W, Weng J, Yu L, Huang Q, Jiang Y, Guo X. Role of TLR4-p38 MAPK-Hsp27 signal pathway in LPS-induced pulmonary epithelial hyperpermeability. *BMC Pulm Med* (2018) 18:178. doi: 10.1186/s12890-018-0735-0
191. Khan MA, Farahvash A, Douda DN, Licht J-C, Grasemann H, Sweezey N, Palaniyar N. JNK Activation Turns on LPS- and Gram-Negative Bacteria-Induced NADPH Oxidase-Dependent Suicidal NETosis. *Sci Rep* (2017) 7:3409. doi: 10.1038/s41598-017-03257-z
192. Sha T, Sunamoto M, Kitazaki T, Sato J, li M, Iizawa Y. Therapeutic effects of TAK-242, a novel selective Toll-like receptor 4 signal transduction inhibitor, in mouse endotoxin shock model. *Eur J Pharmacol* (2007) 571:231–239. doi: 10.1016/j.ejphar.2007.06.027
193. Landmann R, Ludwig C, Obrist R, Obrecht JP. Effect of cytokines and lipopolysaccharide on CD14 antigen expression in human monocytes and macrophages. *J Cell Biochem* (1991) 47:317–329. doi: 10.1002/jcb.240470406
194. Casals C, Barrachina M, Serra M, Lloberas J, Celada A. Lipopolysaccharide Up-Regulates MHC Class II Expression on Dendritic Cells through an AP-1 Enhancer without Affecting the Levels of CIITA. *The Journal of Immunology* (2007) 178:6307–6315. doi: 10.4049/jimmunol.178.10.6307
195. Tierney JB, Kharkrang M, la Flamme AC. Type II-activated macrophages suppress the development of experimental autoimmune encephalomyelitis. *Immunol Cell Biol* (2009) 87:235–240. doi: 10.1038/icb.2008.99
196. Tsukamoto H, Takeuchi S, Kubota K, Kobayashi Y, Kozakai S, Ukai I, Shichiku A, Okubo M, Numasaki M, Kanemitsu Y, et al. Lipopolysaccharide (LPS)-binding protein stimulates CD14-dependent Toll-like receptor 4 internalization and LPS-induced TBK1–IKK ϵ –IRF3 axis activation. *Journal of Biological Chemistry* (2018) 293:10186–10201. doi: 10.1074/jbc.M117.796631
197. Labadie K, Larcher T, Joubert C, Mannioui A, Delache B, Brochard P, Guigand L, Dubreil L, Lebon P, Verrier B, et al. Chikungunya disease in nonhuman primates involves long-term viral persistence in macrophages. *Journal of Clinical Investigation* (2010) 120:894–906. doi: 10.1172/JCI40104

198. Kumar S, Jaffar-Bandjee M-C, Giry C, Connen de Kerillis L, Merits A, Gasque P, Hoarau J-J. Mouse macrophage innate immune response to chikungunya virus infection. *Virology* (2012) 9:313. doi: 10.1186/1743-422X-9-313
199. Gardner J, Anraku I, Le TT, Larcher T, Major L, Roques P, Schroder WA, Higgs S, Suhrbier A. Chikungunya Virus Arthritis in Adult Wild-Type Mice. *J Virol* (2010) 84:8021–8032. doi: 10.1128/JVI.02603-09
200. Hoarau J-J, Jaffar Bandjee M-C, Krejbich Trotot P, Das T, Li-Pat-Yuen G, Dassa B, Denizot M, Guichard E, Ribera A, Henni T, et al. Persistent Chronic Inflammation and Infection by Chikungunya Arthritogenic Alphavirus in Spite of a Robust Host Immune Response. *The Journal of Immunology* (2010) 184:5914–5927. doi: 10.4049/jimmunol.0900255
201. Shirato K, Kizaki T. SARS-CoV-2 spike protein S1 subunit induces pro-inflammatory responses via toll-like receptor 4 signaling in murine and human macrophages. *Heliyon* (2021) 7:e06187. doi: 10.1016/j.heliyon.2021.e06187



OPEN ACCESS

EDITED BY

Rongtuan Lin,
McGill University, Canada

REVIEWED BY

David Marchant,
University of Alberta, Canada
Marceline Côté,
University of Ottawa, Canada
Robert E. Cone,
University of Connecticut Health Center,
United States

*CORRESPONDENCE

Subhasis Chattopadhyay
✉ subho@niser.ac.in
Soma Chattopadhyay
✉ sochat.ils@gmail.com

SPECIALTY SECTION

This article was submitted to
Viral Immunology,
a section of the journal
Frontiers in Immunology

RECEIVED 07 January 2023

ACCEPTED 29 March 2023

PUBLISHED 20 April 2023

CITATION

Mahish C, De S, Chatterjee S, Ghosh S,
Keshry SS, Mukherjee T, Khamaru S,
Tung KS, Subudhi BB, Chattopadhyay S and
Chattopadhyay S (2023) TLR4 is one of the
receptors for Chikungunya virus envelope
protein E2 and regulates virus induced
pro-inflammatory responses in
host macrophages.
Front. Immunol. 14:1139808.
doi: 10.3389/fimmu.2023.1139808

COPYRIGHT

© 2023 Mahish, De, Chatterjee, Ghosh,
Keshry, Mukherjee, Khamaru, Tung, Subudhi,
Chattopadhyay and Chattopadhyay. This is
an open-access article distributed under the
terms of the [Creative Commons Attribution
License \(CC BY\)](https://creativecommons.org/licenses/by/4.0/). The use, distribution or
reproduction in other forums is permitted,
provided the original author(s) and the
copyright owner(s) are credited and that
the original publication in this journal is
cited, in accordance with accepted
academic practice. No use, distribution or
reproduction is permitted which does not
comply with these terms.

TLR4 is one of the receptors for Chikungunya virus envelope protein E2 and regulates virus induced pro-inflammatory responses in host macrophages

Chandan Mahish^{1,2}, Saikat De^{3,4}, Sanchari Chatterjee^{3,4},
Soumyajit Ghosh^{3,4}, Supriya Suman Keshry^{3,5},
Tathagata Mukherjee^{1,2}, Somlata Khamaru^{1,2},
Kshyama Subhadarsini Tung^{1,2}, Bharat Bhusan Subudhi⁶,
Soma Chattopadhyay^{3*} and Subhasis Chattopadhyay^{1,2*}

¹School of Biological Sciences, National Institute of Science Education and Research Bhubaneswar, Jatni, Odisha, India, ²Homi Bhabha National Institute, Training School Complex, Anushaktinagar, Mumbai, Maharashtra, India, ³Institute of Life Sciences, Bhubaneswar, India, ⁴Regional Centre for Biotechnology, Faridabad, India, ⁵School of Biotechnology, Kalinga Institute of Industrial Technology (KIIT) University, Bhubaneswar, India, ⁶School of Pharmaceutical Sciences, Siksha O Anusandhan Deemed to be University, Bhubaneswar, Odisha, India

Toll like receptor 4 (TLR4), a pathogen-associated molecular pattern (PAMP) receptor, is known to exert inflammation in various cases of microbial infection, cancer and autoimmune disorders. However, any such involvement of TLR4 in Chikungunya virus (CHIKV) infection is yet to be explored. Accordingly, the role of TLR4 was investigated towards CHIKV infection and modulation of host immune responses in the current study using mice macrophage cell line RAW264.7, primary macrophage cells of different origins and *in vivo* mice model. The findings suggest that TLR4 inhibition using TAK-242 (a specific pharmacological inhibitor) reduces viral copy number as well as reduces the CHIKV-E2 protein level significantly using p38 and JNK-MAPK pathways. Moreover, this led to reduced expression of macrophage activation markers like CD14, CD86, MHC-II and pro-inflammatory cytokines (TNF, IL-6, MCP-1) significantly in both the mouse primary macrophages and RAW264.7 cell line, *in vitro*. Additionally, TAK-242-directed TLR4 inhibition demonstrated a significant reduction of percent E2-positive cells, viral titre and TNF expression in hPBMC-derived macrophages, *in vitro*. These observations were further validated in TLR4-knockout (KO) RAW cells. Furthermore, the interaction between CHIKV-E2 and TLR4 was demonstrated by immuno-precipitation studies, *in vitro* and supported by molecular docking analysis, *in silico*. TLR4-dependent viral entry was further validated by an anti-TLR4 antibody-mediated blocking experiment. It was noticed that TLR4 is necessary for the early events of viral infection, especially during the attachment and entry stages. Interestingly, it was also observed that TLR4 is not involved in the post-entry stages of CHIKV infection in host macrophages. The administration of TAK-242 decreased CHIKV infection significantly by reducing disease manifestations, improving survivability (around

75%) and reducing inflammation in mice model. Collectively, for the first time, this study reports TLR4 as one of the novel receptors to facilitate the attachment and entry of CHIKV in host macrophages, the TLR4-CHIKV-E2 interactions are essential for efficient viral entry and modulation of infection-induced pro-inflammatory responses in host macrophages, which might have translational implication for designing future therapeutics to regulate the CHIKV infection.

KEYWORDS

Chikungunya virus (CHIKV), toll-like receptor 4 (TLR4), CHIKV-E2, pro-inflammatory cytokines, inflammation

1 Introduction

Since the first report in 1952, the Chikungunya virus (CHIKV) (Family: *Togaviridae*; Genus: *Alphavirus*) has been considered a global public threat over the years. Two massive outbreaks in the last two decades (2004 and 2013) across different regions of the globe emphasize the severity and re-emerging nature of Chikungunya. One of the major governing factors for these repeated outbreaks are mainly unhygienic densely populated habitat with ineffective mosquito control capacity as Chikungunya in mosquito-borne (*Aedes* sp.) disease. Other associated factors are favorable climate for mosquito breeding, lack of available vaccines and proper medications (1, 2).

The pathophysiological manifestations of Chikungunya can be classified into three stages, namely, acute, sub-acute and chronic. The major symptoms of the acute stage are mainly high fever, polyarthralgia, headache, loss of appetite and rashes. The symptoms may last up to 3 months for the sub-acute stage. Although the acute stage has less severity, it may bring severe complications in neonates, pregnant women, patients suffering from comorbidities and aged people (over 65 years). The reported complications are failure of either neuronal, cardiovascular, renal, or respiratory systems. The chronic stage of infection may affect around 40% of the patients and the major symptoms are chronic arthralgia, myalgia, long term fatigue which might lead to permanent physical disability (1, 3, 4).

The mechanistic view on CHIKV entry in the host is not well understood till date. However, several entry pathways, for example, the clathrin-mediated pathway, epidermal growth factor receptor substrate 15 (Eps15)-dependent pathway and macropinocytosis have been experimentally demonstrated to be associated with CHIKV attachment and entry in the host (5–7). For CHIKV attachment, cell surface glycosaminoglycans (GAG), glycoprotein T-cell immunoglobulin and mucin 1 (TIM-1), TIM-4, Axl, C-type calcium-dependent lectin DC-SIGN (DC-specific intercellular adhesion molecule-3-grabbing non-integrin) and prohibitin (PHB) 1 and 2 were found as interaction and attachment factors in the host (8–17). Recently, a cell adhesion molecule, Mxra8 has been found to block CHIKV infection in presence of an anti-Mxra8 monoclonal antibody, although the absence of functional Mxra8 could not completely block CHIKV infection *in vitro* and *in vivo* (18).

Therefore, Mxra8 acts as one of the enhancers for CHIKV attachment and internalization process into the host cell.

Several clinical and experimental studies have revealed that the Chikungunya virus (CHIKV) infection leads to the profound production of pro-inflammatory cytokines and chemokines such as tumor necrosis factor (TNF), interleukin (IL)-6, 4, 1 β and 12 in human as well as in mouse macrophages *via* p38 and Jun N-terminal protein kinase (JNK)-mitogen-activated protein kinase (MAPK) mediated pathway, which may aggravate host immune system towards CHIKV infection mediated fever (CHIKF) and polyarthralgia (19–22). However, the initial pathways behind CHIKV-driven pro-inflammatory responses are still unexplored. Interestingly, the role of toll like receptor 4 (TLR4) has been critically investigated for mediating inflammatory responses in various cases of microbial infections, immune regulation in cancer and autoimmunity (23–25). TLR4 has also been well reported to induce massive pro-inflammatory responses upon binding of lipid A region of lipopolysaccharide (LPS), a cell wall component of Gram-negative bacteria (26). Moreover, the functional association of TLR4 is well established for other pro-inflammatory clinical abnormalities such as inflammatory bowel disease (IBD) and necrotizing enterocolitis (NEC) (27, 28). To establish the role of TLR4 in various *in vivo* inflammatory conditions such as mice sepsis model or LPS-induced lung injury model, a cyclohexene derivative molecule, TAK-242, has been used as a specific blocker of TLR4-dependent inflammation (24, 29). Furthermore, TLR4-dependent viral entry and infection progression of respiratory syncytial virus (RSV) has been described in mice model (30). Recently, several viral structural proteins are proposed to act as potential ligands for TLR4 activation (31, 32).

CHIKV-induced host cell activation and a rise in associated pro-inflammatory responses are already reported by us and others (19, 22, 33). Earlier studies have revealed that the pro-inflammatory cytokines along with MAPKs are induced during CHIKV infection in the host macrophages (19, 22). Since TLR4 activation could be connected with TNF response and MAPK activation (34, 35), the possible interaction of TLR4 with CHIKV infection along with subsequent regulation of host immune responses, if any, needs to be explored. Hence, it has been hypothesized that TLR4 might be pivotal to regulate CHIKV infection and associated host immune

responses. Accordingly, in the current study, the probable role of TLR4 has been investigated in CHIKV infection, inflammation and modulation of host immune responses using different *in vitro* models, *in silico* studies and *in vivo* mice model.

2 Materials and methods

2.1 Cells, virus and reagents

The RAW264.7 (ATCC[®] TIB-71[™]), BALB/c and C57BL/6 mice-derived peritoneal monocyte-macrophage cells were maintained in complete RPMI media consisting RPMI-1640 (Gibco, USA), supplemented with antibiotic-antimycotic solution, L-glutamine (HiMedia Laboratories Pvt. Ltd, MH, India) and 10% heat-inactivated Fetal bovine serum (Gibco, USA) at 37°C in a humidified incubator with 5% CO₂. The TLR4KO RAW (RAW-Dual KO[™]-TLR4; catalog number: rawd-kotlr4, Invivogen, USA) (36) and the Vero Cells were maintained in DMEM (catalog number: 11965-092; Gibco, USA) supplemented with 10% FBS, L-glutamine and antibiotic-antimycotic solution. The CHIKV-Indian Strain (IS) (accession no- EF210157.2), anti-CHIKV-E2 antibody and Vero cells were kind gifts from Dr. M.M. Parida, DRDE, Gwalior, India. The anti-CHIKV-E1 antibody was a kind from Dr. T.K. Chowdary, NISER, Bhubaneswar, India. TAK-242 (catalog no: 614316-5MG), a well-cited TLR4 inhibitor was purchased from Merck Millipore, USA (24, 34, 37). The antibodies against CD86 (Fluorochrome: APC; Catalogue number: 17-0862-82) and MHC-II (Fluorochrome: PE; Catalogue number: 12-5321-82) were purchased from eBiosciences, USA. PerCP-Cy5.5 conjugated CD14 antibody (catalog number: 560638) was purchased from BD Biosciences, USA. The unconjugated antibodies against p-NF-κB p65 (Catalogue number: 3031), total p38 (catalog number: 9212), phosphorylated p38 (catalog number:9211), total SAPK-JNK (catalog number:9252) and phosphorylated SAPK-JNK (catalog number: 4668) proteins were bought from Cell Signaling Technology (Denver, USA). Alexa fluor (AF)-647 conjugated TLR4-MD2 monoclonal antibody (clone Number: MTS510, catalog number: NBP2-24865AF647), used in flow cytometry, was purchased from Novus Biologicals (Littleton, Colorado, USA). The TLR4 polyclonal antibody (catalog number: 48-2300), used in co-immunoprecipitation and Western Blot, was purchased from Invitrogen (Carlsbad, USA). Fluorochrome (AF488/AF647) conjugated anti-mouse and rabbit secondary antibodies (used for flow cytometry) and HRP-conjugated anti-mouse and rabbit secondary antibodies (used in Western Blot and co-immunoprecipitation analysis) were purchased from Invitrogen, USA. The GAPDH (catalog number: 10-10011) and β-actin (catalog number: 11-13012) antibodies were bought from Abgenex India Pvt. Ltd, Bhubaneswar, India.

2.2 hPBMC isolation

Human blood was drawn from healthy donors following the guidelines of the Institutional Ethics Committee, NISER,

Bhubaneswar (NISER/IEC/2022-04). The procedure for generating myeloid adherent cells from human peripheral blood mononuclear cells (hPBMC) was followed as described elsewhere with little modifications (38–41). Briefly, circulating monocytes were enriched by 2 h adherence after Hi-Sep LSM (catalog number: HiSep LSM[™] 1077- LS001; HiMedia Laboratories Pvt Ltd, India) based density gradient-centrifugation according to the manufacturer's instructions. The adherent cells were cultured in RPMI-1640 supplemented with 10% FBS, antibiotic-antimycotic solution and L-glutamine for 3–5 days. The adherent cells obtained after 96 h were of monocyte-macrophage lineages (more than 97%) as found enriched with CD14⁺CD11b⁺ population (42, 43). The monocyte-macrophage cells derived from hPBMC were seeded in 12 well plates (Thermo Fischer, USA) at a density of 0.8x10⁶ cells/well. After 24 h of seeding, pre-incubation was carried out for 3 h with 1 μM of TAK-242, followed by CHIKV infection with MOI 5 for 2 h (19). The infected cells were harvested at 8 hours post-infection (hpi) and downstream experiments were conducted.

2.3 Cell viability assay

The working concentrations of TAK-242 in different host macrophage systems were determined using either the AnnexinV-7-AAD-based method (Annexin V: PE Apoptosis detection kit I, catalog number: 559763; BD Biosciences, USA) or MTT assay-based method (EZcount[™] MTT cell assay kit, catalog number: CCK-003-2500; HiMedia laboratories Pvt. Ltd, India) as per manufacturer's protocol.

2.4 LPS induction in RAW264.7 cells

The RAW264.7 cells were induced with LPS as per earlier reports with required modifications (44). Around 4.5x10⁶ cells were seeded per 90 mm cell culture dishes (Genetix Biotech Asia Pvt Ltd, India) for 16-18 h. The cells were washed with 1X PBS (RT) twice and pre-incubated with either DMSO or 1μM TAK-242 for 3 h. Next, the cells were treated with 500 ng/mL of LPS (catalog number: L5293-2ML, Sigma-Aldrich, Germany) for 6 h. Finally, the cells were scraped using a sterile cell scraper (Genetix, India) with 1X PBS and processed for downstream experiments.

2.5 CHIKV infection

The RAW264.7 cell line, TLR4KO RAW cell line, BALB/c and C57BL/6 mice-derived peritoneal monocyte-macrophages were infected with CHIKV-IS as reported earlier with minute modifications (19, 22, 40, 41, 45, 46). Briefly, 4.5x10⁶ cells were seeded in 90 mm dishes and allowed to grow for 16-18 h. Next, the cells were washed with 1X PBS 2 times and pre-incubated with either TAK-242 or DMSO for 3 h. For TAK-242 treated conditions, the cells were incubated with 0.5 and/or 1 μM concentrations of TAK-242 for 3 h before infection, during infection and post-infection. After pre-incubation, the cells were washed followed by

CHIKV infection at 5 MOI for 2 h. Post-CHIKV infection, the cells were washed and supplemented with complete RPMI media till the harvesting time point (8 hpi).

2.6 Flow cytometry

The expression of intracellular and surface markers was investigated using a flow cytometry-based study as described before (19, 22). Briefly, the cells were scrapped out with a cell scraper at 8 hpi time point and washed with 1X PBS before distribution to microcentrifuge tubes. For surface staining, the washed cells were subjected to Fc blocking using Fc blocking reagent (catalog number: 130-092-575; Miltenyi Biotec, Germany) as per the manufacturer's protocol. Next, the cells were incubated with antibodies against surface markers for 30 minutes at 4°C in dark. Finally, the cells were washed with FACS buffer (1X PBS, 1% BSA, 0.01% NaN₃) and acquired immediately in the flow cytometer. TLR4 and the macrophage activation markers such as CD86, MHC-II and CD14 were tested by surface staining using fluorochrome-conjugated monoclonal antibodies and acquired in the flow cytometer. To study the intracellular markers, such as CHIKV-E2, p-NF-κB or total TLR4, the cells were initially fixed with 4% paraformaldehyde (HiMedia Laboratories Pvt. Ltd., India) for 10 minutes at room temperature and washed with chilled 1X PBS two times to remove any remnant paraformaldehyde. The fixed cells were permeabilized with permeabilization buffer (1X PBS, 0.5% BSA, 0.1% Saponin and 0.01% NaN₃) for 15 minutes at RT followed by blocking with blocking buffer (1X PBS, 1% BSA, 0.1% Saponin and 0.01% NaN₃) for 30 minutes at RT. Next, the cells were further treated with primary (anti-M-CHIKV-E2, anti-R-p-NF-κB antibodies) and their respective fluorochrome-conjugated secondary antibodies sequentially diluted in permeabilization buffer. For TLR4 staining, the cells were incubated with fluorochrome-conjugated antibody (anti-M-TLR4-AF647) diluted in permeabilization buffer. Finally, the cells were washed and re-suspended in FACS buffer and kept at 4°C in dark till acquisition in the flow cytometer. The intracellular cytokine staining starter kit -Mouse (catalog number: 51-2041-AK; BD Biosciences, USA) and BD Golgispot Solution (catalog number-554724, BD Biosciences, USA) were used as per the manufacturer's protocol for dual staining of intracellular cytokine (TNF) and CHIKV-E2 protein together. All samples were acquired using BD LSRFortessa flow cytometer and analyzed by the FlowJo™ software (BD Biosciences, USA). Around ten thousand cells were acquired per sample per experimental set (minimum three biological replicates were performed).

2.7 ELISA

The cell-free culture supernatants from different experimental conditions were subjected to cytokine quantification using the BD OptEIA™ Sandwich ELISA kit (BD biosciences, USA) as per the manufacturer's instructions. Quantification of cytokines was done with respect to the standard curves prepared using the recombinant

cytokines with different concentrations at pg/mL, as reported earlier (19, 22, 45).

2.8 qRT-PCR and plaque assay

The viral RNA from cell-free culture supernatants was isolated using the QIAamp Viral RNA mini kit (Qiagen, Germany) as performed earlier (40). Briefly, an equal volume of the viral RNA from all experimental conditions was taken for cDNA synthesis using the Primescript™ 1st strand cDNA synthesis kit (Takara Bio Inc, Japan) obeying the manufacturer's protocol. The E1 gene was amplified using specific primers (CL11F: 5'-TGCCGTCACAGTTAAGGACG-3', CL12R: 5'-CCTCGCATGACATGTCCG-3') and the PowerUp™ SYBR™ Green Master Mix (Thermo Fisher Scientific, USA) in Applied Biosystems™ QuantStudio™ 7 Flex Real-Time PCR System (Applied Biosystems, USA) as per the manufacturer's instructions. The C_t values were plotted against the standard curve to determine the corresponding viral copy number as mentioned earlier (19, 40). To study the intracellular CHIKV copy numbers, the total RNA isolation kit (Catalogue number: MB602-50PR, HiMedia laboratories Pvt. Ltd., India) was used to isolate RNA from the cells. 1 µg of total RNA was converted to cDNA followed by qRT-PCR analysis using the above-mentioned kits and reagents. The intracellular viral copy numbers were normalized against GAPDH, the housekeeping gene (Forward:5'-CAAGGTCATCCATGACAACCTTTG-3', Reverse:5'-GTCCACCACCCTGTTGCTGTAG-3').

The plaque assay was performed using Vero cells to assess the viral titre as per the protocol mentioned earlier (19). In brief, the CHIKV-infected cell-free culture supernatants were used to infect Vero cells. Post-infection, 5% FBS-supplemented DMEM media mixed with 20% methyl-cellulose (catalog number: M0387; Sigma-Aldrich, USA) was laid over the infected cells for 3-4 days. Next, the cells were fixed using 8% formaldehyde (catalog number: M0387; HiMedia Laboratories Pvt. Ltd, India) and stained with crystal violet to determine the plaque forming units (PFU) manually under the white light of trans-illuminator (Vilber Lourmat, France).

2.9 Effect of TAK-242 before, during and after CHIKV infection

To investigate the possible anti-CHIKV effect of TAK-242, in specific stages of viral infection, the following experiment was performed in RAW264.7 cells as per the method described earlier (40, 46). Briefly, the TAK-242 treatment was given at different stages of CHIKV infection namely, before CHIKV infection (only pre-incubation), during CHIKV infection, both before and during CHIKV infection (pre+during incubation), post-infection incubation at 0 hpi (the drug was added at 0 hpi) and 8 hpi (the drug was added at 8 hpi). Besides the drug treatment, the CHIKV infection was given in all of the conditions in a similar way as described above i.e., infection was given with MOI 5 for 2 h. The cell

culture supernatants were collected at 9 hpi and qRT-PCR was carried out to determine the CHIKV copy numbers.

2.10 Viral attachment assay

To investigate whether TAK-242 has any role in CHIKV adsorption during virus infection, a study was performed to quantitate the unbound CHIKV particles as performed earlier (45). Briefly, the RAW264.7 cells were pre-treated with either DMSO or 1 μ M TAK-242 for 3 h and further subjected to CHIKV infection with MOI 5 for 2 h. After CHIKV infection, the inoculum volume containing unbound virus particles was collected and subjected to plaque assay and/or qRT-PCR to assess the effect of the drug on viral attachment to the cells.

2.11 Time of addition experiment

To study the role of TLR4 in specific stages of the CHIKV life cycle, a time of addition experiment was carried out as described earlier (40, 46). To perform the experiment, no drug treatment was given before or during viral infection. Following the CHIKV infection, TAK-242 was added to the cells at different time points post-infection (0,2,4,8,10,12 and 14 hpi). The cell culture supernatants from all of the time points were collected at 15 hpi for the determination of viral titre using plaque assay.

2.12 Western blot

The differential expression of viral E2, E1, TLR4 and MAPK proteins pathways was investigated using Western blot analysis as described before (22). Briefly, the cells were scraped from different experimental groups and washed with cold 1X PBS two times before preparation of whole cell lysate using Radio Immuno Precipitation Assay (RIPA) lysis buffer (150 mM NaCl, pH-8, 1% NP-40, 0.5% Sodium deoxycholate, 0.1% SDS, 50 mM Tris). After lysis, the solutions were centrifuged at 15000 rpm for 30 minutes at 4°C and the supernatants were collected. The protein lysates were quantified using Bradford reagent (catalog number: B6916-500 ML, Sigma-Aldrich, USA). 2X Sample buffer (pH-8, 130mM Tris-Cl, 20% glycerol (v/v), 4.6% SDS (w/v), 2% DTT, and 0.02% Bromophenol blue) was mixed with samples in a ratio of 1:1 and 30 μ g of total protein was loaded in each well of 10% SDS-PAGE gel. Next, the proteins on the gel were transferred to a PVDF membrane (catalog number: IPVH00010; Millipore, USA) followed by blocking with 3% BSA (catalog number: MB083; HiMedia Laboratories Pvt Ltd, India). Then, overnight primary antibody incubation was performed using different antibodies like the total and phospho-p38 and SAPK-JNK (1:1000), GAPDH and Beta-Actin (1:2000) and CHIKV-E2 (1:1000). The blots were thoroughly washed five times with 1X tris buffer with 0.1% Tween-20 (TBST) and corresponding anti-Mouse and Rabbit HRP conjugated secondary antibodies (catalog number: 31430 and 31460 respectively; Invitrogen, USA)

were probed for 2 h at RT. The blots were washed three times with 1X TBST and the images were captured using the ChemiDoc XRS⁺ imaging system and analyzed by the Image Lab software (Bio-Rad, USA).

2.13 *In silico* analysis

The ZDOCK webserver was used to study the protein-protein interaction. The protein-protein docking is based on the Fast Fourier Transform algorithm that utilizes a combination of shape complementarity, electrostatics and statistical potential terms for predicting the interaction complex (47). The MD2-TLR4 activated complex (PDB ID: 2Z64) was used as the receptor. The CHIKV-E2 structure extracted from the mature envelope glycoprotein complex of CHIKV (PDB ID: 3N41) was used as a ligand. The top-ranked output was visualized by the PyMol software.

2.14 Co-immunoprecipitation

For TLR4-E2/E1 interaction study, the cells were lysed with 1X RIPA buffer (the composition is the same as described in the WB section) after viral infection. The lysates were subjected to immunoprecipitation by the Dynabeads[®] Protein G Immunoprecipitation Kit (Thermo Fisher Scientific, USA) as per the protocol mentioned earlier (22). Briefly, both the mock and CHIKV-infected whole cell lysates were incubated with primary antibody (E2 or E1) and Dynabeads[®] protein G. The Dynabeads[®]-Ab-Ag complexes were washed, eluted and processed further for Western blot analysis.

2.15 Anti-TLR4 blocking assay

The anti-TLR4 blocking assay was performed in the RAW264.7 macrophage cells as per the protocol described elsewhere with little modifications (48). Before pre-incubation with DMSO or TAK-242, either anti-TLR4 antibody (Catalogue number: 48-2300, Invitrogen, USA) or anti-rabbit IgG antibody (Catalogue Number: 2729s, Cell signaling technology, USA) was added to the pre-incubation media at 5 μ g/ml concentration. The cells with different treatments were preincubated for 3 h. Next, the cells were given CHIKV infection at MOI 5 for 2 h. The cells were harvested at 8 hpi and subjected to flow cytometry and Western blot-based analysis. The cell culture supernatants were analyzed for secretory TNF level using ELISA based method. Here anti-rabbit IgG antibody was used as a negative control to conduct the experiment.

2.16 Animal studies

All animal experiments were conducted by following the guidelines of the Committee for the Purpose of Control and Supervision of Experiments on Animals (CPCSEA) of India with

the approval of the Institutional Animal Ethics Committee, NISER (1634/GO/ReBi/S/12/CPSCEA) and Institutional Animal Ethics Committee, ILS Bhubaneswar (76/Go/ReBi/S/1999/CPCSEA).

Six to eight-weeks aged male BALB/c and C57BL/6 mice were used to perform isolation of peritoneal macrophages as mentioned earlier with little modifications (49). In brief, 4-5 mice per set of the experiment were injected with 1 ml of 3.8% Brewer's Thioglycolate solution in the peritoneum cavity. After 3 days of injection, the mice were sacrificed and the peritoneal lavages were collected from the peritoneum cavity using chilled 1X PBS with 2% FBS in a sterile manner. Around 6×10^6 total cells were plated in each 90 mm cell culture dish. After 24 h of seeding, cells were washed with 1X PBS at RT and further experiments were performed with the adherent monocyte-macrophage population.

In vivo mice model work on CHIKV infection was performed in a similar way as mentioned earlier (40, 46). In brief, 8-9 days old C57BL/6 mice were housed under specific germ-free conditions for 2-3 days before experimentation. For CHIKV infected mice group (n=5), 10-12 days old mice were injected subcutaneously with 1×10^7 PFU of CHIKV-IS at the flank region of the right hind limb. For the mock mice group (n=5), serum-free medium was injected at the same position. For TAK-242 treated group (n=5), (dose:1 mg/kg body weight of mice) the drug was given orally from a day before CHIKV infection to 6 days after infection at every 24 h intervals. The mock and CHIKV-treated groups received an equal volume of serum-free media with DMSO for the same duration of the study. The dose of TAK-242 used in the current study was determined based on previously published data where 3 mg/kg dose was shown to be non-toxic and effective for similar mouse model experimentation (24, 37). Depending on their symptoms, the mice were sacrificed on the 5th or 6th-day post-infection (dpi) followed by the collection of blood serum, quadriceps muscles and spleens from the mock, CHIKV infected with solvent (DMSO) or TAK-242 treated mice groups. The serum TNF level was quantified by ELISA-based cytokine assay. The quadriceps muscles and spleen samples were snap-frozen followed by lysis with RIPA buffer for Western blot analysis. To quantitate the viral titre, an equal amount of tissues from each group was homogenized in serum-free RPMI media followed by syringe filtration using 0.22 μ M filters. The solutions were further centrifuged and the supernatants were collected for plaque assay. For, the survival curve and clinical score analysis, a similar protocol was followed as mentioned above (n=6 for all three groups). The mice were monitored every day for the tabulation of clinical score and final survival curve analysis for up to 8 dpi and scored according to the phenotypic symptom-based disease outcomes [no symptoms-0, fur rise-1, hunchback-2, one hind limb paralysis-3, both hind limb paralysis-4, death-5] (40, 46, 50).

2.17 Statistical analysis

The GraphPad Prism 9 software (GraphPad Software Inc., San Diego, USA) was used for statistical analysis. All comparisons among different groups were performed by either the One-way ANOVA with Tuckey posthoc test or the unpaired t-test. All data

were represented as mean \pm SEM. All analyzed data are representative of at least 3 independent experiments where $p < 0.05$ was taken as statistically significant (ns: non-significant, * $p < 0.05$; ** $p \leq 0.01$; *** $p \leq 0.001$; **** $p \leq 0.0001$).

3 Results

3.1 TLR4 inhibition abrogates LPS-induced macrophage activation and pro-inflammatory responses in the host macrophages, *in vitro*

The previously published literature already reports that TAK-242-driven TLR4 inhibition abrogates the upregulation of LPS-mediated pro-inflammatory responses in the RAW264.7 macrophages as well as in the BALB/c-derived peritoneal macrophages (34). Therefore, the effect of TAK-242 in LPS induced RAW264.7 cells has been studied as the experimental control for the current investigation.

To determine the working concentration of TAK-242, Annexin V-7-AAD staining was carried out in the RAW264.7 cells and peritoneal macrophages from BALB/c and C57BL/6 mice. For, the hPBMC-derived monocyte-macrophage cells, a MTT assay was carried out. The cells were incubated with different concentrations of TAK-242 for 24 h and more than 95% of the cells were found viable at 2 μ M concentration (Figures S1A-D). According to the previously studied data, TAK-242 effectively inhibits the upregulation of LPS-driven pro-inflammatory responses at 1 μ M concentration in the RAW264.7 cells (34). To investigate the effect of TAK-242 against LPS-mediated pro-inflammatory responses, the RAW264.7 cells were pre-incubated with either DMSO or 1 μ M of TAK-242 for 3 h and further treated with 500 ng/mL LPS for 6 h (44). TAK-242 was found not to affect the cell surface as well as total TLR4 expressions significantly in the mock RAW264.7 cells (data not shown).

As previously reported, the reduction in the cell surface TLR4 and increase in the total TLR4 occurs upon LPS or virus-mediated stimulations (32, 51, 52). The flow cytometry dot plot analysis revealed that the percent positive cells for the total TLR4 were increased during LPS and LPS with TAK-242 treated conditions with respect to mock significantly [66.5 \pm 2.22% (Mock) to 89.5 \pm 1.59% (LPS) and 85.5 \pm 1.68% (TAK-242+LPS)] (Figure S2A). However, the percent positive cells for the cell surface TLR4 expression were reduced during LPS or LPS+ TAK-242 treatment [43.4 \pm 1.42% (Mock) to 27.6 \pm 1.1% (LPS) and 36.1 \pm 0.757% (LPS+TAK-242)] (Figure S2B), which coincides with previous reports.

Based on LPS mediated TLR4 signaling mechanism (53, 54), CD14, a macrophage activation marker (43), was investigated as one of the TLR4 signaling molecules for the current study. Moreover, inducible activation markers on macrophages such as CD86 and MHC-II were also studied to demonstrate macrophage activation (19). The flow cytometry dot plot analysis of CD14 showed a significant increment during LPS treatment and further reduction upon TAK-242 treatment [16.233 \pm 2.44% (Mock) to 25.2 \pm 2.97% (LPS) and 21 \pm 3.03% (LPS+TAK-242)] (Figure S2C).

CD86 was found to increase during LPS treatment and reduce further in TAK-242 with LPS treated condition [$65.17 \pm 1.337\%$ (Mock) to $71.30 \pm 1.553\%$ (LPS) and $66.13 \pm 1.325\%$ (LPS+TAK-242)] (Figure S2D). MHC-II also showed a similar pattern of expression to CD86 under the same experimental conditions [$40.07 \pm 1.707\%$ (Mock) to $51.07 \pm 1.598\%$ (LPS) and $47.33 \pm 1.338\%$ (LPS+TAK-242)] (Figure S2E).

The p-NF- κ B activation-driven upregulation of pro-inflammatory cytokines (such as TNF) is already reported upon TLR4 activation (34, 55). The p-NF- κ B expression was increased during LPS treatment and decreased further upon TAK-242 treatment in the LPS-induced cells [$14.73 \pm 2.153\%$ (Mock) to $37.15.6 \pm 3.762\%$ (LPS) and $25.23 \pm 2.533\%$ (LPS+TAK-242)] (Figure S2F).

Furthermore, the earlier reports have described TLR4-directed upregulation of p38 and JNK-MAPK phosphorylation during LPS-induced pulmonary epithelial hyperpermeability and LPS treatment in human neutrophils respectively in a concentration-dependent manner (56, 57). Western Blot analysis revealed upregulation of TLR4 in both the LPS and LPS with TAK-242 treated conditions with respect to mock [2.328 ± 0.067 fold (LPS) and 2.205 ± 0.25 fold (LPS+TAK-242)] (Figures S2G, H). The assessment of phosphorylation of the SAPK-JNK pathway revealed that the LPS induction upregulates p-SAPK-JNK expression during LPS treatment which gets reduced during TAK-242 treatment in LPS induced cells [9.826 ± 0.62 fold (LPS) and 2.573 ± 0.09 fold (LPS+TAK-242)] (Figures S2G, I). Similarly, p-p38 expression showed a similar pattern in the LPS and LPS with TAK-242 treated conditions [2.373 ± 0.39 fold (LPS) and 1.044 ± 0.2465 fold (LPS+TAK-242)] (Figure S2G, J).

An earlier report has suggested that the upregulation of LPS-mediated pro-inflammatory responses was inhibited in presence of TAK-242 (34). In the current study, ELISA-based quantification of the secretory TNF showed a massive upregulation of TNF due to the LPS treatment and subsequent restoration upon TAK-242 treatment in a significant manner [394.4 ± 17.4 pg/mL (Mock) to 2585 ± 57.69 pg/mL (LPS) and 552.5 ± 13.06 pg/mL (LPS+TAK-242)] (Figure S2K).

Altogether, these results infer that TAK-242-directed TLR4 inhibition significantly inhibits the upregulation of the LPS-induced pro-inflammatory responses where TLR4 internalization might have a possible implication.

3.2 TLR4 antagonism reduces CHIKV infection in the host macrophages of different origins, *in vitro*

3.2.1 Inhibition of TLR4 abrogates CHIKV infection in the RAW264.7 cells, significantly

Based on our previous reports, where it was established that maximum CHIKV infection occurs at 8 hours post-infection (hpi) time point in the RAW264.7 macrophages, 8 hpi was selected for cell harvesting to carry out all the experiments of viral infection (19, 22).

E2, an envelope protein of CHIKV, was taken as a marker to assess CHIKV infection in different host systems (19, 40, 41, 45, 46).

To understand the role of TLR4 in CHIKV infection, the TAK-242 treated RAW264.7 cells were infected and harvested at 8 hpi. The cells were subjected to flow cytometry to assess viral infection and macrophage activation. The culture supernatants were used to estimate the viral copy number by qRT-PCR and cytokine levels by ELISA. The reduction of E2 percent positive cells [$15.43 \pm 0.5175\%$ (CHIKV) to $9.813 \pm 0.8411\%$ (TAK-242)] (Figure 1A) and significant decrease of corresponding viral copy number [58%] in presence of TAK-242 ($1\mu\text{M}$) (Figure 1B) indicated that TLR4 antagonism reduces CHIKV infection.

In addition, the flow cytometry data showed that the surface expression of TLR4 was reduced upon infection in a significant manner [from $45.33 \pm 1.805\%$ to $23.03 \pm 2.266\%$] and it was further decreased nonsignificantly [$18.2 \pm 0.76\%$] in presence of TAK-242 treatment (Figure 1C). Interestingly, the upregulation of the total TLR4 was observed up on CHIKV infection and in presence of TAK-242 ($1\mu\text{M}$) [from 56.3 ± 2.066 (mock) to 75.5 ± 3.057 (CHIKV) and 73.2 ± 1.172 (TAK-242)] (Figure 1D).

To determine the differential macrophage activation, the percent expressions of CD86, MHC-II and CD14 were investigated in the RAW264.7 cells. It was observed that the percent expression of CD14 was increased in infection and decreased in the presence of TAK-242 ($1\mu\text{M}$) [from $5.57 \pm 0.13\%$ (mock) to $27.9 \pm 2.088\%$ (CHIKV) and $10.24 \pm 1.157\%$ (TAK-242)] (Figure 1E). Similarly, the CD86 expression was found to increase during CHIKV infection which was further reduced in presence of TAK-242 ($1\mu\text{M}$) [from $71.67 \pm 0.29\%$ (mock) to $89.03 \pm 1.467\%$ (CHIKV) and $77.6 \pm 0.7234\%$ (TAK-242)] (Figure 1F). The MHC-II expression was found to be upregulated during CHIKV infection significantly and reduced nonsignificantly during TAK-242 ($1\mu\text{M}$) treatment [from $42.87 \pm 4.889\%$ (mock) to $63.53 \pm 1.12\%$ (CHIKV) and $50.07 \pm 2.896\%$ (TAK-242)] (Figure 1G). Therefore, the data indicate that TLR4 antagonism might reduce CHIKV-mediated macrophage activation.

The level of p-NF- κ B was determined by flow cytometry to assess the effect of TAK-242 in TLR4 signaling during CHIKV infection. It was observed that CHIKV infection resulted in an increase of p-NF- κ B which was subsequently decreased upon the TAK-242 ($1\mu\text{M}$) treatment, significantly [from $19.37 \pm 2.87\%$ (mock) to $33.43 \pm 3.083\%$ (CHIKV) and $17.03 \pm 2.854\%$ (TAK-242)] (Figure 1H). As per reports, p-NF- κ B activation is directly associated with inflammation (58, 59) and pro-inflammatory cytokines such as TNF, IL-6 and MCP-1 which are already reported to be involved with CHIKV-induced immune activation by us and others (19, 33). Accordingly, TNF was found to increase during CHIKV infection and decrease further upon TAK-242 ($1\mu\text{M}$) treatment, significantly [from 161.2 ± 28.34 (Mock) to 1340 ± 79.26 pg/mL (CHIKV) to 681.5 ± 97.3 pg/mL (TAK-242)] (Figure 1I). Similarly, secretory IL-6 was found to decrease significantly in presence of TAK-242 ($1\mu\text{M}$) treatment [from 411.1 ± 25.34 pg/mL (CHIKV) to 73.61 ± 8.047 pg/mL (TAK-242)] (Figure 1J). Additionally, reduced MCP-1 expression was

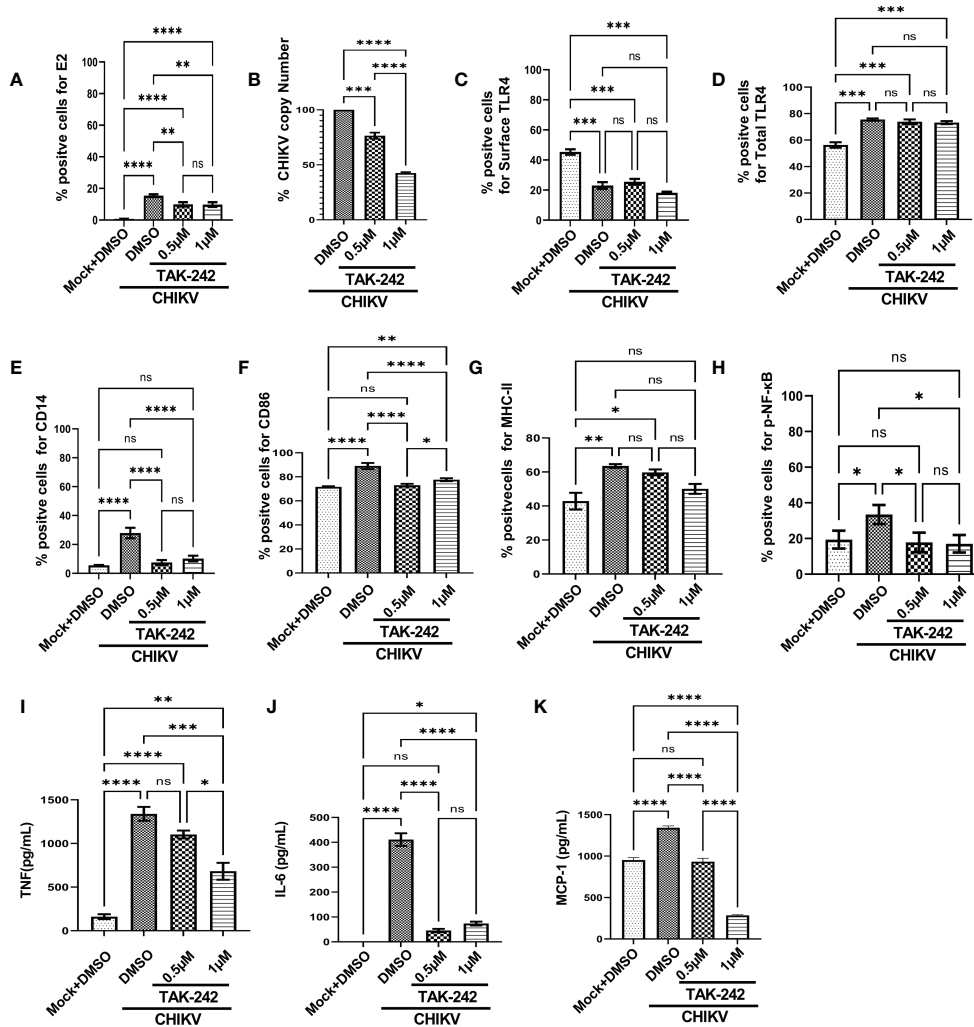


FIGURE 1

TLR4 inhibition decreases CHIKV infection and pro-inflammatory responses in RAW264.7 macrophage cells, *in vitro*. The RAW264.7 cells were either pre-treated with DMSO or TAK-242 for 3 h before CHIKV infection. CHIKV infection was given at 5 MOI for 2 h followed by the cells were harvested at 8 hpi. (A) The bar diagram denotes flow cytometry dot plot analysis based on % positive cells for CHIKV-E2, (B) q-RT PCR-based analysis showing decreased CHIKV-E1 copy number in presence of TAK-242. The bar diagrams represent percent positive cells obtained by flow cytometry dot plot analysis for (C) surface TLR4, (D) total TLR4, (E) CD14, (F) CD86 and (G) MHC-II and (H) p-NF-κB expression. (I–K) ELISA-based cytokine analysis showing differential expression of TNF-α, IL-6 and MCP-1. Data represent the Mean ± SEM of three independent experiments. $p < 0.05$ was considered as a statistically significant difference between the groups (ns: non-significant, * $p < 0.05$; ** $p \leq 0.01$; *** $p \leq 0.001$; **** $p \leq 0.0001$).

also found upon TAK-242 (1μM) treatment [from 951.6 ± 17.19 pg/mL (Mock) to 1342 ± 12.85 pg/mL (CHIKV) and 286.2 ± 4.242 pg/mL (TAK-242)] (Figure 1K). The representative flow cytometry dot plots of all of the above-mentioned markers were shown in the supplementary section (Figure S3).

Further, the current study aimed to elucidate whether TAK-242-directed TLR4 antagonism promotes reduced activation of macrophages or whether overall macrophage activation is solely dependent on the number/percentage of CHIKV-infected cells. To get a detailed insight, flow cytometry-based ICS cytokine staining analysis of TNF-producing cells was performed in CHIKV-E2 positive cells (Figure S4). The treatment with TAK-242 (1μM) decreased the frequency of the E2 positive RAW264.7 cells in a significant manner [$15.67 \pm 1.477\%$ (DMSO+CHIKV) and $9.49 \pm$

0.9% (TAK-242+CHIKV)]. Respective E2 populations from TAK-242 untreated and treated groups were further analyzed to determine the frequency and expression of TNF in the aforementioned population. The frequency (% positive cells) of TNF-positive cells in both TAK-242 treated and untreated cells was found to be comparable under the E2-selected (gated) population. Interestingly, the mean fluorescence intensity (MFI) of TNF in the E2-gated cells was reduced significantly, which complies with the ELISA data mentioned earlier. The expression of TNF is possibly decreased due to lowered frequency of the E2-positive cells upon TAK-242 treatment. Taken together, the results suggest that TAK-242-directed TLR4 inhibition reduces the CHIKV infection (around 58%) and pro-inflammatory responses, significantly, in the RAW264.7 cells.

3.2.2 Inhibition of TLR4 abrogates CHIKV infection in the primary mouse peritoneal macrophages, significantly

The study was further extended to the CHIKV-infected peritoneal macrophages obtained from the BALB/c mice. It was observed that the percent E2 positive cells [from 26.73 ± 0.98 to 13.27 ± 0.5840] (Figure S5A) and the corresponding viral copy number were reduced [60%] significantly in presence of TAK-242 ($1\mu\text{M}$) (Figure S5B). Flow cytometry-based analysis showed that the surface expression of TLR4 was reduced upon infection and TAK-242 ($1\mu\text{M}$) treatment, significantly [from 75.87 ± 1.247 to $51.07 \pm 0.6360\%$ (CHIKV) and $53.5 \pm 0.611\%$ (TAK-242)] (Figure S5C). However, the total expression of TLR4 was found to increase during infection and TAK-242 ($1\mu\text{M}$) treatment in comparison to mock, significantly [from 81.5 ± 1.592 (Mock) to $90.73 \pm 1.874\%$ (CHIKV) and $89.15 \pm 1.084\%$ (TAK-242)] (Figure S5D). Moreover, the CD14 expression was found to increase during CHIKV infection and decrease further upon TAK-242 ($1\mu\text{M}$) treatment, significantly [from 22.53 ± 0.97 (Mock) to 30.73 ± 0.58 (CHIKV) and 26.37 ± 0.44 (TAK-242)] (Figure S5E). The CD86 expression was increased during CHIKV infection and further decreased in the presence of TAK-242 ($0.5\mu\text{M}$), significantly, although a non-significant reduction was observed in presence of $1\mu\text{M}$ TAK-242 [from 37.47 ± 0.8 (Mock) to 65.23 ± 1.389 (CHIKV), 55.77 ± 0.67 ($0.5\mu\text{M}$ TAK-242) and 60.93 ± 2.009 ($1\mu\text{M}$ TAK-242)] (Figure S5F). Moreover, the MHC-II expression was also reduced upon TAK-242 ($1\mu\text{M}$) treatment, significantly [from 58.2 ± 1.25 (Mock) to 77.67 ± 0.09 (CHIKV) and 69.6 ± 1.513 (TAK-242)] (Figure S5G). Next, the p-NF- κB expression was found to increase during CHIKV infection and decrease further upon TAK-242 ($1\mu\text{M}$) treatment, significantly [from 29.2 ± 3.351 (Mock) to 52.63 ± 3.973 (CHIKV) and 40.87 ± 2.826 (TAK-242)] (Figure S5H). To further validate the total TLR4 level, Western blot analysis revealed a significant increase of TLR4 during CHIKV infection and TAK-242 ($1\mu\text{M}$) treatment [2.123 ± 0.3 fold (CHIKV) and 2.06 ± 0.16 fold (TAK-242)] (Figures S5I, J). In order to estimate the inflammatory responses, the levels of TNF, IL-6 and MCP-1 were determined. TNF was found to increase during CHIKV infection and decrease further upon TAK-242 ($1\mu\text{M}$) treatment, significantly [from 773.2 ± 62.88 pg/mL (CHIKV) to 398.6 ± 27.58 pg/mL (TAK-242)] (Figure S5K). IL-6 was found to increase during CHIKV infection and decrease further upon TAK-242 ($1\mu\text{M}$) treatment, significantly [from 5.33 ± 1.294 pg/mL (Mock) to 1078 ± 147.9 pg/mL (CHIKV) and 186.4 ± 22.98 pg/mL (TAK-242)] (Figure S5L). The MCP-1 expression was found to increase during CHIKV infection and decrease further upon TAK-242 ($1\mu\text{M}$) treatment, significantly [from 145.4 ± 6.667 pg/mL (Mock) to 2117 ± 152.8 pg/mL (CHIKV) and 377.5 ± 76.98 pg/mL (TAK-242)] (Figure S5M). The data indicate that the TLR4 inhibition reduces the CHIKV infection (around 60%) and associated pro-inflammatory responses, significantly in the peritoneal monocyte-macrophages obtained from BALB/c mice.

Furthermore, a similar study was carried out using the C57BL/6 mice-derived peritoneal macrophages. The percent E2 positive cells [from 18.6 ± 0.95 to 6.558 ± 0.89] (Figure S6A) and corresponding viral copy number were significantly reduced [50%] in presence of

TAK-242 (Figure S6B). Flow cytometry-based analysis showed a similar kind of change in the surface and total expression of TLR4 upon TAK-242 treatment, significantly (Figures S6C, D). It was further noticed that although the CD14 and MHC-II expressions were significantly modulated in a similar way, the CD86 expression showed a nonsignificant decrease in presence of TAK-242 treatment ($1\mu\text{M}$) (Figures S6E–G). Accordingly, the p-NF- κB expression was estimated and it was found to increase during CHIKV infection and decrease further upon TAK-242 treatment ($1\mu\text{M}$), significantly [from 29.6 ± 1.793 (Mock) to 50.7 ± 0.66 (CHIKV) and 35.03 ± 0.5175 (TAK-242)] (Figure S6H). The Western blot analysis revealed significant upregulation of TLR4 upon CHIKV infection and also during TAK-242 treatment ($1\mu\text{M}$) [1.553 ± 0.08 fold (CHIKV) and 1.489 ± 0.14 fold (TAK-242)] (Figures S6I, J). As observed before, TNF, IL-6 and MCP-1 followed a similar pattern, significantly (Figures S6K–M), indicating that TLR4 inhibition significantly lowers the CHIKV infection (around 50%) and associated pro-inflammatory responses in the peritoneal monocyte-macrophages obtained from C57BL/6 mice as well.

3.2.3 Inhibition of TLR4 abrogates CHIKV infection in the hPBMC-derived macrophages, significantly

To study the effect of TLR4-mediated regulation of CHIKV infection in the higher-order mammalian system, hPBMC derived adherent macrophage population (97% CD14⁺CD11b⁺ cells) (Figures S7A, B) was subjected to infection in the presence and absence of TAK-242 ($1\mu\text{M}$). The hPBMC-derived adherent populations collected from 3 healthy donors showed around a 52% decrease in the E2 level with TAK-242 treatment (Figures S7C, D). Similarly, there was a 32.38% reduction in CHIKV infection after TAK-242 treatment as observed by the plaque assay (Figures S7E). To assess the pro-inflammatory responses, secretory TNF level was determined using ELISA, where around 44% reduction was observed in TAK-242 treated condition (Figure S7F). Collectively, these data indicate that TLR4 inhibition in the hPBMC-derived monocyte/macrophages may lead to reduced CHIKV infection (around 33%) and associated inflammatory responses.

3.3 TLR4 inhibition reduces CHIKV infection driven p38 and SAPK-JNK phosphorylation

The role of the p38 and JNK-MAPK pathways towards CHIKV infection and inflammation was recently reported (2). To investigate the possible role of TLR4 in MAPK-mediated CHIKV-induced inflammation, differential induction of p-p38 and p-SAPK-JNK-MAPK was observed by Western blot experiment. Significant upregulations of p-p38 (2.9-fold) and p-JNK (4.03-fold) were observed after CHIKV infection in the RAW264.7 cells (Figures 2A–C). However, phosphorylation of p38 and JNK was reduced by 4.69 and 1.61-fold respectively following TAK-242 treatment (Figures 2A–C). Furthermore, a reduction of the

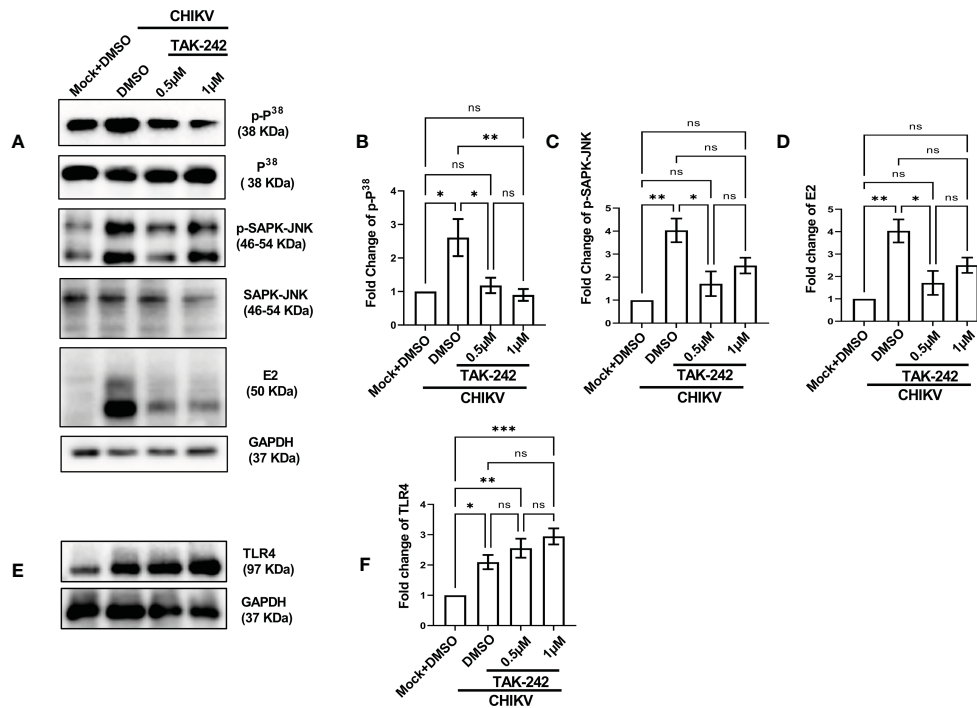


FIGURE 2

TLR4 inhibition lowers p38 and SAPK-JNK phosphorylation in host macrophages, *in vitro*. RAW264.7 cells were either pre-treated with DMSO or TAK-242 for 3 h before CHIKV infection. The CHIKV infection was given at 5 MOI for 2 h followed by the cells were harvested at 8 hpi. (A–D) Western blot analysis showing differential expression of p-p³⁸, p-SAPK-JNK, E2 and their quantification normalized against GAPDH, in respective order. (E, F) Western blot analysis showing TLR4 expression with the corresponding quantification normalized against GAPDH. Data represent the Mean ± SEM of three independent experiments. $p < 0.05$ was considered as a statistically significant difference between the groups (ns: non-significant, * $p < 0.05$; ** $p \leq 0.01$; *** $p \leq 0.001$).

CHIKV-E2 expression (3.27-fold) in presence of TAK-242 (Figures 2A, D) was also observed. In correlation with the total expression of TLR4 measured in flow cytometry-based analysis, an increase in the TLR4 expression was found during CHIKV infection (2.09-fold) and TAK-242 treatment (2.9-fold) (Figures 2E, F). Collectively, these data indicate that the inhibition of TLR4 might lead to reduced viral infection and induction of the p38, and JNK-MAPK pathways.

3.4 CHIKV-E2 and functional TLR4 interaction is necessary for the efficient infection in host macrophages

In order to understand the functional association of TLR4 with CHIKV infection, viral infection was performed in the RAW264.7 and TLR4 functional knockout TLR4KO RAW cells. Interestingly, the TLR4KO RAW cell line was used for the current experiment, which is previously reported to show reduced interferon response against SARS-CoV2 specific protein E antigen (36). Therefore, it seems that the functional presence of TLR4 is necessary to implement the SARS-CoV2-specific antiviral responses. The flow cytometry dot plot analysis suggests that the percent E2 positive population in the RAW264.7 cells was reduced in the case of TLR4KO RAW cells ($16.60 \pm 0.75\%$ to $3.877 \pm 0.43\%$) during CHIKV infection (Figures 3A, B). Next, Western blot analysis

revealed an around 8.651 ± 0.72 -fold decrease of the E2 protein level in the CHIKV-infected TLR4KO RAW cells in comparison to RAW264.7 (Figures 3C, D). Assessment of viral titre also showed a $48.11 \pm 3.23\%$ reduction in the TLR4KO RAW cells (Figure 3E). The total and surface expressions of TLR4 were found to be non-significantly altered (Figures 3F, G). Moreover, macrophage activation markers like CD14, CD86 and MHC-II were found to increase in a modest yet non-significant manner during CHIKV infection in the TLR4KO RAW cells in comparison to RAW264.7 (Figures 3H–J). However, p-NF- κ B was found to increase significantly during CHIKV infection in TLR4KO RAW in comparison to RAW264.7 (Figure 3K). To investigate the differential pro-inflammatory responses during CHIKV infection, comparative levels of TNF, IL-6 and MCP-1 levels were quantified by ELISA. These findings report the elevated expressions of TNF, IL-6 and MCP-1 in RAW264.7 by 2.305 ± 0.2219 , 1.702 ± 0.1797 and 1.541 ± 0.05658 -fold respectively in comparison with TLR4KO RAW (Figures 3L–N). Hence, the results obtained from functionally knockout TLR4KO RAW delineate that TLR4 is functionally essential for eliciting the CHIKV-induced pro-inflammatory responses.

The RAW264.7 cells were infected with CHIKV with MOI 5 and harvested at 8 hpi for further analysis. Co-immunoprecipitation followed by Western blot analysis demonstrated that TLR4 could be pulled with the CHIKV-E2 protein in host macrophages indicating that CHIKV-E2 interacts

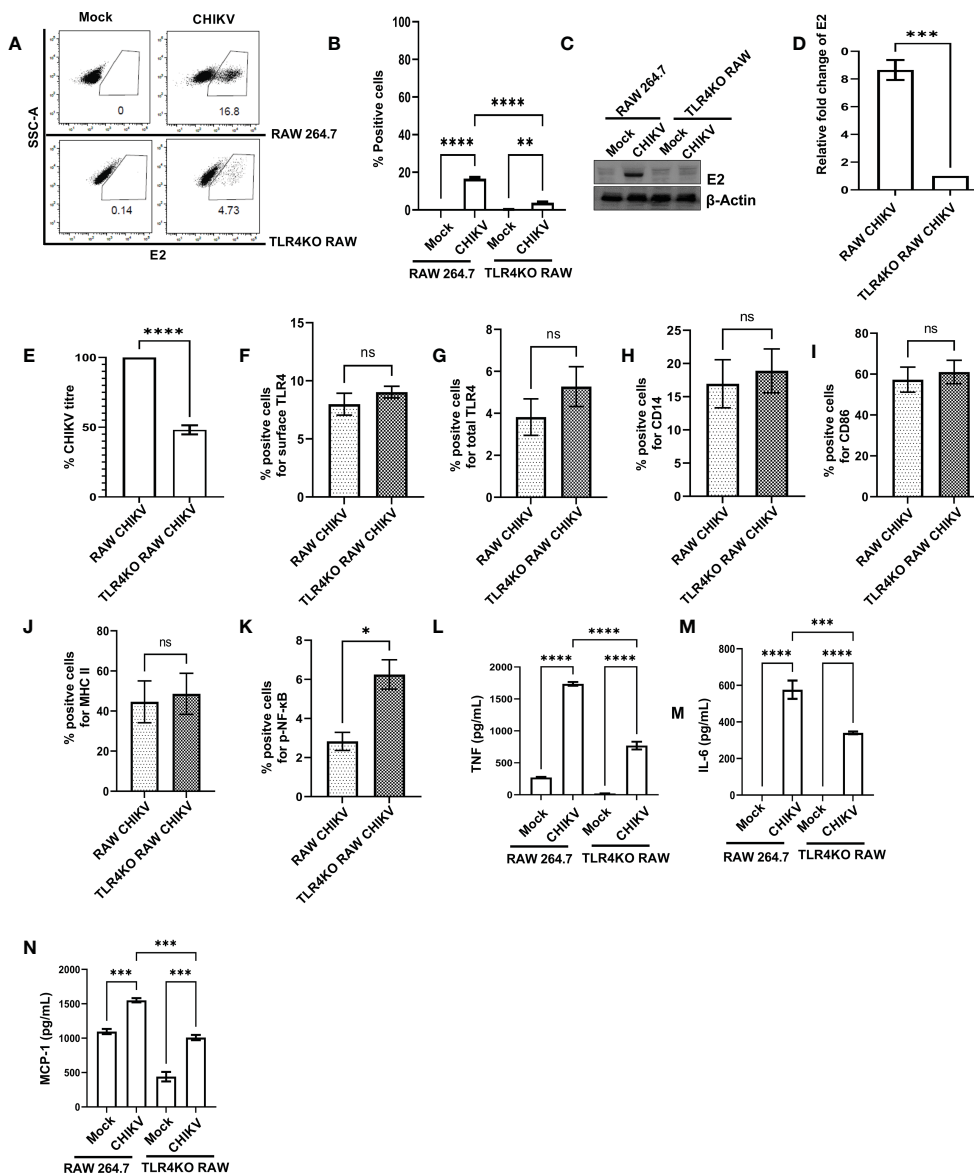


FIGURE 3
 The presence of functional TLR4 facilitates CHIKV infection in host macrophages, *in vitro*. RAW264.7 and TLR4KO RAW cells were subjected to CHIKV infection at 5 MOI and harvested at 8 hpi (A, B) The flow cytometry dot plot analysis depicts comparative CHIKV-E2 expression. (C, D) Western blot analysis showing comparative E2 level. Normalization of E2 expression was done using β -actin as a housekeeping gene. (E) The bar diagram showing comparative CHIKV titre obtained from plaque assay (F–K) The flow cytometry dot plot-based bar diagram analysis showing percent positive cells expressing surface TLR4, total TLR4, CD14, CD86, MHC-II and p- NF- κ B respectively in mock and CHIKV infected TLR4KO RAW cells. (L–N) Bar diagrams depicting ELISA-based TNF- α , IL-6 and MCP-1 quantification respectively in RAW 264.7 and TLR4KO RAW cells. Data represent the Mean \pm SEM of three independent experiments. $p < 0.05$ was considered as a statistically significant difference between the groups (ns: non-significant, * $p < 0.05$; ** $p \leq 0.01$; *** $p \leq 0.001$; **** $p \leq 0.0001$).

with host TLR4 (Figure 4A). To further validate the results, a study on the interaction of E2 and TLR4 was carried out in the TLR4KO RAW cells under similar experimental conditions. However, no detectable interaction between E2 and TLR4 was observed (Figure 4B). To investigate the specificity of the results, the interaction of E1 and TLR4 was studied in the RAW264.7 cells under similar experimental conditions. However, no detectable interaction between E1 and TLR4 was observed (Figure 4C). Moreover, less interaction between CHIKV-E2 and host TLR4 was observed in the presence of TAK-242 (Figure 4D). The interaction of the extracellular domain of TLR4 and CHIKV-E2

was also validated further by *in-silico* analysis using the mouse TLR4-MD2 complex (PDB ID: 2Z64) and CHIKV structural protein E2 (PDB ID: 3N41) (Figure 4E). The analysis showed 12 probable interactions between the amino acid residues of these two structures through molecular docking (Figure 4F) suggesting the possibility of TLR4 activation through the interaction of CHIKV-E2 at the extracellular domain of TLR4 that might be required for the efficient viral infection in host macrophages.

To further validate the positive regulation of TLR4 on CHIKV infection in host macrophages, the anti-TLR4 antibody-mediated blocking experiment was performed. The flow cytometry-based dot

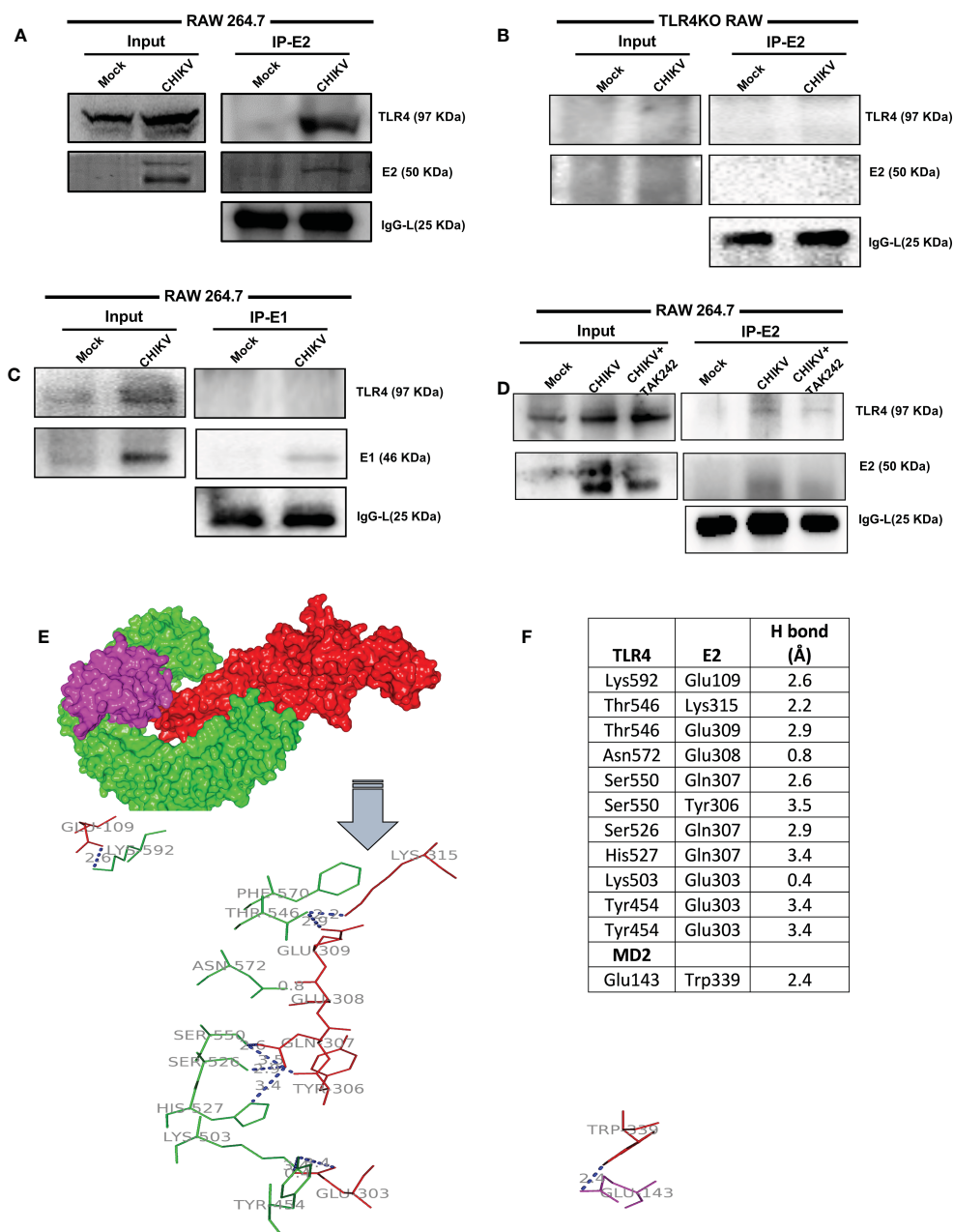


FIGURE 4

TLR4-E2 interaction facilitates CHIKV infection in host macrophages. The RAW264.7 and TLR4KO RAW cells were subjected to study functional TLR4 and E2 interaction. Both mock and CHIKV-infected cells were processed for immunoprecipitation followed by Western blot analysis. **(A)** For RAW264.7 cells, Western blot analysis showing the expressions of E2 and TLR4 in the whole cell lysate (left), co-immunoprecipitation analysis depicting the interaction of CHIKV E2 and TLR4 (right). **(B)** For TLR4KO RAW cells, Western blot analysis showing the levels of E2 and TLR4 in the whole cell lysate (left), co-immunoprecipitation analysis depicting the interaction of CHIKV E2 and TLR4 (right). **(C)** For RAW264.7 cells, Western blot analysis showing the expressions of E1 and TLR4 in the whole cell lysate (left), co-immunoprecipitation analysis depicting the interaction of CHIKV-E1 and TLR4 (right). **(D)** For RAW264.7 cells, Western blot analysis showing the expressions of E2 and TLR4 in the whole cell lysate (left), co-immunoprecipitation analysis depicting the interaction of CHIKV-E2 and TLR4 (right) in the presence/absence of TAK-242. **(E)** Protein-protein docking analysis reveals probable molecular interaction of MD2-TLR4 (PDB ID: 2Z64) with Chikungunya virus (CHIKV) envelope proteins E2 (PDB ID: 3N41). The protein-protein docking was done in the ZDOCK webserver using MD2-TLR4 as receptor and CHIKV-E2 as ligand. **(A)** Interaction complex of MD2 (magenta) and TLR4 (green) with E2 (red). The polar interactions are labeled (blue) in the line diagram. **(F)** The residues involved in polar interactions between CHIKV-E2 and TLR4.

plot analysis revealed a significant decrease in CHIKV infection in the RAW264.7 cells in presence of pre-incubation with the anti-TLR4 antibody. However, in presence of both TAK-242 and anti-TLR4 antibody, CHIKV infection didn't show any marked change in comparison to only the anti-TLR4 antibody, which might be

indicative towards saturation of TLR4 inhibition [from $19.58 \pm 0.375\%$ (CHIKV) to $10.57 \pm 0.8168\%$ (TAK-242), $10.87 \pm 1.546\%$ (CHIKV+Antibody) to $11.88 \pm 1.316\%$ (TAK-242+CHIKV +Antibody)] (Figures 5A, B). Moreover, Western blot analysis revealed the decrease in fold change of CHIKV-E2 level in the

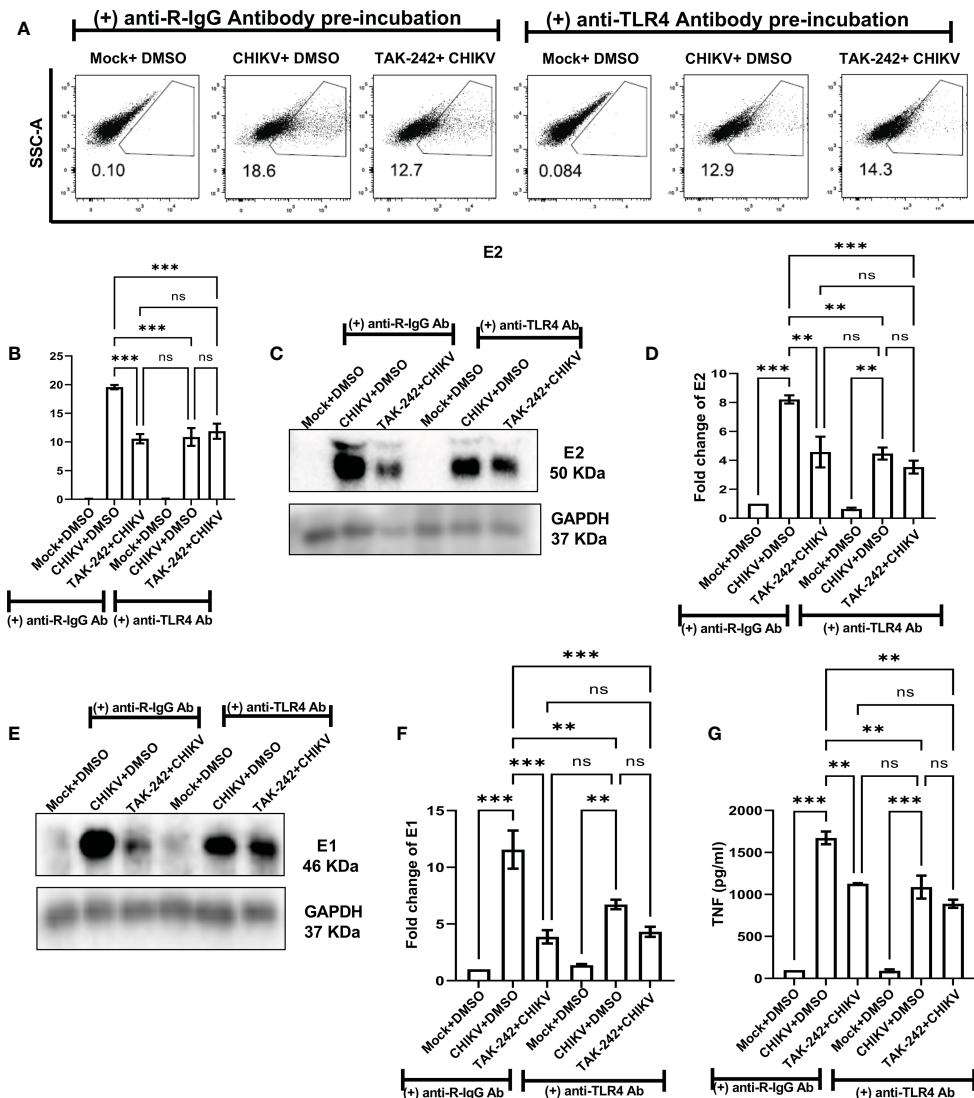


FIGURE 5 Pre-incubation with anti-TLR4 antibody alleviates CHIKV infection in host RAW264.7 macrophages, *in vitro*. Before pre-incubation of the RAW264.7 cells with either DMSO or TAK-242, the anti-TLR4 antibody or anti-R-IgG antibody was added in the pre-incubation volume in respective conditions at 4 μg/ml concentration and the cells from all conditions were preincubated for 3 h. The CHIKV infection was given at 5 MOI for 2 h and the cells were harvested at 8 hpi. (A, B) The flow cytometry dot plot analysis shows comparative CHIKV-E2 levels at different conditions. (C, D) Western blot analysis shows E2 expression in different experimental conditions. (E, F) Western blot analysis shows differential E1 expression. All densitometric quantifications were performed with respect to GAPDH. (G) The bar diagram represents ELISA-based cytokine analysis of TNF.

anti-TLR4 antibody preincubated condition [from 8.212 ± 0.29-fold (CHIKV) to 4.577 ± 1.062-fold (TAK-242), 4.469 ± 0.42-fold (CHIKV+Antibody) to 3.53 ± 0.45-fold (TAK-242+CHIKV +Antibody)] (Figures 5C, D). Furthermore, the CHIKV-E1 level showed a similar trend of expression to CHIKV-E2 [from 11.56 ± 1.6775-fold (CHIKV) to 3.868 ± 0.59-fold (TAK-242), 6.725 ± 0.42-fold (CHIKV+Antibody) to 4.315 ± 0.44-fold (TAK-242+CHIKV +Antibody)] (Figures 5E, F). Next, ELISA-based cytokine analysis of TNF revealed the reduced level of secretory TNF in presence of the anti-TLR4 antibody-driven pre-incubation, significantly [from 98.84 ± 0.49 pg/ml (Mock) to 1673 ± 75.33 pg/ml (CHIKV), 1127 ± 6.685 pg/ml (TAK-242), 90.68 ± 17.12 pg/ml (Mock+Antibody) 1088 ± 136.6 pg/ml (CHIKV+Antibody) to 889.4 ± 48.26 pg/ml

(TAK-242+CHIKV+Antibody)] (Figure 5G). Therefore, the anti-TLR4 antibody-driven blocking study reconfirms the possible engagement of host TLR4 as a potential receptor of CHIKV.

3.5 TLR4 is required to regulate the CHIKV entry in host macrophages

To investigate the possible anti-CHIKV role in specific stages of viral infection, the TAK-242 treatment was given in different stages of the CHIKV life cycle as before CHIKV infection (only pre-incubation), during CHIKV infection, both before and during CHIKV infection (pre+during incubation), only during infection

(during incubation), post-infection incubation at 0 hpi (the drug was added at 0 hpi) and post-infection incubation at 8 hpi (the drug was added at 8 hpi). It was noticed that the presence of TAK-242 before CHIKV infection (only pre-incubation) and before as well as during CHIKV infection (pre+ during incubation) is most efficient (62% and 59% decrease of CHIKV-E1 copy number, respectively) to regulate the CHIKV infection. Interestingly, a 45% decrease of CHIKV copy number was observed while TAK-242 was added specifically during CHIKV infection only (during incubation), indicating its anti-CHIKV effect. However, no decrease in the

CHIKV copy number was observed during the post-infection incubation condition (Figure 6A). Therefore, the data suggest that the TAK-242-mediated TLR4 inhibition probably plays a pivotal role in the initial phase of CHIKV infection i.e., the entry and/or attachment stage.

To further confirm whether TLR4 is required in the entry and/or attachment phase of viral infection, TAK-242 (1 μM) was added to the RAW264.7 cells before infection for 3 h. Once viral adsorption was over at 37°C, the unbound virus particles (CHIKV in SFM) were collected and subjected to plaque assay

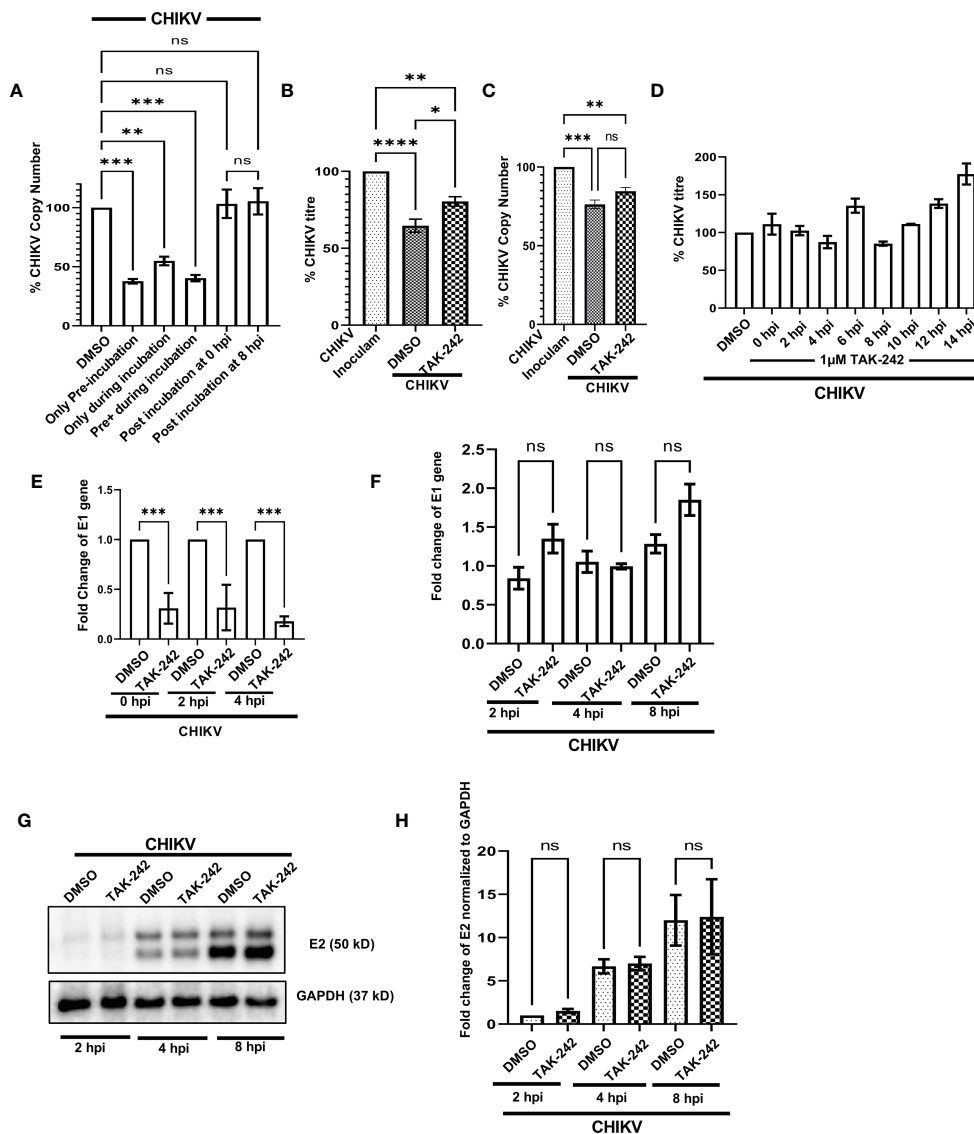


FIGURE 6

TLR4 promotes viral entry at the early stages of CHIKV infection in host macrophages, *in vitro*. (A) TLR4 inhibition before CHIKV infection is most effective to regulate viral copy number at 8 hpi (B, C) Viral entry assay in RAW 264.7 cells showing the internalization of around 24% and 11% less virus in TAK-242 treated condition using plaque assay-based viral titre determination and q-RT PCR based viral copy number determination respectively. (D) Time of addition assay in RAW 264.7 cells showed no significant decrease in viral infection during post-infection treatment. (E) TAK-242 pre-treatment decreases CHIKV copy number in different time points inside the RAW264.7 macrophage cells. (F) Post-infection TLR4 inhibition (TAK-242 was added at 0 hpi) does not have a role in CHIKV E1 gene transcription in the RAW264.7 cells. (G, H) Post-infection TLR4 inhibition (TAK-242 was added at 0 hpi) does not have a role in CHIKV-E2 translation in the RAW264.7 cells. The densitometry was performed with respect to the corresponding GAPDH expression. Data represent the Mean ± SEM of three independent experiments. $p < 0.05$ was considered as a statistically significant difference between the groups (ns: non-significant, * $p < 0.05$; ** $p \leq 0.01$; *** $p \leq 0.001$; **** $p \leq 0.0001$).

and qRT-PCR analysis to determine the viral titre and viral copy number, respectively. It was observed that pre-treatment with TAK-242 resulted in the presence of $24.38 \pm 2.302\%$ and 10.86% more CHIKV particles in the wash solution containing unbound virus particles as compared to untreated cells by plaque assay and qRT-PCR-based method respectively (Figures 6B, C). Therefore, the data suggest that TLR4 might be required for efficient CHIKV attachment and/or entry in the host macrophages.

In order to confirm whether TAK-242 has any role in a specific phase of the CHIKV life cycle, the “Time of Addition” experiment was carried out as mentioned in the materials and method section. The viral titres were determined for all of the supernatants collected at 15 hpi. The data showed no significant reduction in CHIKV infection at any time point when the drug was added after infection (Figure 6D). Hence, the result suggests that TLR4 might not be required for CHIKV once the virus enters inside the host macrophages.

To understand the role of TLR4 in CHIKV replication, E1 mRNA copy numbers were determined inside the cells at different time points after infection. To perform this experiment, the RAW264.7 cells were pre-incubated with TAK-242 ($1\mu\text{M}$), followed by CHIKV infection at MOI 5 for 2 h with TAK-242 ($1\mu\text{M}$) and post-infection incubation with TAK-242 ($1\mu\text{M}$). Next, the cells were harvested at 0, 2 and 4 hpi and subjected to total RNA isolation, cDNA preparation and qRT-PCR analysis of the E1 gene. It was observed that the copy number of the CHIKV-E1 gene was always lower in TAK-242 treated condition inside the cells (Figure 6E). This result confirms that TLR4 abrogation leads to the reduced CHIKV replication when TAK-242 is added in pre and pre+ during conditions at different time points as it has been already noticed that post-treatment doesn't regulate CHIKV infection.

To investigate whether TLR4 inhibition has any role in the transcription of the CHIKV E1 gene, the CHIKV-infected RAW264.7 cells were subjected to post-infection incubation (0 hpi) with TAK-242 ($1\mu\text{M}$) or DMSO. The cells were harvested at 2, 4 and 8 hpi and subjected to RNA isolation followed by cDNA synthesis and q-RT PCR analysis of the E1 gene to estimate the CHIKV copy number inside the cells. It was found that there is no marked change of the CHIKV-E1 gene in the TAK-242 treated/untreated group at different time points (Figure 6F) supporting that post-treatment does not affect the CHIKV transcription.

Similarly, to study the effect of TLR4 inhibition on the translation of E2 protein, the CHIKV-infected RAW264.7 cells were subjected to post-infection incubation (0 hpi) with TAK-242 ($1\mu\text{M}$) or DMSO. The cells were harvested at 2, 4 and 8 hpi and subjected to Western blot analysis of E2 protein (as representative of CHIKV structural proteins) which depicted no significant difference in the E2 protein level in the TAK-242 treated/untreated group at different time points. (Figures 6G, H). These data, therefore, suggest that TLR4 inhibition might not have any role in the viral translation step.

Taken together, all these mechanism-based studies denote that TLR4 might be involved in the CHIKV attachment and entry process in host macrophages and probably doesn't affect post-entry phases of the CHIKV life cycle.

3.6 TLR4 inhibition efficiently reduces the CHIKV infection and inflammation in mice, *in vivo*

The inhibitory role of TAK-242 against CHIKV infection was assessed in 10-12 days old C57BL/6 mice. Interestingly, it was found that TAK-242 treated mice group showed reduced CHIKV-mediated arthritogenic symptoms and impaired limb movements (indicated with an arrow mark in the figure) compared to the only infected group (Figure 7A). Following TAK-242 treatment, the viral titre was found to be reduced to $41.26 \pm 2.664\%$ and $47.01 \pm 0.4225\%$ in the quadriceps muscle and spleen respectively (Figures 7B, C). In addition, Western blot analysis revealed the reduction of E2 level to $56.08 \pm 2.020\%$ and $50.04 \pm 0.6860\%$ in muscle and spleen respectively (Figures 7D-F). Moreover, to determine the functional immune response, the serum TNF level was assessed and a reduction of $38.47 \pm 2.128\%$ was observed (Figure 7G). The clinical score of the TAK-242 treated group of mice showed significantly reduced arthritogenic symptoms as compared to the only infected mice (Figure 7H). Additionally, to analyze the survival efficiency of mice in presence of TAK-242, the survival curve was determined and it was found that all of the CHIKV-infected mice died on the 8th-day post-infection, while TAK-242 treatment provided 75% better survival during CHIKV infection (Figure 7I). Together, the data suggest that TLR4 antagonism effectively reduces CHIKV infection and inflammation and may ensure better survivability (75%) in mice.

4 Discussion

TLR4, an important member of the innate immune system, acts as one of the earliest determinants of foreign immunogenic components associated with different sets of pathogens. Starting from its discovery, TLR4 has been known to play a critical role to study the functional aspects of host-pathogen interactions and associated pro-inflammatory immune responses, thus it has evolved as a suitable target for modern-age bio-medical research in the field of rheumatoid arthritis, necrotizing enterocolitis, and inflammatory bowel disease (25, 27, 28). Moreover, the prominent regulatory role of TLR4 has also been explored in the LPS-mediated endotoxin shock and sepsis model in mice using TAK-242 as a probable TLR4 antagonist (24, 37). In the case of LPS-driven TLR4 activation, LPS binding protein (LBP), an extracellular protein, first interacts with LPS present over bacterial outer membrane or in micelle form. A single LPS-LBP complex then interacts with either soluble or the membrane-bound CD14 protein, a co-stimulator of the TLR4 signaling pathway. CD14 acts as a carrier to transfer a single molecule of LPS to MD2 which results in the TLR4-MD2 heterodimer formation which represents the functional LPS receptor. The TLR4-MD2 dimerization occurs to initiate a downstream signaling cascade (60). The LPS induction enhances macrophage activation markers like CD14, MHC-II and CD86 expressions and results in the internalization of cell surface TLR4 (51, 52, 61-64). As reported previously, activation of TLR4 leads to

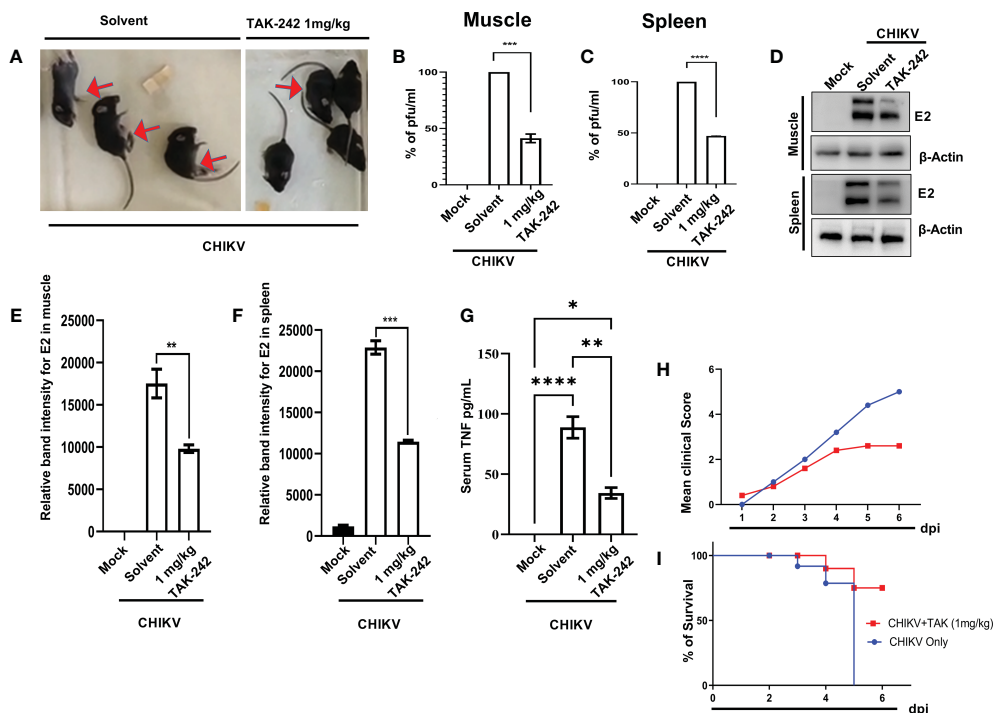


FIGURE 7

TAK-242 protects mice from CHIKV-driven pro-inflammatory responses and increases survival. 10–12 days old C57BL/6 mice ($n=5$ /group) were injected subcutaneously with 10^6 CHIKV-IS and treated with TAK242 (dose:1mg/Kg bodyweight of mice) at every 24h intervals up to 4 dpi. After the mice were sacrificed at 5dpi, serum and different tissues were collected for further downstream experiments. To quantitate viral titre, plaque assay was performed using homogenous and filtered tissues sample. For this, an equal amount of quadriceps muscle and spleen were homogenized and filtrated using 0.22 μ M membrane filter (A) The image showing CHIKV-infected mice in the presence and absence of TAK-242 treatment. The arrows indicate mice with impaired limb movement. (B, C) The bar diagram shows % of pfu/mL in infected and TAK-242 treated mice muscle and spleen respectively. (D) Western blot showing the CHIKV E2 protein in muscle and spleen. Beta-actin was used as a loading control. (E, F) The bar diagram showing the relative band intensities of E2 in muscle and spleen respectively in mock, CHIKV and CHIKV with TAK-242 treated groups (G) The bar diagram depicting serum TNF level in mock, infected and TAK-242 treated mice serum (H) The line diagram showing the disease symptoms of CHIKV infection which were monitored from 1dpi to 6dpi. (I) The survival curve showing the efficacy of TAK-242 against CHIKV-infected C57BL/6 mice ($n=6$ /group). All bar diagrams were obtained through the GraphPad Prism software. Data represent the Mean \pm SEM of three independent experiments. $p < 0.05$ was considered as a statistically significant difference between the groups (ns: non-significant, * $p < 0.05$; ** $p < 0.01$; *** $p < 0.001$; **** $p < 0.0001$).

phosphorylation of NF- κ B (55) and thus has a direct correlation with inflammation (58, 59). TAK-242, a cyclohexene derivative, has been found to bind selectively to the Cys747 residue of the Toll/interleukin 1 receptor (TIR) domain of TLR4 and inhibits the downstream signaling mechanism (24, 34). According to the previous report, it has been shown that the pre-incubation with 1 μ M of TAK-242 for 5 minutes can reduce LPS-induced TNF production by 80% in the mouse peritoneal macrophages and the efficacy of the specific anti-inflammatory role of TAK-242 is concentration and time-dependent (34). They have also shown a reduced activation of the NF- κ B pathway upon TAK-242-mediated TLR4 inhibition (34). Therefore, the effect of TAK-242-mediated TLR4 inhibition has been simultaneously investigated in the LPS-induced pro-inflammatory model as an experimental control of the current study. Additionally, the re-emergence of CHIKV is considered as one of the global public health threats especially due to the unavailability of possible anti-CHIKV drugs or vaccine to date. The literature on CHIKV infection and pathogenesis report on pro-inflammatory cytokine burst in the host immune system (19). Hence, the current study is intended to explore the involvement of

TLR4 during CHIKV infection and associated pro-inflammatory responses.

Earlier studies have already reported that the macrophages could be infected with CHIKV, both *in vivo* as well as *in vitro*, and thus may generate a huge pro-inflammatory cytokine burst (19, 22, 65, 66). The published literature on both mice and macaque models showed that macrophages are one of the immune cells which get recruited at the site of inoculation and generate strong immune responses by pro-inflammatory cytokine release, which might be associated with the CHIKV-induced arthritis, myositis and tenosynovitis (67, 68). CHIKV has already been reported to persist for several months or even years within macrophages and may reappear to cause disease symptoms (65). Therefore, investigating the viral infection-mediated host immune modulation in macrophages might give detailed insight into CHIKV persistence and associated future therapeutic strategies.

TAK-242 (Resatorvid), a well-established TLR4-specific drug has currently been used for clinical trials for several inflammatory diseases, for example, severe sepsis (69) and acute alcoholic hepatitis (ClinicalTrials.gov.Identifier: NCT04620148, <https://>

clinicaltrials.gov/ct2/show/NCT04620148). Therefore, TAK-242 has been used to explore the regulatory role of TLR4, if any, during CHIKV-induced pro-inflammatory responses. The current findings suggest that TAK-242-mediated TLR4 inhibition may abrogate CHIKV infection, cellular activation and pro-inflammatory responses in mouse and human macrophages, *in vitro*. It also demonstrates that TLR4 inhibition-mediated decrease of CHIKV infection is driven by p38 and SAPK-JNK phosphorylation. Interestingly, it is found that CHIKV-E2 interacts with TLR4 during infection which is essential for efficient viral infection in host macrophages. The interaction of the extracellular domain of TLR4 and CHIKV-E2 has been further validated by *in-silico* analysis using the mouse TLR4-MD2 complex as the ligand and CHIKV structural protein, E2 as the receptor. The analysis demonstrates 12 probable interactions where Thr546, Ser550 and Tyr454 residues of TLR4 are found to be critically essential to interact with CHIKV-E2, *in silico*. Therefore, the study depicts TLR4 as one of the possible receptors of the CHIKV-E2 protein to facilitate viral infection. Moreover, anti-TLR4 antibody-dependent blocking assay strengthens the role of TLR4 as a possible receptor for CHIKV-E2 and thus TLR4-mediated CHIKV entry in the RAW264.7 macrophages. Furthermore, it has also been observed that TLR4 plays a key role in CHIKV attachment process and thus TLR4 inhibition might lead to an overall decrease in viral titre. The study also suggests that TLR4 inhibition has no role in post-entry stages of viral infection i.e. viral transcription, replication and translation inside the host macrophages. Additionally, the TLR4 antagonism effectively reduces CHIKV infection and inflammation, *in vivo* by reducing the disease score, significantly with improved survival of CHIKV-infected mice. Therefore, the positive regulation of TLR4 on CHIKV infection in different host systems could be associated with the inflammation and viral pathogenesis.

An earlier report on the respiratory syncytial virus (RSV) describes that the functional TLR4 is an essential component to promote viral infection and the infection-induced inflammasome activation, vascular damage, T cell activation, B cell maturation and NK cell activation in mice model (30). Recent studies on SARS-CoV2 imply that TAK-242 mediated TLR4 inhibition significantly abolishes viral spike protein-induced pro-inflammatory cytokine responses in association with the p-NF- κ B protein in the murine and human macrophages (31, 70). VP3, a structural protein of the foot and mouth disease virus (FMDV) is already reported to interact and induce TLR4 to promote viral infection and associated inflammation (32). Furthermore, previous reports on the reduction in the surface expression of TLR4 and increase in the total TLR4 upon LPS or virus-mediated stimulation are found to be similar to this current investigation (32, 51, 52). Hence, the current study suggests a positive regulation of TLR4 on CHIKV entry, infection and associated inflammation in the host.

Although this study proposes probable TLR4-mediated CHIKV entry, TLR4 inhibition doesn't completely hinder viral entry in the host. Therefore, it seems that the possible involvement of other cellular receptor/s (18) to execute viral entry and pathogenesis

might be crucial under the current experimental scenario, which is yet to be explored. Moreover, siRNA-mediated gene silencing could be explored as a suitable tool to investigate the detailed role of TLR4 during viral infection.

The *in-silico* study reveals the association of specific amino acids of TLR4-MD2 complex and CHIKV-E2 proteins in the current investigation. Two amino acid residues, Asn572 and Lys503 of TLR4 (PDB ID: 2Z64) have been found to show high-affinity polar interactions ($< 2 \text{ \AA}$) with Glu308 and Glu 303 of CHIKV-E2 (PDB ID: 3N41), respectively. Furthermore, Thr546, Ser550 and Tyr454 residues of TLR4 and Gln307 and Glu303 residues of CHIKV-E2 protein have been shown to exhibit multiple polar interactions to emphasize their prominent role in terms of CHIKV-TLR4 association. Further, it will be interesting to investigate the role of these amino acid residues in this interaction through mutational studies in future.

In addition to the mice model, earlier reports are also available on the CHIKV-driven pro-inflammatory cytokine burst and associated symptoms in human patient studies, *in vivo* (20, 21). Accordingly, the effect of TLR4 inhibition could be further explored in experimental *in vitro* or *in vivo* setups with CHIKV-infected patient samples. Therefore, the probable efficacy of TLR4 inhibition against CHIKV infection might be explored in higher-order mammalian systems in future.

In conclusion, the current study reveals the possible regulatory role of TLR4 at the attachment as well as entry stages of viral infection *via* interaction with the CHIKV structural protein E2. Therefore, TLR4 could be considered as a potential receptor of CHIKV and a positive regulator of the virus driven pro-inflammatory host immune responses. Considering this regulatory role of TLR4, this current study might have translational implications for designing future therapeutic strategies against CHIKV infection to modulate the disease pathogenesis.

Data availability statement

The original contributions presented in the study are included in the article/[Supplementary Material](#). Further inquiries can be directed to the corresponding authors.

Ethics statement

The studies involving human participants were reviewed and approved by Institutional Ethics Committee, NISER, Bhubaneswar (NISER/IEC/2022-04). The patients/participants provided their written informed consent to participate in this study. The animal study was reviewed and approved by Institutional Animal Ethics Committee, NISER (1634/GO/ReBi/S/12/CPSCEA) and Institutional Animal Ethics Committee, ILS Bhubaneswar (76/Go/ReBi/S/1999/CPCSEA) under the affiliation of Committee for the Purpose of Control and Supervision of Experiments on Animals (CPCSEA) of India.

Author contributions

SuC, SoC, and CM conceived the idea and designed the experiments. CM, SD, SaC, SG, and SSK did the wet lab experiments. BS performed the *in-silico* experimentation and analysis. SuC and SoC provided the reagents. SuC, SoC, and CM analyzed and interpreted the results. SuC, SoC, CM, TM, SK, and KT wrote the manuscript and prepared the figures. All authors contributed to the article and approved the submitted version.

Funding

The work has been mainly supported by core funding from the Department of Atomic Energy (DAE), Govt. of India and a DST-FIST grant received by the School of Biological Sciences, NISER (Grant No.- SR/FST/LSI-652/2015). The work has been partly supported by the Council of Scientific and Industrial Research (CSIR), India (Grant No.- 37(1542)/12/EMR-II, 37(1675)/16/EMR-II) and Department of Biotechnology, India (Grant No.- BT/NBM0101/02/2018).

Acknowledgments

We are thankful to the central Flow Cytometry facility, Animal House facility and Health Center of NISER, Bhubaneswar for the *in*

vitro mouse and human model experiments. We sincerely acknowledge the Animal House facility of ILS, Bhubaneswar for the *in vivo* mouse model experiments.

Conflict of interest

The authors declare that the research was conducted in the absence of any commercial or financial relationships that could be construed as a potential conflict of interest.

Publisher's note

All claims expressed in this article are solely those of the authors and do not necessarily represent those of their affiliated organizations, or those of the publisher, the editors and the reviewers. Any product that may be evaluated in this article, or claim that may be made by its manufacturer, is not guaranteed or endorsed by the publisher.

Supplementary material

The Supplementary Material for this article can be found online at: <https://www.frontiersin.org/articles/10.3389/fimmu.2023.1139808/full#supplementary-material>

References

- Webb E, Michelen M, Rigby I, Dagens A, Dahmash D, Cheng V, et al. An evaluation of global chikungunya clinical management guidelines: A systematic review. *EClinicalMedicine* (2022) 54:101672. doi: 10.1016/j.eclinm.2022.101672
- Suhrbier A. Rheumatic manifestations of chikungunya: emerging concepts and interventions. *Nat Rev Rheumatol* (2019) 15:597–611. doi: 10.1038/s41584-019-0276-9
- Simon F, Javelle E, Cabie A, Bouquillard E, Troisgros O, Gentile G, et al. French Guidelines for the management of chikungunya (acute and persistent presentations). *November 2014 Med Mal Infect* (2015) 45:243–63. doi: 10.1016/j.medmal.2015.05.007
- Cunha RV, Trinta KS. Chikungunya virus: clinical aspects and treatment - a review. *Mem Inst Oswaldo Cruz* (2017) 112:523–31. doi: 10.1590/0074-02760170044
- Kielian M, Chanel-Vos C, Liao M. Alphavirus entry and membrane fusion. *Viruses* (2010) 2:796–825. doi: 10.3390/v2040796
- Bernard E, Solignat M, Gay B, Chazal N, Higgs S, Devaux C, et al. Endocytosis of chikungunya virus into mammalian cells: Role of clathrin and early endosomal compartments. *PLoS One* (2010) 5:e11479. doi: 10.1371/journal.pone.0011479
- Lee CHR, Mohamed Hussain K, Chu JJH. Macropinocytosis dependent entry of chikungunya virus into human muscle cells. *PLoS Negl Trop Dis* (2019) 13:e0007610. doi: 10.1371/journal.pntd.0007610
- Bernard KA, Klimstra WB, Johnston RE. Mutations in the E2 glycoprotein of Venezuelan equine encephalitis virus confer heparan sulfate interaction, low morbidity, and rapid clearance from blood of mice. *Virology* (2000) 276:93–103. doi: 10.1006/viro.2000.0546
- Gardner CL, Burke CW, Higgs ST, Klimstra WB, Ryman KD. Interferon-alpha/beta deficiency greatly exacerbates arthritogenic disease in mice infected with wild-type chikungunya virus but not with the cell culture-adapted live-attenuated 181/25 vaccine candidate. *Virology* (2012) 425:103–12. doi: 10.1016/j.virol.2011.12.020
- Gardner CL, Hritz J, Sun C, Vanlandingham DL, Song TY, Ghedin E, et al. Deliberate attenuation of chikungunya virus by adaptation to heparan sulfate-dependent infectivity: A model for rational arboviral vaccine design. *PLoS Negl Trop Dis* (2014) 8:e2719. doi: 10.1371/journal.pntd.0002719
- Klimstra WB, Ryman KD, Johnston RE. Adaptation of sindbis virus to BHK cells selects for use of heparan sulfate as an attachment receptor. *J Virol* (1998) 72:7357–66. doi: 10.1128/JVI.72.9.7357-7366.1998
- Smit JM, Waarts B-L, Kimata K, Klimstra WB, Bittman R, Wilschut J. Adaptation of alphaviruses to heparan sulfate: Interaction of sindbis and semliki forest viruses with liposomes containing lipid-conjugated heparin. *J Virol* (2002) 76:10128–37. doi: 10.1128/JVI.76.20.10128-10137.2002
- Weber C, Berberich E, von Rhein C, Henß L, Hildt E, Schnierle BS. Identification of functional determinants in the chikungunya virus E2 protein. *PLoS Negl Trop Dis* (2017) 11:e0005318. doi: 10.1371/journal.pntd.0005318
- Moller-Tank S, Kondratowicz AS, Davey RA, Rennert PD, Maury W. Role of the phosphatidylserine receptor TIM-1 in enveloped-virus entry. *J Virol* (2013) 87:8327–41. doi: 10.1128/JVI.01025-13
- Jemielity S, Wang JJ, Chan YK, Ahmed AA, Li W, Monahan S, et al. TIM-family proteins promote infection of multiple enveloped viruses through virion-associated phosphatidylserine. *PLoS Pathog* (2013) 9:e1003232. doi: 10.1371/journal.ppat.1003232
- Prado Acosta M, Geoghegan EM, Lepenies B, Ruzal S, Kielian M, Martinez MG. Surface (S) layer proteins of lactobacillus acidophilus block virus infection via DC-SIGN interaction. *Front Microbiol* (2019) 10:810. doi: 10.3389/fmicb.2019.00810
- Wintachai P, Wikan N, Kuadkitkan A, Jaimipuk T, Ubol S, Pulmanasahakul R, et al. Identification of prohibitin as a chikungunya virus receptor protein. *J Med Virol* (2012) 84:1757–70. doi: 10.1002/jmv.23403
- Zhang R, Kim AS, Fox JM, Nair S, Basore K, Klimstra WB, et al. Mxra8 is a receptor for multiple arthritogenic alphaviruses. *Nature* (2018) 557:570–4. doi: 10.1038/s41586-018-0121-3
- Nayak T, Mamidi P, Kumar A, Singh L, Sahoo S, Chattopadhyay S, et al. Regulation of viral replication, apoptosis and pro-inflammatory responses by 17-AAG during chikungunya virus infection in macrophages. *Viruses* (2017) 9:3. doi: 10.3390/v9010003
- Jacob-Nascimento LC, Carvalho CX, Silva MMO, Kikuti M, Anjos RO, Fradico JRB, et al. Acute-phase levels of CXCL8 as risk factor for chronic arthralgia following chikungunya virus infection. *Front Immunol* (2021) 12:744183. doi: 10.3389/fimmu.2021.744183
- Guerrero-Arguero I, Høj TR, Tass ES, Berges BK, Robison RA. A comparison of chikungunya virus infection, progression, and cytokine profiles in human PMA-

- differentiated U937 and murine RAW264.7 monocyte derived macrophages. *PLoS One* (2020) 15:e0230328. doi: 10.1371/journal.pone.0230328
22. Nayak TK, Mamidi P, Sahoo SS, Kumar PS, Mahish C, Chatterjee S, et al. p38 and JNK mitogen-activated protein kinases interact with chikungunya virus non-structural protein-2 and regulate TNF induction during viral infection in macrophages. *Front Immunol* (2019) 10:786. doi: 10.3389/fimmu.2019.00786
23. Wu K, Zhang H, Fu Y, Zhu Y, Kong L, Chen L, et al. TLR4/MyD88 signaling determines the metastatic potential of breast cancer cells. *Mol Med Rep* (2018). doi: 10.3892/mmr.2018.9326
24. Takashima K, Matsunaga N, Yoshimatsu M, Hazeki K, Kaisho T, Uekata M, et al. Analysis of binding site for the novel small-molecule TLR4 signal transduction inhibitor TAK-242 and its therapeutic effect on mouse sepsis model. *Br J Pharmacol* (2009) 157:1250–62. doi: 10.1111/j.1476-5381.2009.00297.x
25. Samarrita S, Kim JY, Rasool MK, Kim KS. Investigation of toll-like receptor (TLR) 4 inhibitor TAK-242 as a new potential anti-rheumatoid arthritis drug. *Arthritis Res Ther* (2020) 22:16. doi: 10.1186/s13075-020-2097-2
26. Poltorak A, He X, Smirnova I, Liu M-Y, van HC, Du X, et al. Defective LPS signaling in C3H/HeJ and C57BL/10ScCr mice: Mutations in *Tlr4* gene. *Sci* (1999) 282:2085–8. doi: 10.1126/science.282.5396.2085
27. Yu R, Jiang S, Tao Y, Li P, Yin J, Zhou Q. Inhibition of HMGB1 improves necrotizing enterocolitis by inhibiting NLRP3 via TLR4 and NF- κ B signaling pathways. *J Cell Physiol* (2019) 234:13431–8. doi: 10.1002/jcp.28022
28. Han C, Guo L, Sheng Y, Yang Y, Wang J, Gu Y, et al. FoxO1 regulates TLR4/MyD88/MD2-NF- κ B inflammatory signalling in mucosal barrier injury of inflammatory bowel disease. *J Cell Mol Med* (2020) 24:3712–23. doi: 10.1111/jcmm.15075
29. Seki H, Tasaka S, Fukunaga K, Shiraishi Y, Moriyama K, Miyamoto K, et al. Effect of toll-like receptor 4 inhibitor on LPS-induced lung injury. *Inflammation Res* (2010) 59:837–45. doi: 10.1007/s00011-010-0195-3
30. Marzec J, Cho H-Y, High M, McCaw ZR, Polack F, Kleeberger SR. Toll-like receptor 4-mediated respiratory syncytial virus disease and lung transcriptomics in differentially susceptible inbred mouse strains. *Physiol Genomics* (2019) 51:630–43. doi: 10.1152/physiolgenomics.00101.2019
31. Zhao Y, Kuang M, Li J, Zhu L, Jia Z, Guo X, et al. SARS-CoV-2 spike protein interacts with and activates TLR4. *Cell Res* (2021) 31:818–20. doi: 10.1038/s41422-021-00495-9
32. Zhang J, Li D, Yang W, Wang Y, Li L, Zheng H. Foot-and-mouth disease virus VP3 protein acts as a critical proinflammatory factor by promoting toll-like receptor 4-mediated signaling. *J Virol* (2021) 95. doi: 10.1128/JVI.01120-21
33. Felipe VLJ, Paula AV, Silvio U-I. Chikungunya virus infection induces differential inflammatory and antiviral responses in human monocytes and monocyte-derived macrophages. *Acta Trop* (2020) 211:105619. doi: 10.1016/j.actatropica.2020.105619
34. Matsunaga N, Tsuchimori N, Matsumoto T, Ii M. TAK-242 (Resatorvid), a small-molecule inhibitor of toll-like receptor (TLR) 4 signaling, binds selectively to TLR4 and interferes with interactions between TLR4 and its adaptor molecules. *Mol Pharmacol* (2011) 79:34–41. doi: 10.1124/mol.110.068064
35. Lin F-Y, Chen Y-H, Tasi J-S, Chen J-W, Yang T-L, Wang H-J, et al. Endotoxin induces toll-like receptor 4 expression in vascular smooth muscle cells via NADPH oxidase activation and mitogen-activated protein kinase signaling pathways. *Arterioscler Thromb Vasc Biol* (2006) 26:2630–7. doi: 10.1161/01.ATV.000024725.9.01257.b3
36. Anand G, Perry AM, Cummings CL, Raymond E, Clemens RA, Steed AL. Surface proteins of SARS-CoV-2 drive airway epithelial cells to induce IFN-dependent inflammation. *J Immunol* (2021) 206:3000–9. doi: 10.4049/jimmunol.2001407
37. Sha T, Sunamoto M, Kitazaki T, Sato J, Ii M, Iizawa Y. Therapeutic effects of TAK-242, a novel selective toll-like receptor 4 signal transduction inhibitor, in mouse endotoxin shock model. *Eur J Pharmacol* (2007) 571:231–9. doi: 10.1016/j.ejphar.2007.06.027
38. Chattopadhyay S, Chakraborty NG. Continuous presence of Th1 conditions is necessary for longer lasting tumor-specific CTL activity in stimulation cultures with PBL. *Hum Immunol* (2005) 66:884–91. doi: 10.1016/j.humimm.2005.06.002
39. Chattopadhyay S, Mehrotra S, Chhabra A, Hegde U, Mukherji B, Chakraborty NG. Effect of CD4⁺ CD25⁺ and CD4⁺ CD25⁻ T regulatory cells on the generation of cytolytic T cell response to a self but human tumor-associated epitope *In vitro*. *J Immunol* (2006) 176:984–90. doi: 10.4049/jimmunol.176.2.984
40. De S, Mamidi P, Ghosh S, Keshry SS, Mahish C, Pani SS, et al. Telmisartan restricts chikungunya virus infection *in vitro* and *in vivo* through the AT1/PPAR- γ /MAPKs pathways. *Antimicrob Agents Chemother* (2021). doi: 10.1128/AAC.01489-21
41. Chatterjee S, Kumar S, Mamidi P, Datey A, Sengupta S, Mahish C, et al. DNA Damage response signaling is crucial for effective chikungunya virus replication. *J Virol* (2022). doi: 10.1128/jvi.01334-22
42. Hogg N, Palmer DG, Revell PA. Mononuclear phagocytes of normal and rheumatoid synovial membrane identified by monoclonal antibodies. *Immunology* (1985) 56:673–81.
43. Ziegler-Heitbrock HWL, Ulevitch RJ. CD14: Cell surface receptor and differentiation marker. *Immunol Today* (1993) 14:121–5. doi: 10.1016/0167-5699(93)90212-4
44. Liu G, Xie J, Shi Y, Chen R, Li L, Wang M, et al. Sec-o-glucosylhamaudol suppressed inflammatory reaction induced by LPS in RAW264.7 cells through inhibition of NF- κ B and MAPKs signaling. *Biosci Rep* (2020) 40. doi: 10.1042/BSR20194230
45. Sanjai Kumar P, Nayak TK, Mahish C, Sahoo SS, Radhakrishnan A, De S, et al. Inhibition of transient receptor potential vanilloid 1 (TRPV1) channel regulates chikungunya virus infection in macrophages. *Arch Virol* (2021) 166:139–55. doi: 10.1007/s00705-020-04852-8
46. De S, Ghosh S, Keshry SS, Mahish C, Mohapatra C, Guru A, et al. MBZM-N-IBT, a novel small molecule, restricts chikungunya virus infection by targeting nsP2 protease activity *In vitro*, *In vivo*, and *Ex vivo*. *Antimicrob Agents Chemother* (2022) 66. doi: 10.1128/aac.00463-22
47. Pierce BG, Wiehe K, Hwang H, Kim B-H, Vreven T, Weng Z. ZDOCK server: interactive docking prediction of protein-protein complexes and symmetric multimers. *Bioinformatics* (2014) 30:1771–3. doi: 10.1093/bioinformatics/btu097
48. Yang K, Zhang XJ, Cao LJ, Liu XH, Liu ZH, Wang XQ, et al. Toll-like receptor 4 mediates inflammatory cytokine secretion in smooth muscle cells induced by oxidized low-density lipoprotein. *PLoS One* (2014) 9:e95935. doi: 10.1371/journal.pone.0095935
49. Layoun A, Samba M, Santos MM. Isolation of murine peritoneal macrophages to carry out gene expression analysis upon toll-like receptors stimulation. *J Visualized Experiments* (2015). doi: 10.3791/52749
50. Dhanwani R, Khan M, Lomash V, Rao PVL, Ly H, Parida M. Characterization of chikungunya virus induced host response in a mouse model of viral myositis. *PLoS One* (2014) 9:e92813. doi: 10.1371/journal.pone.0092813
51. Wang J, Feng X, Zeng Y, Fan J, Wu J, Li Z, et al. Lipopolysaccharide (LPS)-induced autophagy is involved in the restriction of escherichia coli in peritoneal mesothelial cells. *BMC Microbiol* (2013) 13:255. doi: 10.1186/1471-2180-13-255
52. Akashi S, Shimazu R, Ogata H, Nagai Y, Takeda K, Kimoto M, et al. Cutting edge: Cell surface expression and lipopolysaccharide signaling via the toll-like receptor 4-MD-2 complex on mouse peritoneal macrophages. *J Immunol* (2000) 164:3471–5. doi: 10.4049/jimmunol.164.7.3471
53. Gioannini TL, Teghanemt A, Zhang D, Coussens NP, Dockstader W, Ramaswamy S, et al. Isolation of an endotoxin-MD-2 complex that produces toll-like receptor 4-dependent cell activation at picomolar concentrations. *Proc Natl Acad Sci* (2004) 101:4186–91. doi: 10.1073/pnas.0306906101
54. Schromm AB, Lien E, Henneke P, Chow JC, Yoshimura A, Heine H, et al. Molecular genetic analysis of an endotoxin nonresponder mutant cell line. *J Exp Med* (2001) 194:79–88. doi: 10.1084/jem.194.1.79
55. Küper C, Beck F-X, Neuhofer W. Toll-like receptor 4 activates NF- κ B and MAP kinase pathways to regulate expression of proinflammatory COX-2 in renal medullary collecting duct cells. *Am J Physiol-Renal Physiol* (2012) 302:F38–46. doi: 10.1152/ajprenal.00590.2010
56. Wang W, Weng J, Yu L, Huang Q, Jiang Y, Guo X. Role of TLR4-p38 MAPK-Hsp27 signal pathway in LPS-induced pulmonary epithelial hyperpermeability. *BMC Pulm Med* (2018) 18:178. doi: 10.1186/s12890-018-0735-0
57. Khan MA, Farahvash A, Douda DN, Licht J-C, Grasemann H, Sweezey N, et al. JNK activation turns on LPS- and gram-negative bacteria-induced NADPH oxidase-dependent suicidal NETosis. *Sci Rep* (2017) 7:3409. doi: 10.1038/s41598-017-03257-z
58. Li C, Zhao B, Lin C, Gong Z, An X. TREM2 inhibits inflammatory responses in mouse microglia by suppressing the PI3K/NF- κ B signaling. *Cell Biol Int* (2019) 43:360–72. doi: 10.1002/cbin.10975
59. Hop HT, Reyes AWB, Huy TXN, Arayan LT, Min W, Lee HJ, et al. Activation of NF- κ B-Mediated TNF-induced antimicrobial immunity is required for the efficient brucella abortus clearance in RAW 264.7 cells. *Front Cell Infect Microbiol* (2017) 7:437. doi: 10.3389/fcimb.2017.00437
60. Fitzgerald KA, Kagan JC. Toll-like receptors and the control of immunity. *Cell* (2020) 180:1044–66. doi: 10.1016/j.cell.2020.02.041
61. Landmann R, Ludwig C, Obrist R, Obrecht JP. Effect of cytokines and lipopolysaccharide on CD14 antigen expression in human monocytes and macrophages. *J Cell Biochem* (1991) 47:317–29. doi: 10.1002/jcb.240470406
62. Casals C, Barrachina M, Serra M, Lloberas J, Celada A. Lipopolysaccharide up-regulates MHC class II expression on dendritic cells through an AP-1 enhancer without affecting the levels of CIITA. *J Immunol* (2007) 178:6307–15. doi: 10.4049/jimmunol.178.10.6307
63. Tierney JB, Kharkrang M, la Flamme AC. Type II-activated macrophages suppress the development of experimental autoimmune encephalomyelitis. *Immunol Cell Biol* (2009) 87:235–40. doi: 10.1038/icb.2008.99
64. Tsukamoto H, Takeuchi S, Kubota K, Kobayashi Y, Kozakai S, Ukai I, et al. Lipopolysaccharide (LPS)-binding protein stimulates CD14-dependent toll-like receptor 4 internalization and LPS-induced TBK1-IKKe-IRF3 axis activation. *J Biol Chem* (2018) 293:10186–201. doi: 10.1074/jbc.M117.796631
65. Labadie K, Larcher T, Joubert C, Mannioui A, Delache B, Brochard P, et al. Chikungunya disease in nonhuman primates involves long-term viral persistence in macrophages. *J Clin Invest* (2010) 120:894–906. doi: 10.1172/JCI40104
66. Kumar S, Jaffar-Bandjee M-C, Giry C, Connen de Kerillis L, Merits A, Gasque P, et al. Mouse macrophage innate immune response to chikungunya virus infection. *Virol J* (2012) 9:313. doi: 10.1186/1743-422X-9-313

67. Gardner J, Anraku I, Le TT, Larcher T, Major L, Roques P, et al. Chikungunya virus arthritis in adult wild-type mice. *J Virol* (2010) 84:8021–32. doi: 10.1128/JVI.02603-09
68. Hoarau J-J, Jaffar Bandjee M-C, Krejbich Trotot P, Das T, Li-Pat-Yuen G, Dassa B, et al. Persistent chronic inflammation and infection by chikungunya arthritogenic alphavirus in spite of a robust host immune response. *J Immunol* (2010) 184:5914–27. doi: 10.4049/jimmunol.0900255
69. Rice TW, Wheeler AP, Bernard GR, Vincent J-L, Angus DC, Aikawa N, et al. A randomized, double-blind, placebo-controlled trial of TAK-242 for the treatment of severe sepsis*. *Crit Care Med* (2010) 38:1685–94. doi: 10.1097/CCM.0b013e3181e7c5c9
70. Shirato K, Kizaki T. SARS-CoV-2 spike protein S1 subunit induces pro-inflammatory responses via toll-like receptor 4 signaling in murine and human macrophages. *Heliyon* (2021) 7:e06187. doi: 10.1016/j.heliyon.2021.e06187

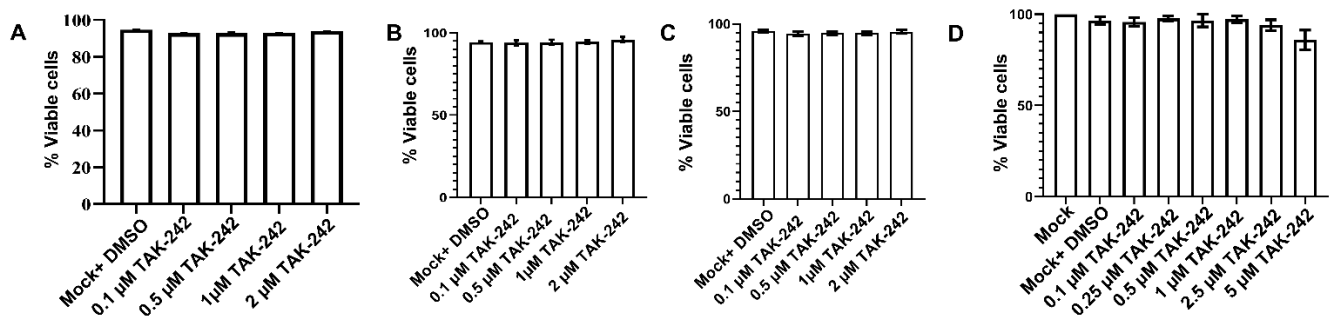


Figure S1: Determination of working concentration of TAK-242 in different host macrophages. (A, B and C) represents Annexin V-7AAD based viability assay in RAW 264.7, C57BL/6 and BALB/c derived peritoneal macrophages, respectively, which is showing > 95% viable cells at 1 μ M concentration. (D) represents MTT assay-based cell viability assay in hPBMC-derived monocyte-macrophage population where >95% cells are viable at 1 μ M.

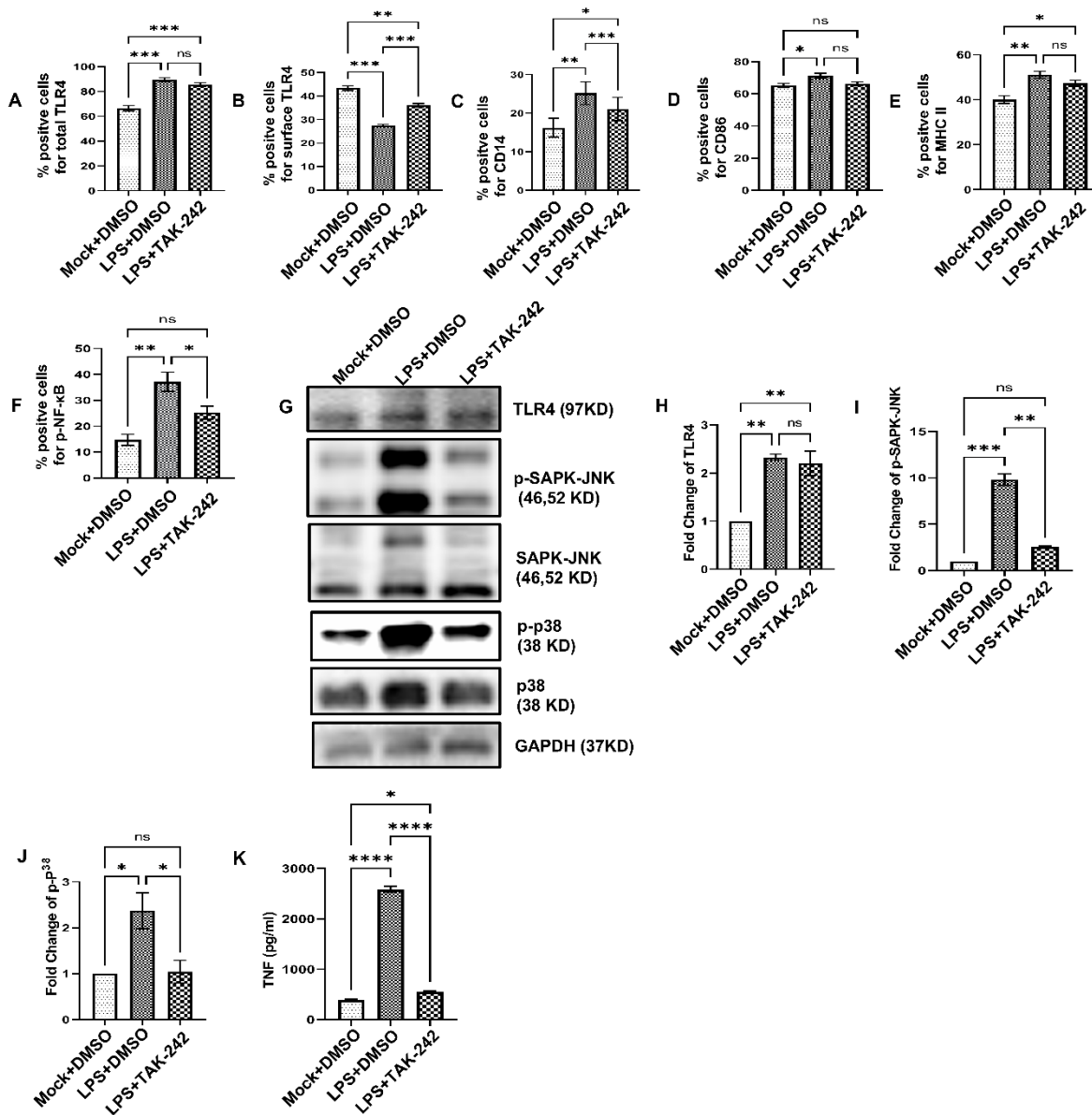


Figure S2: TLR4 inhibition lowers LPS-induced pro-inflammatory responses in RAW264.7 macrophage cells, *in vitro*. The RAW264.7 cells were treated with either DMSO or TAK-242 for 3 h before LPS treatment. LPS treatment was given to the above conditions for 6 h at 1 $\mu\text{g/ml}$ concentration followed by cell harvest. The bar diagrams showing flow cytometry dot plot analysis based on % positive cells for (A) total TLR4, (B) Surface TLR4, (C) CD14, (D) CD86 (E) MHC-II and (F) p-NF- κ B. The cells were also subjected to Western blot analysis to show (G, H) TLR4, (G, I) p-SAPK-JNK and (G, J) p-p38 expression. All of the proteins were normalized against GAPDH. (K) The cell culture supernatants were used for ELISA-based cytokine analysis to show secretory TNF levels. Data represent the Mean \pm SEM of three independent experiments. $p < 0.05$ was considered as a statistically significant difference between the groups (ns: non-significant, * $p < 0.05$; ** $p \leq 0.01$; *** $p \leq 0.001$; **** $p \leq 0.0001$).

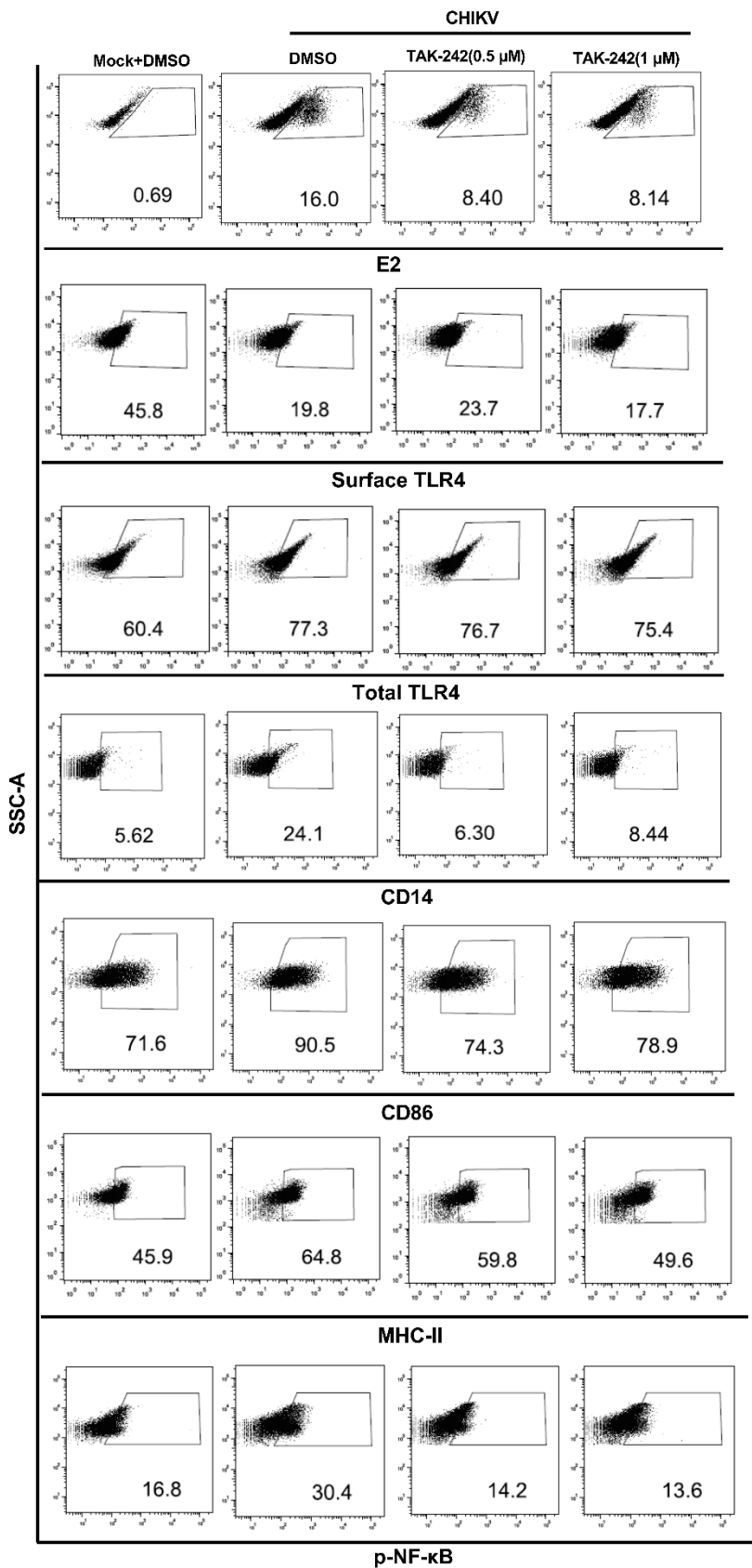


Figure S3: Representative flow cytometry dot plots denoting the percent positive cells for CHIKV-E2, surface TLR4, total TLR4, CD14, CD86, MHC-II and p-NF- κ B in the presence or absence of CHIKV and TAK-242 in RAW264.7 macrophage cells.

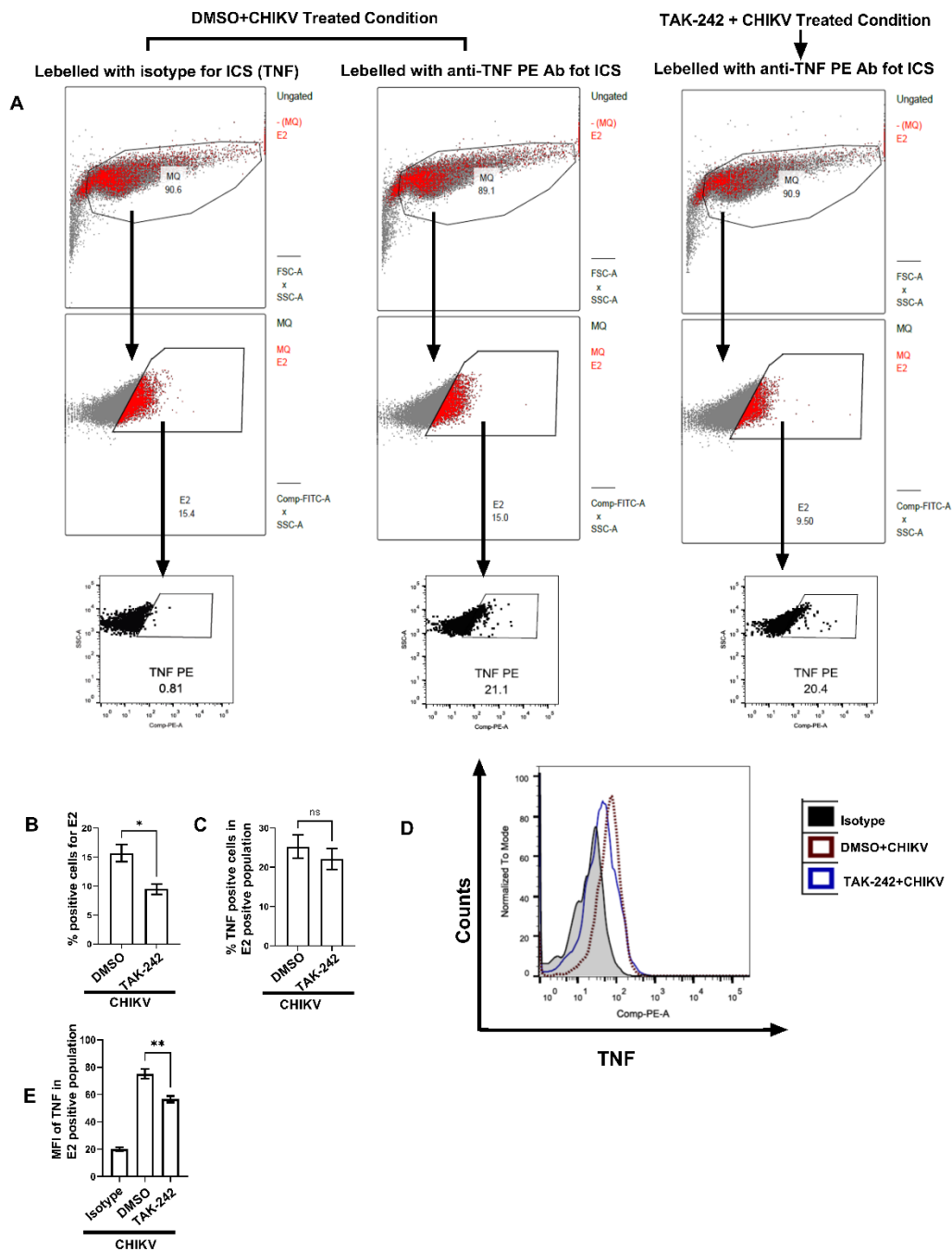


Figure S4: Pharmacological inhibition of TLR4 reduces CHIKV infection and associated proinflammatory response in RAW264.7 cells. ICS staining was performed to characterize the CHIKV-infected population in RAW264.7 cells. The cells were pre-treated with DMSO or TAK-242 3 h before infection. After 4 h post-infection, Golgistop was added to the cells and further incubated for another 4 h. Finally, the cells were harvested at 8 hpi. Dual intracellular staining for E2 and TNF was performed in harvested cells and analyzed via flow cytometry. From the scattered plot, a population devoid of debris was gated and demarcated as **MQ**. E2-positive cells were further gated in the **MQ** population. Furthermore, TNF positive cells were gated in the E2 positive population with respect to their isotype control (**A**) The scattered plots and E2 positive populations of isotype control, DMSO+ CHIKV and TAK-242+CHIKV were represented. Out of the E2-positive population, TNF-PE-positive cells were represented in above mentioned conditions. (**B**) The bar diagram represents % of E2-positive cells (**C**) The bar diagram depicts % of TNF-PE-positive cells within the E2-positive populations. (**D**) The MFI plot denotes the mean fluorescence intensity of TNF-PE positive cells. (**E**) The bar diagram indicates the MFI values of TNF-PE positive cells. The Data represent the mean \pm SEM of three independent experiments. $p < 0.05$ was considered as a statistically significant difference between the groups (ns: non-significant, * $p < 0.05$; ** $p \leq 0.01$).

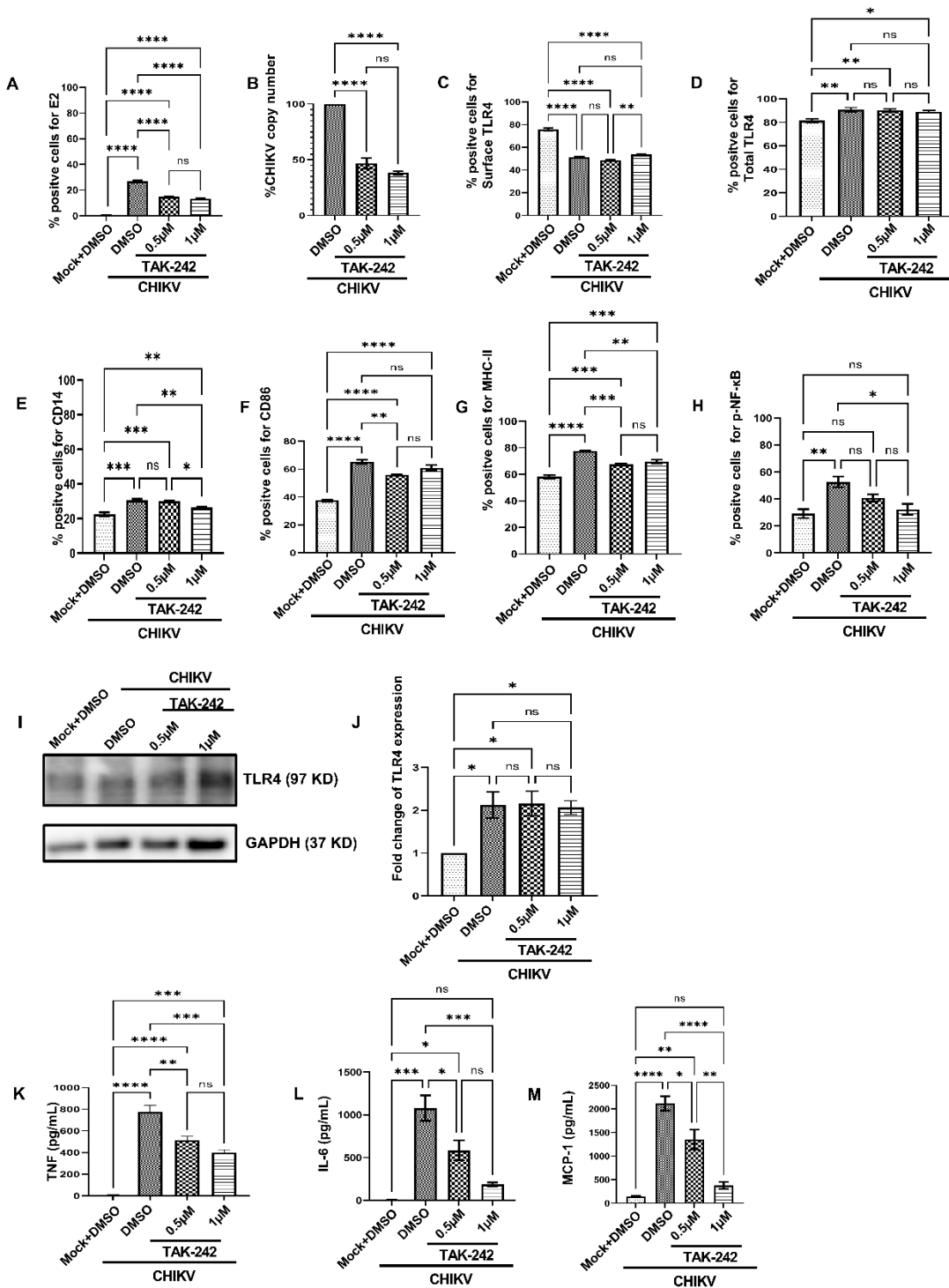


Figure S5: TAK-242 directed TLR4 inhibition reduces CHIKV infection and pro-inflammatory responses in BALB/c derived peritoneal monocyte-macrophage populations, *in vitro*. The cells were either pre-treated with DMSO or TAK-242 for 3 h before CHIKV infection. CHIKV infection was given at 5 MOI for 2 h followed by the cells were harvested at 8 hpi. (A) The bar diagram represents flow cytometry dot plot analysis derived percent positive cells for CHIKV-E2. (B) q-RT PCR-based analysis representing CHIKV copy numbers. The bar diagrams represent flow cytometry dot plot analysis-based percent positive cells for (C) surface TLR4, (D) Total TLR4, (E) CD14, (F) CD86 (G) MHC-II and (H) p-NF-κB, respectively. (I, J) Western blot analysis showing TLR4 level and the densitometric analysis normalized against GAPDH, respectively. (K-M) ELISA-based cytokine analysis showing differential expression of TNF-α, IL-6 and MCP-1, respectively. Data represent the Mean ± SEM of three independent experiments. $p < 0.05$ was considered as a statistically significant difference between the groups (ns: non-significant, * $p < 0.05$; ** $p \leq 0.01$; *** $p \leq 0.001$; **** $p \leq 0.0001$).

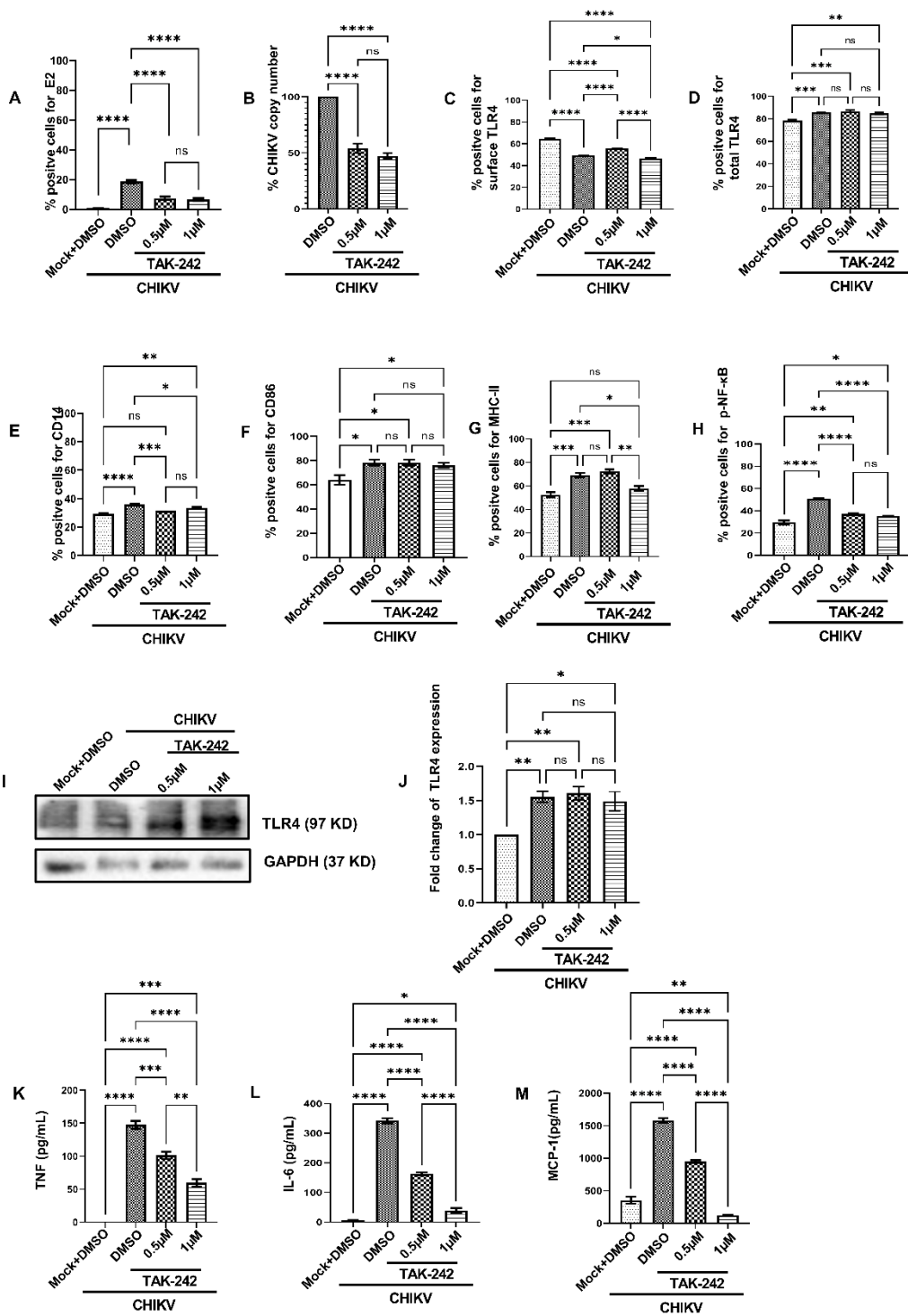


Figure S6: TAK-242 directed TLR4 inhibition reduces CHIKV infection and pro-inflammatory responses in C57BL/6 derived peritoneal monocyte-macrophage populations, *in vitro*. The cells were either pre-treated with DMSO or TAK-242 for 3 h before CHIKV infection. CHIKV infection was given at 5 MOI for 2 h followed by cells were harvested at 8 hpi. (A) The bar diagram represents flow cytometry dot plot analysis derived percent positive cells for CHIKV-E2. (B) q-RT PCR-based analysis representing CHIKV copy numbers. The bar diagrams represent flow cytometry dot plot analysis-based percent positive cells for (C) surface TLR4, (D) Total TLR4, (E) CD14, (F) CD86 (G) MHC-II and (H) p-NF-κB, respectively. (I, J) Western blot analysis showing TLR4 level and the densitometric analysis normalized against GAPDH, respectively. (K-M) ELISA-based cytokine analysis showing differential expression of TNF-α, IL-6 and MCP-1, respectively. Data represent the Mean ± SEM of three independent experiments. $p < 0.05$ was considered as a statistically significant difference between the groups (ns: non-significant, * $p < 0.05$; ** $p \leq 0.01$; *** $p \leq 0.001$; **** $p \leq 0.0001$).

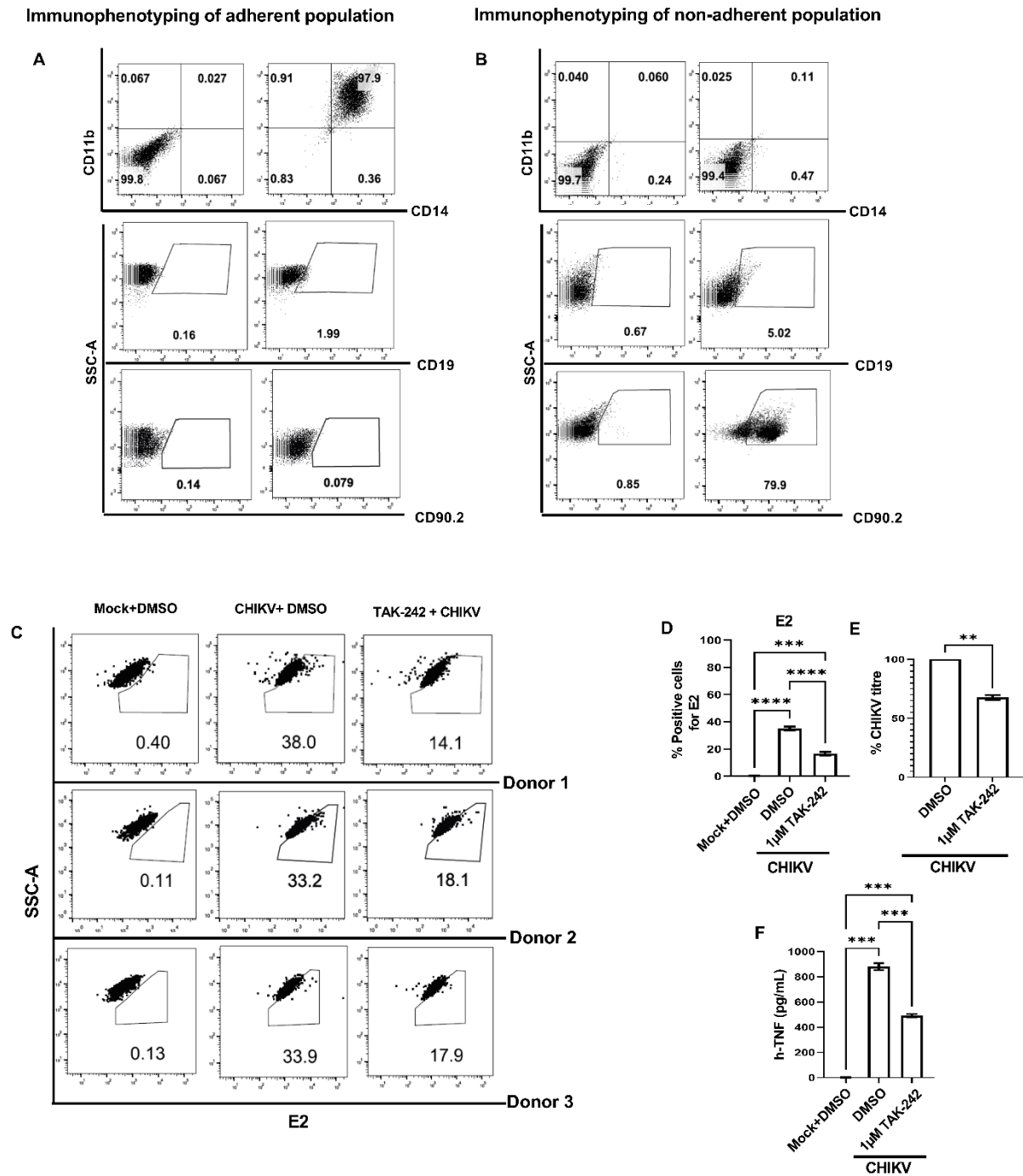


Figure S7: TAK-242 directed TLR4 inhibition decreases CHIKV infection and pro-inflammatory responses in hPBMC-derived monocyte-macrophage populations, *in vitro*. The hPBMC-derived adherent monocyte-macrophage cells were either pre-treated with DMSO or TAK-242 for 3 h prior CHIKV infection. The CHIKV infection was given at 5 MOI for 2 h followed by cells were harvested at 8 hpi. (A, B) The flow cytometry-based immunophenotyping analysis of adherent and non-adherent populations of the hPBMC-derived myeloid cells. (C, D) The flow cytometry dot plot analysis showing percent E2 positive cells under differential conditions. (E) Plaque assay-based % CHIKV titre analysis showing viral titre in the presence and absence of TAK-242. (F) Cytokine ELISA analysis showing differential h-TNF expression. Data representing Mean \pm SEM of three independent experiments with $p < 0.05$ was considered as a statistically significant difference between the groups (ns: non-significant, * $p < 0.05$; ** $p \leq 0.01$; *** $p \leq 0.001$; **** $p \leq 0.0001$).



P38 and JNK Mitogen-Activated Protein Kinases Interact With Chikungunya Virus Non-structural Protein-2 and Regulate TNF Induction During Viral Infection in Macrophages

OPEN ACCESS

Edited by:

Constantinos Petrovas,
Vaccine Research Center (NIAID),
United States

Reviewed by:

Shinya Suzu,
Kumamoto University, Japan
Lucio Gama,
Johns Hopkins Medicine,
United States

*Correspondence:

Subhasis Chattopadhyay
subho@niser.ac.in

† Present Address:

Tapas Kumar Nayak,
Infectious Disease Biology, Institute of
Life Sciences (ILS), Bhubaneswar,
India

Specialty section:

This article was submitted to
Viral Immunology,
a section of the journal
Frontiers in Immunology

Received: 29 November 2018

Accepted: 25 March 2019

Published: 12 April 2019

Citation:

Nayak TK, Mamidi P, Sahoo SS,
Kumar PS, Mahish C, Chatterjee S,
Subudhi BB, Chattopadhyay S and
Chattopadhyay S (2019) P38 and JNK
Mitogen-Activated Protein Kinases
Interact With Chikungunya Virus
Non-structural Protein-2 and Regulate
TNF Induction During Viral Infection in
Macrophages.
Front. Immunol. 10:786.
doi: 10.3389/fimmu.2019.00786

Tapas Kumar Nayak^{1†}, Prabhudutta Mamidi², Subhransu Sekhar Sahoo¹,
P. Sanjai Kumar¹, Chandan Mahish¹, Sanchari Chatterjee², Bharat Bhusan Subudhi³,
Soma Chattopadhyay² and Subhasis Chattopadhyay^{1*}

¹ School of Biological Sciences, National Institute of Science Education and Research, HBNI, Bhubaneswar, India, ² Infectious Disease Biology, Institute of Life Sciences, Bhubaneswar, India, ³ School of Pharmaceutical Sciences, Siksha O Anusandhan University, Bhubaneswar, India

Chikungunya virus (CHIKV), a mosquito-borne Alphavirus, is endemic in different parts of the globe. The host macrophages are identified as the major cellular reservoirs of CHIKV during infection and this virus triggers robust TNF production in the host macrophages, which might be a key mediator of virus induced inflammation. However, the molecular mechanism underneath TNF induction is not understood yet. Accordingly, the Raw264.7 cells, a mouse macrophage cell line, were infected with CHIKV to address the above-mentioned question. It was observed that CHIKV induces both p38 and JNK phosphorylation in macrophages in a time-dependent manner and p-p38 inhibitor, SB203580 is effective in reducing infection even at lower concentration as compared to the p-JNK inhibitor, SP600125. However, inhibition of p-p38 and p-JNK decreased CHIKV induced TNF production in the host macrophages. Moreover, CHIKV induced macrophage derived TNF was found to facilitate TCR driven T cell activation. Additionally, it was noticed that the expressions of key transcription factors involved mainly in antiviral responses (p-IRF3) and TNF production (p-c-jun) were induced significantly in the CHIKV infected macrophages as compared to the corresponding mock cells. Further, it was demonstrated that CHIKV mediated TNF production in the macrophages is dependent on p38 and JNK MAPK pathways linking p-c-jun transcription factor. Interestingly, it was found that CHIKV nsP2 interacts with both p-p38 and p-JNK MAPKs in the macrophages. This observation was supported by the *in silico* protein-protein docking analysis which illustrates the specific amino acids responsible for the nsP2-MAPKs interactions. A strong polar interaction was predicted between Thr-180 (within the phosphorylation lip) of p38 and Gln-273 of nsP2, whereas, no such polar interaction was predicted for the phosphorylation lip of JNK which indicates the differential roles of p-p38 and p-JNK during CHIKV infection in the host macrophages. In summary, for the first time it has

been shown that CHIKV triggers robust TNF production in the host macrophages via both p-p38 and p-JNK/p-c-jun pathways and the interaction of viral protein, nsP2 with these MAPKs during infection. Hence, this information might shed light in rationale-based drug designing strategies toward a possible control measure of CHIKV infection in future.

Keywords: Chikungunya, Alphavirus, MAPK, Macrophages, TNF, p38, JNK, c-jun

INTRODUCTION

Chikungunya virus (CHIKV), a mosquito-borne Alphavirus belongs to *Togaviridae* family, is transmitted through either *Aedes aegypti* or *Aedes albopictus* mosquito. CHIKV mediated disease is one of the global challenges due to its endemics in different parts of the world (103 countries), such as Tanzania (1–3), Reunion island (4–7), India (8–12), Italy (13, 14), and Thailand (15–18). Among Alphaviruses, CHIKV is considered as one of the most successfully evolved virus. The Arboviruses including CHIKV have been evolving and re-emerging from centuries and their emergence and dispersion are more rapid and geographically extensive. This might be due to increase in global communication, mass immigration, vector adaptation to urbanization and land perturbation (19). Even though mortality due to CHIKV is very rare and restricted to children's (below 1 year), old age (above 65 years) or immune compromised patients, the pathogenesis (mainly inflammatory responses) may persist for very long periods of time both in humans and macaque model (20, 21). Currently, arboviruses raise a serious threat to the global public health, due to unavailability of effective drugs or vaccines (22, 23).

Recent studies on CHIKV induced immune responses suggest that the host immune system is found to be both beneficiary in one hand by controlling viral infection, whereas deleterious on the other hand by promoting severe inflammatory responses (24–28). Studies have shown that CHIKV induces different inflammatory cytokines/chemokines (TNF, IL-1 β , IL-6, IFN- γ , IL-8, and MCP-1) (24, 29–37), which might be associated with arthritis like pathogenesis during CHIKV infection. In different *in vivo* systems (both mouse and non-human primates), predominant cellular infiltration of macrophages, monocytes, NK cells and T cells to the site of inoculation and other tissues have been observed (38, 39). Moreover, immunohistochemistry and flow cytometry based analysis of muscles and synovial biopsies revealed that macrophages are major infiltrating cells among MPS (mononuclear phagocytic system) (25, 40). Blood monocytes and tissue macrophages are the major immune cells infected by CHIKV (21, 31, 41). In macaque, synovial macrophages have been identified as the major host cell for long-term viral persistence (21). This productive infection of CHIKV in the host macrophages might be associated with arthritis like pathogenesis despite robust immune activation (41, 42).

T cell immune responses specific to CHIKV is not clearly understood yet. Teo TH et al. have suggested that CD4⁺ T cells (but not CD8⁺ T cells) are essential for the development of CHIKV induced pathogenesis without affecting virus infection and dissemination in mice and this is independent of IFN- γ (43). Flow cytometry based analysis of circulating lymphocytes in CHIKV patients confirms that there are both CD4⁺ and

CD8⁺ T cell responses during early and late phases of infection, respectively. Moreover, CD95 mediated apoptosis was also detected in CD4⁺ T cells after 2 days of symptom appearance (44), which might be one of the strategies to evade host immunity. Purified T cells (both CD4⁺ and CD8⁺) from the chronic and recovered patients from 2005 to 2006 La Reunion islands showed immune activation when challenged with synthetic CHIKV peptides and inactivated virus particles (42). The DNA vaccine based on the consensus sequences of E1/2 and capsid protein (with several modifications) of CHIKV resulted in robust IFN- γ and IgG production suggesting that CHIKV induces both T and B cell specific responses (45, 46).

There are three major studied ser/thr kinases under the mitogen-activated protein kinase (MAPK) family, such as p38, JNK, and ERK, which are known to regulate multiple cellular pathways such as cell proliferation, activation, inflammation, cytokine and chemokine productions and different pathological conditions (47–53). In addition, activation of MAPKs by different pathogens and other inflammatory diseases have been reported to induce pro-inflammatory cytokines such as TNF in the host cells (48–51, 53, 54). The MAPKs have been shown to be activated by phosphorylation in specific positions (Ser/Tyr/Thr) by several viral infections, such as coronavirus type 2, Hepatitis C virus, Rhinovirus and Epstein-Barr virus (54–58). CHIKV is also known to induce MAPKs during infection in various non-immune cells and treatment of an alkaloid berberine, reduces viral infection and joint swelling in mice (59, 60).

We have shown earlier that CHIKV triggers robust TNF production in the host macrophages, which might be a key mediator of virus induced inflammation (37) and macrophages are identified as the major cellular reservoirs during the late stages of CHIKV infection in macaques (21). However, the precise role of MAPK activation pathways in terms of CHIKV infection and associated robust TNF induction in macrophages (immune cell) remains largely unknown. Hence, an attempt was made to understand the involvement of MAPKs in CHIKV infection and TNF induction in the host macrophages.

MATERIALS AND METHODS

Cells and Viruses

DRDE-06 (accession no. EF210157.2), an Indian outbreak strain of CHIKV and Vero cells (African green monkey kidney epithelial cell line) were kind gifts from Dr. M. M. Parida, DRDE, Gwalior, India. The mouse monocyte/macrophage cell line, Raw264.7 (ATCC[®] TIB-71[™]) was maintained in RPMI-1640 (HiGlutaXL[™] RPMI-1640) supplemented with 2.0 mM L-glutamine, Penicillin 100 U/ml, Streptomycin 0.1 mg/ml (Himedia Laboratories Pvt. Ltd, MH, India), 10% Fetal bovine

serum (FBS; PAN Biotech, Germany) at 37°C under a humidified incubator with 5% CO₂. The Vero cells were maintained in Dulbecco's modified Eagle's medium (DMEM; PAN Biotech, Germany) supplemented with 5% FBS, Gentamycin (Sigma-Aldrich, MO, USA). The enzyme-free cell dissociation reagent (ZymeFree™; Himedia Laboratories Pvt. Ltd, MH, India) was used for the maintenance of the Raw264.7 cells.

Eight to ten weeks old male or female BALB/c mice were used for this experiment. The animals used in these experiments were approved by Institutional Animal Ethics Committee, NISER and followed the guidelines by Committee for the Purpose of Control and Supervision of Experiments on Animals (CPCSEA).

Antibodies and Reagents

The mouse anti-CHIKV-nsP2 antibody used in the current study was developed by us (61). Anti-mouse CD3 antibody, anti-TNF antibody, anti-CD69 FITC, HRP linked anti-mouse, and HRP linked anti-rabbit secondary antibodies were purchased from BD Biosciences (CA, USA). Anti-mouse CD28 and CD90.2 APC were procured from Tonbo Biosciences (CA, USA). The monoclonal antibodies for p38, p-p38, JNK, p-JNK, ERK1/2, p-ERK1/2, p-IRF3, and p-c-jun were purchased from cell signaling technology (MA, USA). The anti-mouse Alexa Fluor 488 and anti-rabbit Alexa Fluor 647 were purchased from Invitrogen (CA, USA). The rabbit polyclonal antibodies against p-p38 and p-JNK used for immunoprecipitation were purchased from Santa Cruz biotechnology (TX, USA). Mouse IgG, rabbit IgG isotype control, and anti-GAPDH antibody were purchased from Abgenex India Pvt. Ltd (OD, India). Saponin and Bovine serum albumin fraction V were purchased from Sigma-Aldrich (MO, USA). SB203580 (p-p38 inhibitor, SB), and SP600125 (p-JNK inhibitor, SP) were purchased from Merck Millipore (MA, USA).

MTT Assay

MTT assay was performed to assess the cytotoxicity of SB and SP according to the methods described before (37). Briefly, the Raw264.7 cells were seeded in 96 well plates at a density of 5×10^3 cells per well before 18–20 h of drug treatment. Then, the cells were washed in 1X PBS and incubated with different concentrations of drugs in triplicate. As both SB and SP were dissolved in the Dimethyl Sulfoxide (DMSO), it was taken as solvent control. After 12 h, the cells were incubated with the MTT reagent to a final concentration of 10% (v/v) in RPMI media. Then, the cells were placed in the incubator for upto 2 h for the formation of visible crystals. Later, the media (containing MTT) were removed without disturbing the cells and 100 µl of solubilization solution was added per well followed by incubation for 15 min at room temperature (RT). The percent viable cells were calculated after taking the absorbance of the solution at 550 nm by Microplate Reader (Bio-Rad, CA, USA).

CHIKV Infection in Macrophage

Raw 264.7 cell line has been well-reported to study CHIKV infection, replication and associated altered host immune

responses (31, 37). The Raw264.7 cells were seeded in six-well cell culture plates before 18–20 h of infection with around 70% confluency. The cells were infected with the DRDE-06 strain of CHIKV with multiplicity of infection (MOI) 5 as reported previously (37). Briefly, after washing the cells in 1X PBS, the virus was added over confluent monolayer for 2 h in the incubator with manual shaking at an interval of 15 min. Then, the virus inoculum was washed in 1X PBS to remove unbound viruses and the cells were maintained in the complete RPMI-1640 media. The infected cells and the supernatants were collected at different time points and subjected to further processing according to the assay.

SB and SP treatments were given as described before (62). Briefly, cells were pretreated with the desired concentrations of SB, SP or DMSO for 2 h in serum free media (SFM). Then the infection was carried out in the presence of either solvent control (DMSO), SB or SP. The cells were washed thoroughly with 1X PBS after 2 h and cultured in SFM containing the drug for 3 h. Then, serum was added to the cells and maintained in the incubator until harvesting (37).

Plaque Assay

Viral plaque assay was performed to determine the titer of CHIKV as described previously (10). In brief, after infecting the Vero cells with different dilutions of cell culture supernatants (collected from CHIKV infected Raw cells), the cells were overlaid with complete DMEM containing methyl cellulose and maintained in the incubator. After the development of the visible plaques (usually 4–5 days), the cells were fixed in formaldehyde at room temperature, washed gently in tap water and stained with crystal violet. Then, the numbers of plaques were counted manually under white light.

Flow Cytometry (FC)

Flow cytometric assay was carried out as reported previously (37). Briefly, both mock and CHIKV infected Raw264.7 cells were harvested and fixed in 4% paraformaldehyde for 10 min at RT. Then, the cells were re-suspended in FACS buffer and stored at 4°C until staining. For intracellular staining (ICS), the cells were permeabilized in freshly prepared 1X permeabilization buffer followed by blocking buffer (1% BSA in permeabilization buffer) for 30 min at RT. Then, the cells were incubated with different primary antibodies for 30 min at RT, followed by washing with 1X permeabilization buffer twice. After that, the cells were incubated in Alexa Fluor® 488 and Alexa Fluor® 647 conjugated secondary antibodies followed by washing with 1X permeabilization buffer. The mouse IgG and rabbit IgG were taken as isotype control during ICS. The FcR blocking reagent (Miltenyi Biotec, Bergisch Gladbach, Germany) was used prior to the primary antibody incubation to prevent non-specific binding of antibodies to the Fc receptors on macrophages. Then, the cells were acquired by the BD FACS Calibur™ flow cytometer (BD Biosciences, CA, USA) and analyzed by the CellQuest Pro software (BD Biosciences, CA, USA). A total of approximately 10×10^3 cells were acquired per sample.

Sandwich ELISA for Cytokine Analysis

TNF production from the macrophage cell culture supernatants was quantified by the BD OptEIA™ sandwich ELISA kit (BD Biosciences, CA, USA) according to the manufacturer's instructions (37). The cytokine concentrations in the test samples were calculated in comparison with the corresponding standard curve prepared by using different concentrations of the recombinant TNF in pg/ml.

Western Blot Analysis

Western blot analysis was performed to assess the levels of different protein expressions according to the protocol mentioned before (37). In brief, both the mock and CHIKV infected cells were washed with ice-cold 1X PBS and the whole cell lysate (WCL) was prepared by Radio Immuno Precipitation Assay (RIPA) lysis buffer. The protein concentration was quantified by the Bradford reagent (Sigma-Aldrich, MO, USA). Equal amount of protein was loaded in the 10% SDS-PAGE after mixing with 2X Laemmli buffer (1:1) and blotted on to a PVDF membrane (Millipore, MA, USA). Then the transferred membranes were blocked with 3% BSA followed by overnight incubation with different primary antibodies. Then, the membranes were thoroughly washed with TBST and incubated with the HRP conjugated secondary antibodies for 2 h at RT. After washing with TBST, the blots were subjected to chemiluminescence detection by the Bio-Rad gel doc with the Quantity One software (Bio-Rad, CA, USA). For band intensity quantification, Western blot images were subjected to further analysis by the Quantity One 1-D analysis software while normalizing to the corresponding GAPDH loading control.

Co-immunoprecipitation

Raw cells were infected with CHIKV as described above and harvested at 6 hpi. The cells were lysed with NP-40 (Nonidet P-40) lysis buffer (250 mM NaCl, 5 mM EDTA, 10% glycerol, 1% NP-40, 50 mM Tris, pH 7.4, supplemented with protease inhibitor and phosphatase inhibitor cocktail). The resultant whole cell lysates were subjected to immunoprecipitation by Immunoprecipitation Kit Dynabeads® Protein A (Thermo Fisher Scientific, MA, USA) according to the manufacturer's instructions. Briefly, both the mock and CHIKV infected whole cell lysates were incubated with primary antibodies overnight on the vertical rotor at 4°C. Then, 30 µl of dynabeads® protein A was added to the cell lysate and incubated for another 4 h on the vertical rotor at 4°C. The Dynabeads®-Ab-Ag complexes were washed three times in lysis buffer followed by elution with elution buffer supplied in the kit. Then, the eluted complexes were re-suspended in 4X Laemmli buffer, boiled at 90°C for 10 min and processed further for Western blot analysis as described above.

Protein-Protein Docking Studies

The protein-protein docking was performed using the ClusPro 2.0 webserver (63, 64). This server performs three computational steps. In the first step, it does rigid-body docking using the PIPER. This docking program is based on the Fast Fourier Transform (FFT) correlation approach and uses pairwise interaction potential as part of its scoring function $E = w1E_{rep} +$

$w2E_{attr} + w3E_{elec} + w4EDARS$. While E_{rep} and E_{attr} represent the repulsive and attractive contributions, E_{elec} denotes electrostatic energy term and EDARS refers to the pairwise structure-based potential (64, 65). In the second step, 1,000 lowest energy docked structures are clustered using pairwise interface RMSD (IRMSD) (64, 66). Based on the IRMSD values the structure with the highest neighbors within a 9 Å radius is defined as the center of the first cluster. Further clustering is performed within the remaining structures to generate 30 clusters. The energy minimization is done for the structures using the van der Waals terms of the CHARMM potential in the third step (64, 67), following which the structures at the center of the 10 most populated clusters are taken as the output. Since there was no satisfactory template available in PDB to build the homologous model of nsP2, the structure was generated earlier using the I-TASSER algorithm (68). This was used as a ligand in the study. X-ray crystallographic structures of JNK1 (PDB ID: 3ELJ) and p38 (PDB ID: 1A9U) were taken as receptors for the protein-protein docking. These structures were recovered from the protein data bank. The co-crystallized ligands were extracted and energy was minimized before submission of chain A of these structures as receptors. The output of docking generated four types of models using the scoring algorithms designated as balanced, electrostatic-favored, hydrophobic-favored, and van der waals+electrostatic. Amongst these, the balanced outputs were analyzed. The docking solution with largest members was taken for further visualization using the PyMol software.

TCR Driven T Cell Activation Assay

Mouse splenocytes isolation and splenic T cell purification from BALB/c mice were performed as reported earlier (69). In brief, using a 70 µM cell strainer the splenocytes were collected from mice spleens. After RBC lysis and washing with 1X PBS, cells were suspended in RPMI-1640 media supplemented with 10% FBS. According to instructions given by the manufacturer's protocol, mouse splenic T cell purification was carried out using Dynabeads Untouched Mouse T Cells Kit (Invitrogen, CA, USA). TCR driven T cell activation was carried out with those purified T cells (CD90.2⁺) in the presence of either CHIKV infected or uninfected (mock) macrophage culture supernatants (0.22 µM membrane filtered) to study the status of CD69 (a T cell activation marker) as described earlier for other infection model (70). For TNF neutralization, anti-TNF purified antibody (BD Bioscience) was incubated for 90 min with the CHIKV infected supernatant prior TCR stimulation.

Statistical Analysis

Statistical analysis was performed by using the GraphPad Prism 5.0 software (GraphPad Software Inc. USA). Data were represented as Mean ± SEM. The comparison between the groups was performed by either one- or two-way ANOVA with Tukey or Bonferroni *post-hoc* test, respectively. Data presented here were representative of at least three independent experiments. $p < 0.05$ was considered as statistically significant difference between the groups.

RESULTS

CHIKV Induces Both p38 and JNK Phosphorylation in Macrophages in a Time-Dependent Manner

To determine whether any MAPK (p38, JNK, and ERK) is activated during CHIKV infection in macrophages, Raw cells were infected with the virus at MOI 5 and harvested at different time points (0–12 hpi). Both the cells and cell culture supernatants were subjected to various downstream assays. As shown in **Figure 1A**, the p-p38 and p-JNK expressions were increased significantly as compared to the corresponding mock cells. The p-p38 MAPK expression was found to be increased around 1.5-fold as early as 3 and 6 hpi, followed by approximately 3-fold increments toward 12 hpi as compared to the corresponding mock cells. Similarly, the expression of the p-JNK was found to be increased rapidly around 2-fold during early hours (3 and 6 hpi), whereas, it increased up to 3-fold with respect to the mock in later time points. The total p38 and JNK (t-p38 and t-JNK) expressions remain unaffected in both the groups. Moreover, p-ERK1/2 and t-ERK1/2 (total-ERK1/2) expressions remain unchanged throughout all the time points as compared to the corresponding mock (**Figures 1A,B**). This data suggests that CHIKV induces activation of both p38 and JNK by phosphorylation in a time-dependent manner in macrophages.

SB203580 Treatment Reduces CHIKV Infection in Macrophages

Since CHIKV induces both p38 and JNK activation in the host macrophages, next we sought to assess whether these two MAPKs are crucial for the viral infection and replication in the macrophages. For that, pharmaceutical inhibitors of p38 (SB203580) and JNK (SP600125) were used. First, different concentrations of both SB (0.1, 0.5 and 1.5 μM) and SP (1, 5 and 10 μM) were assessed for cytotoxicity in Raw cells by MTT assay. It was observed that around 100% cells were viable in all the concentrations of SB, whereas up to 95 and 100% cells were found to be viable at 10 and 5 μM concentrations of SP, respectively (**Figures 2A,E**). Thus, both 5 and 10 μM concentrations of SP were selected for further experiments. As SB treatment with $>2 \mu\text{M}$ concentration was known to inhibit phosphorylation and activation of PKB non-specifically (71), both 0.5 and 1.5 μM concentrations of SB was used in the current study.

Raw cells were inoculated with CHIKV in the presence of SB, SP, or solvent control DMSO as described above. At 12 hpi both mock and CHIKV infected cells were harvested and the expressions of nsP2, p-p38, and p-JNK were assessed by Flow cytometry. It was observed that the percent positive cells for nsP2 were reduced from 8.19 ± 0.35 (CHIKV+DMSO) to 2.50 ± 0.08 (CHIKV+SB 0.5 μM) and 1.36 ± 0.02 (CHIKV+SB 1.5 μM), whereas the percent positive cells for p-p38 were reduced from 8.05 ± 0.73 (CHIKV+DMSO) to 1.31 ± 0.15 (CHIKV+SB 0.5 μM) and 0.46 ± 0.04 (CHIKV+SB 1.5 μM) (**Figures 2B,C**). Likewise, the MFI for both the p-p38 and nsP2 were reduced at 12 hpi in the SB treated cells as compared to the DMSO control (**Figure 2D**). The inhibition of p-JNK by SP at 5.0 μM

concentration did not affect nsP2 expression in the macrophages as compared to the DMSO control (CHIKV+DMSO; 7.63 ± 0.40 , CHIKV+SP 5 μM ; 7.21 ± 0.17 , $p > 0.05$), despite significant reduction in the p-JNK percent positive cells (CHIKV+DMSO; 6.08 ± 0.40 , CHIKV+SP; 3.31 ± 0.75 , $p < 0.05$). However, SP at the comparatively higher concentration (10 μM) did reduce nsP2 expression by around 1.5-fold (**Figures 2F–H**). Further, plaque assay of the cell culture supernatants revealed that SB treatment reduces the number of new viral progeny release around 1.5- and 2.5-fold at 0.5 and 1.5 μM , respectively. Whereas, SP at 10 μM concentration treatment reduces the number of new viral progeny release around 1.6-fold as compared to the corresponding DMSO control (**Figure 2I**). This result indicates that the activation of both p38 and JNK MAPKs might be crucial for the CHIKV infection and replication in the host macrophages with SB being more effective comparatively in controlling infection than SP.

Pharmaceutical Inhibitors Specific to p-p38 and p-JNK Reduces CHIKV Induced TNF Production in the Host Macrophages

Activation of MAPKs by different pathogens has been shown to induce pro-inflammatory cytokines such as TNF in the host cells (50, 54). Since, CHIKV triggers robust TNF production (a key mediator of inflammation) in the host macrophages (31, 37), it was interesting to investigate whether any MAPKs are involved in this pathway. Accordingly, macrophages were treated with either SB or SP and infected with CHIKV as mentioned earlier. The cell culture supernatants were subjected to sandwich ELISA for the detection of TNF at early (6 hpi) and late (12 hpi) time post-infection. It was observed that both SB and SP could suppress CHIKV induced TNF significantly at both the time points as compared to the corresponding DMSO control. At 6 hpi the TNF level for CHIKV+DMSO was found to be 737 ± 27 pg/ml (mean \pm SEM), which was reduced to 466 ± 12 pg/ml (mean \pm SEM, $p < 0.05$) and 356 ± 20 pg/ml (mean \pm SEM, $p < 0.05$) in the presence of SB (1.5 μM) and SP (10.0 μM), respectively. Similarly, at 12 hpi, the TNF production was $1,104 \pm 29$ pg/ml (mean \pm SEM) in the CHIKV+DMSO sample, whereas it was reduced to 554 ± 28 pg/ml (mean \pm SEM, $p < 0.05$) for SB and 528 ± 25 pg/ml (mean \pm SEM, $p < 0.05$) for SP treatment (**Figure 3**). Taken together, this result suggests that CHIKV might induce TNF via p38 as well as JNK mediated pathways in the host macrophages.

CHIKV Induced TNF Facilitates TCR Driven T Cell Activation

TNF, one of the potent inflammatory cytokine, which can enhance TCR-dependent T cell activation (72). We and others have previously reported that *in vitro* CHIKV infection in RAW 264.7 cells leads to TNF production (31, 37). Recent studies have shown a pathogenic role of T cells during CHIKV infection associated to host inflammatory responses (43, 44, 46). Here we have investigated whether CHIKV infection induced macrophage derived TNF can facilitate mouse T cell activation associated with cell mediated immunity. For this, CHIKV infected culture

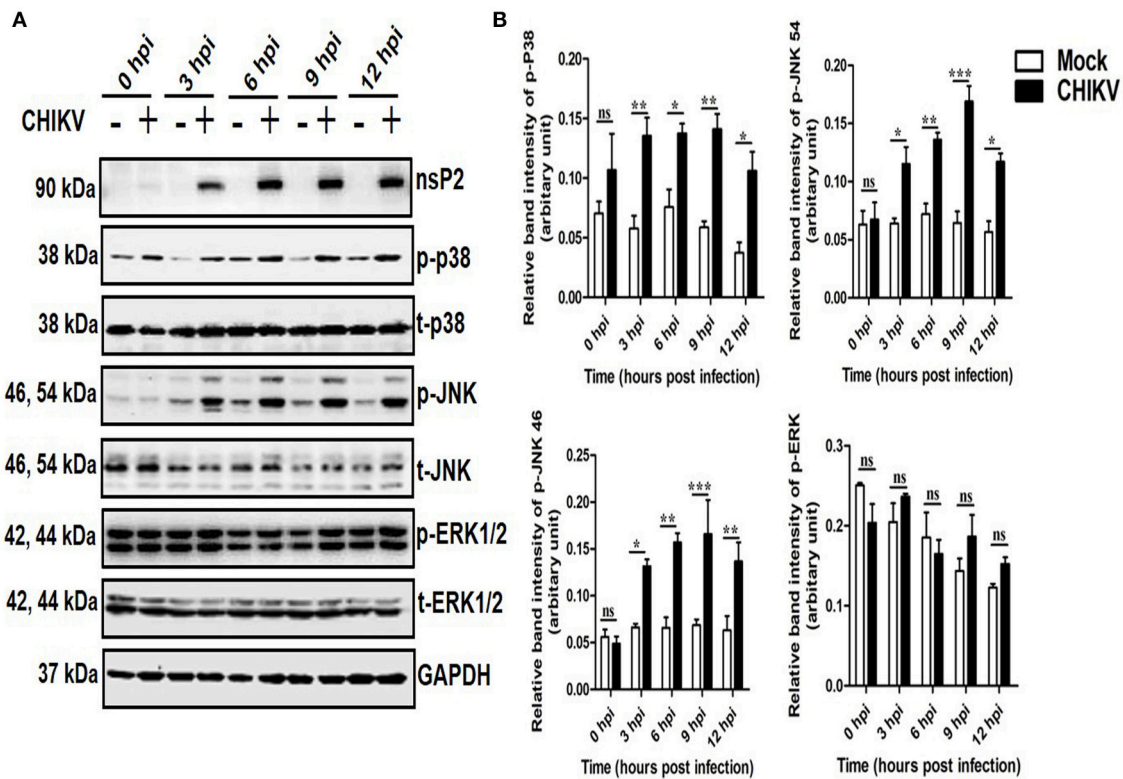


FIGURE 1 | Induction of p-p38 and p-JNK MAPK during CHIKV infection in macrophages. CHIKV infected Raw264.7 cells were harvested at different time intervals followed by Western blot analysis. **(A)** The protein expressions of nsP2, p-p38, t-p38, p-JNK, t-JNK, p-ERK1/2, and t-ERK1/2 were assessed by Western blot analysis. GAPDH was used as loading control. **(B)** Bar diagram showing relative band intensities of p-p38, p-JNK, and p-ERK1/2 at different time post-infection. Data represent mean \pm SEM of three independent experiments. $p < 0.05$ was considered as statistically significant difference between the groups. (ns, non-significant; * $p < 0.05$; ** $p \leq 0.01$; *** $p \leq 0.001$).

supernatant of RAW 264.7 cells were tested toward TCR driven resting T cell activation assay (69). We have found that CHIKV infected macrophage culture supernatant along with TCR activation facilitated the induction of CD69 level (around 81%) as compared to uninfected culture supernatant (around 71%). Interestingly, when the CHIKV infected macrophage culture supernatant was treated with TNF neutralizing antibody, a sharp decrease of CD69 frequency (around 63%) was observed. Beside this, SB and SP treated CHIKV infected Raw 264.7 culture supernatant along with TCR stimulation also showed downregulation of CD69 frequency in T cells (Figures 4A,B). So, the above observations may underscore that the TNF present in CHIKV infected culture supernatant might be able to facilitate the induction of T cell activation.

CHIKV Infection Induces Key Transcription Factors in the Host Macrophages

Often, the viral infection is associated with the activation and localization of several transcription factors (e.g., IRFs, c-jun, p53), which in turn regulates host responses to viruses (73–78). Here, the expressions of key transcription factors involved mainly in antiviral responses (p-IRF3) and TNF production (p-c-jun) were assessed at different hpi by Western blot analysis.

It was observed that both p-IRF3 and p-c-jun were induced significantly in the CHIKV infected macrophages as compared to the corresponding mock (Figures 5A,B). This data suggest that CHIKV infection in the Raw cell line might be associated with the elevation of key antiviral and inflammatory transcription factors.

CHIKV Induces p-c-Jun via JNK MAPK Activation in Macrophages

It has been reported previously that TNF is one of the key mediators for arthritis or arthritis-like diseases in humans by promoting severe inflammation. Although, several other inflammatory cytokines are elevated in RA (rheumatoid arthritis), anti-TNF therapy seems to be promising for the effective treatment against it (79). Since CHIKV induces TNF via p38/JNK MAP kinase pathways and phosphorylation of c-jun is reported to be associated with TNF production in other inflammatory model system (50, 80), phosphorylation of c-jun in both mock and CHIKV infected macrophages was assessed by Western blot analysis. Surprisingly, the expression of p-c-jun was reduced around 1.8- and 4.77-fold in the presence of SP at 5 and 10 μ M indicating a plausible role of JNK toward c-jun phosphorylation, whereas SB treatment at 1.5 μ M did not affect p-c-jun expression significantly. However, both SB and

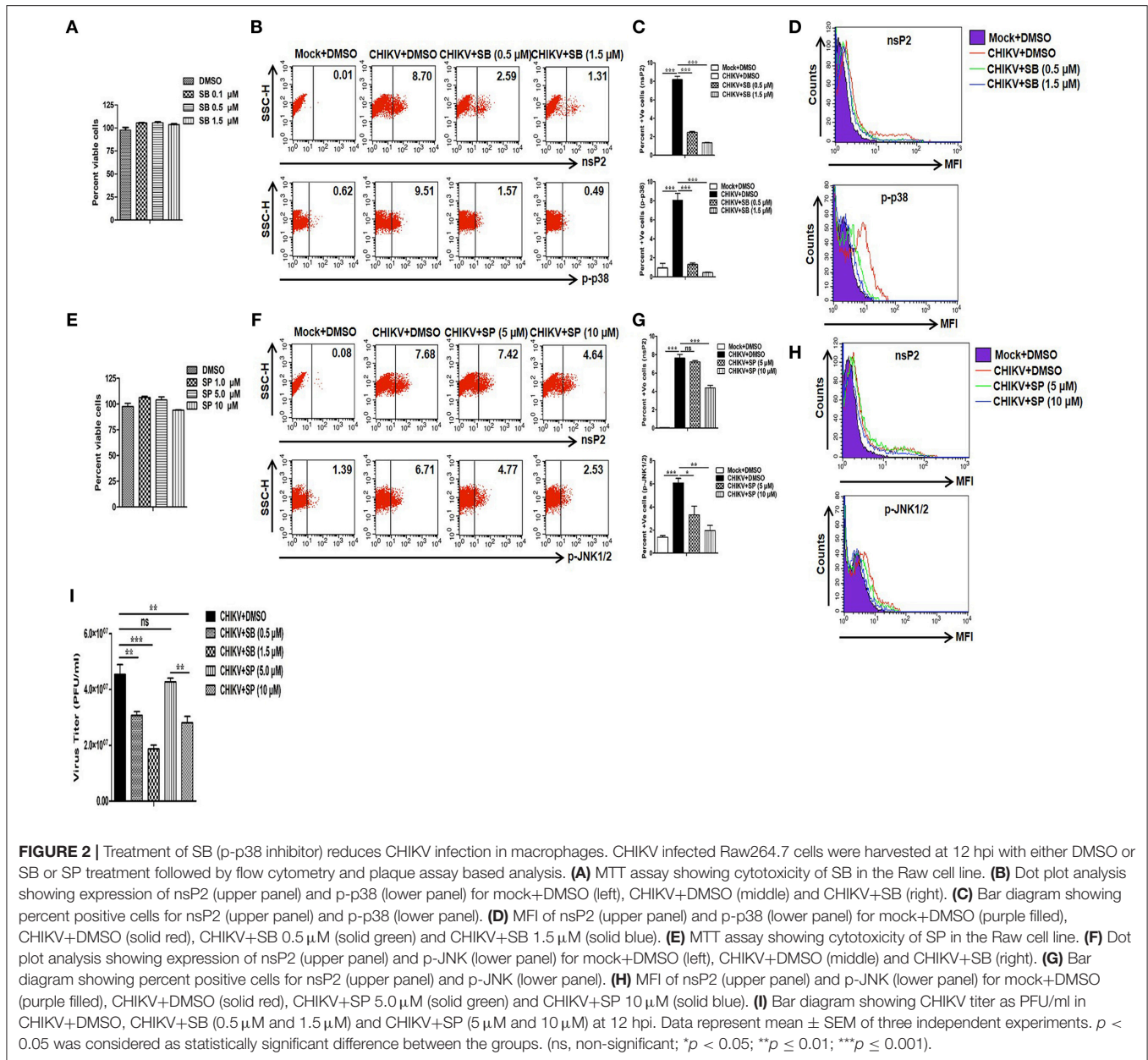


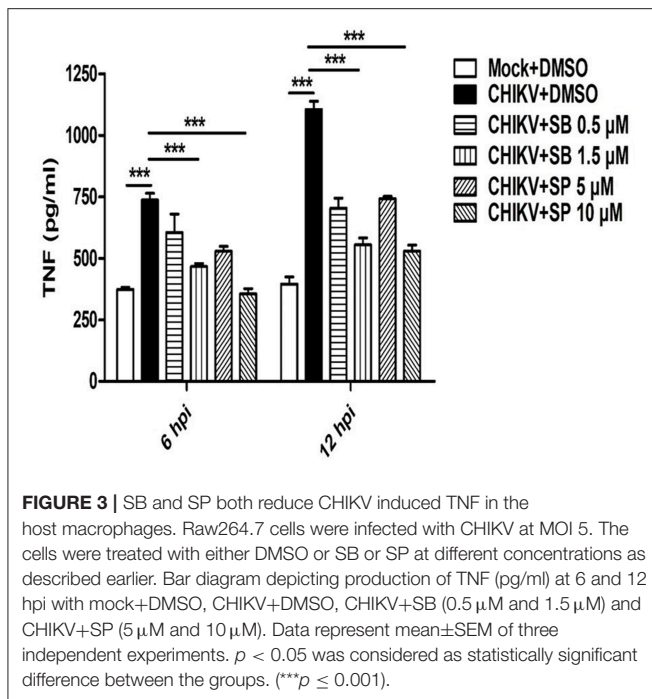
FIGURE 2 | Treatment of SB (p-p38 inhibitor) reduces CHIKV infection in macrophages. CHIKV infected Raw264.7 cells were harvested at 12 hpi with either DMSO or SB or SP treatment followed by flow cytometry and plaque assay based analysis. **(A)** MTT assay showing cytotoxicity of SB in the Raw cell line. **(B)** Dot plot analysis showing expression of nsP2 (upper panel) and p-p38 (lower panel) for mock+DMSO (left), CHIKV+DMSO (middle) and CHIKV+SB (right). **(C)** Bar diagram showing percent positive cells for nsP2 (upper panel) and p-p38 (lower panel). **(D)** MFI of nsP2 (upper panel) and p-p38 (lower panel) for mock+DMSO (purple filled), CHIKV+DMSO (solid red), CHIKV+SB 0.5 μM (solid green) and CHIKV+SB 1.5 μM (solid blue). **(E)** MTT assay showing cytotoxicity of SP in the Raw cell line. **(F)** Dot plot analysis showing expression of nsP2 (upper panel) and p-JNK (lower panel) for mock+DMSO (left), CHIKV+DMSO (middle) and CHIKV+SB (right). **(G)** Bar diagram showing percent positive cells for nsP2 (upper panel) and p-JNK (lower panel). **(H)** MFI of nsP2 (upper panel) and p-JNK (lower panel) for mock+DMSO (purple filled), CHIKV+DMSO (solid red), CHIKV+SP 5.0 μM (solid green) and CHIKV+SP 10 μM (solid blue). **(I)** Bar diagram showing CHIKV titer as PFU/ml in CHIKV+DMSO, CHIKV+SB (0.5 μM and 1.5 μM) and CHIKV+SP (5 μM and 10 μM) at 12 hpi. Data represent mean ± SEM of three independent experiments. $p < 0.05$ was considered as statistically significant difference between the groups. (ns, non-significant; * $p < 0.05$; ** $p \leq 0.01$; *** $p \leq 0.001$).

SP treatment suppressed p-IRF-3 expression which is induced by CHIKV as compared to the DMSO control (Figures 6A–D). Taken together, the current data depict that CHIKV may induce p-c-jun via JNK pathway whereas induction of p-IRF-3 might be dependent on both p38 and JNK MAPKs.

CHIKV nsP2 Interacts With Host p-p38 and p-JNK MAPKs in the Macrophages

Viruses are small obligatory intracellular pathogens utilizes the metabolic pathways of the host for replication. Very often viruses also shut-off host translational process, which might be a strategic decision to contain antiviral responses (81, 82). The integration of complex proteomics studies including *in silico* protein-protein interaction predictions keeps on unraveling the

complex network of interaction with the host cell proteins. Throughout the course of replication, these pathways rely heavily on the dynamic and temporarily regulated virus-host protein-protein interactions which are crucial for the virus replication, pathogenesis, and viral subversion of host defense. The identification and characterization of these interacting partners also help in the delineation of the viral protein functions precisely and might be very helpful in designing rationale drugs for an effective treatment (83–85). The interaction of host MAPK with viral protein has been shown earlier, which in turn regulates infection and replications (86). Since CHIKV infection modulated the phosphorylation of host p38 and JNK, their interaction with the nsP2 protein was investigated. For that, Raw cells were infected with CHIKV and harvested at 6



hpi for further analysis. Co-immunoprecipitation followed by Western blot analysis showed that both the p-p38 and p-JNK proteins were pulled with the CHIKV-nsP2 protein in the host macrophages (Figures 7A,B). This result indicates that CHIKV-nsP2 interacts with both p-p38 and p-JNK and this might be playing a crucial role in the CHIKV infection and TNF mediated inflammatory responses.

Protein-Protein Docking Analysis Shows the Specific Amino Acids Responsible for the nsP2-MAPK Interactions

In order to unravel the amino acid residues responsible for the interaction of nsP2-MAPKs, protein-protein docking was carried out as mentioned above (64, 87, 88). The balanced outputs were preferred from the docking results as this mode takes into account all possible modes of interactions. The most stable complex of nsP2-JNK1 on visualization by using the PyMol software suggested the possible involvement of different residues in the interaction (Supplementary Table S1). No interaction was found between the phosphorylation lip (Thr-183-X-Tyr-185) of JNK1 and nsP2 (Figure 8A). This suggests a poor fit of JNK1 active site with nsP2. Nonetheless, ten polar interactions were observed within 2Å (Figure 8B). Some of these include the interactions of Met-182, Arg-228, Arg-189, Val-196, Arg-150, Lys-68, and Glu-346 of JNK1 with Cys-217, Arg-272, Gln-291, Gly-279, Asp-280, Gly-285, and Lys-282 of nsP2, respectively (Figure 8B). The most stable complex of nsP2-p38 showed a close fit of the phosphorylation lip (Thr-180-X-Tyr-182). In addition to that, a polar interaction was suggested between Thr-180 of p38 and Gln-273 of nsP2 (Figure 8C). Some of the polar interactions were also observed between Lys-66, Ser-329, Asn-196, Ser-252, Ser-254, Asp-177, Glu-178, Arg-173, Lys-152, and Asp-230 of p38 and Asn-288, Gly-285, Asp-280, Cys-278, Asp-351, Cys-257,

Arg-244, Phe-255, Arg-272, and Thr-90 of nsP2, respectively (Figure 8D and Supplementary Table S2). Thus, these results further suggest that CHIKV-nsP2 interacts with p38 as well as JNK MAPKs during viral infection in the host macrophages. Moreover, the phosphorylation lip of p38 interacts more closely with the Gln-273 of CHIKV-nsP2, which supports the findings of IP experiments.

DISCUSSION

The recent epidemics of Chikungunya virus (CHIKV) with unprecedented magnitude and unusual clinical severity have raised a great public health concern worldwide, due to the absence of a vaccine or specific anti-CHIKV therapy. TNF is one of the robustly induced cytokine by CHIKV and in the current study, we have investigated the molecular mechanism involved in the induction of TNF in the host macrophages. Our data suggested that CHIKV induces both p38 and JNK phosphorylation in macrophages in a time-dependent manner. Moreover, p-p38 and p-JNK inhibition by SB and SP were found to reduce CHIKV infection. Interestingly, SB mediated inhibition of CHIKV infection was found to be more effective even at lower concentration as compared to SP. Further, inhibition of both p-p38 and p-JNK reduced CHIKV induced TNF in the host macrophages. Moreover, CHIKV infected cell culture supernatant is found to facilitates T cell activation via TNF in TCR primed T cells. Besides, it was observed that the expressions of key transcription factors involved mainly in antiviral responses (p-IRF3) and TNF production (p-c-jun) were induced significantly in the CHIKV infected macrophages as compared to the corresponding mock cells. Further, it was found that CHIKV mediated TNF production in the macrophages is dependent on p38 and JNK MAPK pathways linking p-c-jun transcription factor. Interestingly, it was also noticed that CHIKV nsP2 interacts with host p-p38 and p-JNK MAPKs in the macrophages. This observation was supported by the *in silico* protein-protein docking analysis which illustrates the specific amino acids responsible for the nsP2-MAPKs interactions and a strong polar interaction was predicted between Thr-180 (within the phosphorylation lip) of p38 and Gln-273 of nsP2. However, no such polar interaction was predicted for the phosphorylation lip of JNK which indicates the differential roles of p-p38 and p-JNK during CHIKV infection in the host macrophages.

The MAPKs have been shown to be activated by several viral infections (54–57). Using the mouse macrophage cell line, Raw264.7 cells, we report for the first time that CHIKV induces both p-p38 and p-JNK significantly, however, the p-ERK1/2 expression remains unchanged. Interestingly, the up-regulation of p-ERK has been reported earlier during CHIKV infection in non-immune BHK cell lines (60). Another report suggested that, the nuclear localization of ERK1/2 (un-phosphorylated form) in the uninfected microglia cells increases after CHIKV infection in astrocytes and this might be due to the release of some factor(s) from infected astrocytes *in vitro* (59).

In this study, it was found that inhibition of p38 signaling by SB reduces nsP2 protein expression and new viral progeny release remarkably, whereas inhibition of JNK signaling by higher concentration of SP could reduce nsP2 moderately as

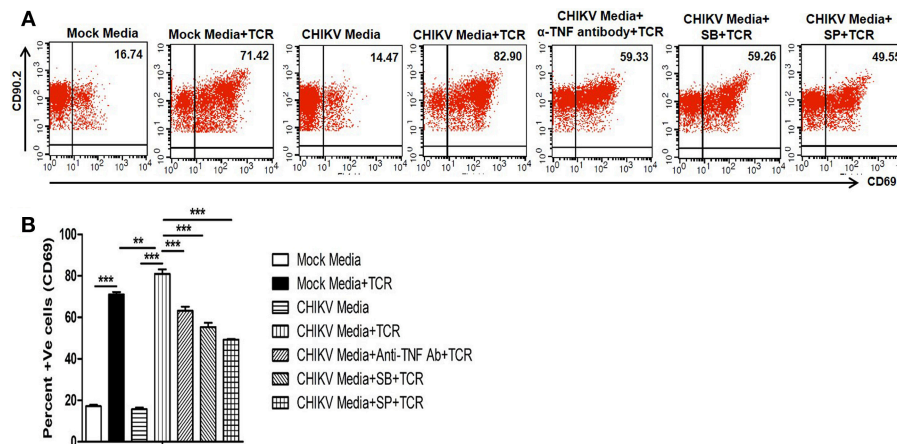


FIGURE 4 | CHIKV induced TNF facilitates TCR driven T cell activation *in vitro*. Both CHIKV infected and mock cell culture supernatants were harvested and used to culture for T cells activation assay *in vitro*. **(A)** Dot plot analysis showing the expression of CD69 in different conditions. **(B)** Graphical representation depicting the percent positive cells for CD69 in T cells. Data represent mean \pm SEM of three independent experiments. $p < 0.05$ was considered as statistically significant difference between the groups. (** $p \leq 0.01$; *** $p \leq 0.001$).

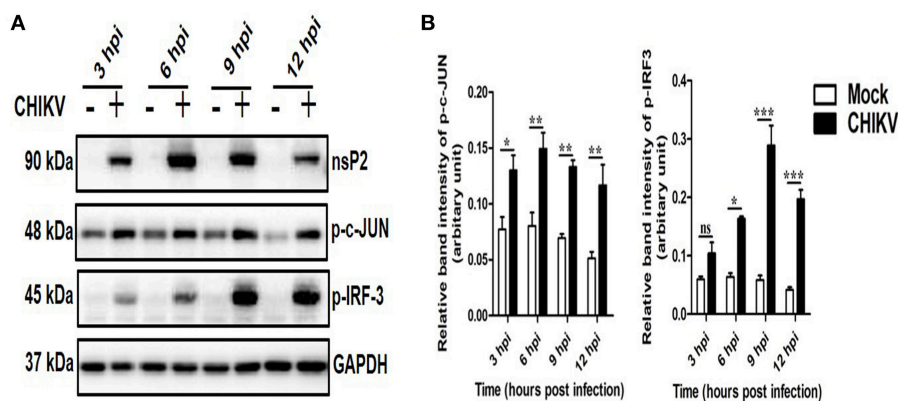


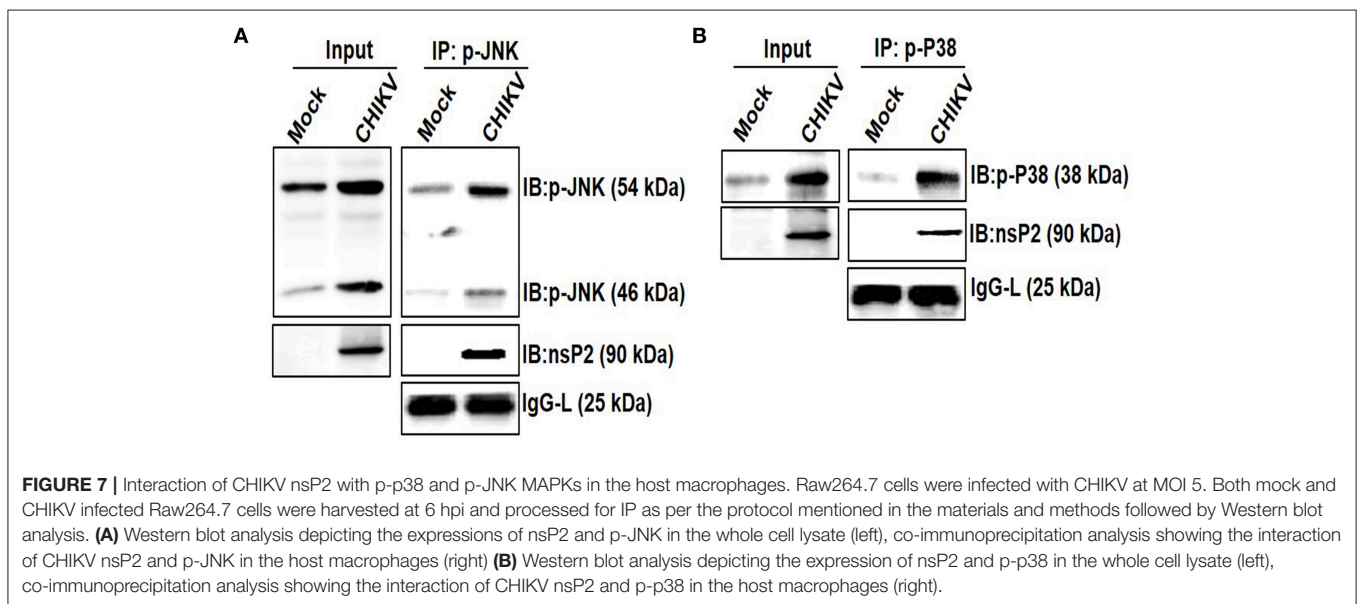
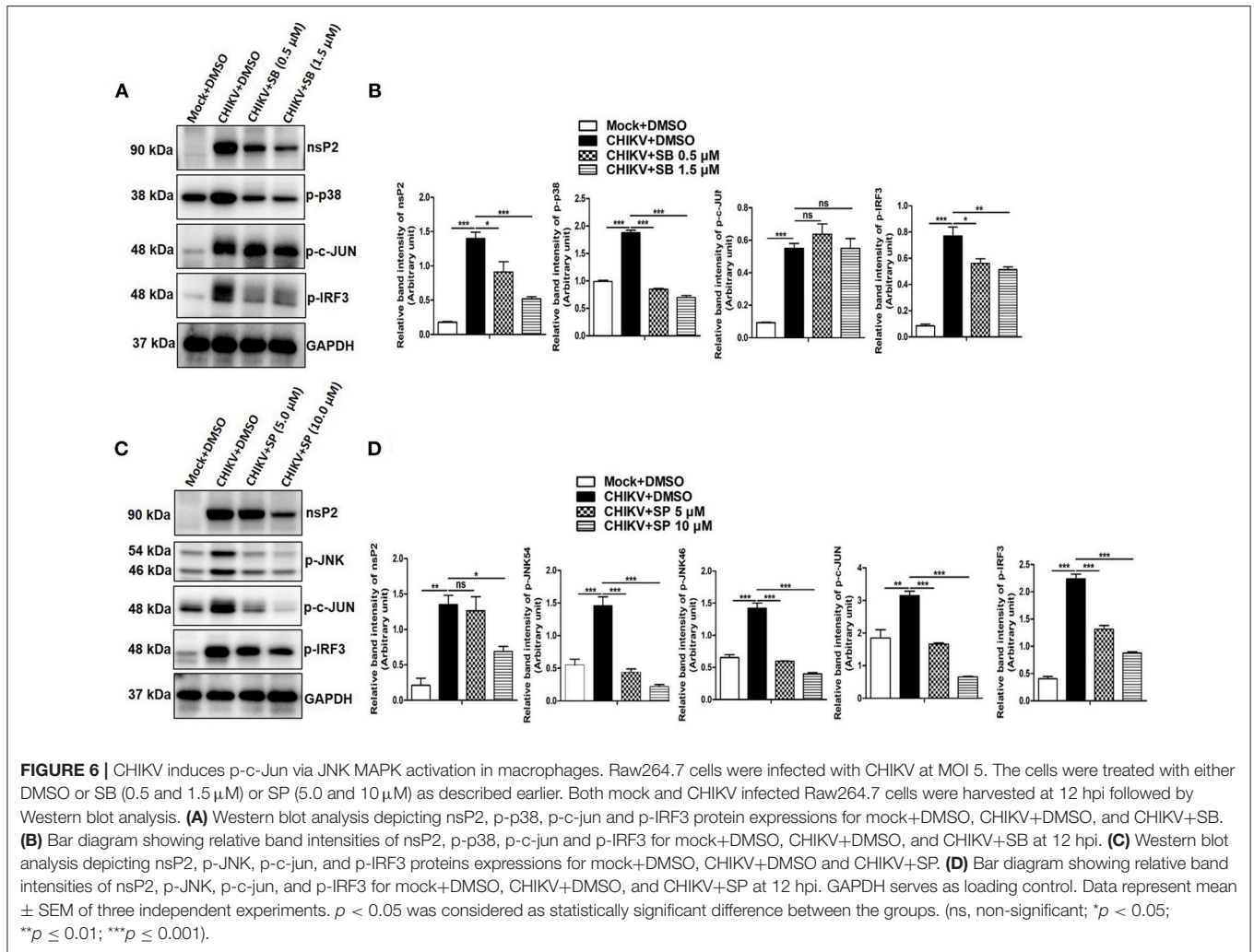
FIGURE 5 | Induction of key transcription factors by CHIKV in macrophages. CHIKV infected Raw264.7 cells were harvested at different time intervals followed by Western blot analysis. **(A)** Western blot analysis depicting p-c-jun and p-IRF-3 protein expressions at different time post-infection. GAPDH serves as loading control. **(B)** Bar diagram showing relative band intensities of p-c-jun and p-IRF-3 at different times post-infection. Data represent mean \pm SEM of three independent experiments. $p < 0.05$ was considered as statistically significant difference between the groups. (ns, non-significant; * $p < 0.05$; ** $p \leq 0.01$; *** $p \leq 0.001$).

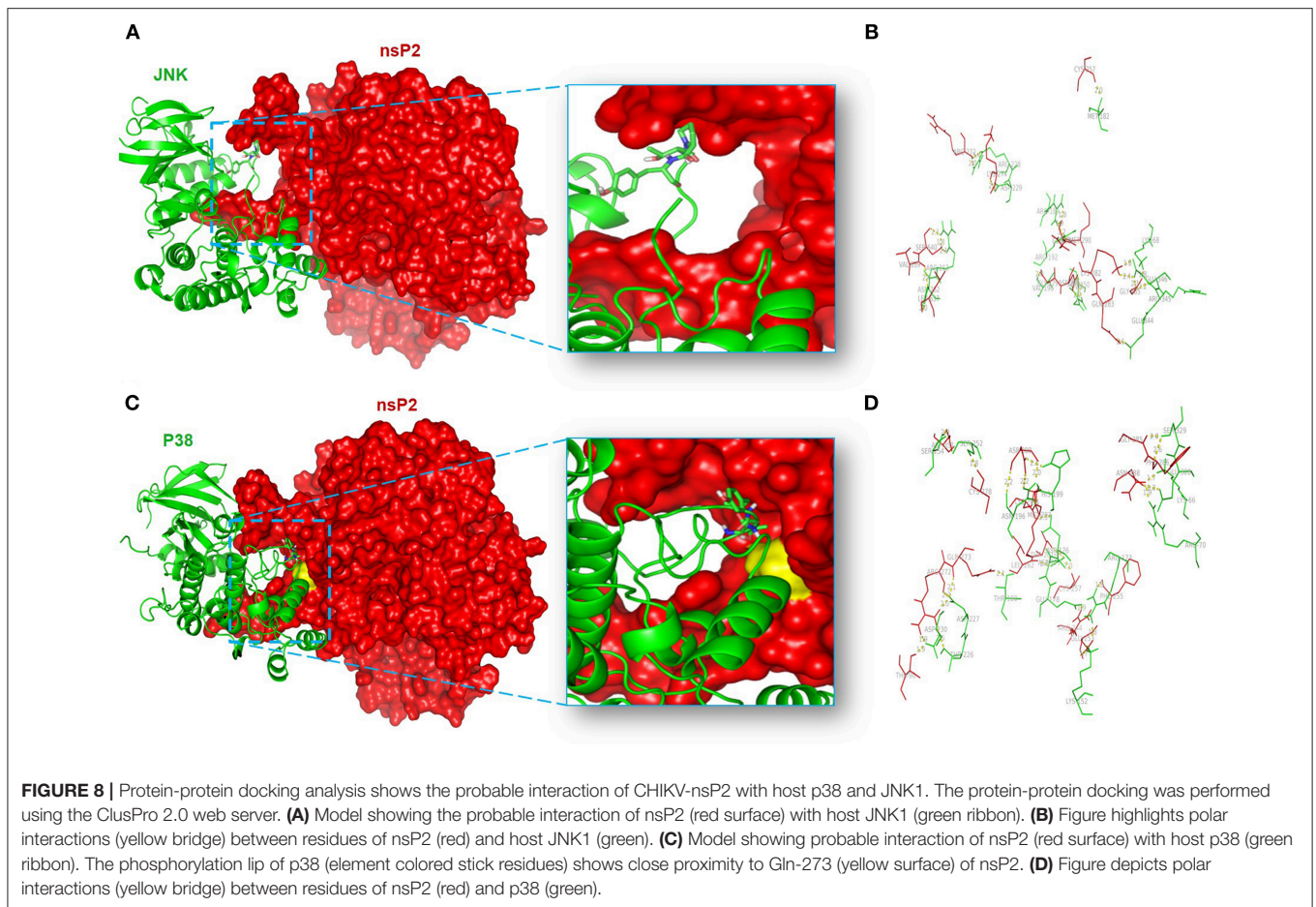
compared to DMSO control. This result indicates that both p38 and JNK play pro-viral role in CHIKV infection in the host macrophages and similar observations have been reported previously in case of other viral infections (60, 89–91). The Encephalomyocarditis Virus infection was suppressed in L929 cells by SB, mainly through the reduction of the viral protein synthesis (89). Whereas, in the Human Enterovirus 71 infection it was shown that the blockage of virus induced p-p38 leads to significant reduction in both viral protein and progeny release (90). Further investigation can be carried out on other CHIKV proteins and RNA synthesis to understand the pro-viral role of the p-p38 in viral replication in details.

MAPKs are known to regulate TNF production via p-c-jun in other inflammation models (50). Here, it was observed that the expression of p-c-jun is dependent on p-JNK pathway (as SP reduces p-c-jun expression in a dose dependent manner),

whereas induction of p-IRF3 is dependent on both MAPKs (p38 and JNK) during CHIKV infection in macrophages. Therefore, it is quite possible that the p-JNK pathway induction by CHIKV leads to the activation of antiviral responses via p-IRF3 and pro-inflammatory responses (TNF) via p-c-jun pathway. On the other hand, p-p38 is involved in activating both pro-viral and antiviral pathways (via induction of p-IRF3) (Figure 9). It has also been observed during this investigation that pro-inflammatory TNF production was decreased significantly during SB treatment. This might be due to the marked inhibition of CHIKV infection, however the possibilities of the involvement of other factors cannot be ignored.

TNF may promote the activation and proliferation of T cells and thereby regulate the overall T cell mediated effector function (72). In mouse model system, it has been demonstrated that host T cells are induced during experimental CHIKV





infection and are associated with CHIKV mediated pathogenesis (43, 44, 46). In the present study, we found that CHIKV infected macrophage culture supernatant may facilitate TCR driven activation of resting T cells as compared to the mock supernatant. Further, the use of neutralizing anti-TNF antibody towards the regulation of the T cell activation suggests that it could be mediated via CHIKV induced macrophage derived TNF. Additionally, presence of either SB or SP in the CHIKV infected macrophage supernatant also able to reduce T cell activation *in vitro*, indicating an effect of macrophage derived TNF on T cell activation during CHIKV infection. Except few cases, CHIKV is not fatal, however, the long-term polyarthralgia, arthritis-like symptoms along with severe inflammation remain a concern for most of the chronic patients (20, 25, 92–95). TNF is one of the key mediator of arthritis or arthritis-like diseases in humans by triggering severe inflammation. Despite the elevation of several other inflammatory cytokines in RA, anti-TNF therapy holds a promise for the effective treatment against it (96, 97), which might be exploited against CHIKV pathogenesis in future.

Further, the co-immunoprecipitation analysis revealed that CHIKV-nsP2 interacts with both p-p38 and p-JNK upon infection in the host macrophages. This was also supported by the *in silico* analysis of the protein-protein interaction of

CHIKV-nsP2 with p38 and JNK. The phosphorylation lip of p38 was found to interact with nsP2 due to the observed close fit model and a polar interaction between Thr-180 of p38 and Gln-273 of nsP2. Residues from the N-terminus of nsP2 were also suggested to have strong ($<2 \text{ \AA}$) polar interactions with the other residues around this active site. Unlike this, the interaction of CHIKV-nsP2 showed poor fit with the phosphorylation lip of JNK and close ($<2 \text{ \AA}$) polar interaction was also observed for residues from N-terminus of nsP2. These interactions might be one of the yet unknown strategies to utilize host signaling pathways through protein-protein interactions for effective viral infection (97–99), which can be explored further in details.

Viral proteins are found to be phosphorylated by various kinases, which in turn regulate its functions, stability and interactions with other cellular and viral proteins (100). However, the precise role of the viral protein phosphorylation (especially in Alphavirus) has not been reported yet. In this investigation, nsP2 was found to interact with the phosphorylation lip of p38, hence, *in silico* analysis was carried out using PTM prediction tools, GPS (group-based phosphorylation scoring method) (101, 102) and NetPhos 3.1, to predict the target phosphorylation sites of nsP2 in a kinase specific manner (103). The GPS is a group-based phosphorylation algorithm, which predicts kinase-specific phosphorylation sites among different host protein kinase groups

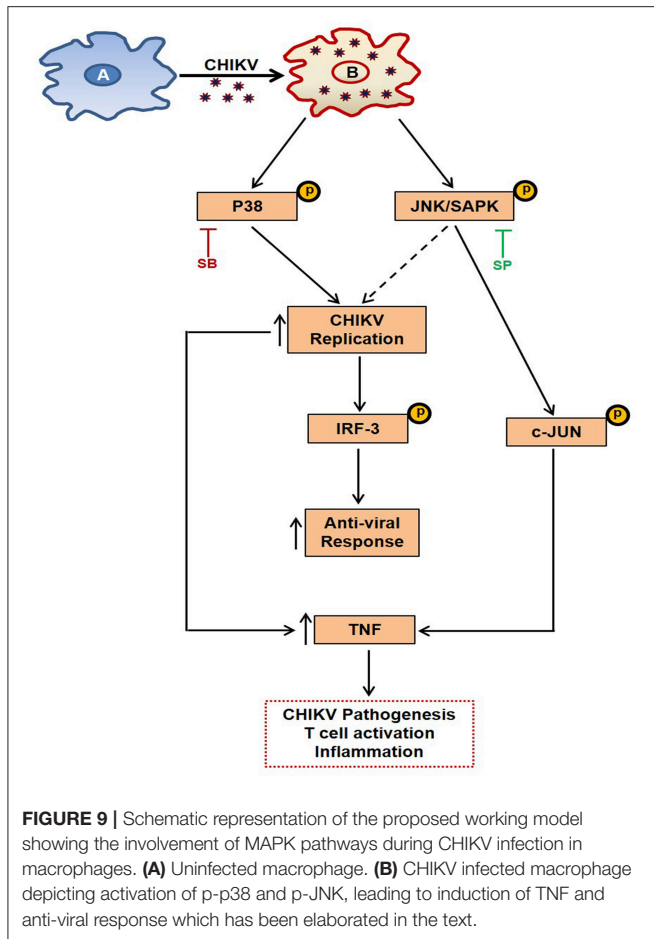


FIGURE 9 | Schematic representation of the proposed working model showing the involvement of MAPK pathways during CHIKV infection in macrophages. (A) Uninfected macrophage. (B) CHIKV infected macrophage depicting activation of p-p38 and p-JNK, leading to induction of TNF and anti-viral response which has been elaborated in the text.

according to specific sequence pattern (101, 102). Whereas, the NetPhos server is based on an artificial neuronal network (ANN) that allows the users to choose between generic predictions based on the given protein sequence or kinase-specific predictions (103, 104). Out of several predictions, both the softwares predicted T5, S28, and S513 sites in CHIKV-nsP2 with a high probability of phosphorylation by p38 (**Supplementary Table S3**). Further, to elucidate whether positions of these amino acids in CHIKV-nsP2 is associated with any consensus regions of functional importance, the predicted peptides were searched in the ExPASy-PROSITE protein database. Surprisingly, the peptide “FKEDKAYSPEVALNE” with S513 (at the middle, red) showed a hit with Alphavirus nsP2 protease domain belonging to the C9 cysteine protease family (105). Since we have shown earlier that p38 interacts strongly with CHIKV nsP2 (with phosphorylation lip) and the inhibition of p38 activation strongly reduces CHIKV infection, it might be possible that, p38 phosphorylates

either nsP2 directly or through the association of other client protein(s) which in turn may modulate its function. However, further studies are required to corroborate the CHIKV-nsP2 phosphorylation by host kinases and its functional consequences on infection and pathogenesis.

In summary, for the first time it has been shown that CHIKV triggers robust TNF production (a key mediator of CHIKV induced inflammation) in the host macrophages via both p-p38 and p-JNK/p-c-jun pathways and viral protein nsP2 interacts with both the MAPKs during infection. Furthermore, CHIKV induced macrophage derived TNF was found to facilitate T cell activation *in vitro*. Hence, this information might shed light in rationale-based drug designing for the control of the disease caused by CHIKV in future.

AUTHOR CONTRIBUTIONS

SuC, SoC, TN, and PM conceived the idea and designed the experiments. TN, PM, SS, PK, SC, and CM performed wet lab experiments. BS, TN, and PM performed *in silico* experiments and analysis. SuC and SoC contributed reagents. SuC, SoC, TN, and PM analyzed and interpreted the data. SuC, SoC, TN, PM, CM, SC, and BS wrote the manuscript. All authors read and approved the final version of this manuscript.

FUNDING

This study has been funded by the Council of Scientific and Industrial Research (CSIR), New Delhi, India, vide grant no 37 (1542)/12/EMR-II and Department of Science and Technology (DST-SERB), New Delhi, India, vide grant no EMR/2016/000854. It was also supported by Institute of life sciences, Bhubaneswar, under Department of Biotechnology and National Institute of Science Education and Research (NISER), Bhubaneswar, under Department of Atomic Energy (DAE), Government of India.

ACKNOWLEDGMENTS

We are thankful to Dr. MM. Parida, DRDE, Gwalior, India for kindly providing DRDE-06 virus strain and Vero cell line. We wish to acknowledge the University Grant Commission (UGC), New Delhi, India for the fellowship to TKN during this study.

SUPPLEMENTARY MATERIAL

The Supplementary Material for this article can be found online at: <https://www.frontiersin.org/articles/10.3389/fimmu.2019.00786/full#supplementary-material>

REFERENCES

1. Lumsden WH. An epidemic of virus disease in Southern Province, Tanganyika Territory, in 1952-53. II. General description and

epidemiology. *Trans R Soc Trop Med Hyg.* (1955) 49:33-57. doi: 10.1016/0035-9203(55)90081-X

2. Mason PJ, Haddow AJ. An epidemic of virus disease in Southern Province, Tanganyika Territory, in 1952-53; an additional note on Chikungunya virus

- isolations and serum antibodies. *Trans R Soc Trop Med Hyg.* (1957) 51:238–40. doi: 10.1016/0035-9203(57)90022-6
3. Robinson MC. An epidemic of viral disease in Southern Province, Tanganyika Territory, in 1952–53. I. clinical features. *Trans R Soc Trop Med Hyg.* (1955) 49:28–32. doi: 10.1016/0035-9203(55)90080-8
 4. Chhabra M, Mittal V, Bhattacharya D, Rana U, Lal S. Chikungunya fever: a re-emerging viral infection. *Ind J Med Microbiol.* (2008) 26:5–12. doi: 10.4103/0255-0857.38850
 5. Jain M, Rai S, Chakravarti A. Chikungunya: a review. *Trop Doc.* (2008) 38:70–2. doi: 10.1258/td.2007.070019
 6. Pialoux G, Gauzere BA, Jaureguierry S, Strobel M. Chikungunya, an epidemic arbovirosis. *Lancet Infect Dis.* (2007) 7:319–27. doi: 10.1016/S1473-3099(07)70107-X
 7. Renault P, Solet JL, Sissoko D, Ballezardier E, Larrieu S, Filleul L, et al. A major epidemic of chikungunya virus infection on Reunion Island, France, 2005–2006. *Am J Trop Med Hyg.* (2007) 77:727–31. doi: 10.4269/ajtmh.2007.77.727
 8. Arankalle VA, Shrivastava S, Cherian S, Gunjkar RS, Walimbe AM, Jadhav SM, et al. Genetic divergence of Chikungunya viruses in India (1963–2006) with special reference to the 2005–2006 explosive epidemic. *J Gen Virol.* (2007) 88(Pt 7):1967–76. doi: 10.1099/vir.0.82714-0
 9. Kaur P, Ponniah M, Murhekar MV, Ramachandran V, Ramachandran R, Raju HK, et al. Chikungunya outbreak, South India, 2006. *Emerg Infect Dis.* (2008) 14:1623–5. doi: 10.3201/eid1410.070569
 10. Kumar A, Mamidi P, Das I, Nayak TK, Kumar S, Chhatai J, et al. A novel 2006 Indian outbreak strain of Chikungunya virus exhibits different pattern of infection as compared to prototype strain. *PLoS ONE.* (2014) 9:e85714. doi: 10.1371/journal.pone.0085714
 11. Lahariya C, Pradhan SK. Emergence of chikungunya virus in Indian subcontinent after 32 years: a review. *J Vector Borne Dis.* (2006) 43:151–60.
 12. Rodriguez-Barraquer I, Solomon SS, Kuganantham P, Srikrishnan AK, Vasudevan CK, Iqbal SH, et al. The hidden burden of dengue and chikungunya in Chennai, India. *PLoS Neglect Trop Dis.* (2015) 9:e0003906. doi: 10.1371/journal.pntd.0003906
 13. Bellini R, Medici A, Calzolari M, Bonilauri P, Cavrini F, Sambri V, et al. Impact of Chikungunya virus on *Aedes albopictus* females and possibility of vertical transmission using the actors of the 2007 outbreak in Italy. *PLoS ONE.* (2012) 7:e28360. doi: 10.1371/journal.pone.0028360
 14. Carrieri M, Angelini P, Venturelli C, Maccagnani B, Bellini R. *Aedes albopictus* (Diptera: Culicidae) population size survey in the 2007 chikungunya outbreak area in Italy. II: estimating epidemic thresholds. *J Med Entomol.* (2012) 49:388–99. doi: 10.1603/ME10259
 15. Mathew AJ, Ganapati A, Kabeerdoss J, Nair A, Gupta N, Chebby P, et al. Chikungunya infection: a global public health menace. *Curr Allergy Asthma Rep.* (2017) 17:13. doi: 10.1007/s11882-017-0680-7
 16. Pulmanusahakul R, Roytrakul S, Auewarakul P, Smith DR. Chikungunya in Southeast Asia: understanding the emergence and finding solutions. *Int J Infect Dis.* (2011) 15:e671–6. doi: 10.1016/j.ijid.2011.06.002
 17. Thavara U, Tawatsin A, Pengsakul T, Bhakdeenuan P, Chanama S, Anantapreecha S, et al. Outbreak of chikungunya fever in Thailand and virus detection in field population of vector mosquitoes, *Aedes aegypti* (L.) and *Aedes albopictus* Skuse (Diptera: Culicidae). *Southeast Asian J Trop Med Pub Health.* (2009) 40:951–62.
 18. Wahid B, Ali A, Rafique S, Idrees M. Global expansion of chikungunya virus: mapping the 64-year history. *Int J Infect Dis.* (2017) 58:69–76. doi: 10.1016/j.ijid.2017.03.006
 19. Gould E, Pettersson J, Higgs S, Charrel R, de Lamballerie X. Emerging arboviruses: why today? *One Health.* (2017) 4:1–13. doi: 10.1016/j.onehlt.2017.06.001
 20. Hawman DW, Stoermer KA, Montgomery SA, Pal P, Oko L, Diamond MS, et al. Chronic joint disease caused by persistent Chikungunya virus infection is controlled by the adaptive immune response. *J Virol.* (2013) 87:13878–88. doi: 10.1128/JVI.02666-13
 21. Labadie K, Larcher T, Joubert C, Mannioui A, Delache B, Brochard P, et al. Chikungunya disease in nonhuman primates involves long-term viral persistence in macrophages. *J Clin Investigat.* (2010) 120:894–906. doi: 10.1172/JCI40104
 22. Lundstrom K. Alphavirus-based vaccines. *Methods Mol Biol.* (2016) 1404:313–28. doi: 10.1007/978-1-4939-3389-1_22
 23. Subudhi BB, Chattopadhyay S, Mishra P, Kumar A. Current strategies for inhibition of chikungunya infection. *Viruses.* (2018) 10:e235. doi: 10.3390/v10050235
 24. Chow A, Her Z, Ong EK, Chen JM, Dimatatac F, Kwek DJ, et al. Persistent arthralgia induced by Chikungunya virus infection is associated with interleukin-6 and granulocyte macrophage colony-stimulating factor. *J Infect Dis.* (2011) 203:149–57. doi: 10.1093/infdis/jiq042
 25. Hoarau JJ, Jaffar Bandjee MC, Krejbich Trotot P, Das T, Li-Pat-Yuen G, Dassa B, et al. Persistent chronic inflammation and infection by Chikungunya arthritogenic alphavirus in spite of a robust host immune response. *J Immunol.* (2010) 184:5914–27. doi: 10.4049/jimmunol.0900255
 26. Kam YW, Ong EK, Renia L, Tong JC, Ng LF. Immuno-biology of Chikungunya and implications for disease intervention. *Microbes Infect.* (2009) 11:1186–96. doi: 10.1016/j.micinf.2009.09.003
 27. Ng LE, Chow A, Sun YJ, Kwek DJ, Lim PL, Dimatatac F, et al. IL-1beta, IL-6, and RANTES as biomarkers of Chikungunya severity. *PLoS ONE.* (2009) 4:e4261. doi: 10.1371/journal.pone.0004261
 28. Robin S, Ramful D, Zettor J, Benhamou L, Jaffar-Bandjee MC, Riviere JP, et al. Severe bullous skin lesions associated with Chikungunya virus infection in small infants. *Euro J Pediatrics.* (2010) 169:67–72. doi: 10.1007/s00431-009-0986-0
 29. Chirathaworn C, Poovorawan Y, Lertmaharit S, Wuttirattanakit N. Cytokine levels in patients with chikungunya virus infection. *Asian Pacific J Trop Med.* (2013) 6:631–4. doi: 10.1016/S1995-7645(13)60108-X
 30. Kelvin AA, Banner D, Silvi G, Moro ML, Spataro N, Gaibani P, et al. Inflammatory cytokine expression is associated with chikungunya virus resolution and symptom severity. *PLoS Neglect Trop Dis.* (2011) 5:e1279. doi: 10.1371/journal.pntd.0001279
 31. Kumar S, Jaffar-Bandjee MC, Giry C, Connen de Kerillis L, Merits A, Gasque P, et al. Mouse macrophage innate immune response to Chikungunya virus infection. *Virol J.* (2012) 9:313. doi: 10.1186/1743-422X-9-313
 32. Lohachanakul J, Phuklia W, Thannagith M, Thongsakulprasert T, Smith DR, Ubol S. Differences in response of primary human myoblasts to infection with recent epidemic strains of Chikungunya virus isolated from patients with and without myalgia. *J Med Virol.* (2015) 87:733–9. doi: 10.1002/jmv.24081
 33. Phuklia W, Kasisith J, Modhiran N, Rodpai E, Thannagith M, Thongsakulprasert T, et al. Osteoclastogenesis induced by CHIKV-infected fibroblast-like synoviocytes: a possible interplay between synoviocytes and monocytes/macrophages in CHIKV-induced arthralgia/arthritis. *Virus Res.* (2013) 177:179–88. doi: 10.1016/j.virusres.2013.08.011
 34. Priya R, Dhanwani R, Patro IK, Rao PV, Parida MM. Differential regulation of TLR mediated innate immune response of mouse neuronal cells following infection with novel ECSA genotype of Chikungunya virus with and without E1:A226V mutation. *Infect Genet Evol.* (2013) 20:396–406. doi: 10.1016/j.meegid.2013.09.030
 35. Priya R, Patro IK, Parida MM. TLR3 mediated innate immune response in mice brain following infection with Chikungunya virus. *Virus Res.* (2014) 189:194–205. doi: 10.1016/j.virusres.2014.05.010
 36. Reddy V, Mani RS, Desai A, Ravi V. Correlation of plasma viral loads and presence of Chikungunya IgM antibodies with cytokine/chemokine levels during acute Chikungunya virus infection. *J Med Virol.* (2014) 86:1393–401. doi: 10.1002/jmv.23875
 37. Nayak TK, Mamidi P, Kumar A, Singh LP, Sahoo SS, Chattopadhyay S, et al. Regulation of viral replication, apoptosis and pro-inflammatory responses by 17-AAG during Chikungunya virus infection in macrophages. *Viruses.* (2017) 9:3. doi: 10.3390/v9010003
 38. Gardner J, Anraku I, Le TT, Larcher T, Major L, Roques P, et al. Chikungunya virus arthritis in adult wild-type mice. *J Virol.* (2010) 84:8021–32. doi: 10.1128/JVI.02603-09
 39. Morrison TE, Oko L, Montgomery SA, Whitmore AC, Lotstein AR, Gunn BM, et al. A mouse model of chikungunya virus-induced musculoskeletal inflammatory disease: evidence of arthritis, tenosynovitis, myositis, and persistence. *Am J Pathol.* (2011) 178:32–40. doi: 10.1016/j.ajpath.2010.11.018
 40. Ozden S, Huerre M, Riviere JP, Coffey LL, Afonso PV, Mouly V, et al. Human muscle satellite cells as targets of Chikungunya virus infection. *PLoS ONE.* (2007) 2:e527. doi: 10.1371/journal.pone.0000527

41. Her Z, Malleret B, Chan M, Ong EK, Wong SC, Kwek DJ, et al. Active infection of human blood monocytes by Chikungunya virus triggers an innate immune response. *J Immunol.* (2010) 184:5903–13. doi: 10.4049/jimmunol.0904181
42. Hoarau JJ, Gay F, Pelle O, Samri A, Jaffar-Bandjee MC, Gasque P, et al. Identical strength of the T cell responses against E2, nsP1 and capsid CHIKV proteins in recovered and chronic patients after the epidemics of 2005–2006 in La Reunion Island. *PLoS ONE.* (2013) 8:e84695. doi: 10.1371/journal.pone.0084695
43. Teo TH, Lum FM, Claser C, Lulla V, Lulla A, Merits A, et al. A pathogenic role for CD4+ T cells during Chikungunya virus infection in mice. *J Immunol.* (2013) 190:259–69. doi: 10.4049/jimmunol.1202177
44. Wauquier N, Becquart P, Nkoghe D, Padilla C, Ndjoi-Mbiguino A, Leroy EM. The acute phase of Chikungunya virus infection in humans is associated with strong innate immunity and T CD8 cell activation. *J Infect Dis.* (2011) 204:115–23. doi: 10.1093/infdis/jiq006
45. Muthumani K, Lankaraman KM, Laddy DJ, Sundaram SG, Chung CW, Sako E, et al. Immunogenicity of novel consensus-based DNA vaccines against Chikungunya virus. *Vaccine.* (2008) 26:5128–34. doi: 10.1016/j.vaccine.2008.03.060
46. Versteeg L, Febres MEC, Beaumier CM. The role of cellular immune responses on Chikungunya virus infection-induced arthritis. *Curr Trop Med Rep.* (2016) 3:60–6. doi: 10.1007/s40475-016-0074-2
47. Arthur JS, Ley SC. Mitogen-activated protein kinases in innate immunity. *Nat Rev Immunol.* (2013) 13:679–92. doi: 10.1038/nri3495
48. Kaminska B. MAPK signalling pathways as molecular targets for anti-inflammatory therapy—from molecular mechanisms to therapeutic benefits. *Biochimica Et Biophysica Acta.* (2005) 1754:253–62. doi: 10.1016/j.bbapap.2005.08.017
49. Kim EK, Choi EJ. Pathological roles of MAPK signaling pathways in human diseases. *Biochimica Et Biophysica Acta.* (2010) 1802:396–405. doi: 10.1016/j.bbadis.2009.12.009
50. Klemm C, Bruchhagen C, van Kruchten A, Niemann S, Löffler B, Peters G, et al. Mitogen-activated protein kinases (MAPKs) regulate IL-6 overproduction during concomitant influenza virus and Staphylococcus aureus infection. *Sci Rep.* (2017) 7:42473. doi: 10.1038/srep42473
51. Thalhamer T, McGrath MA, Harnett MM. MAPKs and their relevance to arthritis and inflammation. *Rheumatology.* (2008) 47:409–14. doi: 10.1093/rheumatology/kem297
52. Turner MD, Nedjai B, Hurst T, Pennington DJ. Cytokines and chemokines: At the crossroads of cell signalling and inflammatory disease. *Biochimica Et Biophysica Acta.* (2014) 1843:2563–82. doi: 10.1016/j.bbamcr.2014.05.014
53. Zhang W, Liu HT. MAPK signal pathways in the regulation of cell proliferation in mammalian cells. *Cell Res.* (2002) 12:9–18. doi: 10.1038/sj.cr.7290105
54. Banerjee S, Narayanan K, Mizutani T, Makino S. Murine coronavirus replication-induced p38 mitogen-activated protein kinase activation promotes interleukin-6 production and virus replication in cultured cells. *J Virol.* (2002) 76:5937–48. doi: 10.1128/JVI.76.12.5937-5948.2002
55. Adamson AL, Darr D, Holley-Guthrie E, Johnson RA, Mauser A, Swenson J, et al. Epstein-Barr virus immediate-early proteins BZLF1 and BRLF1 activate the ATF2 transcription factor by increasing the levels of phosphorylated p38 and c-Jun N-terminal kinases. *J Virol.* (2000) 74:1224–33. doi: 10.1128/JVI.74.3.1224-1233.2000
56. Dumitru CA, Dreschers S, Gulbins E. Rhinoviral infections activate p38MAP-kinases via membrane rafts and RhoA. *Cell Physiol Biochem.* (2006) 17:159–66. doi: 10.1159/000092077
57. Erhardt A, Hassan M, Heintges T, Haussinger D. Hepatitis C virus core protein induces cell proliferation and activates ERK, JNK, and p38 MAP kinases together with the MAP kinase phosphatase MKP-1 in a HepG2 Tet-Off cell line. *Virology.* (2002) 292:272–84. doi: 10.1006/viro.2001.1227
58. Wei L, Zhu Z, Wang J, Liu J. JNK and p38 mitogen-activated protein kinase pathways contribute to porcine circovirus type 2 infection. *J Virol.* (2009) 83:6039–47. doi: 10.1128/JVI.00135-09
59. Das T, Hoarau JJ, Jaffar Bandjee MC, Maquart M, Gasque P. Multifaceted innate immune responses engaged by astrocytes, microglia and resident dendritic cells against Chikungunya neuroinfection. *J Gen Virol.* (2015) 96(Pt 2):294–310. doi: 10.1099/vir.0.071175-0
60. Varghese FS, Thaa B, Amrun SN, Simarmata D, Rausalu K, Nyman TA, et al. The antiviral alkaloid berberine reduces chikungunya virus-induced mitogen-activated protein kinase signaling. *J Virol.* (2016) 90:9743–57. doi: 10.1128/JVI.01382-16
61. Chattopadhyay S, Kumar A, Mamidi P, Nayak TK, Das I, Chhatai J, et al. Development and characterization of monoclonal antibody against non-structural protein-2 of Chikungunya virus and its application. *J Virol Methods.* (2014) 199:86–94. doi: 10.1016/j.jviromet.2014.01.008
62. Wang HQ, Liu BQ, Gao YY, Meng X, Guan Y, Zhang HY, et al. Inhibition of the JNK signalling pathway enhances proteasome inhibitor-induced apoptosis of kidney cancer cells by suppression of BAG3 expression. *Br J Pharmacol.* (2009) 158:1405–12. doi: 10.1111/j.1476-5381.2009.00455.x
63. Kozakov D, Beglov D, Bohnuud T, Mottarella SE, Xia B, Hall DR, et al. How good is automated protein docking? *Proteins.* (2013) 81:2159–66. doi: 10.1002/prot.24403
64. Kozakov D, Hall DR, Xia B, Porter KA, Padhorny D, Yueh C, et al. The ClusPro web server for protein-protein docking. *Nat Protocols.* (2017) 12:255–78. doi: 10.1038/nprot.2016.169
65. Chuang GY, Kozakov D, Brenke R, Comeau SR, Vajda S. DARS (Decoys As the Reference State) potentials for protein-protein docking. *Biophys J.* (2008) 95:4217–27. doi: 10.1529/biophysj.108.135814
66. Kozakov D, Clodfelter KH, Vajda S, Camacho CJ. Optimal clustering for detecting near-native conformations in protein docking. *Biophys J.* (2005) 89:867–75. doi: 10.1529/biophysj.104.058768
67. Brooks B. CHARMM: A program for macromolecular energy, minimization, and dynamics calculations. *J Comput Chem.* (1982) 4:187–217. doi: 10.1002/jcc.540040211
68. Kumar S, Mamidi P, Kumar A, Basantray I, Bramha U, Dixit A, et al. Development of novel antibodies against non-structural proteins nsP1, nsP3 and nsP4 of chikungunya virus: potential use in basic research. *Arch Virol.* (2015) 160:2749–61. doi: 10.1007/s00705-015-2564-2
69. Sahoo SS, Pratheek BM, Meena VS, Nayak TK, Kumar PS, Bandyopadhyay S, et al. VIPER regulates naive T cell activation and effector responses: implication in TLR4 associated acute stage T cell responses. *Sci Rep.* (2018) 8:7118. doi: 10.1038/s41598-018-25549-8
70. Feng H, Zhang D, Palliser D, Zhu P, Cai S, Schlesinger A, et al. Listeria-infected myeloid dendritic cells produce IFN-beta, priming T cell activation. *J Immunol.* (2005) 175:421–32. doi: 10.4049/jimmunol.175.1.421
71. Lali FV, Hunt AE, Turner SJ, Foxwell BM. The pyridinyl imidazole inhibitor SB203580 blocks phosphoinositide-dependent protein kinase activity, protein kinase B phosphorylation, and retinoblastoma hyperphosphorylation in interleukin-2-stimulated T cells independently of p38 mitogen-activated protein kinase. *J Biol Chem.* (2000) 275:7395–402. doi: 10.1074/jbc.275.10.7395
72. Mehta AK, Gracias DT, Croft M. TNF activity and T cells. *Cytokine.* (2018) 101:14–8. doi: 10.1016/j.cyto.2016.08.003
73. Akira S, Takeda K. Toll-like receptor signalling. *Nat Rev Immunol.* (2004) 4:499–511. doi: 10.1038/nri1391
74. Jiang H, Yu K, Kapczynski DR. Transcription factor regulation and cytokine expression following *in vitro* infection of primary chicken cell culture with low pathogenic avian influenza virus. *Virol J.* (2013) 10:342. doi: 10.1186/1743-422X-10-342
75. Kawai T, Akira S. TLR signaling. *Cell Death Different.* (2006) 13:816–25. doi: 10.1038/sj.cdd.4401850
76. Kawai T, Akira S. The role of pattern-recognition receptors in innate immunity: update on Toll-like receptors. *Nat Immunol.* (2010) 11:373–84. doi: 10.1038/ni.1863
77. Tarassishin L, Bauman A, Suh HS, Lee SC. Anti-viral and anti-inflammatory mechanisms of the innate immune transcription factor interferon regulatory factor 3: relevance to human CNS diseases. *J Neuroimmune Pharmacol.* (2013) 8:132–44. doi: 10.1007/s11481-012-9360-5
78. Wang A, Al-Kuhlani M, Johnston SC, Ojcius DM, Chou J, Dean D. Transcription factor complex AP-1 mediates inflammation initiated by Chlamydia pneumoniae infection. *Cell Microbiol.* (2013) 15:779–94. doi: 10.1111/cmi.12071
79. Feldmann M. Development of anti-TNF therapy for rheumatoid arthritis. *Nat Rev Immunol.* (2002) 2:364–71. doi: 10.1038/nri802

80. Zhao J, Wang L, Dong X, Hu X, Zhou L, Liu Q, et al. The c-Jun N-terminal kinase (JNK) pathway is activated in human interstitial cystitis (IC) and rat protamine sulfate induced cystitis. *Sci Rep.* (2016) 6:19670. doi: 10.1038/srep19670
81. Khapersky DA, McCormick C. Timing is everything: coordinated control of host shutoff by influenza A virus NS1 and PA-X Proteins. *J Virol.* (2015) 89:6528–31. doi: 10.1128/JVI.00386-15
82. Walsh D, Mohr I. Viral subversion of the host protein synthesis machinery. *Nat Rev Microbiol.* (2011) 9:860–75. doi: 10.1038/nrmicro2655
83. Lum KK, Cristea IM. Proteomic approaches to uncovering virus-host protein interactions during the progression of viral infection. *Expert Rev Proteomics.* (2016) 13:325–40. doi: 10.1586/14789450.2016.1147353
84. Rowles DL, Terhune SS, Cristea IM. Discovery of host-viral protein complexes during infection. *Methods Mol Biol.* (2013) 1064:43–70. doi: 10.1007/978-1-62703-601-6_4
85. Vidalain PO, Tangy F. Virus-host protein interactions in RNA viruses. *Microb Infect.* (2010) 12:1134–43. doi: 10.1016/j.micinf.2010.09.001
86. Yu JH, Lin BY, Deng W, Broker TR, Chow LT. Mitogen-activated protein kinases activate the nuclear localization sequence of human papillomavirus type 11 E1 DNA helicase to promote efficient nuclear import. *J Virol.* (2007) 81:5066–78. doi: 10.1128/JVI.02480-06
87. Comeau SR, Gatchell DW, Vajda S, Camacho CJ. ClusPro: an automated docking and discrimination method for the prediction of protein complexes. *Bioinformatics.* (2004) 20:45–50. doi: 10.1093/bioinformatics/btg371
88. Kozakov D, Brenke R, Comeau SR, Vajda S. PIPER: an FFT-based protein docking program with pairwise potentials. *Proteins.* (2006) 65:392–406. doi: 10.1002/prot.21117
89. Hirasawa K, Kim A, Han HS, Han J, Jun HS, Yoon JW. Effect of p38 mitogen-activated protein kinase on the replication of encephalomyocarditis virus. *J Virol.* (2003) 77:5649–56. doi: 10.1128/JVI.77.10.5649-5656.2003
90. Leong SY, Ong BK, Chu JJ. The role of Misshapen NCK-related kinase (MINK), a novel Ste20 family kinase, in the IRES-mediated protein translation of human enterovirus 71. *PLoS Pathog.* (2015) 11:e1004686. doi: 10.1371/journal.ppat.1004686
91. Voss K, Amaya M, Mueller C, Roberts B, Kehn-Hall K, Bailey C, et al. Inhibition of host extracellular signal-regulated kinase (ERK) activation decreases new world alphavirus multiplication in infected cells. *Virology.* (2014) 468–470:490–503. doi: 10.1016/j.virol.2014.09.005
92. Josseran L, Paquet C, Zehngoun A, Caillere N, Le Tertre A, Solet JL, et al. Chikungunya disease outbreak, Reunion Island. *Emerg Infect Dis.* (2006) 12:1994–5. doi: 10.3201/eid1212.060710
93. Sam IC, Kamarulzaman A, Ong GS, Veriah RS, Ponnampalavanar S, Chan YF, et al. Chikungunya virus-associated death in Malaysia. *Trop Biomed.* (2010) 27:343–7.
94. Schilte C, Staikowsky F, Couderc T, Madec Y, Carpentier F, Kassab S, et al. Chikungunya virus-associated long-term arthralgia: a 36-month prospective longitudinal study. *PLoS Neglect Trop Dis.* (2013) 7:e2137. doi: 10.1371/journal.pntd.0002137
95. Soumahoro MK, Boelle PY, Gauzere BA, Atsou K, Pelat C, Lambert B, et al. The Chikungunya epidemic on La Reunion Island in 2005–2006: a cost-of-illness study. *PLoS Neglect Trop Dis.* (2011) 5:e1197. doi: 10.1371/journal.pntd.0001197
96. Ma X, Xu S. TNF inhibitor therapy for rheumatoid arthritis. *Biomed Rep.* (2013) 1:177–84. doi: 10.3892/br.2012.42
97. Vasanthi P, Nalini G, Rajasekhar G. Role of tumor necrosis factor-alpha in rheumatoid arthritis: a review. *Int J Rheum Dis.* (2007) 10:270–4. doi: 10.1111/j.1479-8077.2007.00305.x
98. Brito AF, Pinney JW. Protein-protein interactions in virus-host systems. *Front Microbiol.* (2017) 8:1557. doi: 10.3389/fmicb.2017.01557
99. Van Vliet K, Mohamed MR, Zhang L, Villa NY, Werden SJ, Liu J, et al. Poxvirus proteomics and virus-host protein interactions. *Microbiol Mol Biol Rev.* (2009) 73:730–49. doi: 10.1128/MMBR.00026-09
100. Keating JA, Striker R. Phosphorylation events during viral infections provide potential therapeutic targets. *Rev Med Virol.* (2012) 22:166–81. doi: 10.1002/rmv.722
101. Xue Y, Ren J, Gao X, Jin C, Wen L, Yao X. GPS 2.0, a tool to predict kinase-specific phosphorylation sites in hierarchy. *Mol Cell Proteomics.* (2008) 7:1598–608. doi: 10.1074/mcp.M700574-MCP200
102. Xue Y, Zhou F, Zhu M, Ahmed K, Chen G, Yao X. GPS: a comprehensive www server for phosphorylation sites prediction. *Nucleic Acids Res.* (2005) 33:W184–7. doi: 10.1093/nar/gki393
103. Audagnotto M, Dal Peraro M. Protein post-translational modifications: *in silico* prediction tools and molecular modeling. *Comput Struct Biotechnol J.* (2017) 15:307–19. doi: 10.1016/j.csbj.2017.03.004
104. Blom N, Sicheritz-Ponten T, Gupta R, Gammeltoft S, Brunak S. Prediction of post-translational glycosylation and phosphorylation of proteins from the amino acid sequence. *Proteomics.* (2004) 4:1633–49. doi: 10.1002/pmic.200300771
105. Zhang D, Tozser J, Waugh DS. Molecular cloning, overproduction, purification and biochemical characterization of the p39 nsp2 protease domains encoded by three alphaviruses. *Protein Express Purification.* (2009) 64:89–97. doi: 10.1016/j.pep.2008.10.013

Conflict of Interest Statement: The authors declare that the research was conducted in the absence of any commercial or financial relationships that could be construed as a potential conflict of interest.

Copyright © 2019 Nayak, Mamidi, Sahoo, Kumar, Mahish, Chatterjee, Subudhi, Chattopadhyay and Chattopadhyay. This is an open-access article distributed under the terms of the Creative Commons Attribution License (CC BY). The use, distribution or reproduction in other forums is permitted, provided the original author(s) and the copyright owner(s) are credited and that the original publication in this journal is cited, in accordance with accepted academic practice. No use, distribution or reproduction is permitted which does not comply with these terms.